EARLY ANGIOGENIC CHANGE IN DENTAL PULP STROMAL CELLS CULTURED ON BIOMIMETIC MATRICES.

Hugh Russell

Submitted in accordance with the requirements for the degree of

PhD.

The University of Leeds

Dept. of Oral Biology,

School of Dentistry.

February 2016.

The candidate confirms that the work submitted is his/her own and that appropriate credit has been given where reference has been made to the work of others.

Acknowledgements

I would like to thank my principal supervisor Dr. Xuebin Yang who taught me the important fundamentals of dental pulp harvesting and tissue culture; Dr. Howard Davies of OralDent for the GenGiGel® samples; Sue Keates for her immunohistology training; Jackie Hudson for her unfailing patience at my general technological bafflement and SEM training; Yamuna Mohanram and Huiru Zou, the backbone of our mutual support group and their superb Asian cuisine; Dr. Sarah Myers who looked after my experiments during a prolonged period of illness and supervised my FEGSEM images; Dr. Steve Brookes for his unstinting moral support; Dr. Jing Kang for statistical guidance; Adam Steele and Greg Baugh for their secretarial skills; Claire Godfrey for keeping me away from the University ordering system and running the coffee club; Julie McDermott for help during Research Days; Dr. Adam Mitchell for advice on PCR; Dr. Scott Finlay for teaching me EndNote; Dr. Nigel Bubb, master of the University Thesis template and if I've forgotten anyone else I apologise for the oversight, but you all know who you are. I must again thank Dr. Xuebin Yang for his advice and support throughout this study. Finally, two extremely important women! I must give a particularly grateful thank you to Professor Jennifer Kirkham, Head of Department and 'mum' to us all, for her insight, experience and for giving me the chance to pursue this project. Lastly and most importantly, my wife Judith, for her help, encouragement and putting up with me and all of our travails throughout this, because without her none of it would ever have been possible.

Abstract

Revascularisation of the devitalised root canal is the Holy Grail of Endodontics and is being hotly pursued by many teams of clinicians but has yet to be achieved. The overall aim of this work was to attempt to induce early angiogenesis in human dental pulp stromal cells (DPSCS) *in vitro* and *in vivo* using a biomimetic approach based on combining scaffolds comprised of ECM components with DPSCs as a first step towards a tissue engineering strategy for dental pulp regeneration. After isolating DPSCs using collagenase digest, they were cultured on 1% hyaluronic acid (HyA) or Types I and III collagen matrices used either singly or in combination to determine the ability of these scaffolds to support/induce early angiogenic change in DPSCs both *in vitro* and *in vivo*. Angiogenic change was determined using a combined approach of DNA quantification, histology, immunohistochemistry to detect the angiogenic markers CD31 and CD34 and quantitative RT-PCR.

DPSCs were shown to attach and proliferate on Type I and III collagen membranes *in vitro* but early angiogenic change *in vitro* was evidenced only when 1% HyA gel was used, including in the absence of the morphogen $_{rh}VEGF_{165}$ as shown immunohistochemically. PCR at two and five days post-seeding showed an up-regulation of *CD31* and *CD34* genes dependant on culture conditions, with *CD31* being upregulated early and *CD34* later in the culture period.

A modified tooth slice model containing a combination of HyA/collagen scaffold/DPSC constructs within its lumen also showed positive early angiogenic change *in vitro*. SEM examination further confirmed that DPSCs could attach,

colonise and proliferate to/on the combined scaffold. The same combined scaffold-tooth slice model ± DPSCs used *in vivo* in nude mice showed cellular ingress into the lumen with a soft tissue closely resembling dental pulp-like tissues in its appearance with new tubule-like material grown on from the dentinal tubules of the tooth slice. There was a defined demarcation line between this latter material and the dentinal tubules of the tooth slice and the new material closely resembled predentine or dentine-like matrix in appearance and stained strongly for CD31 and CD34 markers. It also had a layer of cells adjacent to and in intimate contact with its deposition front, whose cell processes transited the new tubule-like material and continued into the dentine tubules of the tooth slice for some distance. Interestingly, this neo-tissue was independent of the addition of DPSCs to the construct. The results suggest that biomimetic scaffolds based upon components of the pulp extracellular matrix may provide a useful platform for future engineering of a vascularised replacement dental pulp.

Table of Contents

List of Tables

List of Figures

Chapter 1: General Introduction

The dental pulp, commonly but erroneously called ‘the nerve’ is more accurately described as a neurovascular bundle forming the living soft tissue component found inside every healthy tooth (Luukko et al., 2011). The dental pulp produces dentine throughout its lifetime: primary dentine during tooth development, secondary dentine thereafter and tertiary, or reactive dentine under pathogenic stimuli (Holland and Torabinejad, 2009). It is almost entirely encased by dentine, limiting how much it can expand during inflammatory changes and any symptoms, regardless of cause arising from within a tooth involve and emanate from this structure which connects with the supporting bony tissues of the periodontium, via a periapical foramen or multiple foramina in each root (Zavan et al., 2011, Holland and Torabinejad, 2009).

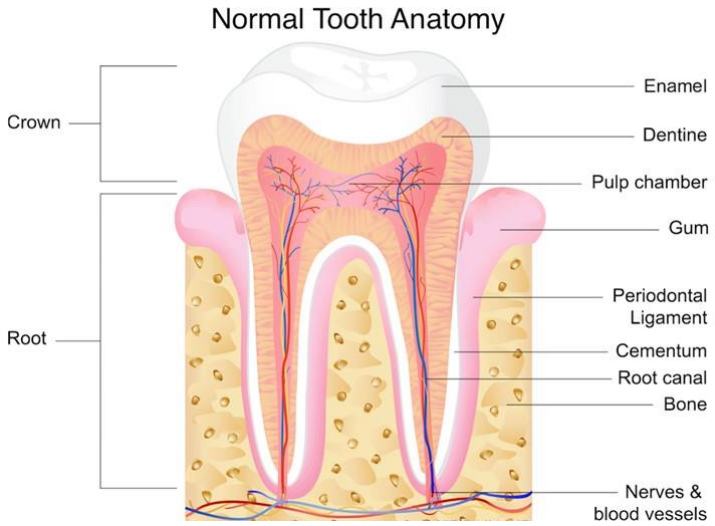

Figure 1. Gross anatomy of the tooth.
From 3MD marketing (public domain).

This constricted vasculature is one of the reasons why dental pulp in the adult tooth has very limited powers of healing, particularly when apexification i.e. complete formation of the constricted part of the root tip is completed, approximately three years following tooth eruption into the oral cavity.

1 Dental pulp embryology

The dental pulp is derived from the cephalic neural crest. Neural crest cells arise from the ectoderm along the lateral margins of the neural plate and begin to migrate. Those which migrate down the sides of the head into the maxilla and the mandible contribute to the formation of the tooth germs and the dental papilla – from which the dental pulp develops – starts as ectomesenchymal cells proliferate and condense adjacent to the dental lamina at the sites where the teeth will develop (Pashley and Liewehr, 2006). The migratory potential of ectomesenchymal cells continues to persist in the ability of pulp cells to move into areas of injury and replace dead odontoblasts. Tooth formation of the primary dentition begins around the sixth week of embryonic life when the proliferation of ectodermal cells gives rise to two horseshoe shaped structures, one on the mandible, the other on the maxilla. These structures are called the primary dental laminae and each divides into a vestibular and a dental lamina. Cells in the dental epithelium and adjacent ectomesenchyme divide rapidly at this stage and the dental lamina can induce tooth formation by its influence on the underlying ectomesenchyme (Mina and Kollar, 1987).

Tooth formation is a continual process, but for convenience is usually divided into three stages: (i) bud, (ii) cap and (iii) bell (Lumsden, 1988, Nanci, 2012, Orban, 1928). The bud stage is the initial stage, where the epithelial cells of the dental lamina proliferate and produce a budlike projection into the ectomesenchyme.

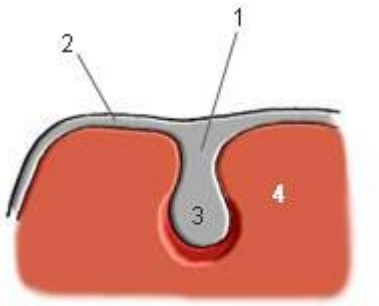

Figure 2. Bud stage (the tooth at 8 weeks embryonic life).
1. The Dental Lamina. 2. The Oral Epithelium. 3. The Tooth Bud. 4. The Jaw Mesenchyme.

The cap stage occurs when the cells of the dental lamina have proliferated to form a concavity. At the transition from bud to cap, enamel knot formation initiates cuspal patterning, an important stage in tooth morphology (Jernvall et al., 1994). The outer cells of the cap are cuboidal and form the outer enamel epithelium. The inner cells are more elongated and form the inner enamel epithelium. Between them is a network of cells called the stellate reticulum. The rim of the enamel organ (where the two layers of cells meet) is called the cervical loop (Parikh, 2004, Pannese, 1962).

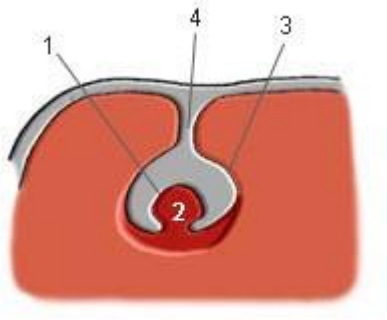

Figure 3. Cap Stage the tooth at 10 weeks embryonic life.

1. The Inner Enamel Epithelium. 2. The dental Papilla. 3. The Outer Enamel Epithelium. 4. The Dental Lamina.

As they continue to proliferate, there is further invagination of the enamel organ into the mesenchyme and the organ assumes a bell shape. During this stage, the ectomesenchyme of the dental papilla becomes partly enclosed by the invaginating epithelium and the blood vessels become established in the dental papilla (D'Souza, 2002). The condensed ectomesenchyme surrounding the enamel organ and dental papilla forms the dental sac and ultimately becomes the periodontal ligament. Differentiation of epithelial and mesenchymal cells into ameloblasts and odontoblasts respectively, occurs during the bell stage.

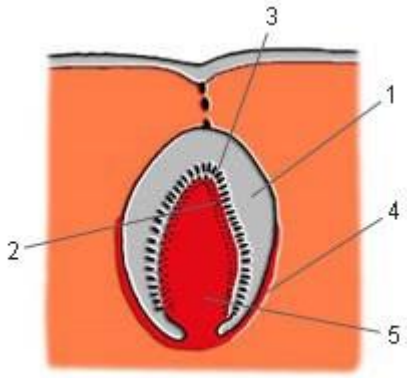

Figure 4. Bell stage (the tooth at 12 weeks embryonic life).

1. Stellate Reticulum. 2. Odontoblasts. 3. Ameloblasts. 4. Dental Sac. 5. Dental Papilla.

By about the sixth month of development, many more of the tooth's structures have become established, including the calcified tissues and the beginning of root formation is about to commence.

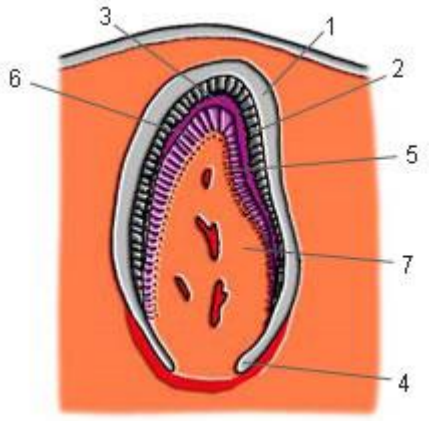

Figure 5. Advanced Bell Stage (about 24 weeks of embryonic life).

1. Stellate Reticulum. 2. Ameloblast layer. 3. Early Enamel formation. 4. Epithelial Root Sheath. 5. Odontoblast Layer. 6. Early dentine formation. 7. Dental Pulp.

As the odontoblast layer differentiates, the cells elongate and take on the ultra-structural characteristics of protein-secreting cells. Cytoplasmic processes extend from the cells and increasing numbers of collagen fibrils (Von Korff fibres) appear

in the extra-cellular matrix (ECM). Both Type I and Type III collagen messenger Ribonucleic Acid (mRNA) can be found in developing odontoblasts (D'Souza et al., 1995) but most of the collagen produced by mature odontoblasts is Type I. Dentinogenesis begins where tooth cusp tips or incisal edges will eventually be and as odontoblasts reach full maturity they become tall columnar cells of up to 50 µm but with a fairly consistent width of about 7 µm. As predentine matrix is laid down the odontoblasts move inwards at between 4 to 8 µm per day leaving matrix behind. In the matrix, an accentuated process from each odontoblast remains to form the primary odontoblast's process and the dentinal tubules are formed around these (Pashley and Liewehr, 2006).

Under the microscope, dental pulp is usually described as having four regions or zones (Zach et al., 1969).

1) The odontoblast layer around the periphery of the pulp, in intimate contact with the tooth dentine.
2) The so-called 'cell free' zone, which has fewer cells than the odontoblast layer but containing capillaries and nerve fibres.
3) The 'cell-rich' zone populated by fibroblasts and undifferentiated mesenchymal cells with a rich vascular supply.

4) The central pulp zone. This region contains the pulp's larger blood vessels and innervative structures. The main cell types are fibroblasts.

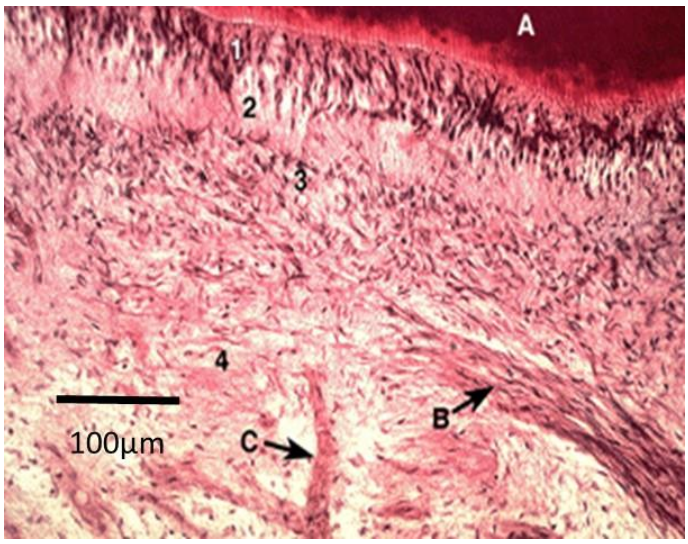

Figure 6. Regions in the Dental Pulp. From Oral Histology Digital Lab (public domain).

1. (white in above image) Odontoblast Layer. 2. 'Cell free' zone. 3. 'Cell Rich' zone. 4. Central Zone.

A: Dentine. B: Nerve Fibril. C. Blood vessel.

Dental pulp is a tissue of ectomesenchymal origin with specialised odontoblasts placed peripherally in intimate contact with dentine. This closeness of this pairing, embryologically, developmentally, anatomically and functionally, has led to them being termed as the pulp-dentine complex and is a reason why the two tissues can be regarded as a single functional entity although made up of histologically distinct components (Pashley, 1996). The pulp has an extensive blood supply (Kishi et al., 1995) but constraints are imposed on the pulp by its rigid mineralised surroundings which limit its ability to expand during periods of vasodilation, inflammation and increased tissue pressure, resulting in an increase in tissue pressure instead of volume (Heyeraas and Berggreen, 1999). As the total volume of fluid in the pulp chamber cannot be greatly increased (although volume changes can occur between

venules, arterioles, lymphatics and extra-vascular tissue) careful regulation of blood flow is crucial to pulp health, with shunting occurring mainly in the apical half of the pulp (Meyer and Path, 1979). Being limited in volume, the microcirculatory system of the pulp contains no true veins or arteries, only venules and arterioles (Zhang et al., 1998). Also there is no collateral system and the vascularity of the pulp decreases progressively with age as the dental pulp shrinks and becomes progressively more fibrous (Bernick and Nedelman, 1975). The pulp contains a mixture of tissues including nerve fibres, vascular tissue, connective tissue, ground substance, interstitial fluid, odontoblasts, fibroblasts and immunocompetent cells. However, its special characteristics and ability to remodel mean that even a mature dental pulp bears a resemblance to embryonic connective tissue and is therefore a fairly good source of stem cells (Pashley and Liewehr, 2006). Odontoblasts continue to lay down matrix and deposit dentine throughout the lifetime of the tooth.

1.1 Extracellular matrix components of the dental pulp

ECM comprises the predominantly non-cellular elements present in all organs and tissues. ECM has been described as the ideal biologic scaffold material and can be divided into two compartments, namely ground substance and fibrous proteins (Badylak, 2007). The ECM is not passive. It supports the blood vessels, nerves and lymphatic tissues and also permits the diffusion of nutrients from the blood to the adjacent cells (Badylak, 2007). As each tissue has its own tailor-made ECM manufactured by its own cells (Badylak, 2007) it provides the necessary physical

and mechanical support medium for the cellular (mostly fibroblasts) constituents. Physiologically, it initiates important biomechanical and biochemical prompts for differentiation, homeostasis and morphogenesis (Frantz et al., 2010). Its importance can be seen by syndromes arising from conditions such as Type IV Ehlers-Danlos syndrome as well as other genetic abnormalities deriving from genetic mutations in ECM proteins (Jarvelainen et al., 2009). Its two main macromolecular components comprise of proteoglycans (PGs) and fibrous proteins (Schaefer and Schaefer, 2010).

1.1.1 Proteoglycans

Proteoglycans (PGs) are a principal component of the tissue ground substance. Ground substance also acts as a molecular sieve, able to exclude large proteins and urea and it can exclude osmotically active molecules, helping to determine the physical characteristics of the pulp. Ground substance can be degraded in the presence of lysosomal enzymes, proteolytic enzymes, hyaluronidases and chondroitin sulphatases. The pathways of inflammatory and infective reactions are strongly influenced by the level of polymerisation of the ground substance components (Pashley and Liewehr, 2006).

PGs are the main component contributing towards the ground substance properties. and are formed of glycosaminoglycan (GAG) polymer chains, covalently attached to a specific protein core (Schaefer and Schaefer, 2010). Hyaluronic Acid (HyA) is also a GAG but is found free in tissues or non-covalently associated with PG aggregates (Iozzo and Murdoch, 1996, Sakamoto et al., 1981). One of their

functions is to act as adhesive molecules binding cell surfaces to other molecules in the ECM (Uitto and Larjava, 1991). Proteoglycans have a net negative charge which attracts water molecules. Thus, within a tissue, PGs can fill most of the extracellular and interstitial spaces giving it the form of a hydrated gel, or hydrogel (Badylak, 2002) with a wide variety of roles reflecting their buffering, force resistance, binding and hydration capabilities (Jarvelainen et al., 2009). PGs are classified by their glycosaminoglycan (GAG) composition, core proteins and localisation, with the main three types being small leucine rich PGs (SLRPs), cell surface proteoglycans and modular proteoglycans. GAG chains bound to the protein cores of PGs comprise of unbranched polysaccharides, of repeating disaccharide units (sulphated *N*-acetylglucosamine or *N*-acetylgalactosamine, *L*-iduronic or *D*-glucuronic acid) and galactose (N-acetylglucosamine-β1 3-galactose-β1) which are subdivided into sulphated (keratin, chondroitin, dermatan and heparan sulphate) and non-sulphated (hyaluronic acid) GAGs (Schaefer and Schaefer, 2010). Their extreme hydrophilic nature gives them highly extended conformations enabling them to absorb high compressive forces and they have been implicated in tooth eruption mechanisms (Dean and Cole, 2013, Picton, 1989). SLRPs have involvement in many signalling pathways including binding to and activating low density lipoprotein related protein 1 (LRP1), regulation of inflammatory response reactions, binding to and activating transforming growth factor β (TGFβ), binding to and activating insulin-like growth factor 1 receptor (IGFIR) and also epidermal growth factor receptor (EGFIR) (Goldoni and Iozzo, 2008) and binding to and directing collagen fibrillogenesis and fibre orientation. Some (but not all) of the actions of modular PGs involve modulating cell adhesion, proliferation and migration (Schaefer and Schaefer, 2010).

Basement membrane modular PGs such as agrin, perlecan and collagen Type XVIII function dually as both pro and anti-angiogenic factors (Iozzo et al., 2009). Cell surface PGs such as syndecan and glypicans facilitate ligand binding with signalling receptors by acting as co-receptors (Schaefer and Schaefer, 2010).

In the pulp, the principal GAGs include dermatan sulphate, heparan sulphate and chondroitin sulphate. The PG content of the pulp reduces greatly following tooth eruption (Linde, 1985). During active dentinogenesis, chondroitin sulphate predominates (Linde, 1973) especially in the odontoblast and predentine layer where it may have a role in the mineralisation process (Bouvier et al., 1990). Predentine contains several types of GAGs and PGs, whereas dentine predominantly contains chondroitin sulphate-containing PGs (Takagi et al., 1990). Following tooth eruption, hyaluronic acid and dermatan sulphate increase and chondroitin sulphate reduces greatly.

1.1.2 Non-collagenous proteins

The ECM of dentine also contains non-collagenous proteins (NCPs) active in controlling collagen fibre mineralisation and crystal growth in predentine as part of its' transition into dentine proper. Mutations in these proteins are manifested by marked phenotype changes in dentine mineralisation and in other calcified tissues such as bone (Feng et al., 2002, Sreenath et al., 2003, Xiao et al., 2001, Xu et al., 1998, Zhang et al., 2001). NCPs such as the small integrin binding ligand, N-linked glycoproteins (SIBLINGs) include osteopontin (OP), bone sialoprotein (BSP), matrix extracellular phosphoglycoprotein (MEPE), dentine sialophosphoprotein

(DSPP) and dentine matrix protein 1 (DMP1) (Fisher et al., 2001). Principally found in bone and dentine, SIBLING proteins are secreted into the ECM as part of the formation and mineralisation of these two tissues although the expression of DMP1, OPN, DSPP and BSP are similar qualitatively but differ quantitatively between these two tissues (Qin et al., 2001).

Fibronectin (FN) is a non-collagenous protein with roles in managing the organisation of interstitial ECM as well as mediating cell function and attachment. Secreted as a dimer joined by two C-terminal disulphide bonds, FN has binding sites to heparin and other FN dimers. It also binds to cell-surface integrin receptors (Pankov and Yamada, 2002). It is able to be stretched by a factor of several times its resting length by cellular traction forces (Smith et al., 2007). This force-dependant unfolding results in the exposure of secret or 'cryptic' binding sites for integrins resulting in pleiotropic changes altering cell behaviour and hint at FN having a role as an extracellular mechano-regulator.

1.1.3 Fibrous proteins

The most commonly found fibrous protein within the ECM is collagen which can comprise up to 30% of the total protein found in a multicellular animal (Frantz et al., 2010). The majority of interstitial collagen is secreted by the fibroblasts residing in the ECM stroma or which are recruited into it from adjacent tissues (De Wever et al., 2008).

1.1.3.1 Collagen

Thus far, twenty eight types of collagen have been identified in vertebrate animals (Gordon and Hahn, 2010). Most collagen molecules form a triple helix which, depending on the collagen type, can subsequently be assembled into supramolecular complexes like fibrils and networks. The importance of Type I collagen structure is evident when seen in patients with osteogenesis imperfecta which is caused by mutations in the Type I collagen gene (Cole, 2002) and in dentinogenesis imperfacta type 1 where there are mutations in the genes encoding collagen Type I, *COL1A1* and ICOL1A2 (Barron et al., 2008). Network collagens are incorporated into basement membranes and fibrous collagens form the basis of collagen fibril bundles within the interstitial tissue stroma (Frantz et al., 2010). Type I collagen synthesis includes several enzymatic post-translational modifications (Myllyharju and Kivirikko, 2004), predominantly the hydroxylation of lysine and proline residues, the cleavage of N- and C- terminal propeptides and the glycosylation of lysine. Post-secretion, lysyl oxidases (LOX) convert the side chains of lysine and hydroxylysine residues of the collagen molecules to their aldehyde forms. These can then go on to react to form covalent inter-molecular cross links, strengthening the collagen fibrils (Robins, 2007). Collagens provide the main structural element for the ECM, where they can direct tissue development, aid chemotaxis and cell migration, help regulate cell adhesion and give tensile strength (Rozario and DeSimone, 2010). Fibroblasts are able to exert tension on the ECM, organising collagen fibrils into sheets and fibres or cables influencing the alignment of the resultant collagen fibres. Normally within any one specific tissue the collagen fibres are a mixture of several types, but one type usually comprises the majority (Frantz et al., 2010). Dental pulp ECM

consists of 56% Type I collagen, 41% Type III collagen, 2% Type V collagen and 0.5% Type VI collagen associated with microfibrillin (Goldberg and Smith, 2004).

1.1.3.2 Elastin

Elastin is another ECM fibre frequently co-expressed with collagen. Elastin fibres are secreted as a precursor tropoelastin which is assembled into fibres, becoming highly crosslinked to each other by their lysine residues. This is carried out by members of the LOX enzyme group which includes LOX and lysyl oxidase like (LOXL) (Lucero and Kagan, 2006). Elastin fibres allow stretch and recoil in tissues subjected to these forces on a repeated basis with the elastin stretch being crucially constrained by its intimate association with collagen fibrils (Wise and Weiss, 2009). The maintenance of the integrity of the elastin fibres is due to their covering of predominantly fibrillin glycoprotein microfibrils (Wise and Weiss, 2009).

1.2 Connective tissue fibres of the pulp

Dental pulp, in common with all connective tissues contains both major and minor fibres within the ECM. Two principal types of structural proteins can be found in the pulp, namely elastin and collagen (see above). Initially during tooth formation thin microfibres called oxytalan fibres are formed (Bradamante et al., 1980) comprised of fibrillin glycoprotein microfibrils, then elastin protein is deposited within them, forming elastic fibres. Elastic fibres are associated with the walls of larger blood vessels and are also part of the ECM. However, collagen Type 1 is by far the most

abundant fibrous protein present in the pulp. By dry weight the amount of total collagen in the dental pulp is approximately 26% in premolars and 32% in third molars (van Amerongen et al., 1983) which is higher than that reported for other mammalian species such as rabbit (Uitto and Antila, 1971). The content is higher in the radicular part of the pulp than the coronal. Collagen Types I and III are both present throughout the majority of pulp collagen, with Type I predominating (Shuttleworth et al., 1978) but with the proportion of Type III collagen also being relatively high at about 43% of the total collagen in human dental pulp (van Amerongen et al., 1983) and over 40% of the total collagen in bovine dental pulp (Lechner and Kalnitsky, 1981) which may contribute to its elasticity (Shuttleworth et al., 1980) enabling it to better adapt during periods of hyperaemia. In the pulp, Type III collagen forms finely branched filaments distributed similarly to reticular fibres (Magloire et al., 1982) and is distributed densely in both the cell rich and cell poor zones (Karjalainen et al., 1986). Dentine and predentine collagens are almost totally Type I (Ruch, 1985) although some investigators have detected Type III collagen (Karjalainen et al., 1986) and Type V collagen in predentine (Lukinmaa and Waltimo, 1992). Pulp fibroblasts can produce both Types I and III collagen but the majority of collagen produced by odontoblasts is Type I (D'Souza et al., 1995). Collagen Types III and V (Tsuzaki et al., 1990) and VI (Hillman and Guertsen, 1997) have been noted in pulp tissue forming a dense, microfibrillar network throughout the stroma of the connective tissue of the pulp. Fibres of Type VI collagen have been found between odontoblasts toward the predentine suggesting they are a component of Korff fibres (Hillman and Guertsen, 1997). Also, collagen Type IV is a component of basement membrane in the pulpal blood vessels (Fried et

al., 1992). Turnover of collagen in the dental pulp is high, compared to other tissues and is associated with the fibroblasts which are able to both synthesise and degrade collagen (Orlowski, 1977). Inflammation consequent to bacterial infection may accelerate collagen degradation as seen in pulps with suppurative pulpitis which show elevated collagenolytic activity (Morand et al., 1981) and in vitro studies have suggested that production of collagenolytic enzymes is up-regulated in fibroblasts in response to infection and inflammation.

1.3 Metabolism of the dental pulp

The metabolic activity of dental pulp tissues has been studied by measuring the rate of O_2 consumption by the bovine dental pulp and the production of CO_2 or lactic acid. Their production was found to be low in comparison to other tissues (Biesterfeld et al., 1979, Fisher, 1967, Fisher et al., 1957, Hamersky et al., 1980, Sasaki, 1959) with one study finding that odontoblasts consumed O_2 at the rate of 3.2 ± 0.2 mL/minute/100grams of pulp tissue (Yu et al., 2002) with others showing it to be much higher, in the region of 40-50 mL/minute/10 grams of tissue as estimated using radioactive microsphere techniques (Kim, 1985, Meyer, 1993, Path and Meyer, 1977). During active dentinogenesis, metabolic activity is higher than after crown development, with the greatest metabolic activity found in the odontoblast layer (Bhussary, 1968, Fisher, 1967). Also, the pulp can produce energy via a phosphogluconate (i.e. pentose phosphate) shunt type of metabolism (Fisher and Walters, 1968), which may be how it survives periods of relative ischaemia

induced by vasoconstrictive anaesthetic agents (Kim et al., 1984). Some dental materials such as amalgam, eugenol, zinc oxide and eugenol and calcium hydroxide appear to reduce O_2 consumption by dental pulp tissue suggesting that they could be able to down-regulate the metabolic activity of dental pulp cells (Jones et al., 1979, Fisher et al., 1957) and it has been shown that sufficient force to elicit orthodontic movement for three days can reduce respiratory activity in dental pulp tissue by 27% (Hamersky et al., 1980).

1.4 Vascular Supply of the dental pulp

The dental pulp has an extensive vascular supply (Kishi et al., 1995). The vessels pass through the apical foramen and accessory foramina in other areas of the root surface, as part of the neurovascular bundle with smaller vessels entering via lateral canals. The arterioles pass up the centre of the pulp, giving off lateral branches which spread towards the odontoblast layer, forming a plexus beneath them. Capillary blood flow in the coronal pulp is nearly twice that in the root area (Kim, 1985). Also, blood flow is greater in the pulp horn regions than elsewhere (Meyer and Path, 1979). From the capillary bed, venous drainage is via progressively larger venules and in multirooted teeth the principal venous drainage may be predominantly down one root (Kramer, 1968). Arteriovenous anastomoses are found in the radicular and coronal pulp, especially the former. It is thought they perform an important regulatory function in shunting blood flow away from areas of inflammation or injury. The blood flow is regulated by sympathetic adrenergic

vasoconstriction (Kim et al., 1989), β-adrenergic vasodilation (Tonder, 1976), a sympathetic cholinergic vasoactive system (Aars et al., 1993) and an antidromic vasodilation system involving sensory nerves including axon reflex vasodilation (Sasano et al., 1994). Despite numerous studies, blood circulation in an inflamed pulp involves complex pathophysiologic mechanisms which have yet to be fully elucidated (Heyerass and Kvinnsland, 1992, Kim et al., 1983). Lymph vessels are also present in the pulp, smaller ones being located on the periphery and larger vessels located in the central pulp, being suggestive of drainage starting from the periphery and progressing to the centre of the pulp (Sawa et al., 1998).

1.5 Innervation of the dental pulp

During the bell stage of development nerve fibres follow the path of blood vessels into the papilla. The sensory innervation of the teeth terminates primarily in the coronal odontoblast layer, predentine and inner dentine. Morphologically, it is made up of at least six types of nerve fibre, each having a preferred location, one example of which being the medium sized Aß myelinated fibres innervating mainly dentine near the pulp horn tip. They are the most sensitive fibres to mechanical/hydrodynamic stimulation of dentine (Chudler et al., 1985, Dong et al., 1985). Between 25% and 50% of dental nerve fibres are small myelinated AΔ fibres containing the neuropeptide calcitonin gene-related peptide (CGRP) and express receptors for nerve growth factor (NGF). Predominantly, they innervate dentine, predentine and the odontoblast layer in the coronal dentine region underlying

enamel (Byers and Narhi, 1999). The majority of nerve fibres in teeth are unmyelinated slowly conducting C-fibres, with most being regulated by NGF in the adult and about half requiring NGF during their development while others use brain-derived neurotrophic factor (BDNF) or glial-derived neurotrophic factor (GDNF) (Byers and Kish, 1976). They terminate in peripheral pulp and are mostly activated by pulpal damage. It is known that nerve fibres are dynamic and continually adjust their association with pulpal cells and dentine (Hattyasy, 1961). This has been further explained by studies showing growth-associated protein-43 in dental nerve fibres and endings (Maeda and Byers, 1996). Ultrastructural and immunocytochemical data show a close association between nerve fibres and odontoblasts, fibroblasts, blood vessels and immunocompetent cells (Ibuki et al., 1996) but specific synaptic or gap junctional connections between pulpal cells and clearly identifiable nerve fibres do not exist (Byers and Kish, 1976)**.** Vasodilatory functions of the sensory innervation of teeth are opposed by vasoconstriction from the sympathetic fibres (Olgart, 1996), which are located mainly in the deeper pulp and around blood vessels (Pohto and Antila, 1972). Parasympathetic activity can affect pulpal blood flow but it is unclear if this is from intradental or periodontal sites and is considered to be of less importance than sympathetic activity (Sasano et al., 1995). Interestingly, it has been shown that a single nerve fibre can innervate multiple tooth pulps (Hikiji et al., 2000). Broadly speaking, the nerve bundles pass through the radicular pulp with the blood vessels and on reaching the coronal pulp they fan out forming the plexus of Raschow. The fibres branch prolifically giving rise to a vast overlap of receptor fields (Harris and Griffin, 1968).

1.6 Dental pulp morphology

In a mature, healthy pulp, the outermost layer consists of odontoblasts. These are found immediately adjacent to and in intimate contact with the layer of predentine, which is in turn in contact with the dentine itself. The odontoblast cell's processes (see Figure 7) extend through the predentine and into the dentine and between each odontoblast there is a gap of 30 to 40 nanometres width. The odontoblast cell bodies are connected by both tight and gap junctional complexes (Bishop and Yoshida, 1992). Odontoblasts are typically columnar in the coronal part of the tooth, cuboidal in the radicular pulp region (Couve, 1986) and flattened in the apical region of the pulp (Kramer, 1968, Nanci, 2012). Immediately adjacent, there is a layer of comparatively few cells approximately 40 μm wide, known as the cell-free zone. Blood capillaries, unmyelinated nerve fibres, and the cytoplasmic processes of fibroblasts cross this area, which may or may not be obvious and sometimes absent, depending on the level of activity the pulp is undergoing e.g. in young pulps, where reparative dentine is being formed, or where dentine is being rapidly laid down (Couve, 1986). Adjacent to this is the cell-rich zone, which contains a relatively high proportion of fibroblasts when compared to the central zone of the pulp. This zone is more prominent in the coronal part of the pulp than elsewhere and also contains varying numbers of lymphocytes, macrophages and dendritic cells. It is thought that this zone arises from the peripheral migration of cells originally found in the central regions of the pulp, which then migrate around the time of tooth eruption (Gotjamanos, 1969). Irreversibly injured odontoblasts are thought to be replaced by cells migrating from the cell-rich zone (Fitzgerald et al., 1990) and their mitotic

activity is likely the first stage in the formation of new odontoblasts (Murray et al., 2000).

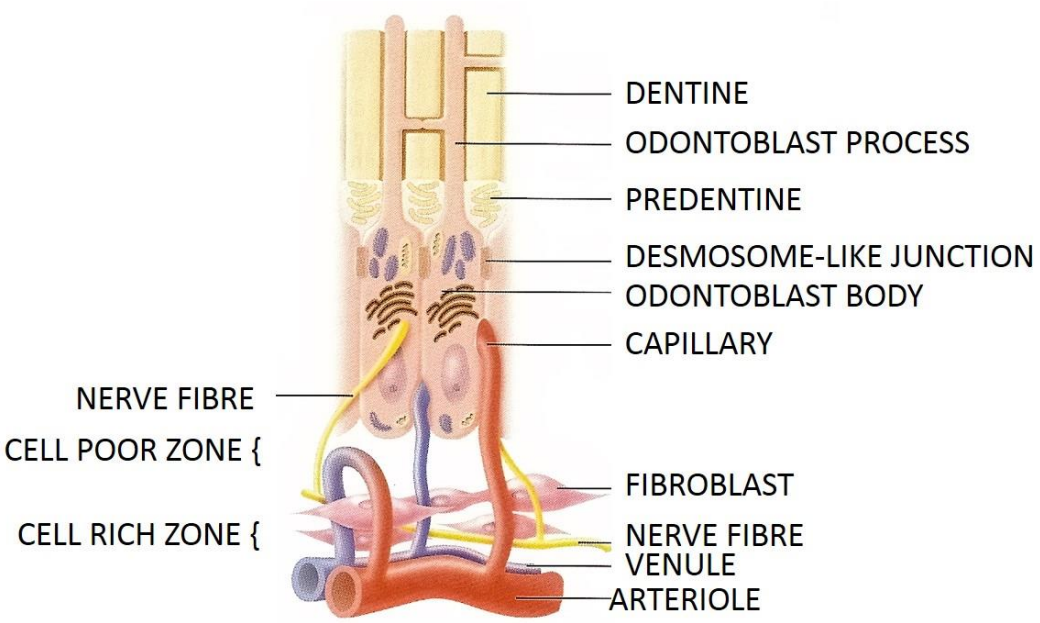

Figure 7. Representation of the odontoblast layer and subodontoblastic layer of the pulp.

Adapted from Pathways of the Pulp 10th edition 2011. Editors K.M. Hargreaves, S. Cohen & L.H. Berman.

Cell division in this zone is uncommon in healthy pulps but odontoblast death causes an increase in the rate of mitosis. Cells migrate from the cell-rich zone to the inner surface of the dentine to replace irreversibly injured odontoblasts and this mitotic activity is the first stage in forming a new odontoblast layer (Fitzgerald et al., 1990). The 'body' or main central mass of the pulp contains the larger blood vessels and nerves and here, the connective tissue cells consisting of fibroblasts and pulpal cells predominate.

1.7 Cells of the Dental pulp

1.7.1 Odontoblasts

These cells are responsible for dentinogenesis throughout the lifetime of a tooth and are the most readily identifiable cells within the pulp with the fully developed odontoblast found in the coronal pulp being a tall columnar cell (Couve, 1986). They form the dentinal tubules and their presence makes dentine a living, vital tissue, responsible for the hydrodynamic theory of pain transduction (Brannstrom, 1966(a), Brannstrom, 1966(b), Gysi, 1900). They share many general similarities with osteoblasts and cementoblasts, such as producing a matrix of collagen fibres and proteoglycans capable of being mineralised (Charadram et al., 2012, Goldberg et al., 1995, Qin et al., 2004). Ultrastructurally, they all exhibit a highly ordered Rough Endoplasmic Reticulum, prominent Golgi complex, secretory granules and numerous mitochondria, reflecting their role as secretory cells.

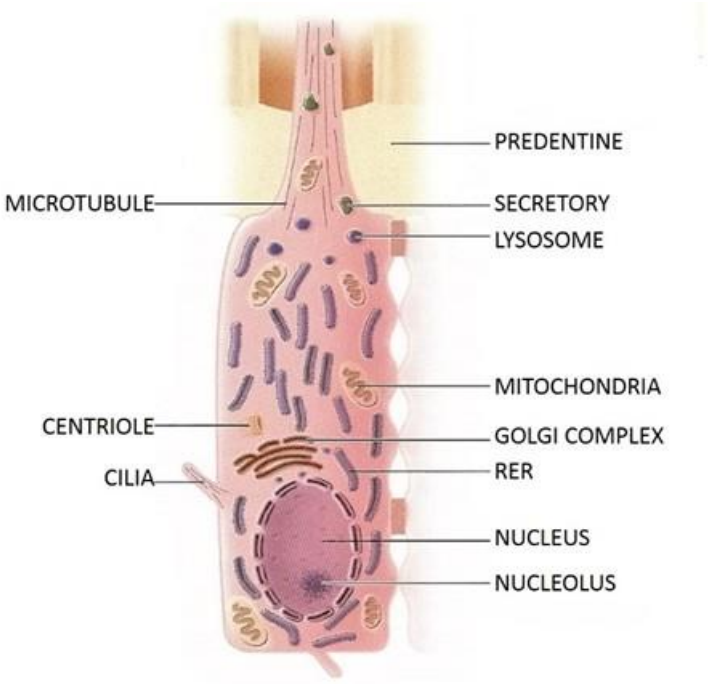

Figure 8. Representation of a fully differentiated odontoblast, showing cell organelles.

Adapted from Pathways of the Pulp 10thth edition 2011. Editors K. M. Hargreaves, S. Cohen & L. H. Berman.

Odontoblasts are rich in RNA and have nuclei with one or more prominent nucleoli. The major differences between odontoblasts, osteoblasts and cementoblasts are their morphology and relationship with the structures they ultimately produce. Osteoblasts and cementoblasts are polygonal to cuboidal in form, whereas the fully mature coronal odontoblast is a long columnar cell (Marion et al., 1991). In bone and cementum some osteoblasts and cementoblasts become trapped in the matrix as osteocytes or cementocytes (Li et al., 2011). Odontoblasts, however, leave behind cellular processes to form the dentinal tubules (Andrew and Matthews, 2000). Lateral branches link the major odontoblastic processes via canaliculi (Mjor and Nordahl, 1996) just as cementocytes and osteocytes link together via the canaliculi in cementum and bone. This provides avenues for inter-cell signalling, circulation of

fluid and metabolites through the mineralised tissues. An active odontoblast has a prominent nucleus, basally situated within a nuclear envelope with up to four nucleoli. A well-developed Golgi complex, numerous evenly distributed mitochondria and prominent rough endoplasmic reticulum (RER) for protein synthesis are also found. Mature odontoblasts mainly secrete Type I collagen, although small amounts of Type V collagen are also found in the ECM. As well as collagen and proteoglycans, odontoblasts secrete alkaline phosphatase (ALP, an enzyme closely linked to mineralisation), dentine sialophosphoprotein (DSPP), a highly phosphorylated phosphoprotein which is involved in extracellular mineralisation and is unique to dentine (D'Souza et al., 1995). Originally thought not to occur in many other mesenchymal cell lines (Butler et al., 1992) it has since been shown to be present in brain, kidney, liver, cartilage and salivary glands, but absent from the heart and spleen. It has also been shown to be expressed at higher levels in salivary glands, cartilage, kidney and liver than in bone and has also been found in the pericytes of dental pulp blood vessels (Prasad et al., 2011). Post secretion, DSPP is rapidly cleaved to produce dental sialoprotein (DSP) (Butler et al., 1992), dentine glycoprotein (Yamakoshi et al., 2005) and dentine phosphoprotein (MacDougall et al., 1997).

Resting odontoblasts have reduced numbers of organelles and may become shorter as seen in the apical region of the pulp, following root completion (Couve, 1986). The odontoblast process forms the template for the dentinal tubule and is responsible for laying down peritubular dentine. Associated with its lateral branches are microtubules and microfilaments. There is much debate as to how far the process extends along the tubule with studies claiming it goes a third of the way into the

dentine (Holland, 1976, Holland, 1985, Thomas and Payne, 1983), up to the amelodentinal junction in some cases (Grossman and Austin, 1983, Kelley et al., 1981) and the amelodentinal junction in all cases (Sakurai et al., 1999, Sasaki and Garant, 1996). Odontoblasts are considered to be fixed postmitotic cells that, once fully differentiated, cannot undergo further cell division.

1.7.2 Dental pulp fibroblasts

Dental Pulp fibroblasts are the most numerous cells within the pulp and seem to be tissue specific, capable of giving rise to cells which are committed to differentiation e.g. odontoblast-like cells, if given the appropriate signal (Luukko et al., 2011). They synthesise Types I and III collagen as well as PGs and GAGS and maintain the matrix proteins of the ECM as well as being responsible for collagen turnover in the pulp (Luukko et al., 2011). Fibroblasts are to be found throughout the pulp but are particularly abundant in the cell-rich zone (Nanci, 2012). In their immature stage, their organelles are rudimentary and inconspicuous with sparse RER. As they mature they become more stellate in form, the RER proliferates, the Golgi complex enlarges and they take on more of the characteristics of protein-secreting cells. With the increase in numbers of blood vessels and nerve fibres in the body of the pulp, the number of fibroblasts becomes relatively reduced. Compared with the fibroblasts of other tissues, pulp fibroblasts remain in a relatively undifferentiated state (Han, 1968) and it has been demonstrated that mitotic activity preceding the differentiation of replacement odontoblasts seems to occur primarily among fibroblasts (Fitzgerald et al., 1990). Cells from the dental pulp with mesenchymal stem cell properties have

been shown to be capable of various types of functional differentiation dependant on the environmental clues provided under the culture conditions, such as neuronal (Arthur et al., 2008), angiogenic (d'Aquino et al., 2007) and osteoblastic (Ramamoorthi et al., 2015).

1.7.3 Macrophages

These are monocytes which have left the bloodstream, entered the tissues and differentiated into various subpopulations. One subpopulation is active in endocytosis and phagocytosis; the other in processing antigen for presentation to T memory cells (Okiji et al., 1992) binding it to major histocompatibility complexes (MHCs) - formerly known as class II antigen molecules - on the macrophage (Hahn et al., 1989) and is an essential part of T cell-dependant immunity.

1.7.4 Dendritic cells

These are accessory cells of the immune system similar to the Langherhans' cells of the epidermis and mucous membranes (Jontell et al., 1987). They are antigen-presenting cells, characterised by dendritic cytoplasmic processes or filopodia and the presence of cell surface MHCs. They are primarily found in lymphoid tissues but also distributed in connective tissues, including the pulp (Sakurai et al., 1999). Their purpose is engulfing proteins and presenting the peptide fragments for T cells to recognise prior to their activation with the majority of the cells co-expressing coagulation factor XIIIa, a marker for antigen-presenting cells of the dermis (Okiji et al., 1997). They are particularly prevalent in the periphery of the pulp, in and

subjacent to the odontoblast layer where their processes sometimes extend into the dentinal tubules (Sakurai et al., 1999). They are also found in the perivascular area arranged parallel to the endothelial cells (Okiji et al., 1997).

1.7.5 Lymphocytes

T lymphocytes are a normal finding in human dental pulp (Hahn et al., 1989) with $CD8^{+}$T (suppressor) lymphocytes outnumbering the $CD4^{+}$T cells subset. During tooth decay, the induction of the cellular immunoresponse is started by T lineage cells and as the lesion progresses this humoral immunoresponse is bolstered by B lineage cells and is accompanied by pulp tissue destruction as a result of the release of proteolytic enzymes by infiltrating macrophages and neutrophils (Izumi et al., 1995). The presence of human immunodeficiency virus (HIV) has also been reported in human dental pulp tissue (Glick et al., 1989). B-lymphocytes and plasma cells are rarely found in the normal human pulp but have been observed in the pulps of impacted teeth (Langeland and Langeland, 1965).

1.7.6 Mast cells

Distributed widely in connective tissues, mast cells are seldom found in the dental pulp although they are a common finding in chronically inflamed pulps (Sakurai et al., 1999).

1.7.7 Dental pulp stem cells

Modern dental pulp cell biology dates from the work originally done by Stanley (Stanley, 1962) and the subsequent culture methods (Pomerat and Contino, 1965) which regarded them as fibroblasts (Kawashima, 2012) along with them being a candidate source for regenerated odontoblasts (Fitzgerald, 1979). Other investigators have also thought them capable of differentiation into odontoblasts (Yamamura, 1985).

The identification of a postnatal mesenchymal stem cell population of dental pulp stem cells (DPSCs) has been a more recent occurrence (Gronthos et al., 2000) and corresponds with the identification of stem cell populations in other tissues (Gronthos et al., 2002). Predominantly neural crest derived cells, they express some of the genes found in embryonic stem cells but don't express mesodermal genes (Dimitrova-Nakov et al., 2014) and despite their obvious existence their precise origin is still uncertain (Dimitrova-Nakov et al., 2014). DPSCs have been compared to other stem cell populations such as bone marrow stem cells (BMSCs) which are the most studied stem cell type and although there are similarities, they express different panels of surface markers from those characteristic of haematopoietic stem cells from bone marrow (Huang et al., 2010) and have never been shown to aid haematopoiesis in transplantation assay experiments (Gronthos et al., 2002). DPSCs are able to regenerate tissues closely resembling the dentine-pulp complex, made up of a mineralised tubule-like matrix aligned with odontoblasts and with a fibrous tissue component containing vasculature similar to that of human teeth (Gronthos et al., 2002). The precise percentage of pulp cells which are definitively stem cells is a

subject of contention but most authors put the number as less than 1% of the total population with an age variation of 0.4% diminishing to 0.1% when comparing young and old rats (Kenmotsu et al., 2010). The multipotency of DPSCs and their ability to exhibit osteoblastic, neuronal and adipogenic differentiation shows them to be different to the pulpal fibroblasts which exhibit monopotency by only being able to differentiate into odontoblasts (Kawashima, 2012).

1.8 Function of the dental pulp

The dental pulp is responsible for several functions. Ironically, a tooth can function perfectly well without one (Yu and Abbott, 2007) as the supply of blood and nutrients to the apparatus of attachment (i.e. the periodontal ligament and the tooth cementum) is unaffected by the pulps' absence. However, the pulp renders a tooth less liable to bacterial ingress as a tooth with a healthy pulp is much more able to resist bacterial invasion than one without (Nagaoka et al., 1995). The dentinal tubules are occupied by the odontoblast processes and pressurised fluid which can in concert act like a positively charged hydrogel (Linden et al., 1995, Vongsavan and Matthews, 1992). The positive outward flow of the dentinal fluid provides an important barrier against the rate at which noxious substances can diffuse into dentinal tubules (Matthews et al., 1996, Vongsavan and Matthews, 1992). Antibodies and other antimicrobial agents can also be present in dentinal fluid as a response to bacterial stimuli (Trowbridge and Kim, 1998). Immune complex build up and the precipitation of higher molecular weight proteins e.g. fibrinogen, carried in the dentinal fluid can

reduce the functional radius of a tubule and slow down the rate and volume of fluid shift potentially reducing dentine permeability and sensitivity (Pashley et al., 1984). Pulp has the cellular constituents necessary to recognise and process antigens, leading to its ability to mount an immune response reaction (Jontell et al., 1988). The major immune cells in a healthy pulp are peripheral T cells of the cytotoxic/suppressor and the helper/inducer types, while the main antigen presenting cells in a healthy pulp are the dendritic cells which are located mainly in association with the odontoblastic layer (Okiji et al., 1997). Pulp also has sensory functions with its sensitivity to differing thermal and osmotic stimuli being obvious (Holland, 1994), in fact regardless of the stimulus whether it be mechanical deformation, thermal or pulp trauma, pulp interprets them all as pain (Yu and Abbott, 2007). Dental pulp tissue contains both autonomic and sensory nerves, enabling it to carry out its defensive and vasomotor roles (Avery et al., 1980, Heyeraas et al., 1993, Inoue et al., 1994, Okamura et al., 1995, Pohto and Antila, 1972). Numerous theories abound regarding the exact mechanism of dental pain transmission such as odontoblastic transduction, dentine innervation and the hydrodynamic theory, with the hydrodynamic theory being the most popular (Matthews and Vongsavan, 1994, West et al., 2013).

Odontoblasts are a cell unique to the dental pulp and are end-differentiated post mitotic cells (Kim and Simmer, 2007) responsible for the deposition of dentine in its various forms throughout the lifespan of a tooth (Yu and Abbott, 2007). The cell resides in the periphery of the pulp at the predentine margin with its process extending into the dentine matrix, possibly all the way to the amelo-dentinal junction (Grossman and Austin, 1983, Holland, 1985, Kelley et al., 1981, Sigal et

al., 1984(a), Sigal et al., 1984(b), Yamada et al., 1983), although other authors dispute this, claiming that it is limited to the inner third (Byers and Sugaya, 1995, Garberoglio and Brannstrom, 1976, Narhi, 1985, Thomas, 1979, Weber and Zaki, 1986). Odontoblasts are also implicated in sensory transduction (Matthews et al., 1996) with the presence of adhering, tight and gap junctions inferring cell to cell communication, with the gap junctions also existing between nerve fibres and odontoblasts (Matthews and Holland, 1975, Sasaki and Garant, 1996). The O_2 uptake of odontoblasts is high with its uptake being significantly higher in the periphery of bovine dental pulps (Fisher, 1967) and the O_2 consumption of rat odontoblasts has been shown to be 3.2 mL of O_2/minute/100grams of tissue, a rate comparable to that of the brain (Chien, 1987). Transmission electron microscope studies have shown that odontoblasts are particularly sensitive to ischaemia (Chen, 1987) and an electron microscope study has shown ultrastructural changes including mitochondrial swelling, chromatin clumping and irregular nuclear membrane in odontoblasts (Torabinejad et al., 1993).

The pulpal circulation's purpose is to provide nutrients and oxygen to its constituent cells and is defined as a microcirculation and given the physical constraints it operates under careful regulation of blood flow is important with alterations in the pulpal microcirculation occurring early during pulpal inflammation (Baumgardner et al., 1996, Kim, 1985). As previously stated, the blood flow in the dental pulp of a mature tooth is comparable to that in the brain and can be in the region of 40-50 mL/minute/10 grams of tissue as estimated using radioactive microsphere techniques (Kim, 1985, Meyer, 1993, Path and Meyer, 1977). Furthermore, one

study has shown pulp vessels in monkeys to be unaffected by atherosclerosis (Krell et al., 1994).

1.9 Historic dental treatment and the current status of endodontics

Human teeth have been the subject of restorative attempts since prehistory, with evidence of prepared cavities being found in teeth from what is now Pakistan dated to between 8,000 to 9,000 years ago (Cohen, 2001). There is also evidence that prehistoric man may have used beeswax as a filling material after a mandible found in what is now modern Slovenia was found to have had a cracked left mandibular canine filled with the material (Barras, 2012). Coming more up to date, prostheses from Etruscan tombs from between the sixth and fourth century B.C. are common archaeological findings and prostheses from Roman cemeteries have been recovered dated from around the first to second century A.D. (Minozzi et al., 2007) that were found to have used gold wire to retain lost or replacement teeth.

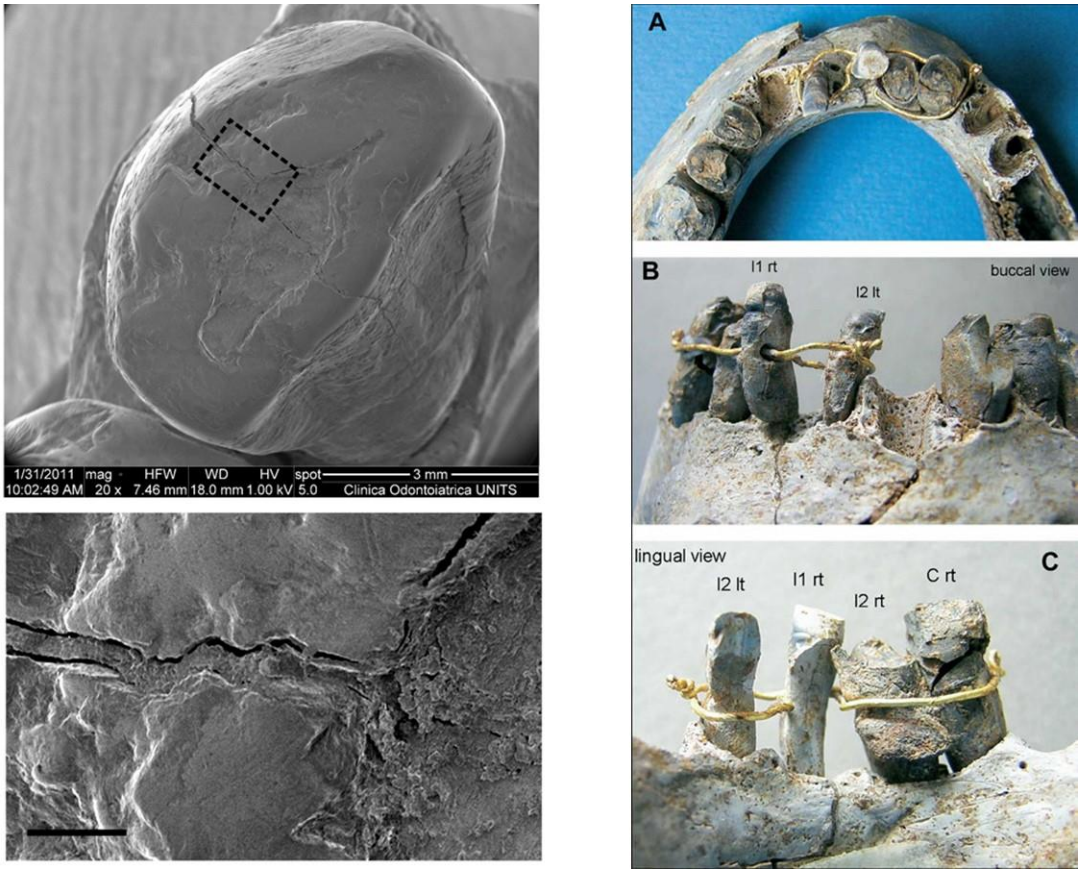

Figure 9. Scanning electron microscope image of a tooth with beeswax filling (left) and Roman prosthodontics (right).

Tooth filled with beeswax (left image, courtesy of New Scientist magazine) and Roman dental prosthesis (right image, courtesy of Dr. Franchesco Coschino, University of Pisa, Italy).

The practice of Endodontics has been attempted for at least two millennia with the oldest bona fide root canal filling being a piece of copper wire, discovered inside the upper right lateral incisor found in the excavated skull of a Nabatean warrior dating from around 200 BC, the tooth having been X-rayed out of curiosity to see why it was green. This root filling came from a time when the prevailing theory of the cause of tooth diseases was that of a worm burrowing inside the tooth (Zias and Numeroff, 1987). Earlier than this, the Chinese had also subscribed to the worm theory of dental caries and an inscription excavated from the 14th century BC (Ying

Dynasty) shows a character clearly designed and intended to mean dental caries, by combining the two characters for worm and tooth.

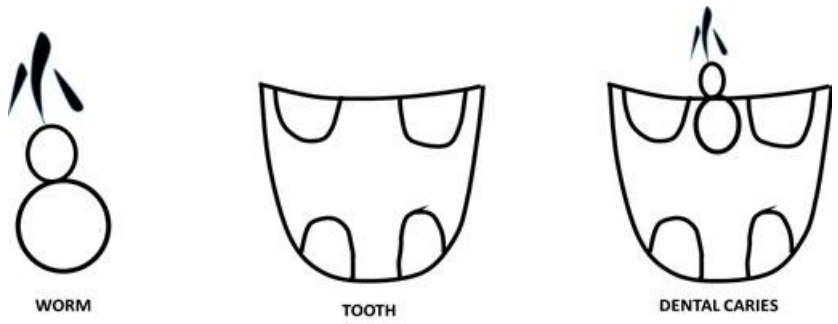

Figure 10. Ancient Chinese characters for worm, tooth and tooth decay. Adapted from Tsai-Fang 1984.

Some fifteen hundred years later, arsenicals were being used by the Chinese to treat pulpitis, some sixteen hundred years before their first use by Europeans and they were also using an amalgam-like material to restore cavities in teeth circa 659 AD (Tsai-Fang, 1984).

The traditional and still current method of rectifying a badly diseased, painful or necrotic pulp is either by tooth extraction or endodontic treatment i.e. pulp removal, followed by instrumentation and the use of medicaments to clean and disinfect the root canal, then obturation of the resulting space using gutta percha cones or points, with a sealing cement followed by definitive restoration such as a crown.

Although endodontic success is high in the hands of a skilled practitioner (West, 2006), the procedure can be technically difficult with the potential at every stage for something to go wrong, with some clinical textbooks even devoting chapters to

‘Procedural Accidents’ (Holland and Torabinejad, 2009). Even after successful endodontic therapy, the tooth remains liable to fracture and reinfection (Goto et al., 2009, Torabinejad and Lemon, 2009).

Teeth in which the dental pulp has become necrotic and consequently non-vital, through whatever process, traditionally suffer one of three fates:

1). They are left untreated because they are symptomless.

2) They are extracted when they eventually initiate pain and sepsis.

3). They undergo endodontic (i.e. root canal) treatment in order that the tooth be retained as a functioning masticatory unit within the oral cavity (Yu and Abbott, 2007).

For several reasons i.e. what the patient desires, operator technical ability or expertise and technical reasons such as ease of access or compromised anatomy, 2 often follows on from 3, despite the best intentions and efforts of the Dental Surgeon.

Orthograde endodontics is usually described as “root canal filling” by conventional methods i.e. sealing the canal hermetically from the inner ends of the dentinal tubules and completely filling and sealing the canal from there, to the floor of the root chamber (Blaney, 1928, Orban, 1930).

The techniques for this have been more accurately expounded as:

1) The isolation of the appropriate tooth,

2.) The removal of organic and inorganic debris from the root canal system and the elimination of any bacteria,

3). Shaping and filling of the resultant non-vital tooth with the appropriate obturation materials to form a hermetic three-dimensional seal (Schilder, 1967).

Endodontic surgery, an extension of these techniques, and usually carried out when conventional therapies have failed, has been considered part of the remit of oral surgery but is now considered to be within the field of specialist endodontics in accordance with the regulations of the American Association of Endodontists (Endodontists., 1994).

More recently, the scope of endodontics has broadened to encompass procedures designed to safeguard and maintain the health of all or part of the dental pulp. This has evolved gradually with the recognition that the pulp has definite powers of recuperation and recovery given the appropriate circumstances and supportive therapy. Procedures such as pulpotomy and pulp capping (Cvek, 1978) are now commonplace. Hence, the aim now when a pulp is diseased or injured is to preserve as much of the normal healthy pulpal tissue as can be retained, wherever possible.

Historically, it could be argued that modern endodontics began with the gold foil capping of cariously exposed pulps by Pfaff about two hundred and fifty years ago (Dammaschke, 2008). It is likely this treatment, or something similar, had been widespread previously before being rediscovered, as there is evidence of attempted endodontic work in countries around the Mediterranean and Middle East (Zias and Numeroff, 1987).

Figure 11. Images of Dental Treatment from Antiquity.
Hesi-Re (left) "Chief of the Toothers". Unknown Arab dentist (right).
Internet images from public domain.

The conventional methods of root canal therapy have been around for decades and a wide variety of materials have been tried including asbestos, silk, cotton, wool, paper, fiddle string in creosote, orange wood dipped in phenol, gold thread, copper thread, ivory cones, beeswax and numerous others (Gethro, 1919).

There is evidence that Asa Hill (1847) developed the first gutta percha root canal filling material, known as "Hill's Stopping" which was composed of powdered quartz, carbonate of lime and bleached gutta-percha and patented it the following year (Thorpe., 1909), thus heralding the beginning of gutta-percha as an endodontic filling material although in some instances it was only placed over the canal orifice and not within the canal (Grossman, 1976). Later in 1867, G. A. Bowman, a St. Louis dentist was attested to have used gutta-percha points to pack root canals (Grossman, 1976) and gutta-percha points began to be marketed to the dental profession in 1887 by S.S. White Co. (Keane, 1944).

Silver points became available in the 1930s but have increasingly fallen out of favour after it was demonstrated that it was virtually impossible to produce round canals to match the diameter of the silver points (Schneider, 1971) and round apical

root canal orifices are only found in a certain percentage of root canals, with other canal orifice shapes being defined as oval, asymmetric, semilunar, hour glass-shaped and serrated (Green, 1956). It was further observed that silver points corrode in the root canal, resulting in toxic corrosion products and leakage (Brady and del Rio, 1975).

Currently, the material most widely used for root canal obturation is gutta percha, a naturally occurring form of rubber (either cis, or trans-polyisoprene), along with sealing cement, or a softening agent, depending on the technique being employed (Goodman et al., 1974). It is generally accepted not to be the perfect material for this purpose as it doesn't fulfil the three main criteria of the ideal endodontic filler namely: entomb any bacteria remaining within the root canal system; prevent the influx of any serum or bodily fluids back into the root canal system to nourish the aforementioned bacteria and prevent coronal leakage of bacteria into the root canal system (Hovland and Dumsha, 1985), but the least bad of those available, as ultimately any material will eventually leak to some degree and can potentially reinfect (Ainley, 1970). Chemically pure gutta percha exists in two different crystalline forms, alpha and beta. These are interchangeable depending on the temperature of the material with both the alpha and beta forms used clinically, usually mixed with other materials such as zinc oxide to produce a material which can be readily used within the root canal.

1). Although the claimed success rates for endodontic treatment can reach as high as 97% after an eight-year period there are still drawbacks in what might appear to be an otherwise successful therapy (Freire and Archegas, 2010, Salehrabi and Rotstein, 2004, Sedgley and Messer, 1992).

2). Endodontically treated teeth often discolour and darken

3). They are more brittle and prone to fracture, especially in the molar region where occlusal forces are higher

4). The increased brittleness requires more extensive restorative procedures in order to 'protect' the tooth leading to further tooth substance loss.

5). Any decay which occurs progresses much more rapidly than in a vital tooth.

6). Removal of dentine bulk can weaken the tooth.

7). Endodontically treated teeth with post-retained restorations have less bone supporting them.

8). Insertion of post-retained restorations can act like a wedge, splitting the tooth during masticatory function.

9). Because of the lack of tissue pressure and immune response, endodontically treated teeth can re-infect and cause abscess formation.

10). If unsuccessful, revision endodontics or further surgery such as apicectomy may be necessary.

In short, the present 'gold standard' root filling materials impart few if any of the tooth's physiological requirements and a new, replacement, tissue engineered dental pulp would be a much better therapeutic option (Aptekar and Ginnan, 2006, Eliasson et al., 1995, Murray et al., 2007).

1.10 Dental pulp tissue engineering

The first usage of the term 'Tissue Engineering' in its current context as opposed to its previous usage to describe prosthetic devices and surgical manipulation of tissues was in an article entitled 'Functional Organ Replacement: The New Technology of Tissue Engineering', published in Surgical Technology International in 1991 (Vacanti, 2006). The first publication to broadly describe the technology behind tissue engineering (in its current usage) was published earlier in 1988 (Vacanti, 2006).

There are many definitions of the term Tissue Engineering, for example 'an interdisciplinary field applying the principles of engineering and life sciences toward the development of biological substitutes that restore, maintain or improve tissue function' (Langer and Vacanti, 1993). Others have defined it as 'understanding the principles of tissue growth and applying this to produce functional replacement tissue for clinical use' (MacArthur, 2005) and it has further been defined as 'the employment of biologic therapeutic strategies aimed at the replacement, repair, maintenance and/or enhancement of tissue function (Murray et al., 2007). Not to be outdone, it has also been described as 'the application of principles and methods of life sciences and engineering combining towards the fundamental understanding of structural and functional relationships found in normal and pathological mammalian tissues and the development of biological substitutes to restore, maintain or improve tissue function' (Shalak, 1988). This has been further expanded as the application of scientific engineering principles to the design, construction, modification, growth and maintenance of living tissue and organs from native or synthetic sources for the

human body to restore function based on principles of molecular developmental biology, cell biology and biomaterial sciences (Boyan et al., 1999). Overall, the goal of tissue engineering is to surpass the limitations of conventional treatments based on organ transplantation and biomaterial implantation (Langer and Vacanti, 1993) and its basic premise is that the repair and regeneration of biologic tissues can be guided through application and control of cells, materials, and the microenvironment into which these cells are delivered (Vacanti and Vacanti, 2000). The normal protocols of tissue engineering require cells, a scaffold for them to attach to, morphogenetic cues and/or growth factors along with nutrients in order to recapitulate the developmental events which served to grow the tissue or organ *ab origine* (Chan and Leong, 2008, Murphy et al., 2013, O'Brien, 2011).

One other avenue of investigation could be gene therapy to convey genes for morphogens/growth factors, transcription factors and extracellular matrix molecules on a local level to somatic cells, with a therapeutic effect. Theoretically, the gene conveyed can stimulate or induce the desired natural biological process by expressing the necessary molecules involved in a regenerative response for the desired tissue (Bonadio et al., 1999). Either viral or non-viral vectors are used for the gene uptake and expression. Presently, adenoviral, retroviral, herpes simplex virus and lentivirus are being developed to eliminate their disease potential for therapeutic gene transference (Jullig et al., 2004, Naldini et al., 1996). Non-viral systems include electroporation, sonoporation, deoxyribonucleic acid (DNA) -ligand complex and gene gun applications to address the safety concerns associated with the viral methods. Most risk from gene therapy seems to arise from the vector used rather than the gene expressed (Jullig et al., 2004). Consequently, widespread

clinical application is unlikely until safe, affordable, simple and efficient vectors are available which can express the required level of transgene for an adequate length of time (Parikh, 2004).

1.11 The model for dental pulp regeneration in nature

In nature there already exists a well-studied model for dental pulp regeneration and the commonest 'naturally-occurring' human model for pulp regeneration occurs when upper incisor teeth are either avulsed or subluxed out of their sockets during facial trauma and then replaced. It has been shown (Kling et al., 1986) that there are several factors that need to be taken in to account for the successful revascularisation of teeth after reimplantation.

1) Time the tooth has spent out of the socket.
2) Interim storage conditions.
3) The state of maturity of the tooth i.e. the width of the apical foramen and the apical-coronal length of the pulp.

Andreasen and Andreasen (Andreasen, 1994) reported that "The relationship between the diameter of the apical foramen and the chance of pulpal revascularisation apparently is an expression of the size of the contact area at the pulpo-dental interface….whereas the length of the root canal probably reflects the time necessary to repopulate the ischaemic pulp. With a favourable ratio (i.e. a broad apical foramen and short canal as opposed to a narrow apical foramen and a long

root canal), the odds for an intervening pulpal infection are reduced. A limiting factor in pulpal revascularisation appears to be an apical diameter of less than 1mm". Thus it would appear that any method of tissue engineering a new dental pulp could require an apical opening of 1mm or greater. However, this could also be described as a simplistic view as most reimplantation studies are done on young or adolescent children who are still growing and have a much better healing response potential. Alternatively, it might also be argued that in a mature adult, the amount of materials and nutrients necessary for a purely soft tissue pulp - as opposed to one which is still involved in laying down large amounts of dentine, root formation and pulp tissue formation - wouldn't be as great, so this might be the more advantageous situation. Other individual case histories support the younger patient. In one case (Iwaya et al., 2001) the 13-year-old female patient had a lower premolar tooth with an open apex and a draining sinus which, following the appropriate washing out of necrotic tissue, double antibiotic therapy and sealing of the access cavity, continued to grow and complete apexification. In another case, an 11-year-old boy with a tooth similar to the above had a similarly successful outcome using a slightly different treatment protocol where the immature apex of the tooth was instrumented to make it bleed in a controlled fashion back up the root canal. The tooth was then sealed with MTA and a temporary dressing, followed by a definitive bonded composite resin restoration two weeks later (Banchs and Trope, 2004). In the former case, there does appear to be radiographic evidence in the article that the pulp space was continuing to calcify and sclerose following the successful apexification of the tooth, which could suggest that any remaining pulp tissue and blood clot which in effect became the scaffold for the soft tissue ingrowth, initiated a repair process as opposed

to a regeneration process following the application of calcium hydroxide to the remaining pulp tissue and that conventional endodontics might be necessary to retain the tooth for the future. When comparing the above two protocols (apexification cf. revascularisation) revascularisation has been shown to increase radicular reinforcement and root length extension (Diogenes et al., 2013) when compared with teeth treated via the apexification protocol using $CaOH_2$ (Jeeruphan et al., 2012, Moreno-Hidalgo et al., 2014).

1.12 Requirements for dental pulp tissue engineering

The dental pulp has recognised, definite powers of repair and regeneration (Nakashima, 1994) and the bridge of reparative dentine produced is biologically superior to any restorative material yet available (Smith and Lesot, 2001). As with any projected tissue engineering construct, any regenerated pulp will need stem cells, morphogens and a scaffold for the cells to attach and differentiate upon into functional tissue (Demarco et al., 2011).

1.12.1 Cells

DPSCs can self-renew and have multi-lineage capacity *in vitro* and it has been suggested that DPSCs are closely associated with pulpal blood vessels, especially pericytes and smooth muscle cells (Shi and Gronthos, 2003). The demonstration of specific markers in DPSC differentiation pathways is still uncertain, as there is as

yet no single definitive marker for odontoblasts or DPSCs. Also, DPSCs would be available in a partially-vital pulp, but would be absent in a completely non-vital pulp, so it is possible that other cells e.g. from the gingival tissues or periodontal ligament cells might have to be used as source cells to regrow a new pulp into an empty pulp canal and chamber system (Rutherford and Gu, 2000). However, DPSCs are capable of long-term cryopreservation and retain their capability to differentiate and their differentiated cytotypes proliferate, produce woven bone tissue and express all their respective surface antigens, confirming cellular integrity (Papaccio et al., 2006).

1.12.2 Scaffold

Following pulp capping with calcium hydroxide, pulp cells eventually adhere to an osteodentine layer before differentiation into odontoblasts (Schroder, 1985). Other studies (Anneroth and Bang, 1972, Nakashima, 1990, Nakashima, 1994, Tziafas and Kolokuris, 1990) suggest that there is a requirement for an appropriate physicochemical surface for odontoblast differentiation. The mechanisms involved in this are still unclear (Nakashima and Reddi, 2003). Fibronectin plays a role in the interactions between ECM and cells to reorganise the cytoskeleton of the polarising odontoblasts overall pulpal wound healing process and also facilitates the binding of signalling molecules. Collagen facilitates arrangement of preodontoblasts and binds newly matured odontoblasts to pulp tissue, thereby supporting a reparative dentinogenesis network (Kitasako et al., 2002). Synthetic extracellular matrix may also be a likely scaffold candidate for reparative dentinogenesis and pulp

regeneration (Bohl et al., 1998). Mineral trioxide aggregate (MTA) – a well-established pulp capping agent - while unlikely to be a scaffold in its present form, is likely to be a good 'lid' to seal any access cavity into the tooth and also to promote odontoblast differentiation and reparative dentine formation on the surface of any regenerated dental pulp (Torabinejad and Chivian, 1999), as would Biodentine, a combination of tri and dicalcium silicate, calcium carbonate and oxide filler, iron oxide shade and zirconium oxide (Malkondu et al., 2014). Previous animal studies have shown that high molecular weight HyA can be used to facilitate reparative dentine formation in amputated rat molar pulps (Sasaki and Kawamata-Kido, 1995).

1.12.3 Morphogens

Morphogens produce inductive signals which function as growth and differentiation factors in odontoblast differentiation. Originally isolated from demineralised bone matrix, bone morphogenic proteins (BMPs) (Urist, 1965) such as BMP2 can have various effects on pulp cells, e.g. adult pulp cells are stimulated to differentiate into odontoblasts in monolayer cultures under the influence of recombinant human BMP2 (Nakashima, 1994, Saito et al., 2004) and also in three dimensional pellet cultures (Iohara et al., 2004). Millipore filters with human TGFβ implanted intrapulpally induced odontoblast differentiation and reparative dentine formation in close proximity to the implants (Tziafas et al., 1998) showing the efficacy of this morphogen for odontoblast differentiation in the pulp (Tziafas, 2004). It is not yet clear what controls the abrupt transition of stem and progenitor cells from quiescent to active state regarding differentiation, proliferation, migration and matrix secretion

as the sequelae of pulp tissue injury and the molecular mechanisms of control for morphogen release require further elucidation to be useful in regenerative endodontics.

1.12.4 Vascular regeneration

The dental pulp vascular system is vital for nutrient supply and removal of waste metabolites. Its contribution to any pulp regeneration would be immense as the importance of vasculature to any tissue repair and regeneration is well known. Vascular endothelial growth factor (VEGF) is a regulator of angiogenesis and increases vascular permeability. It also induces chemotaxis, proliferation and differentiation of dental pulp cells (Artese et al., 2002, Matsushita et al., 2000) and is present in dentine matrix (Roberts-Clark and Smith, 2000). VEGF's presence in dentine suggests there might be endothelial progenitor cells in the pulp tissue alongside the progenitors for neuronal cells and odontoblasts (Gronthos et al., 2002) and it is likely that VEGF and vascular endothelial cells are crucial for dentine regeneration.

1.12.5 Neural regeneration

Firstly, we must remember that were predictable peripheral sensory and motor nerve regeneration possible, spinal cord injuries involving severance would not result in their current sequelae. The rich innervation of the dental pulp includes both sensory and sympathetic nerves (see previous section on innervation). Their interactions, location and function with pulp tissue, vasculature and immune cells all differ

(Byers et al., 2003) and the cytochemical location of neurofilaments, NGF, GDNF and CGRP vary with the type of nerve fibre (Byers et al., 2003). Embryologically, the temporal sequence of pulp innervation depends on gradients of neurotrophic growth factors coming from the pulp cells. Dental pulp expresses NGF, BDNF and GDNF (Nosrat et al., 2004). As already stated, the pulpal innervation is crucial in the homeostasis of the dental pulp. Sensory nerves stimulate invasion of immune and inflammatory cells into sites of injury (Fristad, 1997). Sensory denervation gives rapid necrosis of any exposed pulp cells because of impaired blood flow and extravasation of immune cells (Byers and Taylor, 1993, Fristad, 1997, Holland et al., 2001, Olgart, 1996) and reinnervation leads to recovery in coronal dentine, which Schwann cells seem to play a role in by releasing neurotrophic growth factors and in recruiting sensory and sympathetic nerves during the process. Some members of the BMP family also have effects on neurogenesis (Mabie et al., 1999) possibly enabling them to have a dual role in pulp regeneration. There is also the intriguing possibility that nerve tissue may not be a requirement for functional pulp regeneration, as there is at least one claimed example of mammalian dental pulp tissue which doesn't contain nerve tissue (Fagan et al., 1999) although this has been contradicted by later investigators (Boy and Steenkamp, 2004).

1.13 Dental pulp tissue engineering: Current Status

At present, there is keen interest in the development of a protocol for the tissue engineering of a dental pulp, primarily to encourage better formation of a calcific barrier in the case of cariously or traumatically exposed dental pulps (Hermann, 1952), in the case of immature apex formation to develop apical closure (Damle et al., 2012) or completion of root formation (Diogenes et al., 2013). To this end, there have been numerous studies, usually involving the application of BMPs (Nakashima, 1994) onto exposed pulp tissue and investigation of the resultant calcific barrier. The success of these procedures was probably just as equally attributable to the germ-free conditions as the technique. This had been shown much earlier in tests which showed that any pulp capping material would give rise to a calcific barrier if used in germ-free conditions (Paterson, 1976) and also using no material whatsoever would still give rise to a calcific barrier in germ-free conditions (Kakehashi et al., 1965). However, in another study, exposed dental pulps that had been treated with a bacterial lipopolysaccharide were able to develop little or no reparative dentinogenesis (Rutherford and Gu, 2000). This would potentially seriously limit the clinical applications of BMPs and patient usefulness as most pulp exposures are as a result of involvement with caries with all the concomitant bacterial infection, inflammatory sequelae and resultant complications, often with the added complication of salivary contamination. Currently, there is no uniform protocol for these studies but many investigators use the tooth slice model in immunodeficient rodents as it has a proven track record of success and enables investigators to control desired parameters such as cell types, scaffolds and

morphogens with others using the canine model (Goncalves et al., 2007, Magloire et al., 1996, Mullane et al., 2008, Sakai et al., 2011, Sakai et al., 2010, Sloan et al., 1998, Nakashima and Iohara, 2014).

1.14 Potential clinical problems in dental pulp tissue engineering

Bacterial invasion and colonisation of a devitalised tooth and how to prevent it is a continual complication for all clinicians and patients. One study (Nagaoka et al., 1995) compared the rates of bacterial ingress along dentinal tubules in cervical cavities prepared in vital and non-vital teeth at 30 and 150 days and found that there was a significant difference in the bacterial invasion rate between the two groups of teeth, with the non-vital teeth having much higher levels of bacterial infiltration along the dentinal tubules. This would suggest that any pulpal regeneration would have a finite time to become established, or at least give rise to a positive pulpal pressure, before becoming infected from bacterial ingress along the dentinal tubules of the coronal and radicular sections of the root canal. There would also be the necessity for a good coronal seal preventing leakage as this has a bearing on the success of conventional endodontics (Ray and Trope, 1995) although other authors have elucidated several other factors to be taken into consideration when assessing the success or failure of endodontic treatment (Ng et al., 2011). There is potential, however, to perhaps at least partially negate these effects by inclusion of antimicrobials to diffuse along the tubules far enough to halt or slow down bacterial ingress until any new pulp graft becomes established and this has been successful in

the past (Banchs and Trope, 2004) although antimicrobial levels sufficient to inhibit bacterial ingress may have deleterious effects on new pulp cell growth.

As discussed above, the ideal three-dimensional scaffold has yet to be established and while some researchers have used ground substance components in experimentation (Ferroni et al., 2015, Smith et al., 2015) no one has yet fully expounded its role and relative importance in embryonic pulp development and growth.

The main problem however, would be the re-establishment of a new blood supply into the nascent pulp tissue as no cells would be able to survive without one and it is unlikely that a normal sized mature apical foramen would be large enough to accommodate a blood vessel of sufficient diameter to supply a growing pulp. The likely adopted method to enlarge an apical foramen would be patency filing (Buchanan, 1989) which is to this day a contentious area of both endodontology thought and practice, totally contradicting many areas of teaching and clinical practice promoted by both teachers and practitioners. Addressing the issue of blood vessel construction, since the production of the first tissue engineered blood vessel (Weinberg and Bell, 1986) improvements in static patency (L'heureux et al., 1997), vessel wall thickness, improved suture retention, physiological smooth muscle cell density and patency achieved in pulsed growth conditions (Niklason, 1999) and grafts have all been grown in the recipient's own peritoneal cavity (Campbell et al., 1999). However, the replication of small diameter blood vessels of < 6mm still eludes researchers (Sarkar et al., 2005) and this is still vastly larger than the size of those required for the dental pulp, so not only access to the regenerating pulp would be impossible, the diffusion of nutrients and O_2 limits the distance from blood

vessels to a 500 μm maximum (Sachlos and Czernuszka, 2003) although later studies have made progress in the field of *in vitro* capillary matrices (Montano et al., 2010). Until this most fundamental aspect of regeneration is solved, perhaps by the combined use of proteins more often found in higher levels in the foetus as a microscaffold used down to the nanotopographical level and VEGF, encapsulated in microbead delivery vessels, the risk of necrosis in the centre of any newly grown pulp would be high.

Endodontic treatment of teeth is ripe for change away from a therapeutic protocol and train of thought allied to materials and techniques available and originating in the 19th Century and gradually modified since, in an attempt to alleviate any inherent shortcomings. Tissue Engineering is the logical future pathway to explore and Endodontic regeneration the logical method by which to achieve the re-establishment of a vital living tissue inside a previously wholly or partly devitalised tooth, mimicking what can occur spontaneously when an immature incisor for example, suffers trauma such as sub-luxation and re-establishes vital pulp tissue, continuing root formation and apexification, and there have and continue to be strong calls from Academia to that effect (Murray et al., 2007).

1.15 Angiogenic markers

Cell surface markers of angiogenesis provide useful tools with which to characterise cell populations when investigating tissue engineered constructs where angiogenesis is an important end result. CD 31 and CD34 were chosen because of their conservation between different species, enabling them to be easily accessible for immunohistochemistry purposes and also as they are early markers of angiogenesis, again across most species.

1.15.1 CD31 Angiogenic marker

Cluster of Differentiation 31 (CD31, also known as platelet endothelial cell adhesion molecule-1, or PECAM-1) is a 130-kDa transmembranous glycoprotein and a member of the immunoglobulin (Ig) superfamily. It comprises of six extracellular Ig domains, a cytoplasmic domain and a transmembrane domain (Newman, 1997). CD31 has been shown to contain intracytoplasmic immunoreceptor tyrosine inhibitory motifs (ITIMS), which, following phosphorylation, are able to mediate an inhibitory function via recruitment and activation of protein-tyrosine phosphatases (PTPs), mainly Src homology region 2 domain containing phosphatase 1 (SHP-1) and SHP-2, which are crucial for T cell response (Hua et al., 1998, Jackson et al., 1997, Lorenz, 2009). CD31 is found expressed in leukocytes, monocytes, neutrophils, macrophages (Pusztaszeri et al., 2006), concentrated at the lateral junctions of endothelial cells and obviously, platelets. It was firstly identified as a cell to cell adhesion molecule which mediated cellular adhesion through self-association (Pinter et al., 1997). As a bioactive molecule, CD31 has been shown to

be involved in numerous biological processes such as platelet aggregation and homeostasis, thrombosis, maintenance of the vascular endothelial barrier function, mechanosensing of endothelial cell response to fluid shear stress (Woodfin et al., 2007), leucocyte migration during the inflammatory response to sites of injury and bacterial ingress and development of the vasculature (DeLisser et al., 1997, Ferrero et al., 1995, Thompson et al., 2001). As such, CD31 has been described as more than a marker for endothelial cells (Liu and Shi, 2012).

CD31 has been shown to have an important role in the inhibition of tumour-induced angiogenesis by the use of anti-CD31 antibodies in several animal models and it has been demonstrated that CD31 has a role in the cell to cell association of endothelial cells which is a prerequisite for endothelial tube formation which itself is a precursor to blood vessel formation (Cao et al., 2002, Pinter et al., 1997, Thompson et al., 2001).

1.15.2 CD34 Angiogenic marker

CD34 is a transmembrane glycoprotein initially identified on haematopoietic stem and progenitor cells (Civin et al., 1984), having a molecular weight of approximately 115 kDa with a heavily sialylated, O-linked glycosylated extracellular domain which also contains some N-linked glycosylated sites (Sidney et al., 2014). The commonest ligand for CD34 is L-selectin (or CD62L) but the adapter protein CrkL (Crk-like), a phosphorylated tyrosine, which is involved in adhesion regulation also binds to it (Baumheter et al., 1993, Felschow et al., 2001). It is found in many multipotent precursor cells of the haematopoietic system, hair follicle stem cells, mast cells, embryonic fibroblasts, eosinophils and vascular

endothelial cells (Brown et al., 1991, Fina et al., 1990, Nielsen and McNagny, 2008). The complete functionality of this molecule has not yet been fully elucidated, but amongst others, it has been reported to stimulate proliferation and block differentiation of progenitor cells and to enhance the migration and trafficking of haematopoietic cells (Nielsen and McNagny, 2008). It has been used for the isolation of haematopoietic stem and progenitor cells and as a marker to identify some tissue specific stem cell such as muscle satellite cells and epidermal cell precursors. Thus, it has been widely used both as a haematopoietic stem cell marker and a vascular endothelial cell marker (Fina et al., 1990, Hristov and Weber, 2008, Sato et al., 1999). Peripherally circulating $CD34^+$ cells have been examined for utilising in neovascularisation therapies (Mackie and Losordo, 2011) and can differentiate into osteoblasts (Tondreau et al., 2005) and cardiomyocytes (Zhang et al., 2004). There is also a subset of $CD34^+$, noncirculating adult endothelial cells predominantly found within smaller blood vessels, whereas the majority of endothelial cells in larger arteries and veins are $CD34^-$ (Fina et al., 1990). Endothelial cells typically have a 'cobblestone' morphology, whereas $CD34^+$ cells have a more pronounced elongated morphology and are lacking in tight junctions (Siemerink et al., 2012). Predominantly found on the luminal membrane of cellular processes, CD34 expression can also be detected on the abluminal membrane of cells situated at the tip of vascular sprouts (Fina et al., 1990, Schlingemann et al., 1990). Additionally, $CD34^+$ endothelial cells are quiescent and considered to be involved in adhesion and migration (Fina et al., 1990).

Human umbilical vein endothelial cells (HUVECs) are $CD34^+$ *in vivo* but after several passages of culture CD34 expression is lost and only a relatively small

population of $CD34^+$ cells are left (Fina et al., 1990). They have distinctive morphological characteristics such as numerous filopodia (Siemerink et al., 2012). Migration of these cells is started by angiogenic stimuli and it has been proposed that this $CD34^+$ subpopulation is analogous to sprouting tip cells which are a specialised type of endothelial cell found at the leading edge of *in vivo* angiogenesis (Siemerink et al., 2012). At sites of active angiogenesis, CD34 is strongly expressed on the filopodia of angiogenic tip cells showing the important functional role for CD34 in progenitor cell activity (Sidney et al., 2014).

Chapter 2: Aims and Objectives

The clinical need for a reliable, effective, Dental Surgeon user-friendly method of dental pulp regeneration that is also acceptable to patients is apparent from examining the literature (Murray et al., 2007). The hypothesis to be tested in this thesis is that constructs comprising of DPSCs together with a scaffold suited structurally and physiologically to that found in a dental pulp could be used to regenerate dental pulp-like tissue *in vitro* and *in vivo*. Such a scaffold would ideally comprise of a mixture of the main constituents of dental pulp, incorporating Types I and III collagen and HyA, which are already licenced for therapeutic use in humans and which can incorporate nutrients and if necessary, morphogens.

The overall aim of this work was to induce early angiogenic change in DPSCS *in vitro* and *in vivo* using a biomimetic approach based on combining scaffolds comprised of ECM components with human dental pulp stromal cells as a the first steps towards a tissue engineering strategy for pulp regeneration.

The specific objectives are summarised as follows:

- To determine whether DPSCs can be cultured on biomimetic scaffolds comprising of hyaluronic acid and Types I and III collagen (either singly or in combination) both *in vitro* and *in vivo*.
- To investigate if either hyaluronic acid or Types I and III collagen matrices used either singly or in combination can support/induce early angiogenic change in DPSCs both *in vitro* and *in vivo*.

Chapter 3: Materials and Methods

3.1 General Materials

Cell culture flasks, plates and other plastics were purchased from Corning (Amsterdam, Netherlands). Alpha-modified minimum essential medium (α-MEM), phosphate buffered saline solution (PBS) and foetal calf serum (FCS) were purchased from Lonza (Slough, U.K.). Antibiotics, enzymes, and other reagents were purchased from Sigma (Poole, U.K.). Growth factors and antibodies were purchased from AbCam (Cambridge, U.K.). Other laboratory supplies were obtained as indicated in the text.

DPSCs were isolated from teeth donated for research purposes immediately post-extraction in the Department of Oral Surgery, School of Dentistry, Leeds Dental Institute (LDI) with full written consent from the patient and appropriate ethical approval (LDI Research Tissue Bank: LREC 07/H1306/93; Tissue Bank reference number: 180808/HR/12) and in accordance with the Human Tissue Act. The age and sex of the patient were recorded along with the tooth notation wherever possible for record-keeping purposes but all teeth were anonymised prior to distribution to the researcher.

3.2 Harvesting of the dental pulp organ

Teeth obtained as described above from the Research Tissue Bank were predominantly unrestored upper and lower third molars which were being removed due to their causing cheek trauma and/or pericoronitis, or premolar teeth extracted for orthodontic purposes. The dental pulp organ was harvested in accordance with an established departmental protocol (El-Gendy et al., 2015) as follows. The teeth were transported to the tissue culture laboratory and placed in a sterile petri dish inside a laminar flow hood. Teeth were initially cleaned by scalpel to remove any gross debris such as calculus, obvious food and plaque deposits, blood clots and adherent soft tissues. The teeth were then washed 2 to 3 times with sterile 1x PBS to remove any remaining stubborn debris, sprayed externally with 70% ethanol which was allowed to evaporate, then picked up coronally by a gloved hand (after spraying the glove with 70% ethanol and allowing it to evaporate) between the thumb and the forefinger. The glove was then everted placing the tooth inside the thumb tip which was then wrapped in paper towel, taken to a workshop vice and crushed. After returning to the tissue culture hood and cutting off the thumb tip into a sterile petri dish, the pulp tissue was dissected out using a combination of scalpels, dental explorers and fine tweezers (see Figure 12). After this it was sectioned by scalpel for explant culture or collagenase digest.

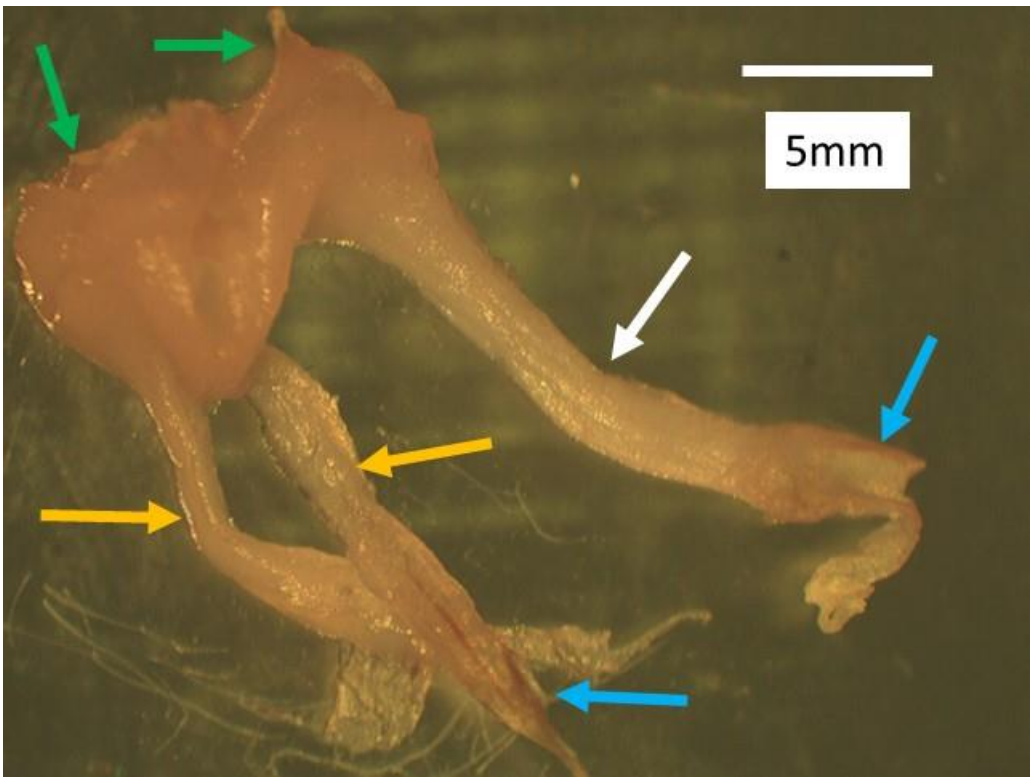

Figure 12. *In situ* image of a dissected dental pulp from a lower left first molar.

Image displaying an intact complete dissected dental pulp, with the entire dental pulp contents: coronal pulp and pulp horns (indicated by the green arrows), the distal root canal dental pulp (indicated by the white arrow) and the two mesial root canal dental pulps (mesio-buccal indicated by the left yellow arrow; mesio-lingual indicated by the right yellow arrow). The two blue coloured arrows indicate the apical blood vessels. The other scuff marks on the dish surface (bottom left) were caused by instruments during dissection and positioning of the sample during image taking.

3.3 Isolation of DPSCs via the pulp explant method

Following the above initial dissection process, the pulp was then transferred into a sterile petri dish and segmented, usually into six pieces comprising of the upper coronal pulp, the lower coronal pulp, the coronal section of the root-canal pulp, the radicular root-canal pulp, the apical root-canal pulp and any extraneous pulpal soft tissue such as the dental papilla beyond the tooth root which came with the tooth during extraction of teeth with open apices (see Figure 14). These sections of pulp were cultured in either a 6 well plate or T25 flasks with αMEM/10% FCS at 37°C in 5% CO_2/air until outgrowth of cells from the explants became observable. If no outgrowth of cells was visible after three weeks, or if the pulp tissue sample had failed to attach to the plate or flask, the sample was discarded. The cells were passaged at 80% confluence until passage 3 then either used for experimentation or frozen for future use. For alkaline phosphatase (ALP) staining, the explant samples were fixed in 98% ethanol overnight prior to use (see Appendix A for complete protocol).

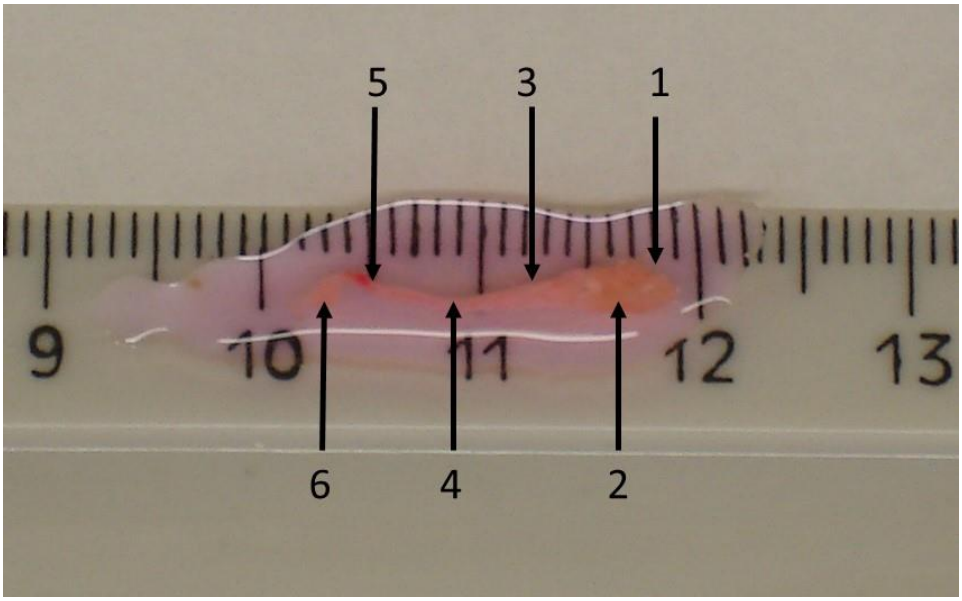

Figure 13. Dissected lower premolar pulp in DMEM/10%FCS. Scale in millimetres

1) Coronal Pulp; 2) Lower Coronal Pulp; 3) Lower Coronal/Upper radicular Root Canal Pulp; 4) Radicular Root Canal Pulp; 5) Apical Root Canal Pulp; 6) Extraneous Pulp Tissue (Apical Papilla – potential source of stem cells from the apical papilla (SCAP) cells).

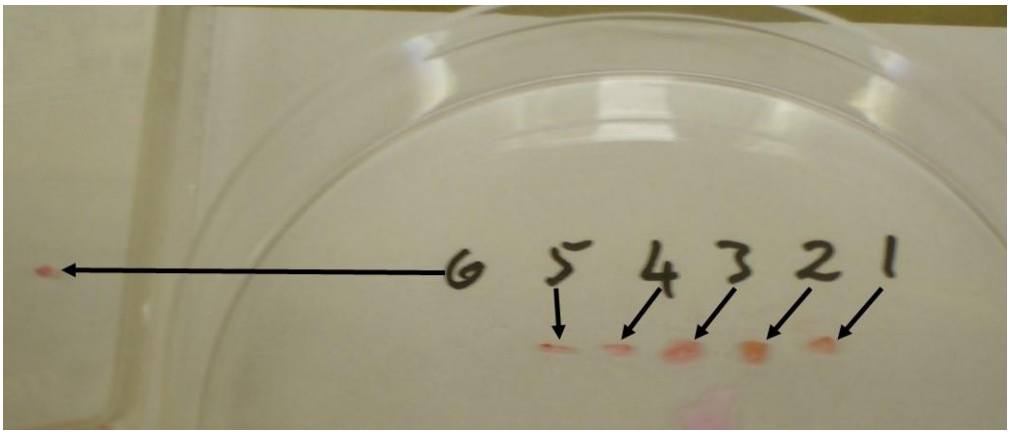

Figure 14. Pulp tissue cut into 3 mm sections.

Site specific culture of dental pulp: 1. Upper coronal pulp. 2. Lower coronal pulp. 3. Upper coronal part of the root canal pulp. 4. Radicular root canal pulp. 5. Apical root canal pulp. 6. Dental papilla in adjacent flask.

For ALP staining, the cell explants were first stopped in 98% ethanol overnight in their 6 well plate. Next day the 98% ethanol was drained off and replaced with PBS

for 10 minutes, during which the following reagent was made up in these proportions: 9.6 mL of distilled water was added to 0.4 mL of Naphthol A5-MX phosphate alkaline solution (Sigma-Aldrich), to which was added 2.4 mg of Fast Violet B salt. This was mixed thoroughly, the PBS was removed from the explant samples and enough reagent was added to cover the explants. It was then left for a minimum of 30 minutes for the reaction to take place. After obvious colour change had occurred, the solution was drained off and images were taken of the explants.

The DPSCs from T175 flasks for cryostorage were collected at passage 3, 4 or 5 by detaching with 10 mL. of 1x trypsin/edta solution. Five millilitres of FCS were added and then they were spun down at 600g for ten minutes. The supernatant was carefully drawn off then the cells were resuspended in FCS/10% dimethyl sulphoxide (DMSO) in cryotubes and placed into the insert of a Mr. Frosty™ freezing container (Thermo Scientific™) containing isopropyl alcohol around the insert holding the cryotubes and placed in a minus 80°C freezer to cool at minus 1°C per minute until frozen, thereby giving optimal cell preservation.

3.4 Isolation of DPSCs by the collagenase digest method

The following method of DPSC isolation was used for all other investigations described in this thesis from Section 3.11.3 onwards. Pulp explants, harvested as described above in section 3.3 were treated with collagenase P (Roche, Pensberg, Germany) to allow release of the cells from the intact tissue. This was a modification of the collagenase/dispase method used by other authors in previous studies (Gronthos et al., 2002, Huang et al., 2006). The collagenase digest method was adopted as it gave a greater and much more rapid release of cells from each pulp sample between the second and third passage, thus giving better yield in comparison to the pulp explant method (see Results section 4.1.2). Following its retrieval from the tooth, the pulp tissue was finely chopped using two scalpels fitted with no. 15 blades (Swann Morton Ltd., Sheffield, England) in the base of a sterile Petri dish. This was done quickly in the laminar air flow hood to avoid dehydration of the tissues, with any small fragments being 'parked' in αMEM/10% FCS or in PBS, in a separate Petri dish until required for the next stage of the protocol. The resultant fragments were placed into a sterile 5 mL test tube and immersed in a solution of collagenase P diluted to a concentration of 5 mg/mL in PBS (with no added Mg^{2+} or Ca^{2+}) for at least 30 minutes at 37°C and 5% CO_2 in a tissue culture incubator, with the test tube lid being 'cracked open' half a turn to allow for gas exchange. Every 5-10 minutes, the test tube was removed from the incubator, its lid secured and then vortexed for one minute at full power to ensure even mixing and exposure of the tissues to the collagenase, then returned to the incubator as before. When the minced fragments of dental pulp were adjudged by eye to have dissociated as far as possible

at a time never greater than 60 minutes, 50% FCS (per volume) was added to the mixture to halt the reaction. The cell suspension was centrifuged at 600 g for 10 minutes, the supernatant carefully pipetted off and the resultant cell pellet resuspended in αMEM. This was then passed through a 70 µm cell strainer (BD Falcon™ California, USA) to obtain a single cell suspension. The cells were then cultured in T75 flasks in αMEM/10% FCS, supplemented with 200 mM L-glutamine and 100 units/mL penicillin/streptomycin at 37°C and 5% CO_2 with weekly changes of medium.

3.5 Counting and passaging DPSCs

After reaching 80-90% confluence (confirmed by light microscopy), the αMEM/10% FCS medium was discarded and the cell layer was washed twice with 5-10 mL of 1× PBS to remove any extraneous FCS (FCS interferes with the serine protease function of the trypsin/EDTA solution). The PBS was drained off, then 10 mL of 1x 0.25 mM trypsin/ethylenediaminetetracetic acid (EDTA) was added to the T 175 flask for approximately 5-10 minutes to detach the cells. Periodic observation by microscope was used to monitor this process. Once all the cells were detached and in solution, the reaction was then halted by adding 2.5 mL of FCS and 5 mL of αMEM to re-suspend the cells, the whole then being placed in a test tube and centrifuged at 1100 rpm for 5 minutes. The supernatant was carefully removed without disturbing the pellet and the pellet was re-suspended in plain (i.e. no FCS) αMEM. This was vortexed to ensure even distribution in the liquid. A 30 µL sample

from this was then applied to the central groove of the haemocytometer and a cover slip applied. Under a microscope, the cells were counted in five demarcated fields with the numbers being added up. This number was then averaged (i.e. divided by five) and multiplied by the haemocytometer constant and again by the volume of the suspension to give the total cells in the suspension. After this the desired volume containing the required number of cells could be calculated in microlitres. No Trypan Blue reaction was recorded. In this way, the cells could be seeded at different densities dependent upon the conditions and requirements of the relevant experiment or split and passaged on into new tissue culture flasks for further culture and expansion.

3.6 Cryopreservation of DPSCs

After the appropriate number of passages cultured in αMEM/10% FCS plus L-glutamine supplement and having achieved 80% confluence in a T175 flask, the cells were then trypsinised, detached and spun down at 1000 rpm for 5 minutes to form a pellet, which was re-suspended in a solution of 90% FCS/10% DMSO (Sigma. Poole, Dorset) in cryotubes and stored in the insert of a Mr Frosty™ freezer box containing isopropanol which would lower the temperature at 1 degree centigrade per minute in a minus 80°C freezer. Then the cells were kept at minus 80°C until required. This same method of cryopreservation was adopted for cells obtained via the collagenase digest method and all other types of cell used during the study.

3.7 Dental pulp explants and DPSCs for alkaline phosphatase staining

Where pulp explants or DPSCs were to be used for alkaline phosphatase staining, following examination under light microscopy to ascertain their suitability, they were fixed in 98% ethanol until required (see Section 3.3). If used the same day, the explants/DPSCs were first stopped in 98% ethanol overnight in their 6 well plate. Next day the ethanol was drained off and replaced with PBS for 10 minutes. Then 0.4 mL of Naphthol A5-MX solution was added to 9.6 mL of distilled water. To this mixture 2.4 mg of Fast Violet B salt was added and mixed thoroughly. The PBS was removed from the samples and sufficient reagent mixture was added to cover the samples. The lid was kept on for at least 30 minutes or longer if necessary until no further colour change was apparent. The liquid was drained off and images taken.

3.8 *In vitro* expansion of control cells

G292 cells

G292 cells were used as a control cell line in some of these studies. The cells are a human osteosarcoma cell line and were obtained from stock held within the Department either from the minus 80°C freezer, or held in cryostorage in liquid nitrogen. These cells had originally been obtained from the European Collection of Cell Cultures (ECACC) and were G292 cells clone A141B1, passage 20 at the time of use. The cells were thawed rapidly, suspended in α-MEM in a 15 mL test tube

then centrifuged for 5 minutes at 1100 rpm. Following removal of the supernatant the pellet was re-suspended in αMEM/10% FCS and cultured in tissue culture flasks until required for experimental purposes, being passaged as and when necessary at approximately 80% confluence. For cryostorage, the cells were treated as per the DPSCs in section 3.6.

3.9 *In vitro* culture of Human Umbilical Vascular Endothelial Cells (HUVECs) as control

HUVECs were obtained from PromoCell GmbH (Cat. No. C-12203; Heidelberg, Germany) and were derived from a pooled donor source. On arrival, the cells were removed from the transportation dry ice and quickly thawed. They were then suspended in 30 mL of basal endothelial growth medium (EGM) (PromoCell catalogue no. C-22210) to which a supplied supplemental mixture had been added (PromoCell catalogue no. C-39210), giving the following concentrations per 500 mL:

TABLE 1: Total amounts of supplement reagents in 500 mL of EGM.

REAGENT	AMOUNT
FCS	20 µL/mL
Endothelial Growth Supplement	4 µL/mL
Epidermal Growth Factor	0.1 ng/mL
Basic Fibroblastic Growth Factor (rh)	1 ng/mL
Heparin	90 µg/mL
Hydrocortisone	1 mg/mL

The initial 500,000 cells received from the supplier were firstly split between two T175 flasks and cultured in EGM to between 80-90% confluence as adjudged by light microscopy. They were then passaged by EGM removal, washing with 30 mL of 1x PBS for thirty minutes and detached with 10 mL of 1 × 0.25 mM trypsin/EDTA solution. Then the cells were either re-suspended to continue passaging, or for experimental use, or stored in FCS/10% DMSO at minus 80°C to build up a working stock. One vial of HUVECs was kept back at each passage and stored in FCS/10% DMSO in case of contamination. A working stock was obtained from cells at passages 3 to 5 with passage 4 being used experimentally. When

required, these were retrieved from the -80°C freezer, rapidly thawed, re-suspended in EGM and cultured for experimental use.

3.10 Culture of G292 cells on GenGiGel® HyA scaffolds

Preliminary work for this thesis was conducted using G292 cells and DPSCs (see below) as a preliminary study of biocompatibility.

3.10.1 Preparation of GenGiGel®

GenGiGel® is a commercial product (OralDent U.K.) made from high molecular weight fractions of HyA which is a constituent of ground substance. It is available in several forms e.g. a low viscosity mouthwash and at higher, more viscous gel concentrations of 0.2 % and 0.8 %, depending on its intended clinical use, which can vary from periodontal application following surgery, soft tissue healing after titanium implant placement and in the management of mouth ulcers. Given that GenGiGel® is already licensed for clinical use in dental applications and in promotion of wound healing, together with the fact that HyA exists within the ground substance of pulp, GenGiGel® was evaluated as a candidate scaffold in pulp tissue engineering.

Differing amounts of granular GenGiGel® powder were autoclaved at 120^{o} C for 15 minutes in 10 mL Pyrex containers with foil lids. After cooling, 10 mL of Dulbecco's modified eagles medium (DMEM, Sigma)/10% FCS was added to the powders and mixed using a magnetic stirrer to final GenGiGel® concentrations of 0.2%, 0.4%, 0.6% and 0.8%. The gels were then left overnight at 4°C. After the

initial experiments were completed it was decided to continue with a concentration of 1% HyA gel as this handled better, shrank less during cooling and its increased viscosity resisted being removed by the Pasteur pipettes during medium changes.

3.10.2 Preliminary study of G292 cells cultured on GenGiGel® HyA gel

G292 human osteosarcoma cells obtained from departmental frozen stock as described in section 3.9 were used in this preliminary study exploring the use of GenGiGel as a possible biomimetic scaffold. The cells were cultured in tissue culture flasks in DMEM supplemented with penicillin and streptomycin (5,000 units per mL penicillin and 5,000 µg per mL streptomycin) and 10 % FCS (Harlan Sera Lab s-0001 AE) at 37^{o}C and under 5 % CO_2/air. The medium was changed weekly until at 70 -80 % confluence, normally after two to three weeks. The cells were then detached by adding 5 mL of 1x trypsin (0.5 g/L trypsin 1:250, 0.2 g/L EDTA (Versene) prior to seeding at a density of 2 x 10^5 cells per mL (300 µL) onto the GenGiGel® preparations (0.2 %, 0.4 %, 0.6 % and 0.8 % GenGiGel® prepared as described above). The cultures were maintained in an incubator for one week at 37°C in a 5% CO_2/air mixture prior to being examined in the light microscope.

One millilitre (mL) of each GenGiGel concentration was placed into a well of a 24 well plate sealed with Parafilm™ and incubated overnight in a tissue culture incubator to allow settling. The gels were then seeded with G292 cells at a concentration of 2 x 10^5 cells in 1 mL of DMEM/10% FCS and cultured for one week prior to image acquisition.

3.10.3 Culture of HPDLCs in EGM on 1% HyA gel ± 5 ng/mL $_{rh}VEGF_{165}$

HPDLCs (Tissue Bank number: D0613673) were suspended in EGM and seeded onto 1% HyA gel at 2×10^5 cells per mL in a 6 well plate. To this was added enough EGM with additional $_{rh}VEGF_{165}$ to give a final concentration of 5 ng/mL $_{rh}VEGF_{165}$ in 3 mL of EGM. After 48 hours the plates were stopped by fixing in 10% NBF for 30 – 40 minutes at room temperature, washed twice with PBS for 10 minutes then stained for CD31 and CD34 biomarkers.

3.11 Culture of DPSCs on other scaffolds

In addition to GenGiGel, further scaffold materials were evaluated for use in these studies in order to investigate the attachment and growth of human dental pulp stromal cells (DPSCs). These included: elephant ivory blocks (obtained with permission from HM Customs & Excise) and poly (DL) -lactic acid (PDLLA)/Bioglass® (45 % SiO_2, 24.5 % Na_2O, 24.5 % CaO and 6 % P_2O_5) foams (provided by Dr Aldo Boccaccini, Imperial College, London, UK) which contain 45S5 Bioglass® particles (0, 5 and 40 wt. %) (Lu et al., 2014, Yang et al., 2006).

3.11.1 Culture of DPSCS on 3-D ivory scaffolds

The ivory blocks (5 x 5 x 5 mm^3) cut from the body of the tusk dentine, were sterilised in 70 % ethanol overnight and washed twice in DMEM for thirty minutes.

Then 20 mL of DMEM was added to the blocks for 4 hours to condition the surface of the substrate. Half of the block samples were placed into 10 mL of 4% GenGiGel/10% FCS/DMEM gel in the base of the test tubes prior to the addition of the ivory blocks and the seeding of the DPSCs, the remainder being kept for future use.

DPSCs (passage 4) were detached using 1 x trypsin/EDTA solution (Sigma, Poole, UK). The cells were then re-suspended in 6 mL of DMEM/10% FCS and 2 x 10^5 cells were seeded onto the conditioned ivory blocks in GenGiGel using a static seeding method in sterile test tubes. The test tubes were then incubated overnight at 37°C and 5 % CO_2 to allow cell attachment. The ivory blocks and GenGiGel were then transferred to a 6 well plate and cultured for a further three days in DMEM/10% FCS prior to being labelled with a live cell fluorescent marker, 5-chloromethylfluorodiacetate (5-CMFDA) (Thermo Fisher Scientific) prior to imaging (see Appendix A for full protocol). The cells growing on the ivory scaffolds were labelled with 5-CMFDA (see Section 4.6) which is taken up by live cells and fluoresces under an excitation wavelength of 497 nm with an emission spectrum of 517 nm producing a green colouration. Briefly, the culture medium was drained off and the cells cultured in plain DMEM for 45 minutes. At the same time, 5-CMFDA was dissolved in 10 µL of DMSO. The DMEM was drained off again and replaced by fresh DMEM with the 5-CMFDA/DMSO added to it. The flask was then wrapped in aluminium foil to exclude light and incubated at 37°C in the tissue culture CO_2 incubator for a further 30 minutes, then viewed at 497 nm wavelength in a fluorescent light microscope. See full staining protocol is given in appendix A.

3.11.2 Culture of DPSCs on 45S5 Bioglass® scaffolds

Scaffold 45S5 poly (DL) -lactic acid (PDLLA)/Bioglass® (45 % SiO_2, 24.5 % Na_2O, 24.5 % CaO and 6 % P_2O_5) foams were provided by Dr Aldo Boccaccini (Imperial College, London). Different amounts of 45S5 Bioglass® particles (0, 5 and 40 wt. %) were used for this study to examine the adhesion, growth and differentiation potential of DPSCs on synthetic scaffolds.

Scaffolds (S5 Bioglass® or ivory) of $5mm^3$ were sterilised under type C ultraviolet (UV) light (wavelength 250 – 260nm) for 30 minutes in 10 mL universal tubes in an aluminium foil tray. The tubes were turned at regular 5 minute intervals to ensure uniformity of exposure. DPSCs (2×10^5) obtained by the cell explant method (see Section 3.1.2), were suspended in 1 mL DMEM and were seeded onto the 45S5 BioGlass® samples and left overnight to allow the cells attach to the scaffolds. The following morning, the 45S5 cell-BioGlass® constructs were transferred to a 24 well plate and cultured in DMEM/10% FCS for up to 12 weeks. At weekly intervals the cultures were stopped for assessment by staining with Sirius Red and Alcian Blue stain. Briefly, after fixing in 10% NBF the sections on the slides were stained with Weigart haematoxylin, using a plastic Pasteur pipette to gently wash the Weigart haematoxylin over each section and left for 10 minutes. Each slide was rinsed gently through a water bath then replaced in the staining rack. The rack was placed into a water bath and rinsed for 10 minutes. The rack of slides was dipped 3x in acid/alcohol (20 mL HCl added to 2 litres 50% methanol) then rinsed in the water bath for one minute. The slides were then stained in molybdophosphoric acid for 30

minutes followed by a one minute rinse in the water bath. The slides were then stained with Sirius Red for one hour, followed by a one minute immersion in water, then immersed in 100% ethanol for 30 minutes then fresh 100% ethanol for a further 30 minutes. They were then mounted in DPX and ready for viewing.

3.11.3 Examination of micro and ultrastructure of unseeded Osseoguard® and BioGide® membranes

Unseeded Type I and III collagen membranes were either coated with gold (Au) in an inert argon gas atmosphere under vacuum, prior to obtaining scanning electron microscope (SEM) images with a Hitachi S-3400N SEM or coated with platinum (Pt) for imaging with a FEI Quanta 650 Field Emission Gun Scanning Electron Microscope (FEGSEM), to provide comparator control images to the seeded samples and higher resolution images of the membrane structure.

3.11.4 DPSCs on Osseoguard® and BioGide® collagen Type I and III membranes *in vitro*

Biomimetic scaffolds containing both collagen Types I and III, (Osseoguard® and BioGide®) were chosen because they have long proven clinical usage in both hospital and private practice. They consist of Types I and III collagen and are readily available commercially. They were either purchased, donated as a gift by commercial representatives or came from the spare pieces left over from my dental practice during implant placement and Guided Bone Regeneration procedures, which were then re-sterilised using UV radiation in a BIO-RAD GS Gene Linker®

UV Chamber, using the sterilisation for UV Resistant Material setting for 90 seconds on each side before experimental use. To ascertain whether DPSCs obtained via the collagenase digest method could attach and proliferate on collagen Type I and III membranes, 25 mm^2 sections of Osseoguard® and BioGide® were conditioned as follows: each membrane was first treated by immersion in DMEM for 1 hour in a 6 well plate at 37°C in air/5% CO_2 mixture. This was done to modify the surface chemistry and condition the surface of the scaffold to promote cell attachment. This was followed by 2 x 10 minute changes of PBS, liquid removal by aspiration via a Vacuubrand vacuum pump unit with two Pasteur pipettes (one to hold the sample in place, the other for evacuation of any liquid) to remove any excess liquid still retained, then seeded with DPSCs at 2 x 10^5 cells per mL in DMEM/10% FCS. These were left for a minimum of four hours to facilitate cell attachment, then transferred to a new 6 well plate and cultured in DMEM/10% FCS for up to 28 days at 37°C in a 5% CO_2/air mixture.

3.11.4.1 5 CMFDA and TOPRO staining

To determine cell viability on the scaffolds, the medium was removed and the samples were then stained with 5-CMFDA and TOPRO-3 iodide (Thermo Fisher Scientific) as follows: the 5-CMFDA was applied as in section 3.11.1. The TOPRO-3 was diluted to 1:100 in PBS to give a working solution. Any culture medium or fluid was removed and the sample lightly fixed in 10% Neutral Buffered Formaldehyde (NBF) for 15 minutes maximum. The samples were then washed for 3 x 5 minutes in PBS, then permeabilised in 0.1% Triton-X in PBS for 20 minutes.

They were then washed in 3 x PBS for 5 minutes and incubated at 37°C for 20 minutes in TOPRO. They were then washed in PBS for 1 x 5 minutes, following which they were examined under confocal microscopy. TOPRO excitation was at 642 nm, emission at 661 nm, 5-CMFDA excitation at 497 nm and emission at 517 nm.

3.11.4.2 Acridine Orange and HCS CellMask™ Deep Red staining

Acridine Orange stain has previously been used for assessing viability of dental pulp tissues (Sloan et al., 1998) so for staining with Acridine Orange/HCS CellMask™ Deep Red, the constructs were fixed by immersion in 10% NBF for 30 minutes at room temperature prior to staining as follows: three washes (10 minutes each) in 1× PBS prior to being stained with a 2 ng/mL working solution of HCS CellMask™ Deep Red stain (Thermo Fisher Scientific) in PBS made up from the stock HCS CellMask™ solution (10 µg/mL). The samples were stained for 30-40 minutes. Then the samples were washed a further three times (10 minutes each) in PBS and stained with 0.01% Acridine Orange working solution for 40 minutes. Whole membrane samples were examined under a scanning electron microscope and confocal laser scanning microscope (Acridine Orange: excitation at 488 nm, emission at 520 nm. HCS CellMask™ Deep Red: excitation at 633 nm, emission at 680 nm). Images were recorded as snapshots or Z-stacks thereof.

3.12 Histochemistry and immunohistochemistry of DPSCs on Type I and III collagen membranes

To assess the ability of DPSCs to attach and proliferate on Osseoguard® and BioGide® collagen Type I and III membranes, DPSCs obtained by the collagenase digest method (see Section 3.4) were seeded onto template-derived 25 mm^2 sections of Osseoguard® and BioGide® Types I and III collagen membranes (see below for seeding protocol).

Each of the membranes was first treated as described in Section 3.11.4. This was done to modify the surface chemistry and condition the surface of the membrane to promote cell attachment. This was followed by 2 changes of PBS (10 minutes in each), then the membrane was subjected to suction using two Pasteur pipettes (one to hold it in place, the other for evacuation) to remove excess liquid, then seeded with DPSCs at 2 x 10^5 cells per mL in DMEM/10% FCS. These were left for a minimum of four hours to facilitate cell attachment, then transferred to a new 6 well plate and cultured in DMEM/10% FCS for up to 15 days at 37°C in a 5% CO_2/air mixture. They were fixed in 10% NBF for 45 minutes to 1 hour at room temperature. They were then tissue processed in an Excelsior ES Tissue Processor (Thermo Shandon), where they were dehydrated in a series of graded alcohols up to 100% ethanol, infiltrated with 100% xylene and then infiltrated with wax before being further wax embedded before being sliced into 5µm sections using a JUNG BIOCUT 2035 microtome and histological evaluation such as H&E staining (see Section 3.12.1 and Appendix A) or immunohistochemistry (see section 3.1.12 and Appendix A).

3.12.1 Immunohistochemistry for CD31, CD34 and STRO-1

DPSCs were seeded onto BioGide® Type I and III collagen membranes (see Section 3.11.4). They were then cultured in αMEM/10% FCS in a 6 well plate in a tissue culture incubator for 14 days then stopped by draining off the αMEM/10% FCS, washing twice in 1× PBS for 30 minutes each, drained, then fixed in 10% neutral buffered formalin for one hour at room temperature. The membrane samples were tissue processed in an Excelsior ES Tissue Processor (Thermo Shandon), where they were dehydrated in a series of graded alcohols up to 100% ethanol, infiltrated with 100% xylene and then infiltrated with wax before being further wax embedded (by hand) in tissue cassettes, then 5 µm sections were cut using a JUNG BIOCUT 2035 microtome. Sections were wetted with 20% ethanol and floated on warm water onto 3-aminopropyltriethoxysilane (APES) coated slides, then dried overnight in an air incubator at 37°C before horseradish peroxidase (HRP) immunohistochemistry staining. This protocol was carried out for CD31, CD34 and STRO-1 markers, or H&E staining (see Section 3.12.1 and Appendix A for full protocol details), with the protocol being common to all CD31, CD34 and STRO-1 samples, only the first antibody differing. Briefly, HRP-immunohistochemistry staining involves use of a primary antibody raised (in this case) in rabbits and directed against a specific antigen molecule (such as CD31, CD34) and normally used at a concentration of 1 in 100 in accordance with the manufacturers data sheet having been further optimised previously by test samples at different serial dilutions (1 in 50; 1 in 100; 1 in 250; 1 in 500) to detect the presence and location of the antigen within a tissue or sample. The sections to be investigated were prepared as described above onto APES (3-aminopropyltriethoxysilane) coated slides (the APES coating gives a

negative charge which improves the attachment of the sections to the surface of the slide). They were then immersed in two stages of 100% xylene, for 20 minutes each, followed by two stages of absolute alcohol for five minutes each and one stage of 2% hydrogen peroxide and absolute methanol for 20 minutes. After washing, the antigenic epitopes were exposed by a process of antigen retrieval. The sample was warmed in a 0.01M citrate buffer for 60 minutes at 60°C in a plastic Copling jar in a covered water bath. The sections were then washed again in PBS and then 150 µL of 20% normal goats serum (NGS) was applied for 5 minutes minimum as a blocking agent. Primary antibody (anti-CD31 Abcam ab 28364, anti-CD34 Abcam 81289, anti-STRO-1 Abcam 102969) used at 1 in 100 dilution in PBS was applied and incubated overnight in a controlled humid environment at room temperature, with the 20% NGS being used for any negative control samples such as the experimental samples themselves. For positive control samples, human or animal tissue (e.g. dental pulp) which should test positive to the primary antibody were used. After leaving overnight, the samples are then washed again in PBS for 5 minutes and then two drops of solution A from the EnVision™ kit was applied for 30 minutes to each slide. A 5 minute wash with PBS was then applied. While this was happening, enough amounts of solutions B and C were mixed in the ratio of 1 mL B to 20 µL C, the slides rapidly moved onto a flatbed and 120 µL of the B and C mixture applied to each slide to develop the brown colouration indicative of the horseradish peroxidase staining. This stage was monitored closely by checking under the microscope and repeated if necessary. The samples were then washed in tap water for a minimum of 5 minutes, counterstained with H&E for 1 minute, washed in tap water for 5 minutes, immersed in Scotts tap water for 1 minute, washed again in tap

water, dried in two changes of absolute alcohol for two minutes each, then washed in two changes of xylene for two minutes each. Finally, a drop of dibutylphthalate in xylene (DPX) was used to exclude any air over the sample, then a coverslip applied prior to viewing and imaging.

3.12.2 Haematoxylin and Eosin (H&E) staining

For H&E staining protocol, as in Section 3.12.1, the sections were firstly dewaxed in xylene twice for 5 minutes each, then immersed in two changes of absolute ethyl alcohol for 5 minutes and then washed under running tap water for 5 minutes. They were then immersed in Harris' haematoxylin solution for 3 minutes, washed under running tap water for 5 minutes, given 3 quick dips (literally) in 1% acid alcohol with a quick look under the light microscope to check the nuclear staining, washed under tap water again for 5 minutes, then immersed in Scott's tap water for 2 minutes, washed again under tap water for 5 minutes, then counterstained in 1% aqueous eosin for 30 seconds and finally given a tap water wash for 5 minutes. This was followed by two changes of absolute ethyl alcohol for 5 minutes each, then clearing in xylene for 5 minutes and then mounting under DPX with a coverslip. Sections of human dental pulp which had been dissected from teeth and fixed in 10% NBF and tissue processed as described in the previous paragraph and stained exactly the same as the experimental samples were used as positive or negative controls during this process.

3.13 Biochemical assay using PicoGreen® for determination of total DNA content of DPSCs

To determine the proliferation rate for DPSCs on BioGide® Type I and III collagen membranes following seeding on both sides, total DNA content was measured using a PicoGreen® assay. Firstly, the membranes were marked with a fine dot on one side with a black Sharpie permanent marker and allowed to dry inside a petri dish in a tissue culture incubator for 30 minutes. This was done so as not to seed the same side twice. Double sided seeding increases the numbers of cells attached and maximises DNA retrieval. DPSCs were seeded onto the 25mm^2 samples of collagen membranes using a modified technique to increase the numbers of cells attaching in the absence of a dynamic-seeding alternative. The membranes were conditioned by application of αMEM for 4 hours followed by three changes of PBS for 30 minutes. Following this, each membrane was skewered onto a sterile hypodermic needle and placed into the base of a 15 mL test tube in which was a 5 mL suspension of 2 x 10^5 DPSCs in αMEM. Each test tube was then placed in a rack with the lids lightly closed to enable air circulation and the rack was then placed in a tissue culture incubator at 37°C in 5% CO_2/air mixture. The samples were left for 4 hours then removed into a tissue culture hood, the cell suspension agitated, the membranes were taken out of the test tube, turned over the other way, placed back on the end of the needle and left for another 4 hours in the cell suspension in a similar fashion. After that, they were placed in a 6 well plate and cultured in 3 mL of αMEM/10% FCS and stopped at days 5, 10 and 15. The samples were stopped by washing in 2 x PBS for 30 minutes then the PBS was removed by suction until the Type I and III

collagen membrane and cell samples were visibly dry. These were then snap-frozen in the 6 well plate at minus 20°C, following which they were then assayed for DNA content via the PicoGreen® assay method to measure the proliferative capacity of the cells (Yang et al., 2006). The membrane samples were placed in 1 mL of 1% triton-X 100 in a 1.5 mL Eppendorf tube to thaw, then completely refrozen. Following defrosting for the first time, the samples were finely minced with sharp pointed scissors in the Eppendorf tube then refrozen. This freeze/thaw cycle was repeated five times in total to ensure as complete membrane disruption as possible. To prepare the solution for measurement, briefly, a stock solution of 10 mM Trizma hydrochloride and 1 mM EDTA buffer (TE) was made up in 500 mL of sterile DNase free water. To make the working solution, 10 mL of the 20 x TE buffer was diluted in 190 mL of DNase free water. To generate a standard curve, a 2 µg/mL stock solution of dsDNA (double stranded Deoxyribonucleic acid) was prepared in TE buffer. Sample fluorescence was measured against standards made up to 5, 10, 25, 50 and 100 ng/mL of salmon sperm DNA (Sigma-Aldrich) using a 2 µg/mL solution of diluted in TE buffer to the desired concentrations. Total dsDNA was measured in the cell lysates by placing 100 µL aliquots of each standard, test samples (15 µL of sample plus 85 µL of TE buffer) and blanks (TE buffer only) were added to 96 well plates in triplicates. Then, 100 µL of PicoGreen® (diluted 1:40 in TE buffer) was added to each well and the plates were incubated in the dark at room temperature for 5 minutes. The fluorescence of the samples was measured using a Thermoscientific (ELISA) microplate reader (Fluoroskan Ascent) with an excitation wavelength of 480 nm and an emission wavelength of 520 nm.

Statistical analysis of the results was carried out with IBM SPSS version 22 using a one way ANOVA test with a post hoc Bonferroni correction.

3.14 Culture of DPSCs and HUVECs on 1% Collagen gel + $_{rh}VEGF_{165}$

3.14.1 Culture of DPSCs and HUVECs

A 1% sterile mixture of Type I collagen gel was prepared by autoclaving 1 gram of collagen gel powder (gelatine) and dissolving it in 100 mL sterile water, then storing it in a sterile bottle at 4°C. It was then warmed to 70°C in a water bath and 100 µL was pipetted into the base of a 12 well plate and allowed to set and cool in a tissue culture incubator at 37°C. DPSCs or HUVECs suspended in EGM were then seeded with 1 mL of cell suspension at a density of 10^4 cells per mL per well with each well receiving another 2 mL of medium along with the appropriate amount of recombinant human Vascular Endothelial Growth Factor$_{165}$ ($_{rh}VEGF_{165}$) next, to give a final concentration of 5 ng/mL (Matsushita *et al*., 2000). This was incubated over 48 hours in a tissue culture incubator at 37°C in a 5% CO^2 and air mixture.

3.14.2 Immunohistochemistry of DSPCs and HUVECs

Plates were stopped by draining off the EGM very carefully using a disposable Pasteur pipette, so as not to disturb the gel and given a light fix by immersion in 10% NBF for 30 minutes at room temperature. This was then carefully drained off

and washed twice with PBS. They were then immunostained for CD31 or CD34 markers in a modified technique from section 3.1.1 where the antigen exposure step was omitted as the samples were not paraffin embedded and the protocol ended at the second alcohol stage with no final xylene steps as these would have dissolved the 12 well plate plastic. After draining, a round coverslip was placed into each well to retain the gel and the plate lid was sealed with parafilm after which the plates were ready for image recording and inverted onto the microscope stage to enable focussing. This methodology was used for all the samples in sections 3.14 and 3.15.

3.15 Culture of DPSCs and HUVECs on 1% Hyaluronic Acid gel ± $_{rh}VEGF_{165}$

3.15.1 Culture of DSPCs and HUVECs

A 50 mL sterile mixture of 1% HyA gel was prepared using the method described earlier in section 3.1.8 and stored in a sterile Schott bottle. The bottle was placed in a water bath and warmed to 70°C. One hundred microlitres of warm 1% HyA gel were pipetted into the base of each well of a 12 well plate which had been pre-warmed in the tissue culture incubator at 37°C and the plate turned to ensure even coverage in the base of each well. The plate was then incubated at 37°C for approximately one hour until needed. DPSCs suspended in EGM were then seeded onto the 1% HyA gel at a density of 10^4 cells per well with each well receiving 2 mL of medium along with the appropriate amount of recombinant human Vascular Endothelial Growth $Factor_{165}$ ($_{rh}VEGF_{165}$) next, to give a final concentration of

5 ng/mL. This was placed for 4 hours in a tissue culture incubator at 37°C in a 5% CO^2 and air mixture and the plates incubated over 48 hours in a tissue culture incubator.

3.15.2 Immunohistochemistry of DSPCs and HUVECs

Samples were treated using the same protocol as described in section 3.14.2.

HUVECs were used as controls for this part of the study and subjected to identical conditions.

This procedure was then repeated, with DPSCs and HUVECs this time with no $_{rh}VEGF_{165}$ being added to the cells and the cultures stained for CD31 and CD34 cell markers as before. As further controls, G292 cells were also cultured and tested using the same methodology, again with no $_{rh}VEGF_{165}$

3.16 *In Vitro* culture of DPSCs on Type I and III collagen membranes and 1% HyA gel in endodontically prepared tooth slices

3.16.1 Preparation of Type I and III collagen membranes and 1% HyA gel

To combine the two elements of culture so far, DPSCs were cultured on Type I and III collagen membranes which had been infiltrated by 1% HyA gel under gentle vacuum overnight. Type I and III collagen membranes were prepared by immersion in a 1% HyA gel in a Schott bottle under a vacuum for one hour in a vacuum vessel with the bottle lid slightly open to allow the vacuum to have an effect on the penetration of the gel. The bottle was then closed and placed in a fridge at 4°C until required.

3.16.2 Preparation of tooth slices

The tooth slice and scaffold model (Sakai et al., 2011) used for dental pulp tissue engineering (Cordeiro et al., 2008) was in turn derived from a combination of the tooth slice organ culture model (Sloan et al., 1998) and the SCID (severe combined immunodeficient) mouse model used in the study of human angiogenesis (Nor et al., 2001). This has been used to study angiogenesis-based therapeutic methods for pulp regeneration and revascularisation (Goncalves et al., 2007, Mullane et al., 2008). The protocol was modified for use in this study. Slices of tooth, 3 mm thick, were cut horizontally from the cervical region of premolar teeth on a Struers Accutom® 5 water-cooled cutting machine to give a ring shaped sample. The rationale behind

this was that anatomically, the pulp chamber is usually largest in this region of the tooth and can be further enlarged by endodontic instrumentation (see figure 15).

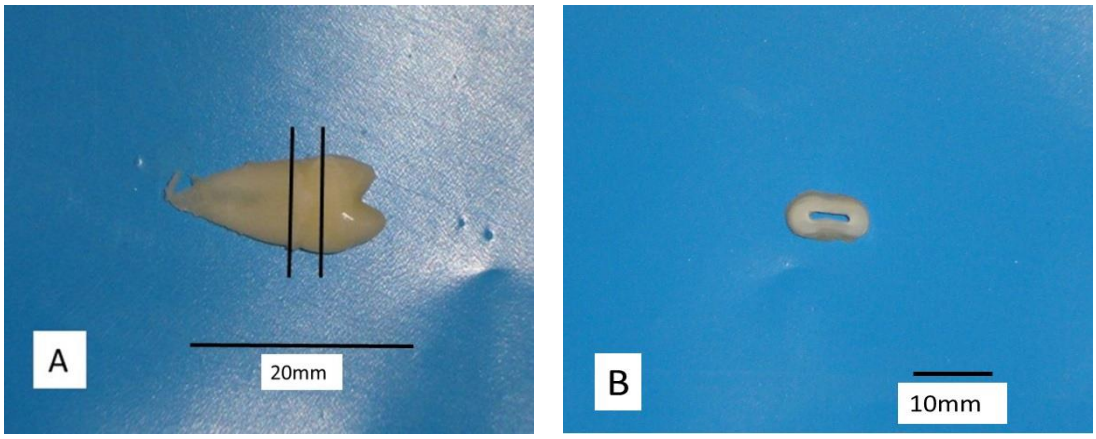

Figure 15. a premolar tooth prior and post-sectioning.

A: The two parallel black lines indicate the cervical region of the tooth from where the slices were sourced. B: resulting tooth slice instrumented up to a size 140 file.

The resultant annular slices were then filed/instrumented to increase the lumen of the root canal with sterile Kerr endodontic files up to a size 140. The tooth slices were then sterilised by placing them in 70% ethanol inside a sealed bijoux container which was then placed in an ultrasonic bath for 30 minutes and sonicated. The ethanol was then removed inside a tissue culture hood, replaced with PBS with added Penicillin/Streptomycin (Pen/Strep) at a concentration of 100 units of each per mL and sonicated again. Lastly this solution was replaced with 1 x PBS and again sonicated. Following this, the tooth slices were incubated overnight in 5 mL of αMEM/10% FCS in a tissue culture incubator to check for contamination before being removed, washed three times for 30 minutes each in PBS then used.

The collagen Type I and III membranes were removed from the 1% HyA gel and placed on a sterile surface inside a tissue culture hood. The tooth slices were removed from the PBS and placed alongside. The tooth slices were then gripped in a pair of locking forceps and the collagen Type I & III membrane was inserted into and pulled through the enlarged root canal using tissue forceps until it jammed whereupon the excess was cut off at both ends with a scalpel. Each tooth sample with the treated membrane in the enlarged canal lumen was then placed into a well in a 6 well plate then seeded with 2 x 10^5 DPSCs suspended in the appropriate volume of EGM. Cells were allowed to attach for four hours in a tissue culture incubator at 37°C in a 5% CO_2/air mixture after which the wells were topped up with 3 mL of EGM then incubated at 37°C in a CO_2/air mixture for two weeks with the medium being changed every three days in accordance with the manufacturer's instructions. After this, the samples were drained, fixed in 10% NBF overnight and radiographs taken using a Phillips Oralux X-ray machine and AGFA size 2 intra-oral films. They were then demineralised in 10% TRIS/EDTA solution, radiographed at weekly intervals and the demineralising solution changed weekly until the slices appeared radiolucent on the radiographs and the dentine showed no difference in radiolucency from the Type I and III collagen membrane. The tooth slices were then prepared for manual embedding by sequential dehydration in a series of alcohols under vacuum in a Dry-Seal desiccator: 70% ethanol for 20 minutes; 95% ethanol for 20 minutes × 2; 100% ethanol for 20 minutes × 2; xylene for 20 minutes × 2 before being placed in tissue cassettes and wax embedded in Gurr® Paramat embedding wax at 40°C under 1000 m bar of vacuum for 40 minutes. The samples were then slowly brought up to atmospheric pressure and placed into a new wax

bath for a further 40 minutes then embedded in fresh paraffin wax. Sections of 5µm thickness were prepared using a microtome and floated onto APES slides before immunohistochemistry staining for CD 31 and 34 markers and H&E staining as described in section 3.12 (see Appendix 1 for full protocol details). Unseeded membrane samples were used as negative controls and subjected to the same histological procedures.

3.16.3 Cold stage SEM imaging of tooth slice-DPSCs/scaffold constructs

Samples for SEM cold stage imaging were stopped in 10% NBF prior to imaging. They were washed twice in PBS for thirty minutes, blotted dry then placed in the SEM cold stage for imaging under vacuum at minus 20 °C.

3.17 Determination of CD31 and CD34 gene expression at 2 and 5 days by DPSCs using qRT-PCR

DPSCs were seeded at 2×10^5 cells per well and cultured under the following four different conditions in 6 well plates for 2 and 5 days. This was to examine the change in gene expression of the angiogenic marker genes *CD31* and *CD34* in comparison to the housekeeping gene Tyrosine 3-monooxygenase/tryptophan 5-monooxygenase activation protein, zeta polypeptide (*YWHAZ*) which acts in signal transduction.

TABLE 2: Culture conditions for DPSCs to determine CD31 and CD34 expression.

Groups	2D/3D	Culture conditions
A	1%HyA gel	EGM
B	1% HyA gel	αMEM/10% FCS
C	monolayer	EGM
D	monolayer	αMEM/10% FCS

As a pre-requisite to carrying out qRT-PCR, RNA was isolated from the cell culture lysates, following which it was reverse-transcribed into cDNA. Initially, cells were disrupted by adding 1.5 mL of RLT buffer, to which had previously been added β-mercaptoethanol at a concentration of 10 µL per mL. The RNA was extracted from the cell lysates using an RNeasy Mini Kit (50) (Cat. No. 74104) with additional DNase digestion (Qiagen, Crawley, UK) in accordance with the manufacturer's instructions. RNA concentrations were quantified using a NanoDrop spectrophotometer (Thermo Scientific, Wilmington, USA). The RNA obtained was then processed, with the amount being used dependant on its concentration, into single stranded cDNA samples using a High Capacity RNA-to-cDNA Kit (Applied Biosystems, Carlsbad, USA) to obtain 200 ng of cDNA in 20 µL reaction volumes in accordance with the manufacturer's instructions. These were then run on an MJ

Research PTC-100 Thermo Cycler for 1 hour at 37°C and then at 95°C for five minutes and were stored at minus 20°C until required.

Amplification and analysis of the angiogenic markers was carried out using Taqman® probe assays in a 20 µL reaction volume in the Roche light cycler as follows:

10 µL of gene expression master mix supplied by Applied Biosystems, UK (ABI, UK) were combined with 9 µL of cDNA template and 1 µL of Taqman® assay probe (ABI, UK). This mixture was added in triplicates to 96 well plates which were sealed and centrifuged for 10 seconds then placed into the light cycler. The amplification program comprised of three steps (as recommended by ABI) for the Taqman® probes:

A pre-incubation cycle for 5 minutes at 95°C;

45 amplification cycles comprising of two steps:1. 95°C for 5 seconds, followed by 2. 65°C for 1 minute.

This was followed by a final cooling cycle with the temperature being dropped to 40°C for 30 seconds.

This experiment was repeated three times, with the results being analysed using the ΔCT method. Details of the Taqman® gene expression assays used follow in the next table. A sample from DPSCs on day 0 was used to provide a baseline.

TABLE 3: Details of Taqman® gene expression assays used in qRT-PCR.

Gene name	Gene group	Taqman® gene expression assay number
YWHAZ	Binds phosphoserine and phosphothreonine proteins. Active during signal transduction, apoptosis, tumour suppression.	Hs00237047
CD31	Cell adhesion molecule/protein binding molecule/angiogenic marker/gene of interest	Hs01065279-m1
CD34	Cell adhesion molecule/protein binding/angiogenic marker/gene of interest	Hs00990732-m1

3.18 *In vivo* study

3.18.1 Preparation of DPSCs-scaffold constructs for *in vivo* implantation

Tooth slices were prepared as in section 3.16 for use in an *in vivo* study to determine the ability of the cell-scaffold constructs to develop vascular-like structures under physiological condition *in vivo*, when implanted subcutaneously in four MF1 Nu/Nu nude mice. These albino mice were selected as they have normal B cell function but have a rudimentary dysfunctional thymus and so are T cell deficient. They are phenotypically hairless, generate no cytotoxic effector cells and show no graft versus host response.

The tooth slices and HyA/Type I and III collagen membrane constructs were prepared in the same manner as described in sections 3.16.1 and 3.16.2. DPSCs were seeded on these scaffolds at a density of $2x10^5$ cells per sample and cultured for two weeks in 6 well plates. Four different scaffold constructs were examined: (a) Tooth slice with Type I and III collagen membrane and HyA gel *in situ* but with no DSPCs; (b) Tooth slice and Type I and III collagen membrane seeded with $2x10^5$ DPSCs. (c) Tooth slice and 1% HyA gel seeded with $2x10^5$ DPSCs and (d) Tooth slice and Type I and III collagen membranes infiltrated with 1% HyA gel and seeded with $2x10^5$ DPSCs as described in section 3.16.1. Each sample was incubated initially in EGM for 2 weeks with the medium being changed every three days, to allow the cells to attach and proliferate before being inserted subcutaneously into the dorsal surface of four MF1 Nu/Nu nude mice.

3.18.2 *In vivo* implantation

Four MF1 Nu/Nu athymic mice (five weeks old, male) were used for this study. The procedure was conducted under general anaesthetic (Project license: PPL40/3361) and carried out by Dr. Xuebin Yang from the Dept. of Oral Biology. After an incision was made on the dorsal surface of the mouse, four subcutaneous pockets were made via blunt dissection (16 sites in total). A scaffold only, or DPSCs-scaffold construct was implanted in this pocket and the wound was closed by non-resorbable suture. The implantation locations (see Figure 17) were in the following order for each of the animals: (a) was inserted into the shoulder area above the left forelimb; (b) was inserted into the shoulder area above the right forelimb; (c) was inserted into the lumbar area above the right rear limb and (d) was inserted into the lumbar area above the left rear limb.

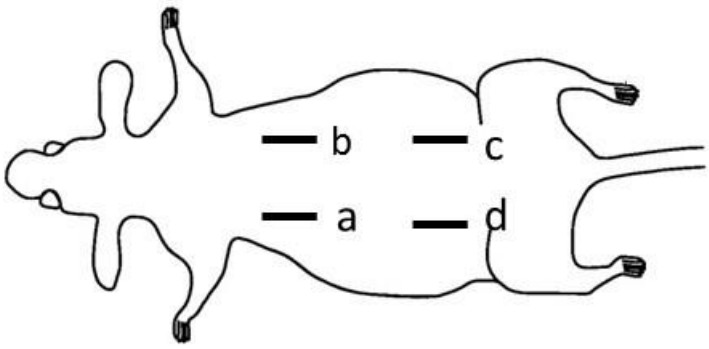

Figure 16. Diagram of incision sites for subcutaneous implantation of constructs.

The mice were housed in the Central Biological Service with normal food and drink available under a 12 hours day/night cycle. Each wound was checked daily for the first week post operation. After four weeks, the four animals were euthanized and the samples (16 in total) dissected out, immersed in 10% NBF for one week then decalcified. They were then tissue processed for histological and immunohistochemical analysis by the same method as described in section 3.16.2.

Chapter 4: Results

4.1 Cell outgrowth from dental pulp explants and cell growth following the collagenase digest method

4.1.1 Cell growth and proliferation from the pulp explant method

Dental pulp explants normally stick onto tissue culture plastic surfaces after a few minutes, although overnight incubation was necessary in some cases. After being cultured for between 1 to 14 days, the cell explants began to show DPSC outgrowth from discreet areas or 'nodes' of their periphery (see Figure 17). Generally, the sooner this happened the better it predicted cell proliferation but it varied between explants as some which had attached showed no growth whatsoever. Donor variation was also seen, with some donor tissue showing early, vigorous growth with rapid proliferation and others proliferating very slowly. This correlates with other investigators' findings in the literature (Moule et al., 1995). Figure 17 (A), shows a pair of DPSCs after 24 hours of attachment, (B) shows a cluster of DPSCs emanating from a single growth node, again at the 24 hour time point, while (C) shows another larger cluster of DPSCs at 24 hours and (D) shows a single DPSC growing out of a dental pulp explant at the 7 day time point. Images of this nature highlighted the donor variability of the procedure, making the predictability of cell proliferation and therefore availability of cells for experimental purposes impossible to predict. It is also possible that the DPSCs grow out of areas where vascular structures have been in contact with the tissue culture plastic as the perivascular

niche has been postulated as the source of DPSCs which differentiate into odontoblasts (Bianco and Cossu, 1999, Senzaki, 1980). In addition, DPSCs associated with "stemness" express surface markers such as CD44, CD106, CD146, 3G5 and STRO-1. See Figure 35 (A), for an example of this latter marker.

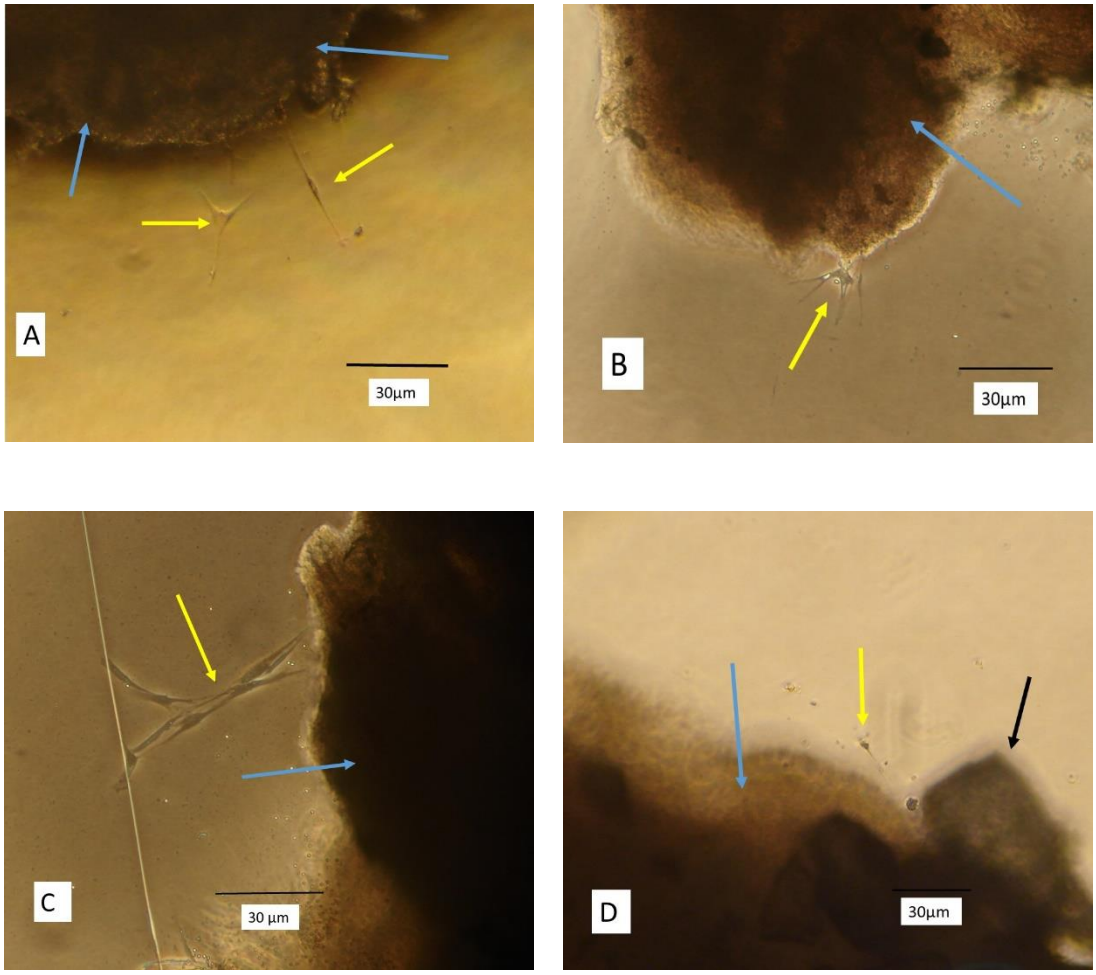

Figure 17. Single cell outgrowth from a dental pulp growth node.

A-D: dental pulp explants are all designated by the blue arrows. DPSCs are indicated by the yellow arrows. The vertical white line in (C) is a scratch on the tissue culture plastic surface and the black arrow in (D) indicates a dentine fragment adhering to the pulp explant.

4.1.2 Comparison of DPSC proliferation from pulp explant and collagenase digest at days 14 and 15

As stated before, cell proliferation from a growth node from pulp explants was unpredictable and could be extremely slow or extremely rapid (see Figure 18).

Figures 18 (A) and (B) show cell outgrowth from the same coronal region of a pulp explant at days 14 and 15. Normally, the DPSC numbers would have been much higher than this, further illustrating the variability in between donor samples. Cell counting showed approximate doubling of cell numbers over a 24 hour period. The piece of fibrous/extraneous tissue attached to the dental pulp explant on the right side of the image was used to accurately locate where the DPSC outgrowth was occurring (the view was moved slightly to accommodate the extra cells on the second day). Figure 18 (C,D) shows cell proliferation data obtained after using the collagenase digest method at days 14 and 15 after original dental pulp collagenase digestion. The cells had undergone an additional passage in that time, one week previously. It can be seen that many more cells were present compared to the explant method and that some of the cells had arranged themselves into circular/oval patterns reminiscent of vascular structures. As a result of the obvious increased proliferation rate of the DPSCs obtained via the collagenase digest method and in accordance with the findings of other authors (Gronthos et al., 2000, Huang et al., 2006) it was decided to adopt this as the method of choice for DPSC harvesting and proliferation for future experiments.

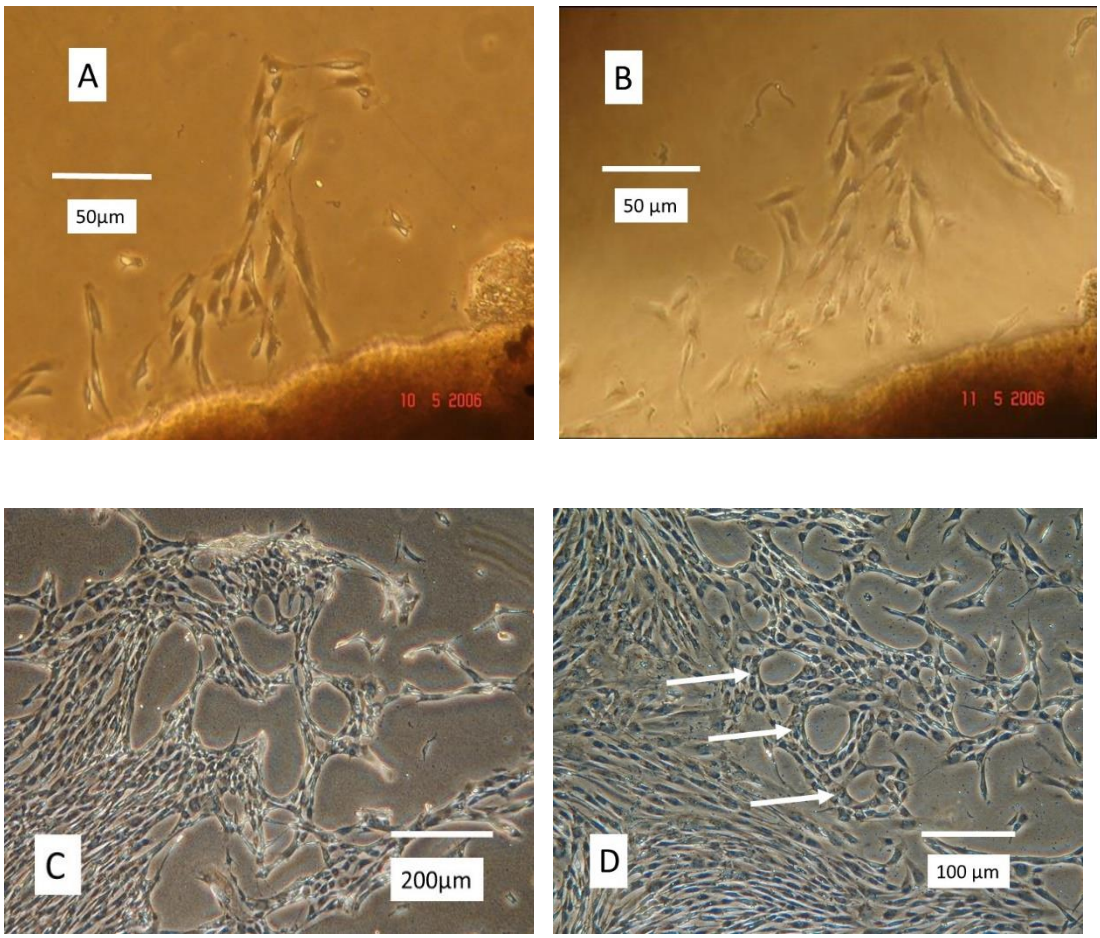

Figure 18. Comparing the proliferation of DPSCs obtained following the dental pulp explant method (A and B) and collagenase digest method (C and D) at the same time points.

Image A: DPSCs outgrowth from a dental pulp explant at day 14.

Image B: DPSCs outgrowth from same dental pulp explant at day 15 (24 hours later).

Image C: DPSCs proliferation following the collagenase digest method one week following P1, at day 14

Image D: DPSCs proliferation following the collagenase digestion method at day 15 (24 hours later). Note the circular/oval pattern of the DPSCs indicated by the white arrows, suggestive of vascular structures.

4.2 Site-specific expression of alkaline phosphatase activity by DPSCs *in vitro*

As part of a general characterisation of the DPSCs harvested from dental pulp explants, pulp explants from three donors were assessed to determine ALP staining as an indication of their osteogenic/calcification potential. Data from one individual is reported here. Again, there was variability in DPSC outgrowth from explants seen between donors and also between different regions of the dental pulp explants. Figure 19 shows site-specific ALP activity for cells outgrowing from different regions of the pulp sections. ALP positive staining was found in the lower coronal region of the pulp and the upper coronal region. Weak staining was observed in the corono-radicular, radicular and apical regions, with this last pulp fragment expressing no staining whatsoever. Figure 19 (A and B) shows obvious red-brown staining. Some weak staining was also visible in C and virtually no DPSC ALP activity towards the tooth apex (D and E). The sample consisting of the apical papilla tissue had proliferated so rapidly that the cells had become over-confluent during the culture period and were unusable. The rapidity of this proliferation was consistent with the findings of other investigators (Sonoyama et al., 2008) where SCAP cells were found to proliferate at a 2 to 3 fold greater rate than those from pulp organ cultures.

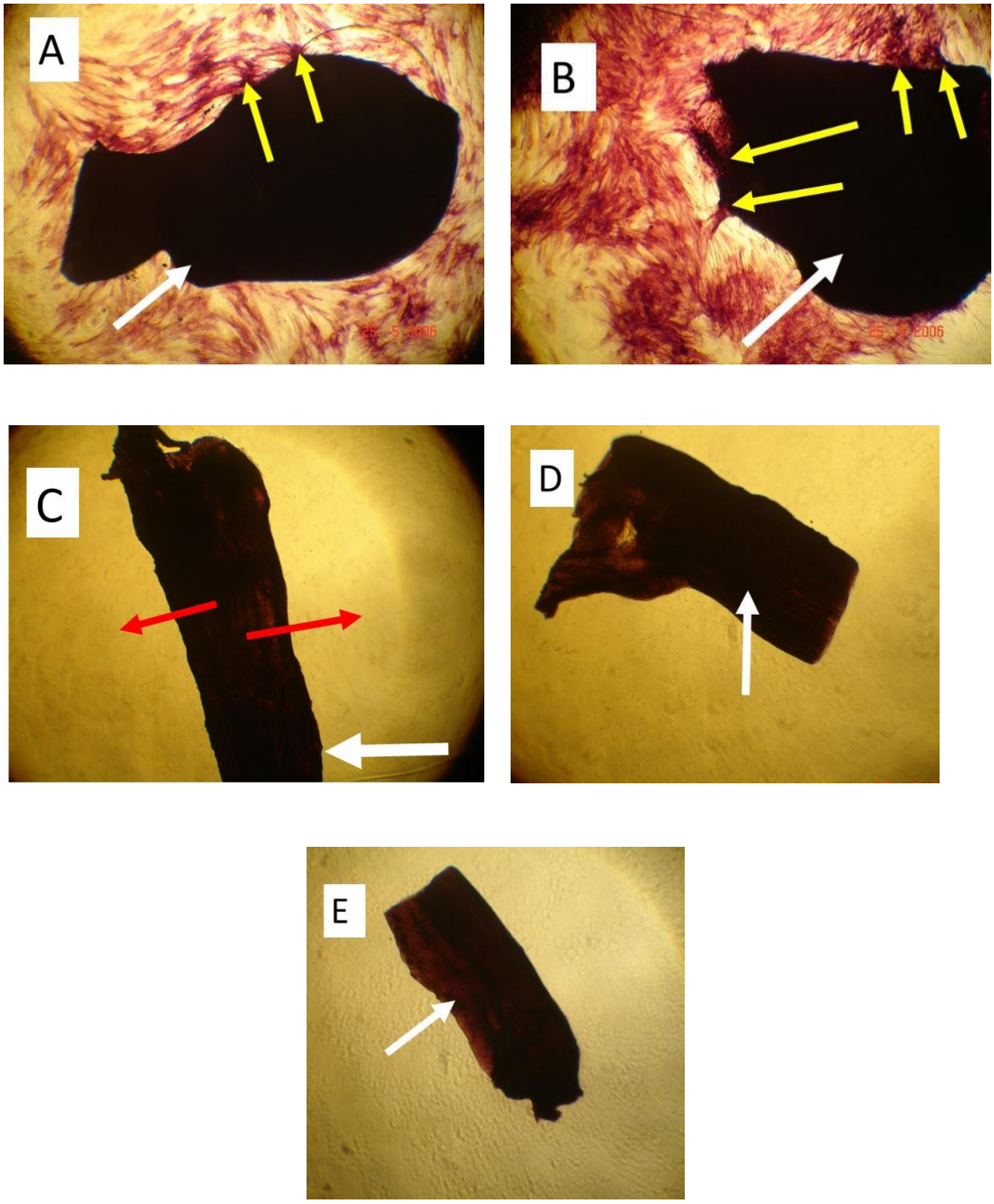

Figure 19. Site - specific ALP staining for cells growing out from the different regions of pulp tissue sections (size = approximately 3 mm each).

A = upper coronal pulp; B = lower coronal pulp; C = upper radicular pulp; D = radicular pulp; E = apical pulp. ALP activity was highest at the growth nodes seen in (B) (yellow arrows), followed by (A), then (C) which was very weak (red arrows), then (D) then (E) with these latter two images showing virtually no positive staining for ALP. White arrow indicates the dental pulp explant in all images.

4.3 Cytocompatability of HyA scaffolds

4.3 1 Cytocompatability of HyA scaffolds with G292 cells as control

G292 cells were cultured on different concentrations of HyA gel as a positive control to ensure scaffold cytocompatibility. After one week of culture in αMEM/10%FCS, G292 cell growth on GenGiGel® scaffolds was examined using light microscopy. Crystalline-like nodule formation, which could represent mineralise deposition (see below) was observed at the two higher GenGiGel® concentrations (0.6 % and 0.8 %) but not in the two lower concentrations of gels (0.2 % and 0.4 %, data not shown). The more obvious nodular growth in 0.8% HyA is shown in Figure 20. Figure 20 (A) shows a group of three nodules, the upper two are out of the plane of focus but a more detailed image of the colony can be seen in the lower right of the image (see white arrows). Figure 20 (B) shows the larger more obvious colony from (A), with fine hair-like growth in the bottom left (see white arrow) and the rest of the colony gradually moving out of focus, indicating a 3D growth pattern within the GenGiGel® structure.

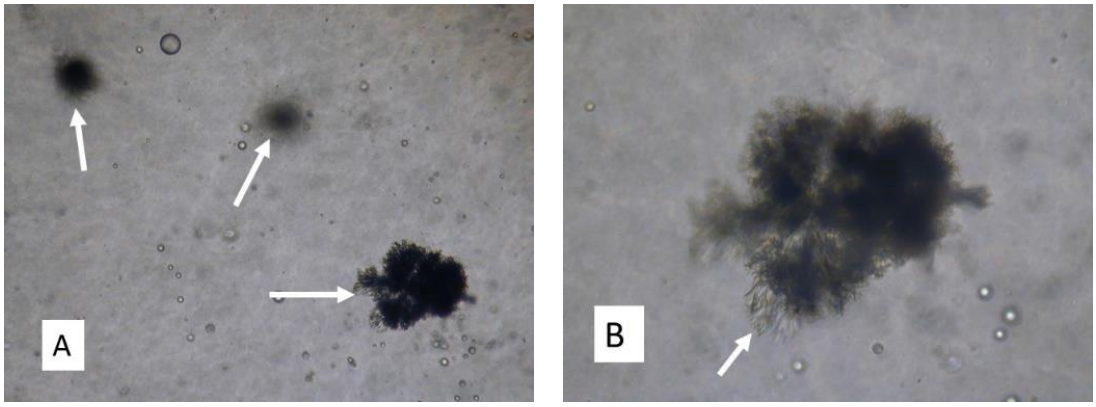

Figure 20. G292 osteosarcoma cell growth on/in 0.8% GenGiGel®.

White arrow shows the crystal-like nodule formation in both images. Image A: magnification: x100. Image B: magnification x400.

4.3.2 DPSCs grown on 2% and 4% HyA gel

Following the data obtained from the G292 cells' culture on HyA gel which indicated good biocompatibility, further experiments using DPSCs were carried out (see Figure 21A and B). There were morphological differences visible between the DPSCs grown on each gel concentration with the 2% gel showing cells exhibiting a more elongated morphology (Figure 21 A) and the higher 4% concentration resulting in cells with shorter cell bodies. This was possibly associated with the increased viscosity of the HyA gel acting in a motility inhibiting fashion, a higher sodium concentration (the HyA was of the sodium salt) or simply a higher concentration of higher molecular weight molecules being present in the gel structure, given that GenGiGel is a high MW gel. This might suggest that higher concentrations of high MW HyA could have an effect on DPSC morphology. Intriguingly, some cells at the periphery of the culture, away from the main cell colony, exhibited a columnar phenotype with long processes, but still with much shortened cell bodies. However, other cells away from the main colony also exhibited a fibroblastic morphology (Figure 21(B)). This is similar to results by other authors (Couble et al., 2000) who noted differences in DPSC phenotype in the presence of βGP in the culture medium, with polygonal cells present centrally and elongated cells present on the periphery of the culture. This could imply that the HyA gel not only has an effect related to its MW but that it could also be concentration and therefore dose-dependent.

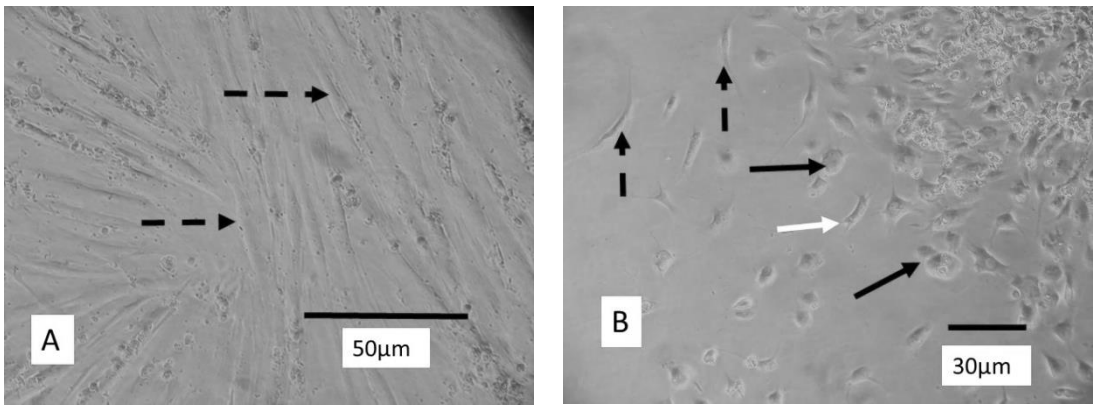

Figure 21. DPSCs grown on different concentrations of HyA (GenGiGel).

A: DPSCs showed fibroblast-like phenotype when cultured for one week on 2% GenGiGel in DMEM/10% FCS based upon their morphological appearance under light microscopy. Elongated cell bodies and multiple processes were present throughout all fields of view.

B: DPSCs cultured on the stiffer, more rigid 4 % gels showed a much more rounded/polygonal cell phenotype after 7 days (Figure 22 (B)).

4.4 DPSCs grown on ivory block scaffolds

It was intended to eventually adopt the tooth slice model (Goncalves et al., 2007, Mullane et al., 2008, Sloan et al., 1998) incorporating other elements of scaffold material, as the experimental model of choice within this thesis. For initial studies, ivory blocks were utilised to overcome a short term shortage in tooth availability from the Tissue Bank as ivory has a very similar chemical composition to dentine (Locke, 2008). DPSCs were seeded at a density of 10^5 cells per block onto sections of ivory block scaffolds which had been prepared as described in section 3.11.1.

As can be seen in Figure 22, the DPSCs were seen to attach, colonise and proliferate successfully on the surface of the ivory blocks after 7 days of culture in DMEM/10% FCS. The cells appeared to be aligned on the ivory surface, with the alignment most likely reflecting the micro or nanotopography of the scaffold substrate. The strong green background staining evident in Figure 22 was seen whenever a collagen-based scaffold of any type was used and stained with 5-CMFDA (see also Figures 25 (A) and (B), section 4.6). However, DPSCs were clearly visible against the background.

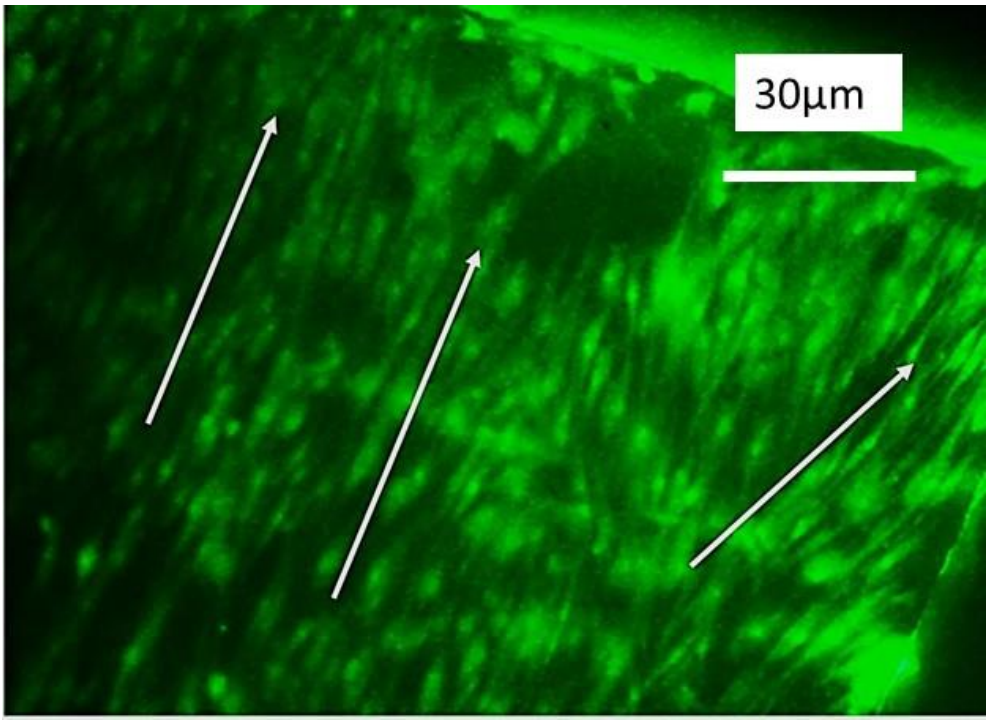

Figure 22. Fluorescent image of DPSCs, labelled with 5-CMFDA, grown on ivory blocks.

The image shows viable DPSCs apparently aligned on the ivory surface, after 7 days of culture in DMEM/10%FCS. Arrows show the approximate direction of the alignment.

4.5 DPSCs grown on biodegradable 45S5 Bioglass® matrices

Following culture to assess ALP activity, DPSCs were cultured on three different concentrations of Bioglass® scaffolds to examine their potential for collagen and glycosaminoglycan/aggrecan deposition on these scaffolds using histological methods. DPSCs were examined after 12 weeks, experiments of shorter time span having failed to show any histological changes. After being stopped and stained as described in section 3.11.2, Sirius Red and Alcian Blue staining showed that more extensive red staining was observed in the 0% and 40% Bioglass® scaffolds compared to that of the 5% Bioglass® scaffold (see Figure 23), although evidence of red staining was seen in all three samples. This indicates more collagen matrix deposition on the 0% and 40% Bioglass® samples. The 5% Bioglass scaffold, showed more blue staining, suggesting greater deposition of glycosaminoglycan/aggrecan, considered a precursor to cartilaginous tissue deposition.

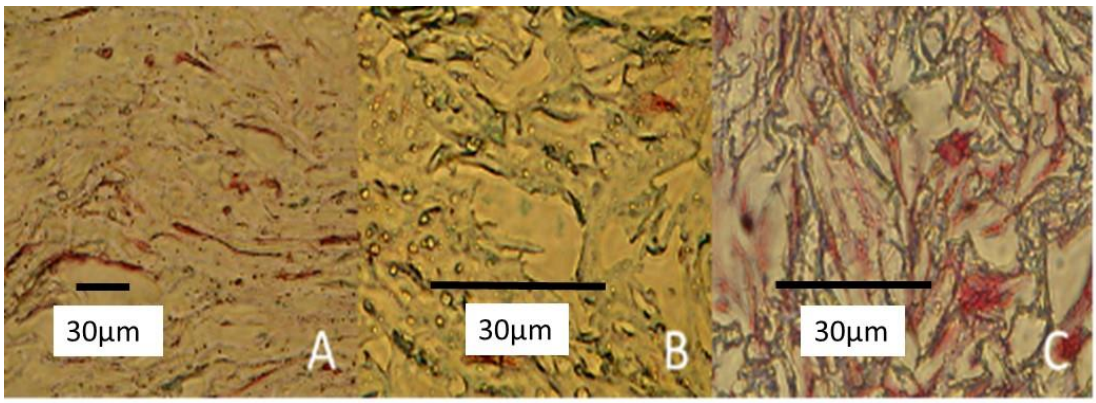

Figure 23. Sirius Red/Alcian Blue staining of DPSCs on different concentrations of Bioglass®.

A: 0% Bioglass scaffold; B: 5% Bioglass scaffold; C: 40% Bioglass scaffold. Red colour indicates presence of collagen as suggested by Sirius Red staining. Blue colouration indicates the presence of possible cartilage precursor material.

4.6 The viability of DPSCs grown on Osseoguard® and BioGide® Type I and III collagen membranes

In order to confirm the viability of DPSCs grown on the two Type I and III collagen membranes, DPSCs were seeded onto them as described in section 3.11.4 and labelled with 5-CMFDA after 7 days of culture. Figures 24 (A) and (B) show DPSCs (bright fluorescent green colour) at 7 days post-cell seeding on both membranes. Images were taken under a fluorescent inverted microscope, indicating strong uptake of 5-CMFDA representing their continuing viability and potential for proliferation, as non-vital cells do not take up the dye. The increased fluorescence at the lower edge of the scaffold in image (B) indicated DPSCs permeating through the thickness of scaffold and not just adherent to the seeded surface. There was no obvious difference in cell fluorescence between either scaffold, suggesting equal viability.

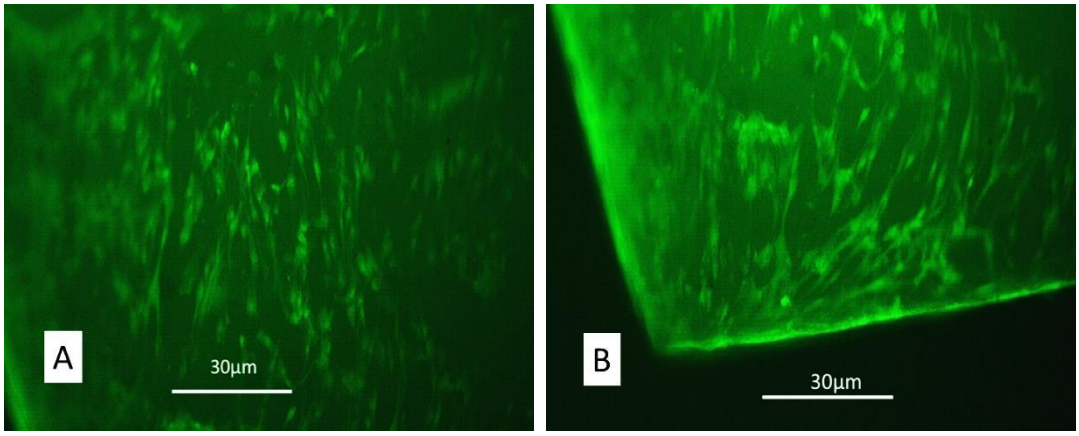

Figure 24. Fluorescent images showing viable 5-CMFDA labelled DPSCs on 3D scaffolds.

Following culture in DMEM/10% FCS for 7 days, both A: Osseoguard® and B: BioGide® show good colonisation by the DPSCs.

4.7 Examination of unseeded Osseoguard® and BioGide® Type I and III collagen membranes by SEM and FEGSEM imaging

4.7.1 Osseoguard® Type I and III collagen membrane

Two Type I and III collagen based scaffold materials were examined as described in section 3.11.3, under SEM and FEGSEM to assess their suitability as the collagenous/fibrillar component of the ECM-type construct. Having been coated in gold (for SEM images) or platinum (for FEGSEM images) in an inert argon gas atmosphere, the samples of Osseoguard® Type I and III collagen membrane were imaged to identify any pattern in their structure. The SEM image shown in Figure 25 (A) shows the upper surface of a sample of Osseoguard® membrane material with the characteristic embossed "zig-zag" pattern, designating the 'open,' 'up' or outer side of the membrane during clinical use (i.e. that which the cells would not be expected to directly colonise *into*, rather a surface which they would be expected to proliferate, populate and colonise *over*). There are also some pieces of extraneous unembossed material left behind during the manufacturing process seen in the image. Figure 25 (B) shows the cut edge of the Osseoguard® Type I and III collagen material, showing the upper surface of the cut material off to the top right hand side with the interior of the material showing an unorganised, random spongiform-like appearance with niches potentially suitable for cell attachment, growth and proliferation. The higher magnification FEGSEM image (Figure 25 (C)) shows the ultrastructure of the Osseoguard® Type I and III collagen membrane material with an apparently random arrangement of the collagen fibrils of varying size and degree of intertwining, which exhibited collagen banding at approximately 65 nm.

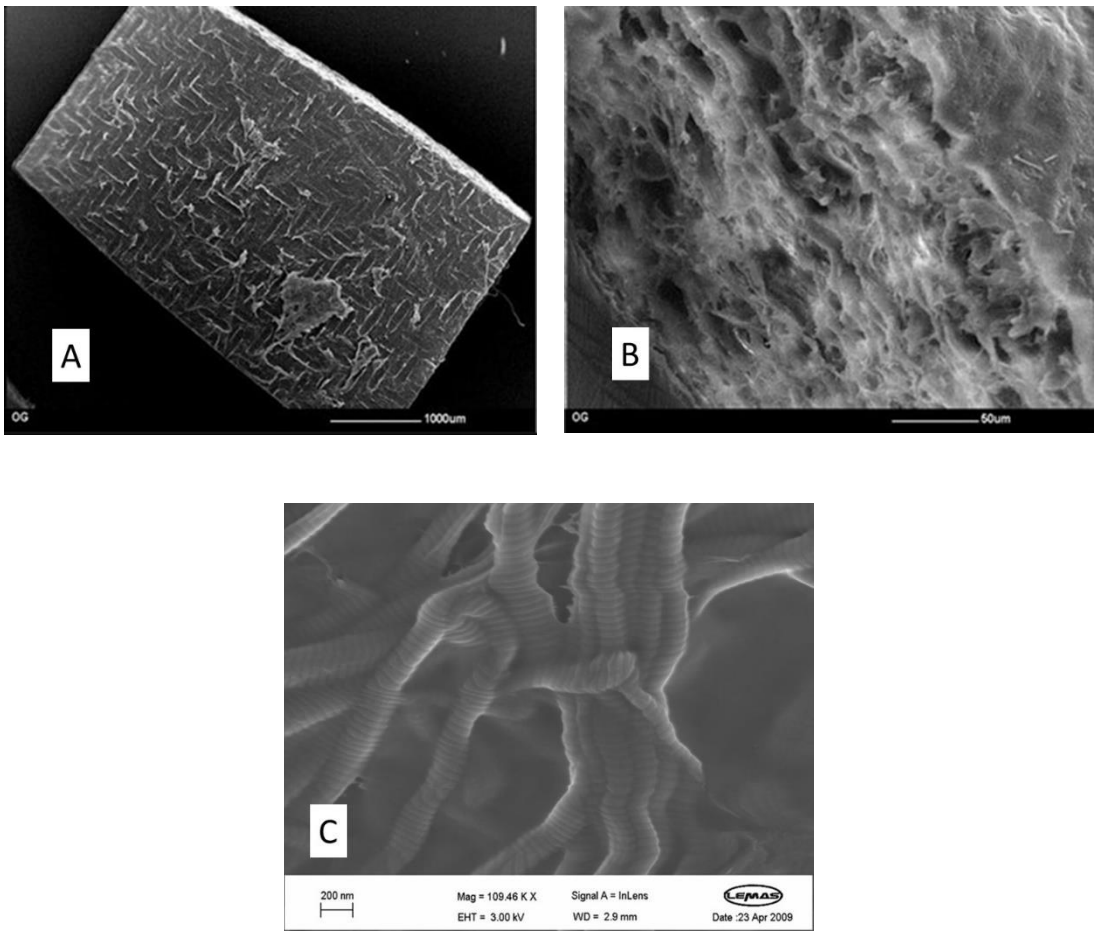

Figure 25. SEM images (A and B) and a FEGSEM image (C), showing the structure of Osseoguard® Type I and III collagen membrane.

A: gross low power view of the top surface of the Osseoguard® membrane material. B: lateral view of the cut edge and upper surface of the Osseoguard® membrane material and C: high resolution image of the Osseoguard® membrane material showing cross banded collagen fibrils. Scale bars shown at the bottom of all the images.

4.7.2 BioGide® Type I and III collagen membrane

Figure 26 (A) shows the gross SEM appearance of the upper surface of the BioGide® Type I and III collagen membrane sample with the cut edge visible at the top edge. The word 'UP' is embossed on the surface. This is an attempt by the manufacturer to make it 'Dentist proof' and designate the side of the membrane which goes towards the outer surface of any wound during normal surgical usage where the cells would be expected to gradually populate and colonise *over* should it be exposed to an open environment, as opposed to *into*, which is the behaviour that any cells within the closed wound environment would be expected to exhibit. Figure 26 (B) shows a higher power view of the BioGide® Type I and III collagen membrane material, demonstrating the random arrangement of collagen fibres with gaps and niches suitable for cell attachment, colonisation, proliferation and differentiation. Figure 26 (C) shows an ultra-high resolution image of the BioGide® Type I and III collagen membrane material with a random arrangement of the collagen fibrils which are exhibiting collagen banding at approximately 65 nm.

The gross, micro- and ultrastructure of both Osseoguard® and BioGide® membranes were near-identical. Although Type III collagen might be expected to be obvious from its' finer structure (smaller diameter fibrils), very few of its' microfibrils were apparent in either membrane. Both membranes showed good pore size of between 50 to 300 µm and porosity (Murphy et al., 2010, Murphy and O'Brien, 2010) which is essential for the dissemination of gases and nutrients as well as expulsion of waste products and providing suitable niches for cell binding, attachment, colonisation, migration, proliferation and differentiation, whilst at the same time avoiding the aggregations of cells at the scaffold edges, which can occur with smaller pore size

scaffolds (O'Brien, 2011). This indicates that both/either would be suitable for future investigation as biomimetic matrices for seeding, attachment and proliferation of DPSCs in this study.

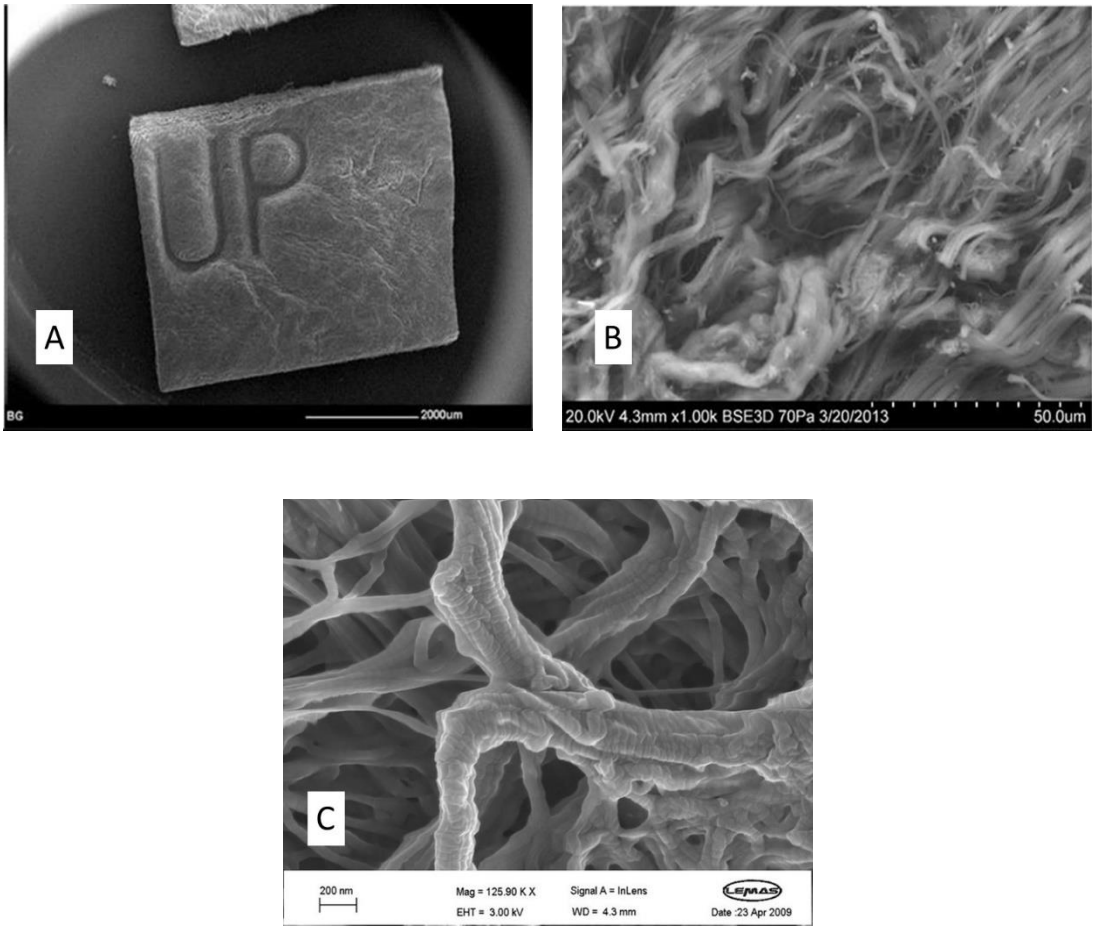

Figure 26. SEM images (A and B) and a FEGSEM image (C) showing the structure of BioGide® Type I and III collagen membrane.

A: shows the gross (low power) view of the top of the BioGide® Type I and III collagen membrane, B: lateral view of the cut edge of the BioGide® material and C: high resolution image of the BioGide® membrane material showing cross banded collagen fibrils (cf . Osseoguard® Figure 24 (C). Scale bars shown at the bottom of all the images.

4.8 Ultrastructural appearance of DPSCs grown *in vitro* on Type I and III collagen membranes in DMEM/10%FCS

4.8.1 DPSCs grown on Osseoguard® Type I and III collagen membrane *in vitro*

DPSCs were cultured on 25mm^2 Osseoguard® membrane samples for 14 days in DMEM/10%FCS, as described in section 3.11.4 to ascertain the membrane's suitability to facilitate DPSC attachment, colonisation, proliferation and differentiation, all of which would be necessary for success as a putative scaffold material. Figure 27 (A) shows an area of approximately 0.36 mm^2 of the Osseoguard® membrane as seen in the SEM. Elements of the gross structure of the membrane were visible with a background of DPSCs apparently embedded in matrix which they had produced. Several groups of cells were visible bridging across gaps, as indicated by the white arrows. Figure 27 (B) shows a high power view of the same area, approximately 0.046 mm^2 showing the cell density more obviously than Figure 27 (A) but again with an extensive area of DPSCs embedded in their own matrix. Figure 27 (C) shows a close up of the cells from images (A) and (B), in an area of approximately 0.004 mm^2. This shows the cells exhibiting a mixed fibroblast/myofibroblastic morphology with some structural features such as fenestrations, attachment 'feet' or focal adhesions and filopodia apparent.

These images confirmed that the Osseoguard® Type I and III collagen membrane was capable of supporting the attachment, colonisation and proliferation of DPSCs over a period of 14 days, enabling them to produce their own extracellular matrix materials with pores and gapping between the cells and cell layers to allow the through flow of nutrients and O_2.

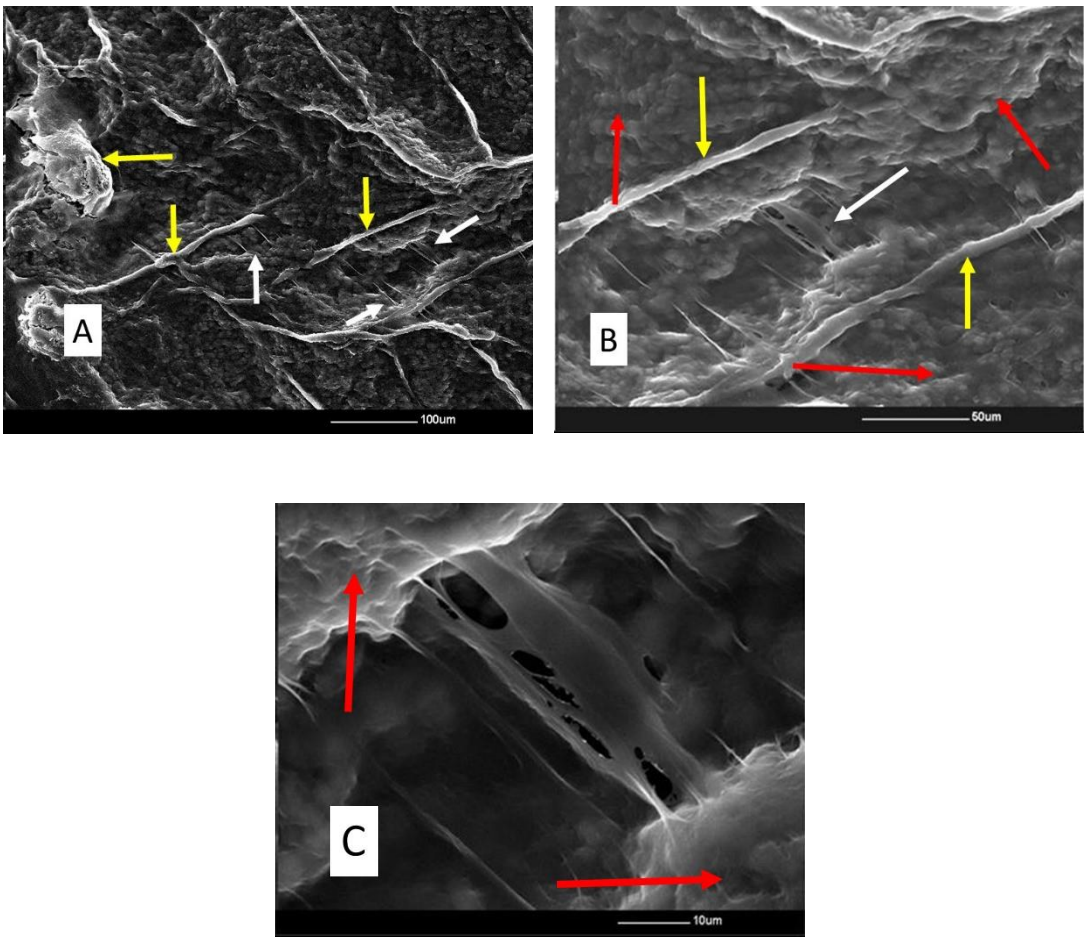

Figure 27. SEM images of DPSCs growth on Osseoguard® Type I and III collagen membrane after 24 days of culture in DMEM/10%FCS.

A: low power view of DPSCs on the Osseoguard® membrane showing structural elements of the scaffold material indicated by the yellow arrows and various groupings of DPSCs, indicated by the white arrows. B: higher power image of the right side of the field in (A) with cells covered in matrix. C: further higher power image detailing individual DPSCs seen here bridging the gaps between scaffold fibres. DPSCs embedded in own matrix indicated by red arrows. Scale at the bottom of the images.

4.8.2 DPSCs grown on BioGide® Type I and III collagen membrane *in vitro*

To decide which Type I and III collagen membrane would be the final choice and as a comparator for Osseoguard®, DPSCs were also cultured on 25mm^2 BioGide® Type I and III collagen membrane samples as described in section 3.11.4. Figure 28 (A) shows an extended grouping of apparently less mature cells in area of cells embedded in their own extracellular matrix. These less mature or 'new' cells are most likely to have derived from other cells *in situ* or they could have migrated there from elsewhere on the scaffold material. They show little or no evidence of alignment with the other cells or matrix production. Figure 28 (B) shows detail of a cell indicated from the bottom centre of image (A), exhibiting an irregular cuboidal morphology with an approximate cell length of 10 μm. Immediately above it is another 'new' cell, this time showing a different 'J'-shaped morphology and above that, a small clump of 'new' oval cells. None of these cells are exhibiting any evidence of any matrix deposition at this stage, although all the other established cells are, as can be seen elsewhere. Figure 28 (C) shows detail of a cell indicated in the top left region of image (A), apparently assuming a differing morphology and commencing matrix deposition as it gradually aligns with the adjacent cells. The outline of the cells in the background can be seen through their blanket of matrix.

Figure 28 (D) shows a colony of cells. The cell to the left of the central pair (indicated by the white arrows) exhibits less matrix deposition. The cell on the right of the pair exhibits more matrix deposition and both this cell and another third cell to the left of this pair (lower to the left in the image) can be seen to be extruding some material (indicated by the yellow arrows) through a pore in the cell membrane.

Overall, these images appear to show that DPSCs can attach, colonise, proliferate, align and thrive sufficiently over the duration of the culture period to produce their own matrix on BioGide® Type I and III collagen membrane with pores and gapping between the cells and cell layers that would allow the permeation of nutrients and O_2 as well as the dispersal of waste products. Their colonisation can be compared with the unseeded material in Section 4.7.2 and also the image in Figure 28 (E).

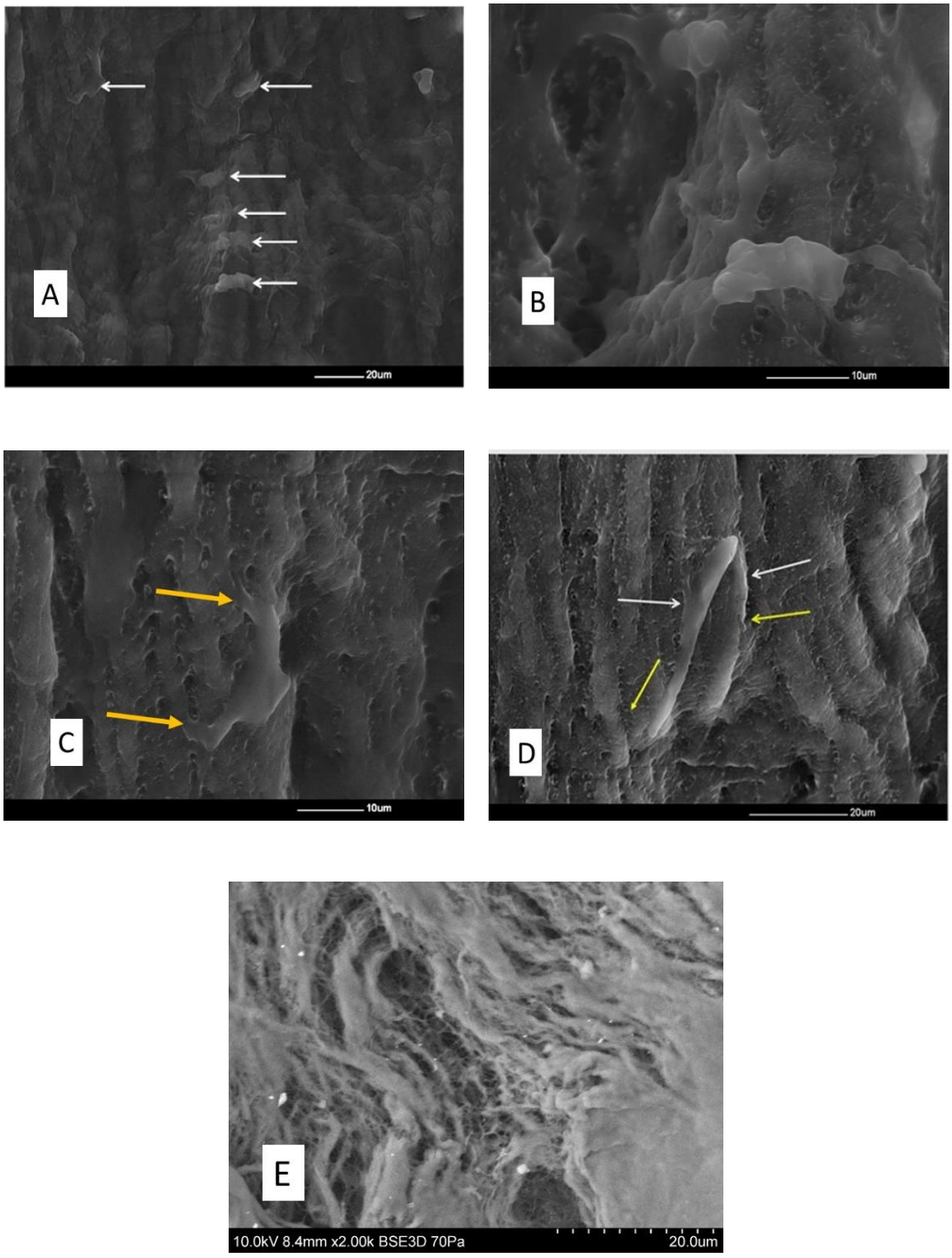

Figure 28. SEM images showing DPSCs growth on BioGide® Type I and III collagen membrane after 14 days of culture in DMEM/10% FCS.

4.9 Appearance of DPSCs grown on Osseoguard® and BioGide® Type I and III collagen membranes in the confocal microscope

4.9.1 DPSCs examined at 7 days post seeding

After 7 days of attachment and culture, Figure 29 (A and B) shows DPSCs with strong uptake of 5-CMFDA and TOPRO indicating their continuing viability at the time of staining and presumed potential for proliferation had culture been allowed to continue. The images show snapshots of z-stacks taken on the confocal microscope to show the depth of penetration of the DPSCs after 7 days in culture in DMEM/10% FCS. There appeared to be no obvious differences seen between the scaffolds, with both scaffolds showing cells several layers deep, confirming that cells survival in the deeper, potentially nutrient poor parts of the scaffold material.

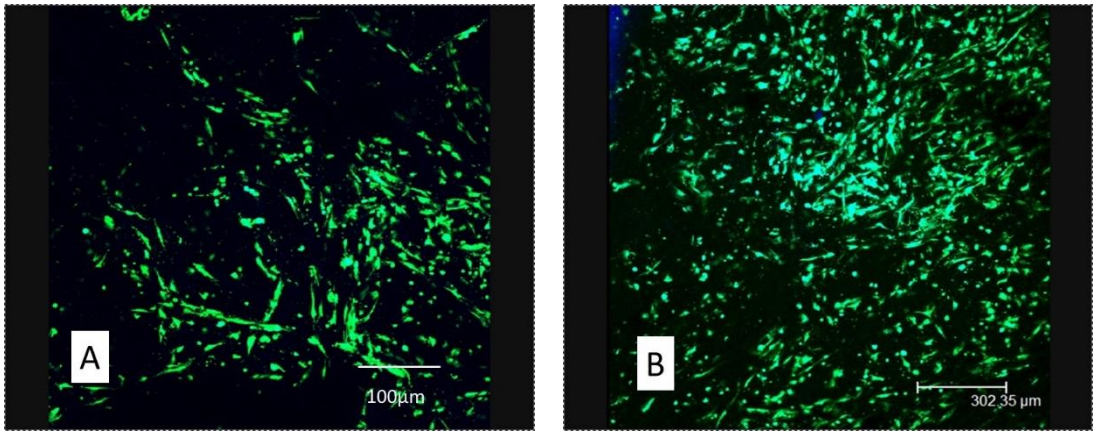

Figure 29. Confocal laser scanning microscope images of DPSCs on (A) Osseoguard® and (B) BioGide® Type I and III collagen membranes. Both images show viable DPSCs penetrating towards the deeper parts of each membrane. Scale at the bottom of each image.

4.9.2 DPSCs examined at 28 days post seeding

Figure 30 (A and B) shows DPSCs cultured in DMEM/10% FCS in 3D Osseoguard® and BioGide® Type I and III collagen membrane scaffolds at 28 days post-seeding with viable cells being stained with Acridine Orange and HCS CellMask™ Deep Red dye, showing strong uptake of these stains and the extent of colonisation and proliferation in both scaffold materials. Both images are from a series of z-stacks taken on the confocal microscope to show the depth of penetration of the DPSCs within both scaffolds after 28 days culture. Both scaffolds exhibited cells several layers deep, confirming that cells could survive in the deeper, potentially nutrient poor parts of the scaffold. It was noted that there were many fewer (if any) gaps between the DPSCs on both scaffolds at this stage of the experiment as the culture period had gone on for 21 days longer than the seven days in Section 4.9.1, Figure 29, where larger numbers of gaps were seen. There were also DPSCs out of focus in parts of both images which are not able to be shown in a snapshot image (areas seen as dark patches). Also, the cells appeared to be more aligned on the Osseoguard® sample compared with the BioGide® although there is apparently an area of uncolonised BioGide® scaffold (the green mesh-like region) in Figure 30 (B). This could be down to one of several reasons such as failure of stain uptake or non-attachment and proliferation of the DPSCs during the seeding procedure, although close examination of Figure 30 (B) does show Acridine Orange stained nuclei within the centre of the green mesh field, indicating failure of stain uptake as the more likely cause.

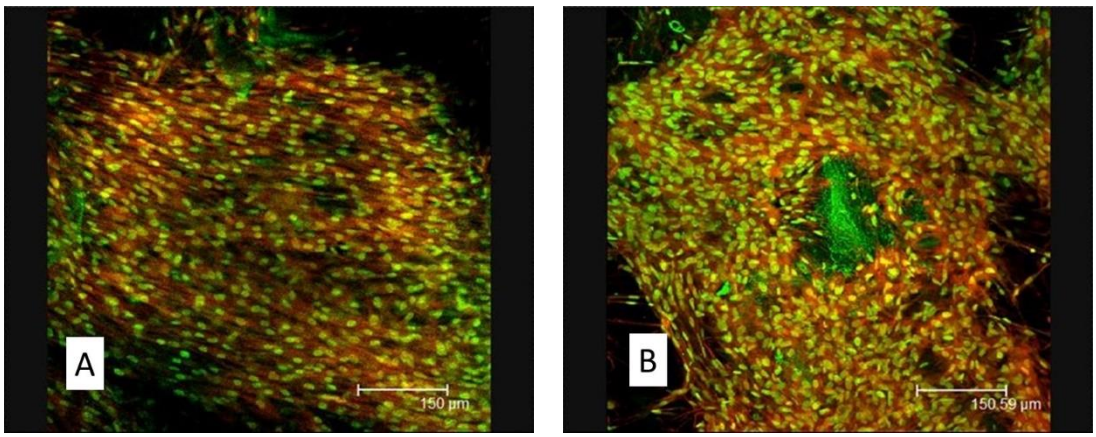

Figure 30. Confocal laser scanning microscope images showing DPSCs growth on (A) Osseoguard® and (B) BioGide® Type I and III collagen membranes after 28 days of culture.

(A) and (B) show extensive colonisation of both scaffolds. Scale shown at the bottom right of each image.

4.10 Measurement of DPSC proliferation on BioGide® Type I and III collagen scaffold membranes using the PicoGreen® method

In order to quantitatively determine DPSC proliferation on BioGide® Type I and III collagen scaffolds, DNA was measured using a PicoGreen® assay at a range of time points, as described in section 3.13. Statistical analysis was carried out by a 1-way ANOVA calculation using Microsoft Excel software. Figure 31 shows the DNA standard calibration curve.

This type of standard curve shown in Figure 31 was used to quantify DNA recovered from DPSCs seeded onto 25 mm^2 sections of BioGide® Type I and III collagen membrane at days 5, 10 and 15 following seeding, as a measure of cell numbers.

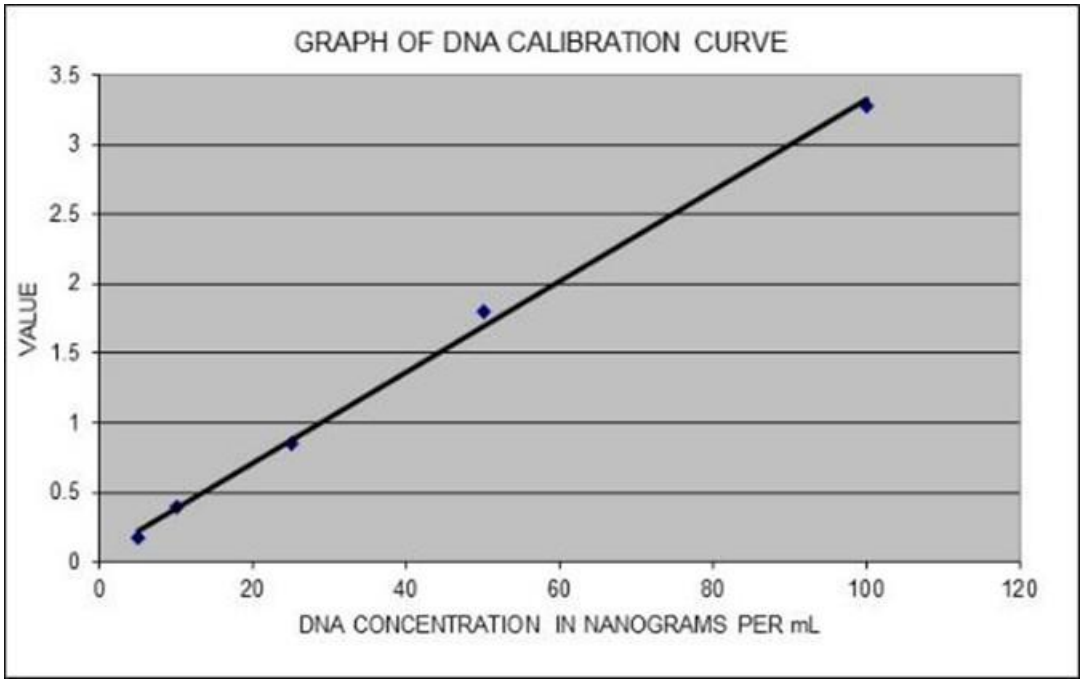

Figure 31. Calibration curve for DNA quantification.

The bar chart in Figure 32 shows that the numbers of cells present in the scaffold increased progressively with time, indicating that the membrane supported DPSCs growth, allowing them to proliferate throughout the time period examined.

However, statistical analysis showed that although there was an apparent increase between day 5 and day 10, it was not statistically significant, with $p = 0.102$. The increase in detectable DNA between day 5 and day 15 was statistically significant, with $p < 0.0001$ and the increase in measurable DNA between days 10 and day 15 was statistically significant with $p<0.0001$.

The more precise values obtained by the calculations are displayed in table 4.

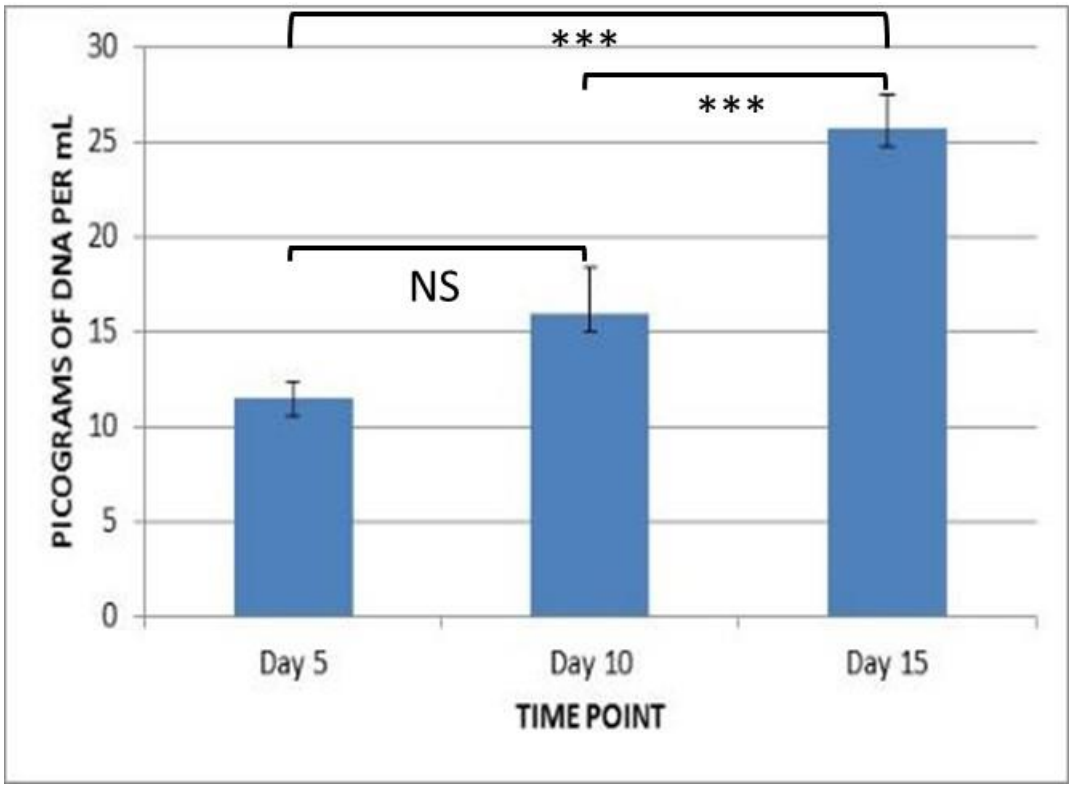

Figure 32. Bar chart showing total of measurable DNA obtained from DPSCs grown on BioGide® Type I and III collagen scaffolds.

DNA was measured at days 5, 10 and 15 using a PicoGreen assay. NS: $p > 0.05$; ***: $p \leq 0.001$. n=9

TABLE 4: Statistical analysis of measurable DNA at days 5, 10 and 15.

Table showing the precise values obtained by statistical analysis.

Groups	Adjusted p value
Day 5 compared with day 10	0.101712
Day 5 compared with day 15	0.000047
Day 10 compared with day 15	0.000195

4.11 H&E Histological staining of DPSCs on BioGide® Type I and III collagen membranes in DMEM/10% FCS

Given the data shown in sections 4.8 and 4.9, it was decided that as neither scaffold material showed any discernible difference from the other and that both had shown good support for DPSCs attachment, colonisation and some evidence of proliferation, further work would proceed using BioGide® Type I and III collagen membrane as there were fewer issues with supply since the material was available cheaply, at short notice and could be both stored and sterilised easily after opening. Figure 33 (A) shows a histological section, stained with H&E, of BioGide® Type I and III membrane scaffold (white arrows) with DPSC ingrowths (yellow arrows) showing cell attachment and colonisation. The matrix deposited by the DPSCs stained pale purple-pink with the scaffold material staining a darker shade of the same colour and showing a coarser-structured ribbon-like appearance.

Figures 33 (B and C) revealed what appeared to be deposition of an extracellular matrix material within the scaffold and attachment of DPSCs to the membrane itself (Figure 33 (D).

A higher power oil immersion image revealed nuclei around circular/oval regions as shown in Figure 33 (D). Taken together, these data suggest that DPSCs can attach to the membrane, continue to grow and to successfully proliferate over a period of 28 days producing a fine extracellular matrix material (see areas indicated by yellow arrows in Figure 33 (A)).

Of particular interest were the areas where small irregular and sometimes oval void areas had formed. These superficially resembled vascular structures in appearance,

with cell nuclei next to what would be the putative vessel lumen. These can be seen in all of the images, most commonly within areas of matrix deposition but also within the scaffold material itself and were more apparent in the higher magnification views. Their presence led to the next avenue of investigation in section 4.12.

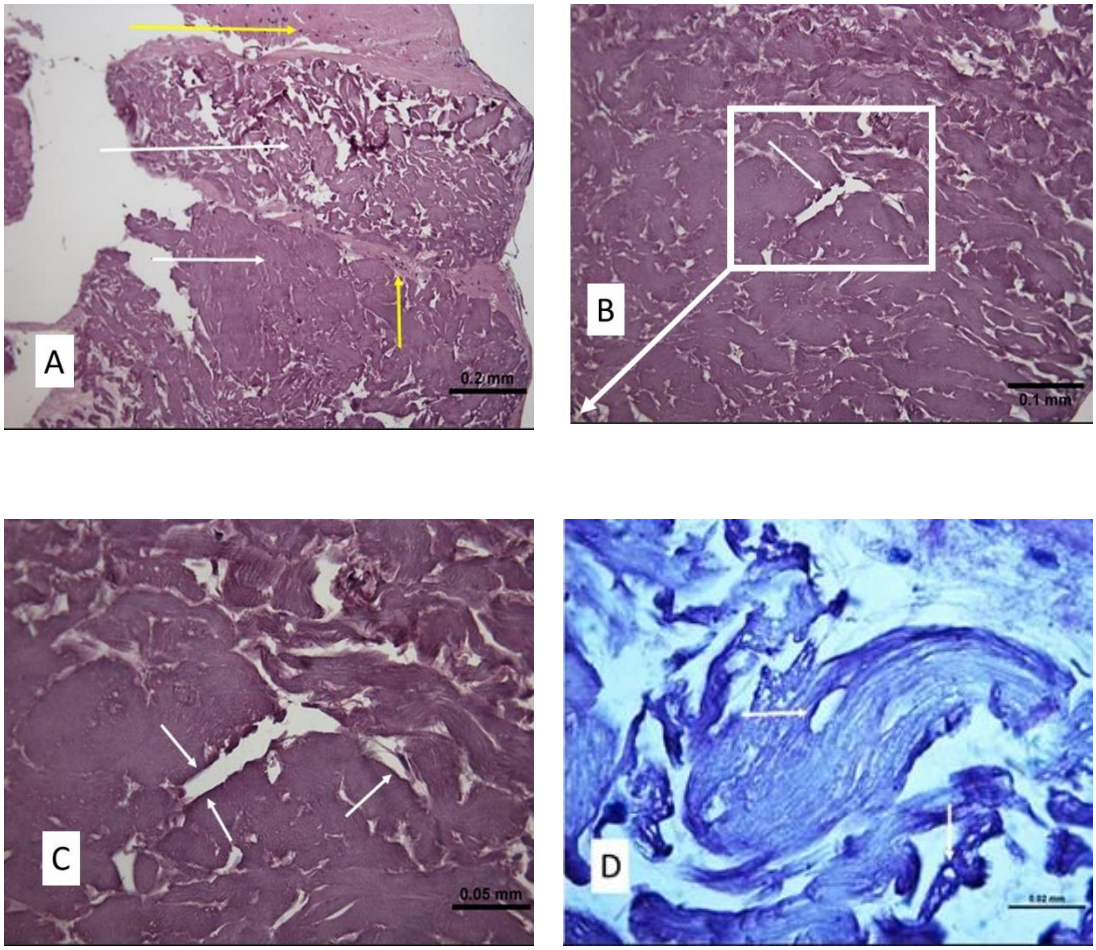

Figure 33. H&E staining showing DPSC growth on BioGide® Type I and III collagen membrane.

A: DPSCs and matrix ingrowths (indicated by the yellow arrows) into the BioGide® membrane. B: area with DPSCs surrounding an area of void or lumen (indicated by the white arrows) with their nuclei prominent into the same. C: same region under higher power with the putative vascular areas indicated by the white arrows. D: oil immersion image showing DPSCs and their deposited matrix. The central void oval area indicated by the white arrow inside the area of deposited matrix would be approximately the size of a capillary. Scale bars in millimetres at the lower right corner of the images.

4.12 Immunolocalisation of angiogenic markers expressed by DPSCs on BioGide® Type I and III collagen scaffolds

Consequent to the findings in section 4.11. it was decided to investigate whether the oval and irregular lumen-like structures were actually neo-vascular. Immunohistochemistry was carried out to determine if they would stain positively for angiogenic markers. Figure 34 shows immunostaining of DPSCs cultured on Type I and III collagen membranes in αMEM/10% FCS, stained for CD31 and CD34 markers. There was no evidence of any positive staining on any of the sections or the negative control. In contrast, the positive control (dental pulp) sections (Figure 35 (B and C)) all showed positive staining for the markers. This suggests that there had been no early angiogenic change in the DPSCs cultured on the scaffolds at 14 days. However, there was evidence of some matrix deposition by the DPSCs (the fine hair-like strands).

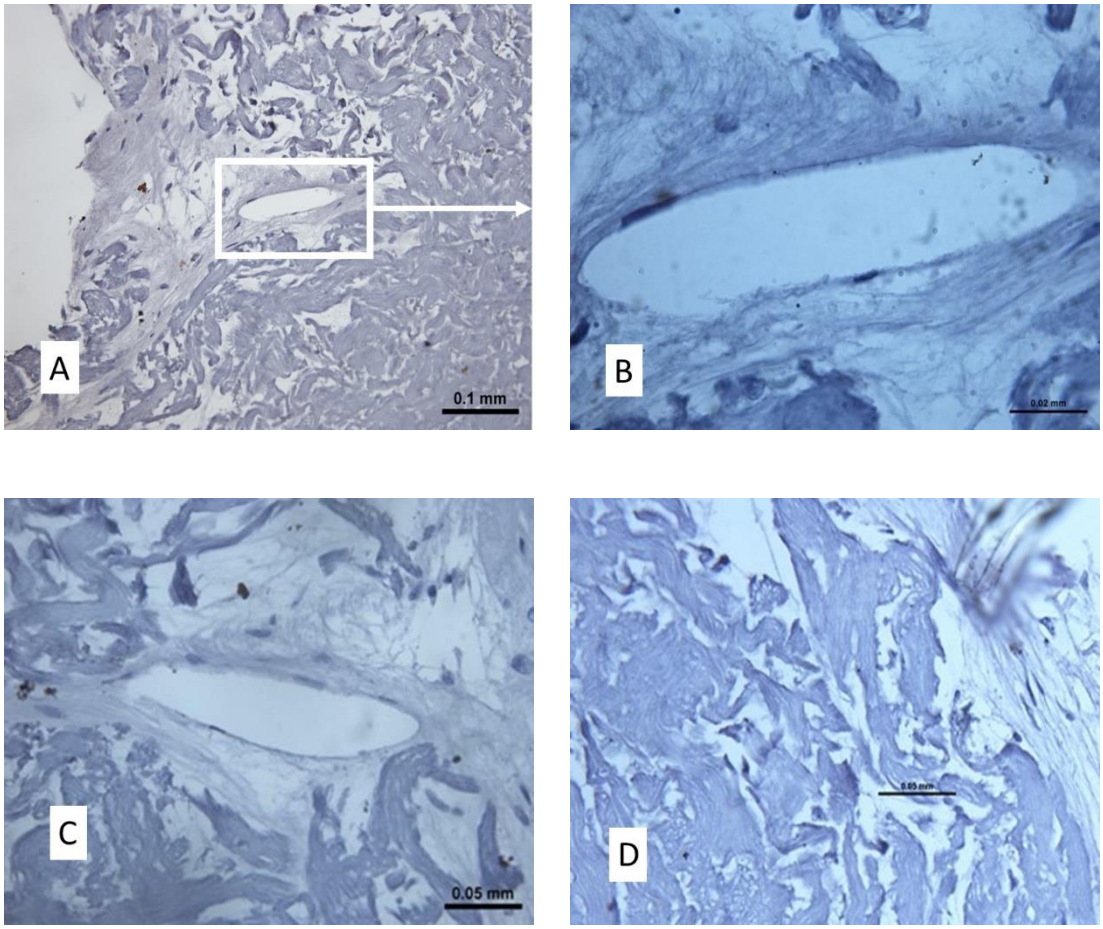

Figure 34. CD31 and CD34 immunohistochemical staining of DPSCs on BioGide® Type I and III collagen membrane.

A: staining for CD31. B: staining for CD31 (magnified view of image A). C: negative control (no 1st antibody). D: staining for CD34 of DPSCs on BioGide® Type I and III collagen membrane after 14 days of culture in αMEM/10% FCS. No positive staining was detected in any of these samples.

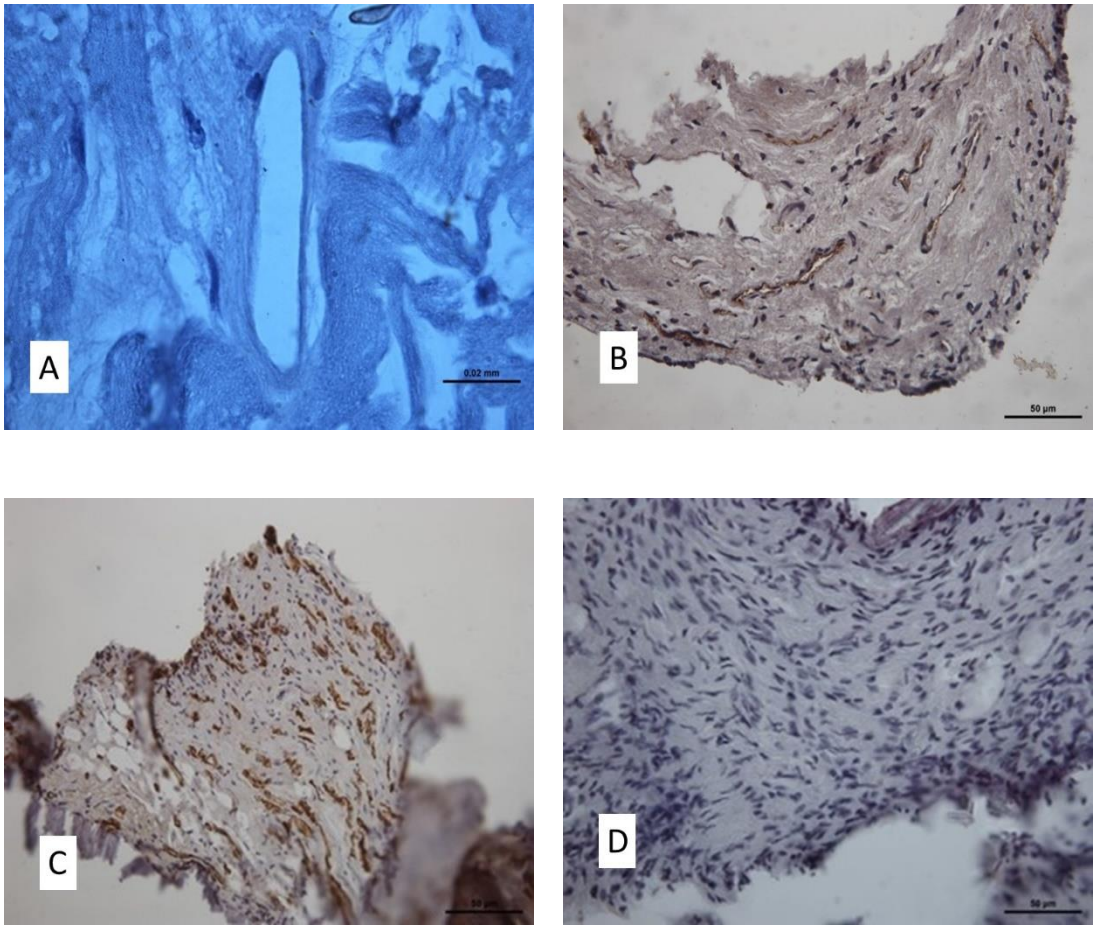

Figure 35. Negative and positive controls used for immunohistochemical staining for CD31 and CD34 antibodies.

A: CD31 negative control (no 1st antibody) for DPSCs on BioGide®. B: positive control (dental pulp section) staining strongly for CD31. C: positive control (dental pulp section) staining strongly for CD34. D: CD34 negative control dental pulp section without 1st antibody. Scale bars at bottom of images.

4.13 Immunostaining of STRO-1 and CD34 staining cells

The images in Figure 36 were taken from consecutive sections of the same dental pulp show the relative proximity of STRO-1 and CD34 positive staining cells. There is marked commonality of staining between the two biomarkers, with the staining patterns being almost identical. This correlates with CD34 being regarded as a marker for ‘precursor’ cells of various lineages as well as haematopoietic precursor cells. Note that despite the commonality of staining pattern between the two biomarkers, there is no evidence of any CD34 staining away from the immediate blood vessel vicinity, but there is definite evidence of positive staining to STRO-1 seen in image A in the surrounding perivascular tissue niche.

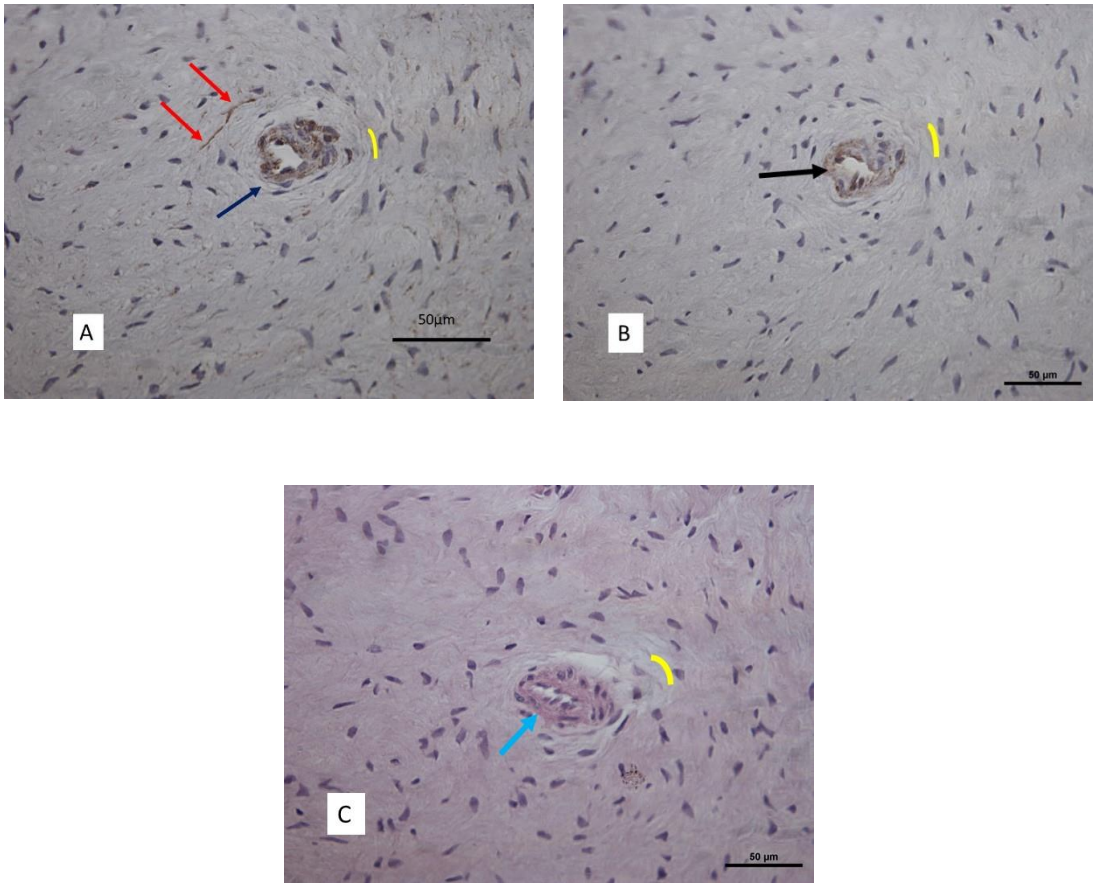

Figure 36. Staining of three consecutive control sections of dental pulp with STRO-1 stain (A), CD34 stain (B) and H&E stain (C).

A: blood vessel in dental pulp indicated by the blue arrow with cells staining strongly positive for STRO-1 antibody (in the perivascular niche, indicated by the red arrows in the top left of the image. The endothelial vessels have also stained strongly for STRO-1. The perivascular tissues are indicated by the yellow arc in each image.

B: consecutive microtome section to (A), immuno-stained for CD34 indicated by the black arrow. The endothelial cells stained strongly positive for CD34 antibody. Note no perivascular staining, with the perivascular tissues indicated by the yellow arc.

C: conventional H&E staining of next consecutive microtome section with blue arrow indicating the blood vessel.

Image C shows another section from the same blood vessel stained for H&E with the vessel walls staining strongly positive for H&E as indicated by the light blue arrow and the region of the perivascular tissues indicated by the yellow arc.

4.14 The effect of added $_{rh}VEGF_{165}$ on the expression of angiogenic markers by DPSCs and HUVECs on 1% collagen gels

As the DPSCs cultured on BioGide® Type I and III collagen scaffolds had not shown any evidence of markers for angiogenic change, it was decided to investigate if the presence of $_{rh}VEGF_{165}$ would have any effect on the expression of angiogenic markers in a collagen gel culture as can be seen in the following images comprising Figure 37. Collagen gel was chosen for these experiments in order to approximate more closely the culture conditions of the HyA gel component of the intended Type I and III collagen/HyA construct. EGM was chosen as the culture medium as it is recommended for cells expressing angiogenic markers e.g. HUVECs. HUVECS were chosen as a comparator cell line as they express angiogenic markers such as CD31, CD34 and Von Willebrand Factor (vWF).

As can be seen in Figure 37, following culture in the presence of $_{rh}VEGF_{165}$ on 1% collagen gels for 48 hours, DPSCs showed minimal positive immunostaining for either CD31 (Figure 37 (A)) or CD34 (Figure 37 (B)) angiogenic markers, similar to the dental pulp positive and negative controls (Figure 35 (B), (C) and (D)). This indicates no, or very slight, differentiation along an angiogenic lineage for DPSCs under these conditions.

In contrast, the HUVEC positive control cell line (Figure 38(A and B)) showed strong positive staining for both CD31 and CD34.

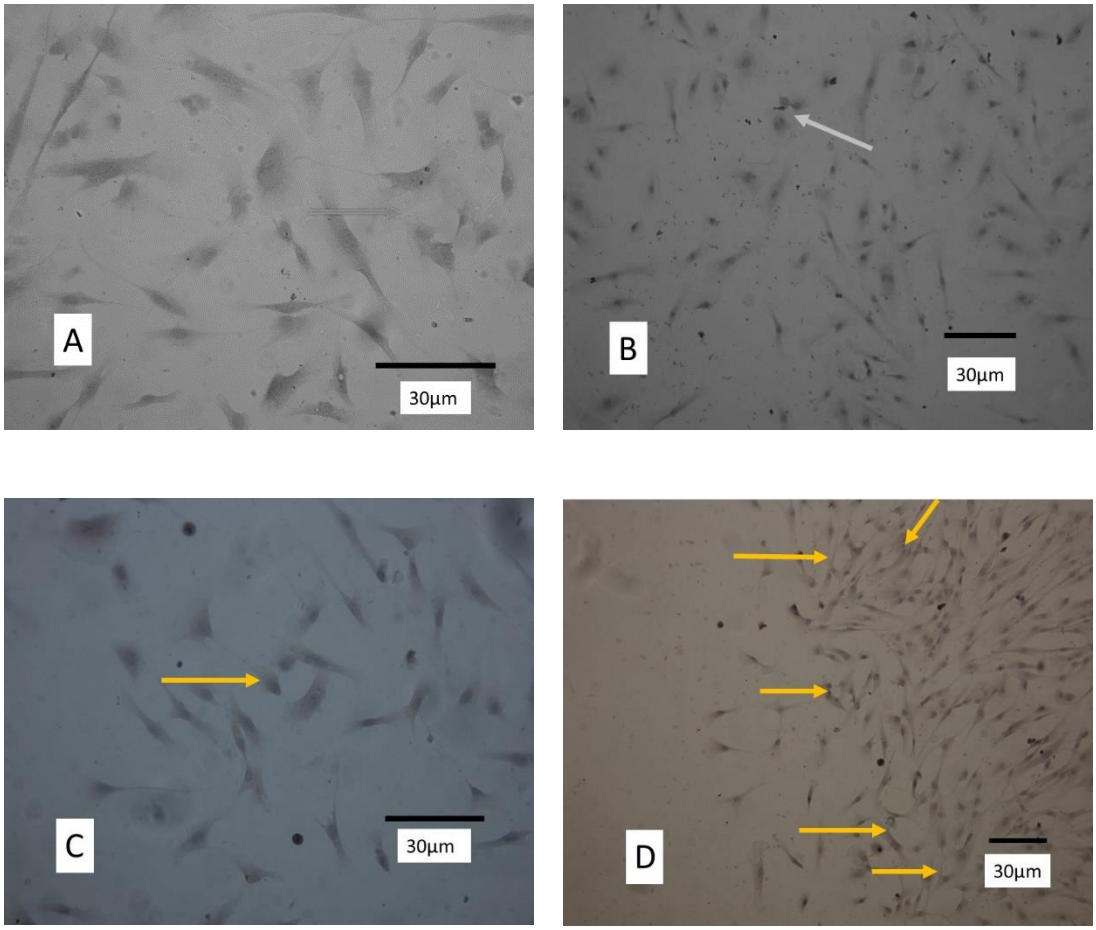

Figure 37. CD31 and CD34 immunohistochemical staining of DPSCs cultured on 1% collagen I gels in EGM with 5 ng/mL $_{rh}VEGF_{165}$ for 48 hours.

A and B: weakly positive immunostaining staining of DPSCs to the target antigens, CD31 and CD34 respectively. C and D: negative controls (no 1st antibody). All images show evidence of annular configuration, suggestive of monolayer vascular structures (gold arrows).

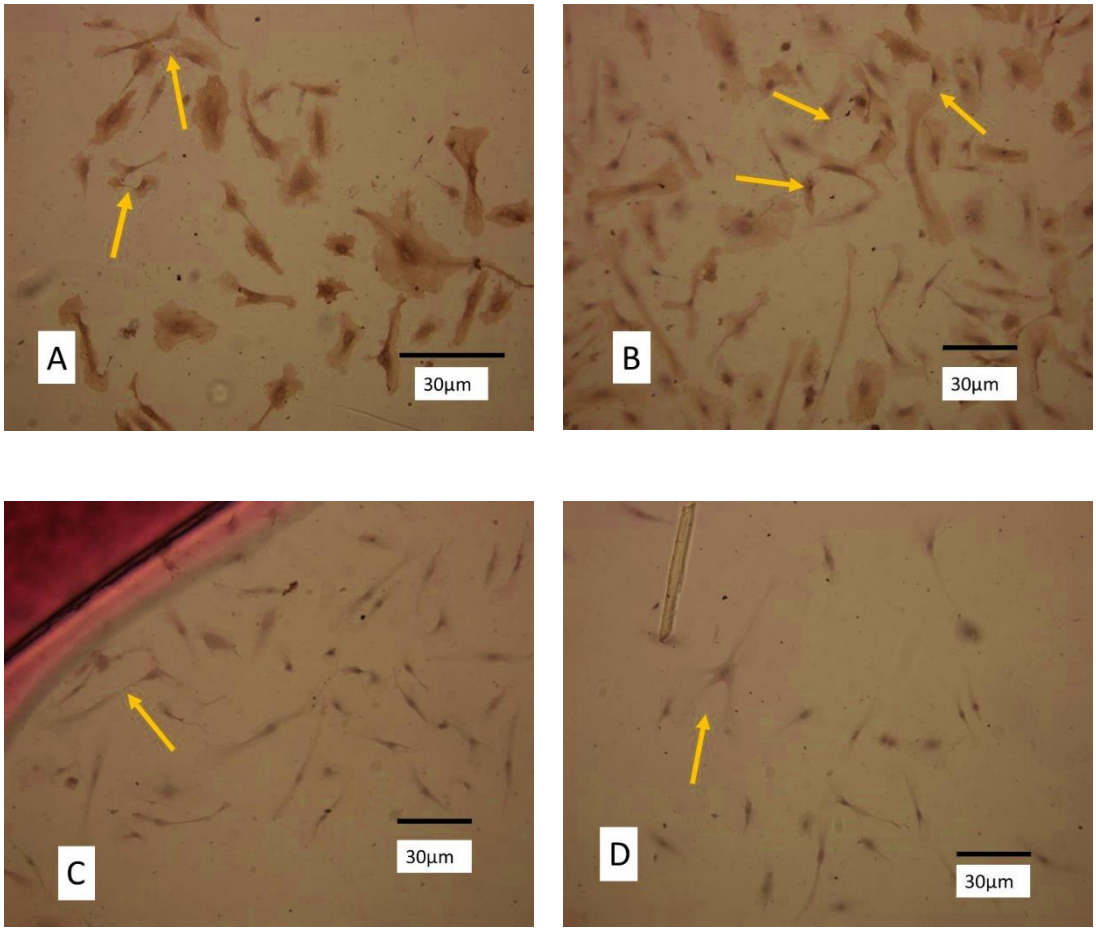

Figure 38. Immunohistochemical staining for CD31 and CD34 of HUVECs cultured for 48 hours on 1% collagen I gel in EGM with 5 ng/mL $_{rh}VEGF_{165}$.

A and B: HUVECs (positive control cell line), showed strong positive immunostaining for CD31 and CD34 markers, respectively. C and D: negative controls, (no 1st antibody) showed minimal staining. Monolayer vascular-like structures indicated by gold arrows.

4.15 Comparison of cells cultured on 1% HyA ± $_{rh}VEGF_{165}$

4.15.1 DPSCs

Cells were cultured on 1% HyA gel with or without $_{rh}VEGF_{165}$ to see if a 1% HyA gel could induce angiogenic change in the absence of $_{rh}VEGF_{165}$. Figure 39 shows strong positive immunostaining for both CD31 and CD34 markers when DPSCs were cultured in 1% HyA in EGM for 48 hours with and without the addition of 5 ng/mL of $_{rh}VEGF_{165}$ to the culture medium. All of the samples exhibited small circular or irregular collections of DPSCs suggestive of vascular structures in monoculture. This suggests that a 1% HyA gel on its own can act as a biomimetic matrix to initiate angiogenic change in DPSCs without needing the addition of $_{rh}VEGF_{165}$ when cultured for 48 hours and is discussed more fully in the discussion, Section 5.4.4.

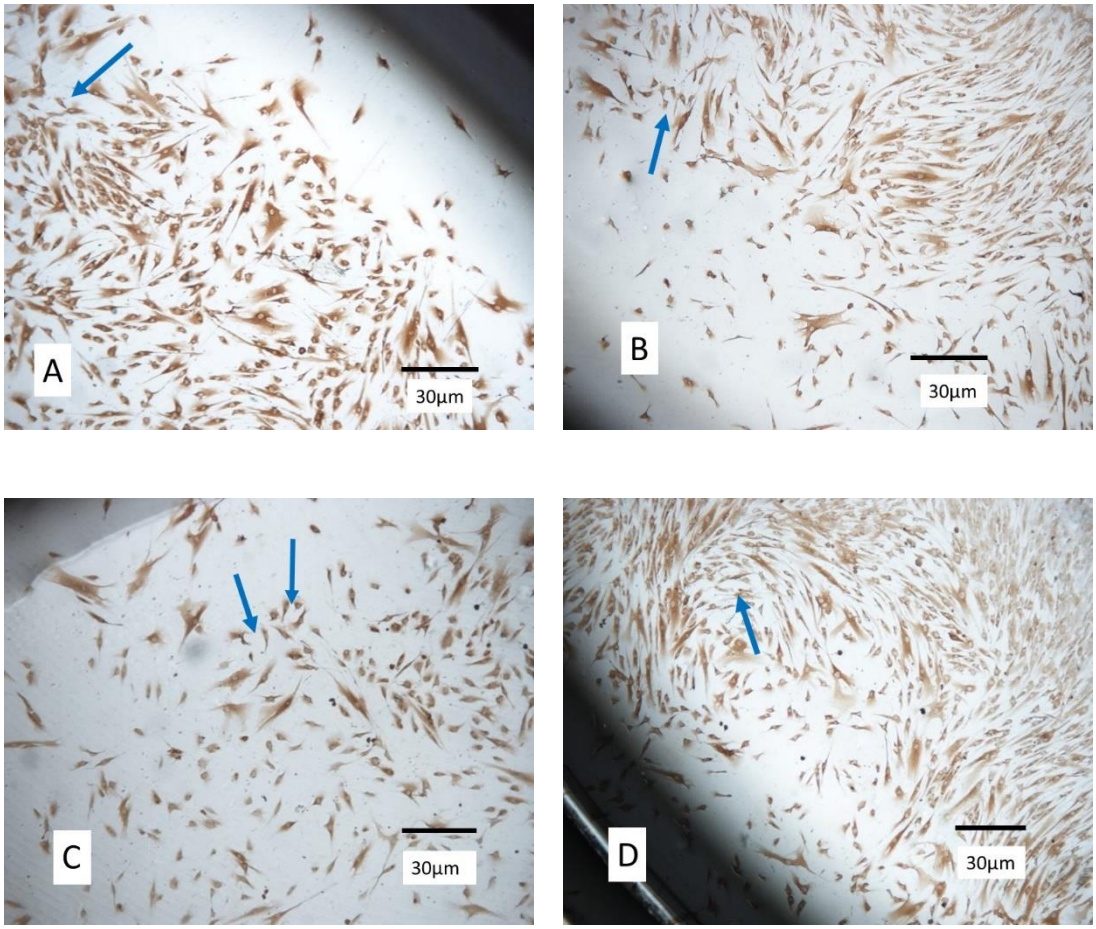

Figure 39. CD31 and CD34 immunohistochemical staining of DPSCs grown on 1%HyA ± 5 ng/mL of $_{rh}$ VEGF$_{165}$ after 48 hours of culture in EGM

A: DPSCs cultured on 1% HyA in EGM for 48 hours showed strongly positive immunostaining for CD31. B: as A, but stained for CD34 antigen also with strong positive staining evident. C and D: DPSCs cultured under the same conditions but with the addition of 5 ng/mL of $_{rh}$VEGF$_{165}$. Strong positive staining was seen for both CD31 and CD34 markers, with the blue arrows indicating cells arranged in a vascular-like configuration.

4.15.2 HUVECs

HUVECs were used as the positive control for these experiments investigating the effect of culture conditions on angiogenic marker expression. Figure 40 shows strong positive staining for both CD31 and CD34 when HUVECS were cultured in 1% HyA in EGM for 48 hours with and without the addition of 5 ng/mL of $_{rh}VEGF_{165}$ to the culture medium, similar to the observations for DPSCs cultured under the same conditions. This further suggests that a 1% HyA gel on its own can act as a biomimetic matrix and can enhance angiogenesis in HUVECs without needing the presence of $_{rh}VEGF_{165}$ when cultured for 48 hours.

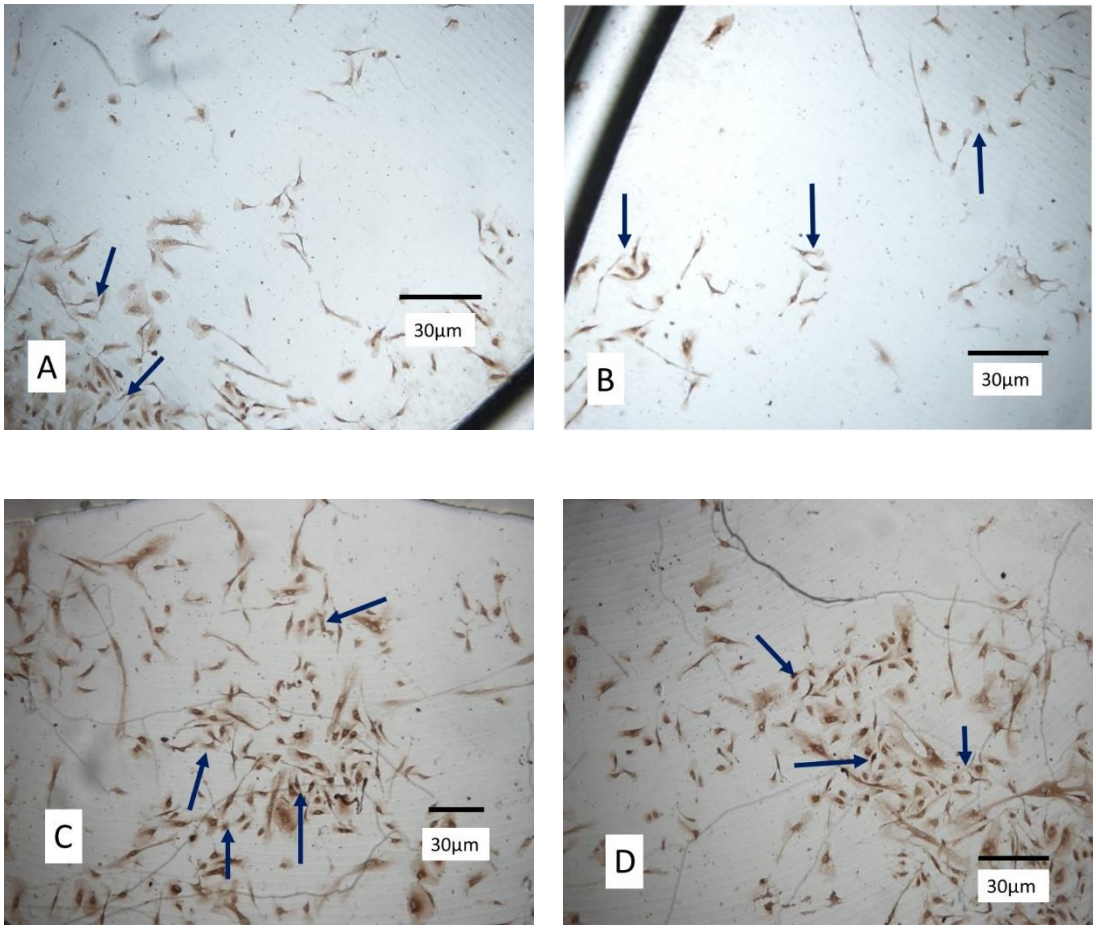

Figure 40. CD31 and CD34 immunohistochemical staining of HUVECs cultured for 48 hours in 1%HyA ± 5 ng/mL of $_{rh}VEGF_{165}$ in EGM.

A: strong CD31 positive immunostaining for HUVECs cultured on 1% HyA gel only. B: similar intense positive staining for HUVECs was seen for CD34 expression, again cultured on 1% HyA gel only. C and D: similar results for HUVECs cultured on 1% HyA gel + 5 ng/mL $_{rh}VEGF_{165}$ and immunostained for CD31 and CD34 respectively. Blue arrows indicate circularly arranged cells.

4.16 Immunohistochemical staining of G292 cells and HPDLCs cultured on 1% HyA in EGM with 5 ng/mL of $_{rh}VEGF_{165}$

4.16.1 G292 cells

G292 cells were used as a negative control and cultured under identical conditions to those described above with no expectation of any sign of early angiogenic change. Figure 41 shows that no obvious positive staining for either CD31 or CD34 was evident in any of the sections, indicating little or no propensity for angiogenic change in the G292 cells cultured on 1% HyA gel in EGM with 5 ng/mL of $_{rh}VEGF_{165}$.

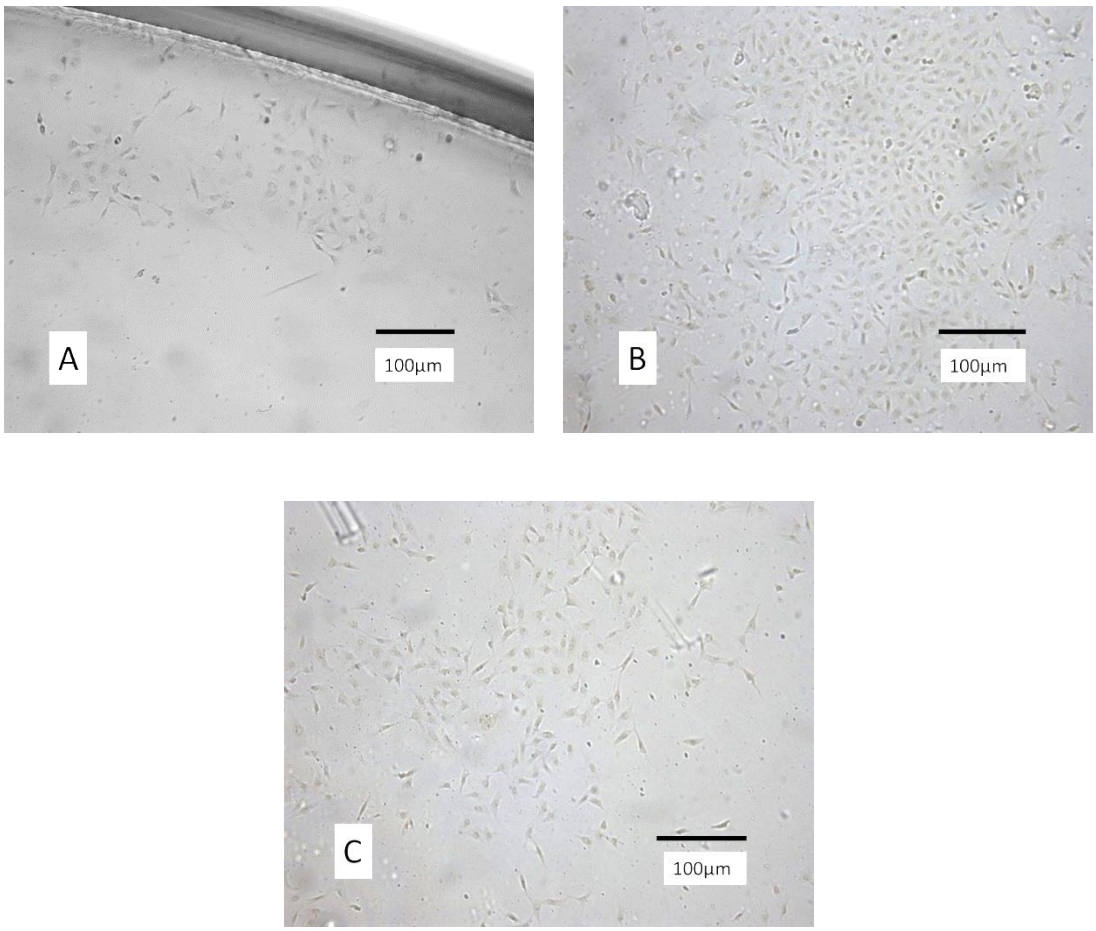

Figure 41. CD31 and CD34 immunohistochemical staining of G292 cells as control, cultured in EGM on 1% HyA with 5 ng/mL of $_{rh}VEGF_{165}$.

A: CD31 immunohistochemistry showed no positive staining. B: CD34 immunohistochemistry also showed no positive staining. C: negative control (no 1st antibody). All images × 100 mag.

4.16.2 HPDLCs

HPDLCs were used as a separate negative control and cultured under identical conditions to those described above as they are derived from a similar embryological source to DPSCs and might be expected to show similar angiogenic change under the same stimuli. Figure 42 (A) and (B) show no definite positive staining for either CD31 or CD34 in any of the sections, probably indicating limited or no propensity for angiogenic change in the HPDLCs cultured on 1% HyA gel in EGM without 5 ng/mL of $_{rh}VEGF_{165}$.

These results are indicative of little or no early angiogenic change. The more pronounced change being in Figure 42 (C), the HPDLCs which were stained for CD31 antibody and which were cultured on 1% HyA gel in the presence of 5ng/mL of $_{rh}VEGF_{165}$, suggesting that $_{rh}VEGF_{165}$ enhances their potential for angiogenic change. There was minimal change in Figure 42 (D). These are cells deriving from a similar embryonic source as DPSCs and given their proximity to the dental pulp organ needing to be regenerated and their already documented pluripotency, they could become a potential recruit cell source for a suitable matrix to repopulate a sterile, prepared root canal and ultimately regenerate a dental pulp.

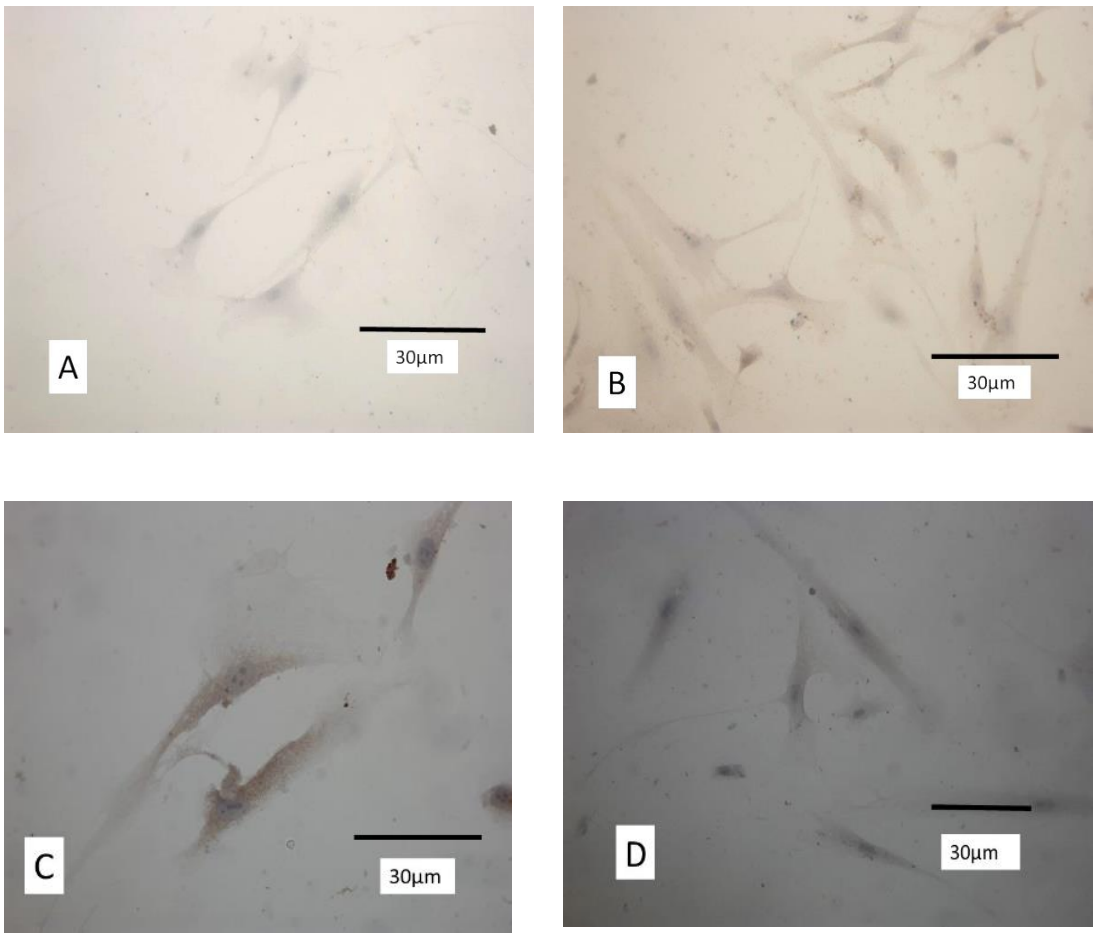

Figure 42. CD31 and CD34 immunohistochemical staining of HPDLCs cultured for 48 hours in 1%HyA ± 5ng/mL of $_{rh}VEGF_{165}$ in EGM.

Images A and B were of cells cultured without $_{rh}VEGF_{165}$, whereas C and D were cultured with $_{rh}VEGF_{165}$. A and C: stained for CD31 antigen. B and D: stained for CD34 antigen. All images show weak staining for both markers but the cells cultured in the presence of $_{rh}VEGF_{165}$ showing stronger staining. Image C showing prominent nuclei and nucleoli.

4.17 Cold stage SEMs of DPSC-scaffold constructs *in situ* within endodontically prepared tooth slices

Tooth slices containing BioGide®/HyA/DPSC constructs were prepared as described in sections 3.16.1 and 3.16.2. They were stopped after two weeks culture in EGM as described in section 3.16.2.1. They were then imaged in the SEM at minus 20 °C.

The ultrastructural appearance of DPSC-scaffold constructs *in situ* within the endodontically prepared tooth slices is shown in Figure 43. The tooth slice cracked following exposure to the minus 20°C temperature in the SEM chamber, probably as a result of insufficient moisture removal and consequent ice crystal formation and expansion within the sample. Nevertheless, Figure 43 (C) shows DPSCs apparently bridging the space between scaffold and dentine with cells arranged in a layer covering the inside of the endodontically prepared dentine surface. Figure 43 (D) shows a prominent hour-glass shaped cell (see the white arrow) with an obvious nucleus, in a field of several other cells, all exhibiting prominent cytoskeletal features.

These results showed that despite the difficulties encountered in obtaining intact tooth sections for immunostaining, the tooth slice/ BioGide®/HyA/DPSC construct successfully maintained DPSCs over the two week period of this experiment (see Section 4. 18).

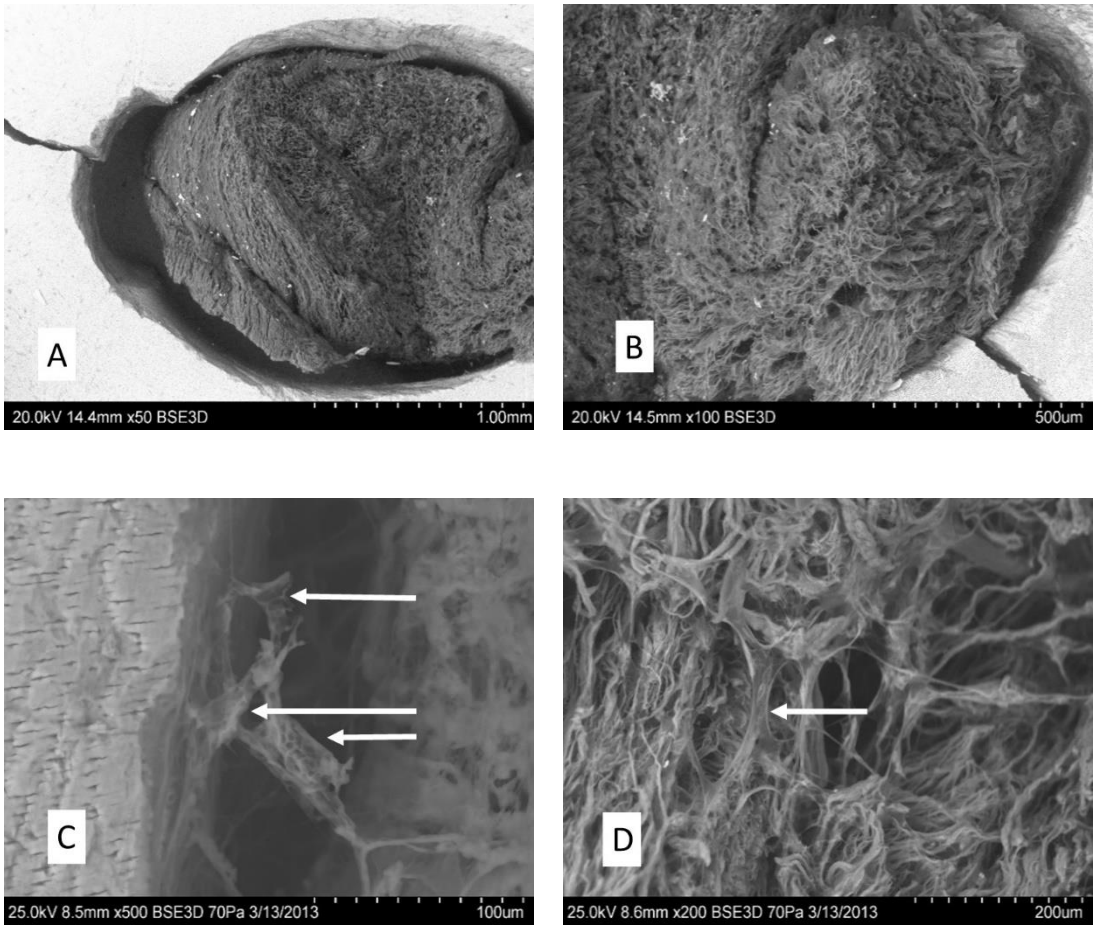

Figure 43. SEM images showing a tooth slice with DPSCs/BioGide®/scaffold *in situ* after 14 days of culture in EGM.

A and B: low power view of the sample. Fracture of the dentine slice due to the minus 20°C temperature is obvious. C: dentine slice on left of field; BioGide® membrane with 1% HyA gel on the right, with cells bridging the space (indicated by the white arrows). D: accumulation of cells including hour-glass shaped cell (indicated by the white arrow) exhibiting prominent cytoskeletal elements amongst the BioGide® membrane fibres.

Further ultrastructural examination of more samples of the DPSC-constructs *in situ* within the endodontically prepared tooth slices showed similar but not identical interesting features. For example, Figure 44 (A) shows a different sample with a DPSC bridging between the scaffold and dentine (see white arrow) with DPSCs growing on the dentine wall to the right of the image showing obvious dentine tubule structure and DPSCs populating the instrumented lumen of the dentine slice.

Figure 44 ((B), (C) and (D)) shows DPSCs within the scaffold material with other DPSCs in the field of view and good evidence of cytoskeletal elements and nuclei.

All of the samples examined showed similar results confirming uniformity of results from the experimental protocol.

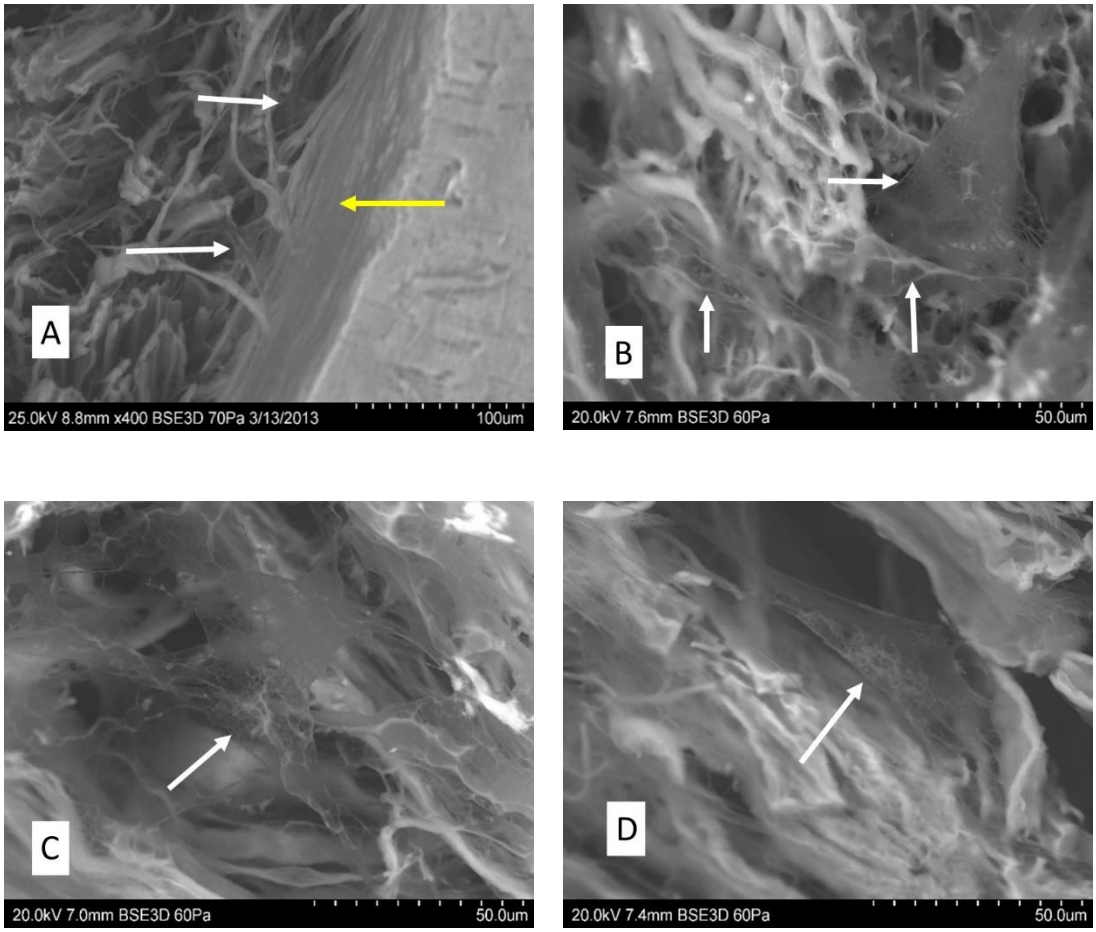

Figure 44. Cold stage SEM images of tooth slice/DPSC/BioGide®/HyA construct samples.

These images appear to show cell groups proliferating within the BioGide® membrane and 1% HyA gel matrices. Cell groups and individual cells indicated by the white arrows.

4.18 Expression of angiogenic markers by DPSC-scaffold constructs *in situ* within endodontically prepared tooth slices

Tooth slices containing DPSC constructs were prepared as described in sections 3.16.1 and 3.16.2. Following preparation for histology and microtomy, sections were immuno-stained for CD31 and CD34 markers to investigate their expression following culture of the slices + constructs as a whole. Figure 45 shows DPSCs cultured in EGM *in vitro* on 1% HyA and BioGide® Type I and III collagen membrane inside a tooth slice. Cells showed positive staining for CD31 and CD34 markers, with blue-staining ribbon-like structures representing fragments of BioGide® Type I and III collagen membrane which had fractured during cutting. Neither this membrane, nor the honeycombed structure representing the dentine of the tooth were positively stained for CD31 or CD34 and had only picked up the counter-staining from the Harris haematoxylin and Scotts tap water. Fragmentation of the BioGide® Type I and III collagen membrane during histological procedures was a constant finding throughout the study.

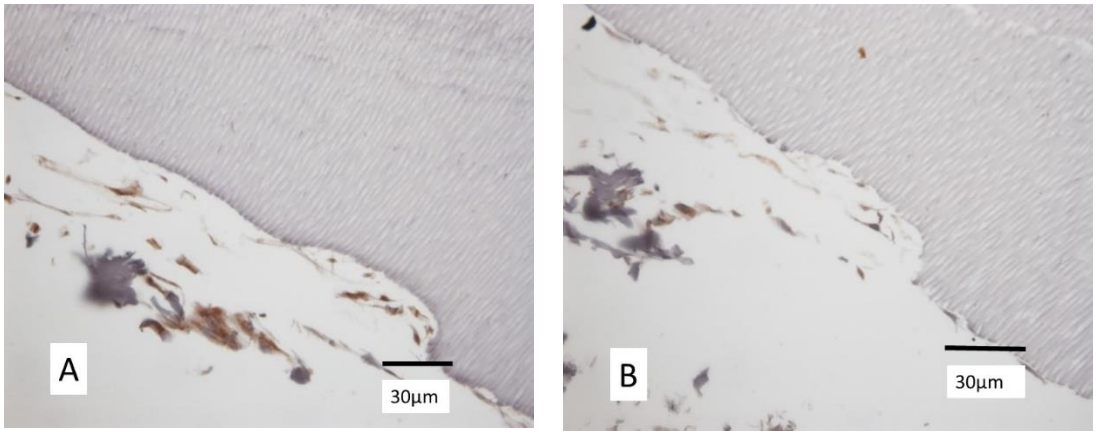

Figure 45. CD31 and CD34 immunohistochemical staining of DPSCs cultured on 1% HyA and BioGide® in EGM in a tooth slice *in vitro* for two weeks.

A: positive staining for CD31. B: positive staining for CD34. Note that in both images, the DPSCs appear to locate in small 'lacunar-shaped' areas off the main endodontically prepared tooth slice lumen.

4.19 Expression of angiogenic marker genes by human dental pulp stromal cells

Quantitative RT-PCR (qRT-PCR) was used to determine gene expression of the angiogenic genes, *CD31* and *CD34* by DPSCs under different culture conditions. Cells were cultured either in 1% hyaluronic acid gels or as monolayers and in either EGM or basal medium (see Methods section 3.18). qRT-PCR was carried out at two and five days after culture using TaqMan gene expression assays for the angiogenic marker genes *CD31* and *CD34* as described in section 3.18. Results are shown relative to the housekeeping gene *YWHAZ* and were analysed using the comparative cycle threshold method (ΔCT). Bar charts of the mean ± standard error were plotted in Microsoft Excel. Statistical analysis between groups was carried out using an ANOVA one way test followed by Bonferroni multiple comparison tests. The analysis of statistical significance was carried out using SPSS version 21. The data is shown in Figure 46 and Tables 5 and 6.

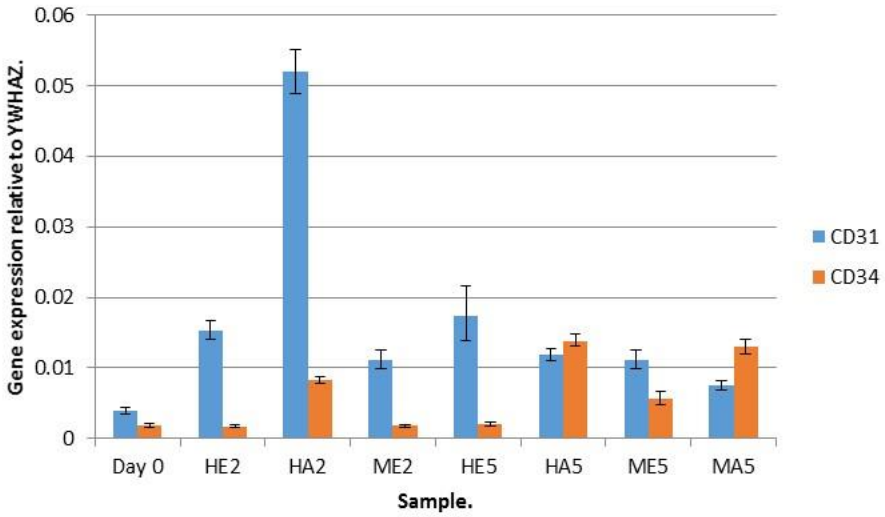

Figure 46. qRT-PCR data showing changes in *CD31* and *CD34* expression by DPSCs under different culture conditions at different time points relative to the housekeeping gene *YWHAZ*.

H = DPSCs cultured on 1% HyA gel; M = DPSCs cultured as monolayers; E = EGM used as culture medium; A = αMEM/10%FCS used as culture medium. Numeric value is the time in days (2 or 5) elapsed since day zero (D0). Bars show mean values ± SE, with n=1. Statistical comparison of data is shown in Tables 5 and 6 below.

TABLE 5: Comparison of *CD31* gene expression between the various cell/culture condition groups at days 0, 2 and 5.

H = DPSCs cultured on 1%HyA gel; M = DPSCs cultured as monolayers; E = EGM used as culture medium; A = αMEM/10%FCS used as culture medium. Statistically significant change is shown by $p \leq 0.05$; NS = not significant; N/A = not applicable.

	Day 0	**HE2**	**HA2**	**ME2**	**HE5**	**HA5**	**ME5**	**MA5**
Day 0	N/A	NS	$p \leq 0.05$	NS	NS	NS	NS	NS
HE2	NS	N/A	$p \leq 0.05$	NS	NS	NS	NS	NS
HA2	$p \leq 0.05$	$p \leq 0.05$	N/A	$p \leq 0.05$	$p \leq 0.05$	$p \leq 0.05$	$p \leq 0.05$	$p \leq 0.05$
ME2	NS	NS	$p \leq 0.05$	N/A	NS	NS	NS	NS
HE5	NS	NS	$p \leq 0.05$	NS	N/A	NS	NS	NS
HA5	NS	NS	$p \leq 0.05$	NS	NS	NA	NS	NS
ME5	NS	NS	$p \leq 0.05$	NS	NS	NS	N/A	NS
MA5	NS	NS	$p \leq 0.05$	NS	NS	NS	NS	N/A

TABLE 6: Comparison of *CD34* gene expression between the various cell/culture condition groups at days 0, 2 and 5.

H = DPSCs cultured on 1%HyA gel; M = DPSCs cultured as monolayers; E = EGM used as culture medium; A = αMEM/10%FCS used as culture medium. Statistically significant change is shown by $p \leq 0.05$; NS = not significant; N/A = not applicable.

	Day 0	**HE2**	**HA2**	**ME2**	**HE5**	**HA5**	**ME5**	**MA5**
Day 0	N/A	NS	NS	NS	NS	$p \leq 0.05$	NS	$p \leq 0.05$
HE2	NS	N/A	NS	NS	NS	$p \leq 0.05$	NS	$p \leq 0.05$
HA2	NS	NS	N/A	NS	NS	NS	NS	NS
ME2	NS	NS	NS	N/A	NS	$p \leq 0.05$	NS	$p \leq 0.05$
HE5	NS	NS	NS	NS	N/A	$p \leq 0.05$	NS	$p \leq 0.05$
HA5	$p \leq 0.05$	$p \leq 0.05$	NS	$p \leq 0.05$	$p \leq 0.05$	N/A	NS	NS
ME5	NS	NS	NS	NS	NS	NS	N/A	NS
MA5	$p \leq 0.05$	$p \leq 0.05$	NS	$p \leq 0.05$	$p \leq 0.05$	NS	NS	N/A

Effect of culture medium on changes in *CD31* gene expression

Comparing *CD31* expression between days 0, 2 and 5 for DPSCs cultured on HyA in EGM showed an apparent upregulation between day 0 and day 2 and day 0 and day 5 but neither of these were statistically significant. In contrast, when DPSCs were grown on HyA in basal medium, there was a significant upregulation in *CD31* expression between days 0 and 2, followed by a significant down regulation between days 2 and 5, with *CD31* expression at day 5 being similar to that at day 0 (NS).

When DPSCs were grown in monolayer culture in EGM, there were also no significant differences in *CD31* expression between days 0 and 5. Unfortunately, data for DPSCs grown in monolayers in basal medium for 2 days was not obtained, so there is no possibility of comparing expression at day 2 with day 0 or at day 5.

Effect of culture medium on changes in *CD34* gene expression

Comparing *CD34* expression between days 0, 2 and 5 for DPSCs cultured on HyA in EGM showed no significant changes with time. When DPSCs were grown on HyA and cultured in basal medium, there were no significant changes to *CD34* gene expression at day 2 but a significant upregulation in *CD34* expression was seen at day 5 compared with day 0.

When DPSCs were grown as monolayers and cultured in EGM, CD34 expression was unaffected at days 2 and 5 of culture compared with day 0. Unfortunately, data for DPSCs grown in monolayers in basal medium for 2 days was not obtained, so there is no way of comparing *CD34* expression at day 2 with day 0 or at day 5.

Taken together, these data suggest that growth of DPSCs on HyA in EGM did not affect the expression of wither angiogenic marker. However, in basal medium, both gene markers were significantly upregulated in culture, with *CD31* being greatly upregulated by day 2 and then returning to baseline values and *CD34* being upregulated by day 5.

Effect of 3D culture on HyA scaffolds on *CD31* gene expression:

The effect of growing DPSCs on HyA scaffolds compared with monolayer culture on angiogenic marker gene expression was also determined for each time point and in both culture mediums. *CD31* expression in EGM was similar at both day 2 and day 5 (NS) irrespective of whether cells were cultured on HyA scaffolds or as monolayers. In basal medium, at day 5, there was also no significant differences in *CD31* expression either between DPSCs grown on HyA scaffolds and those grown as monolayers.

Effect of 3D culture on HyA scaffolds on *CD34* gene expression:

In the case of *CD34* expression, DPSCs grown in EGM also had similar levels of gene expression at days 2 and 5 of culture (NS). In basal medium, *CD34* expression was also similar irrespective of whether the cells were grown on HyA scaffolds or in monolayers at day 5.

These data together suggest that the effect of HyA scaffolds in the expression of angiogenic markers was minimal under the conditions described here.

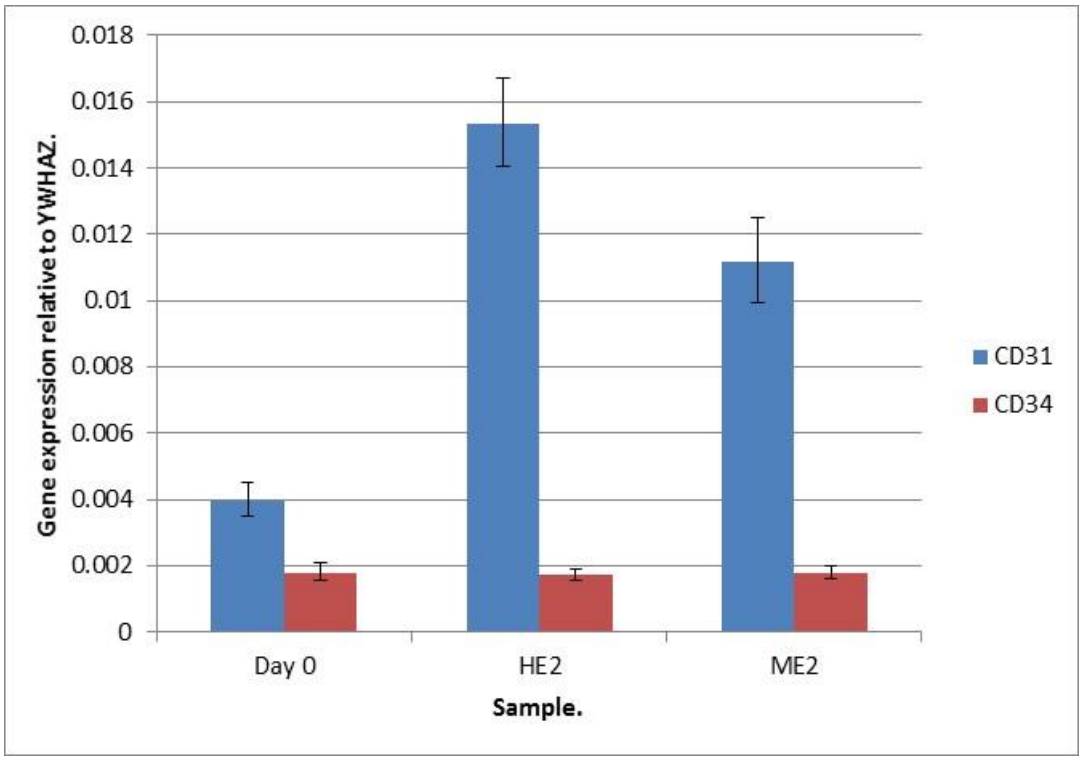

Figure 47. Bar chart showing DPSCs expression of CD31 and CD34 when cultured in EGM either with 1% HyA gel or in monolayer relative to *YWHAZ* housekeeping gene.

Comparing CD31 expression between days 0 and 2 in the HE2 and ME2 groups: although the bar chart shows there was just over a three-fold increase between days 0 and 2, this was not calculated to be statistically significant, with a value of $p = 1$ between day 0 and the HE2 group. In comparing change between day 0 and the ME2 group, although there was again a more than doubling of CD31 expression, it wasn't calculated as statistically significant with $p = 1$.

Comparing CD34 expression between days 0, and day 2 for the HE2 and ME2 groups again shows no statistically significant difference with $p = 1$ although there is an apparent change in expression shown on the bar chart.

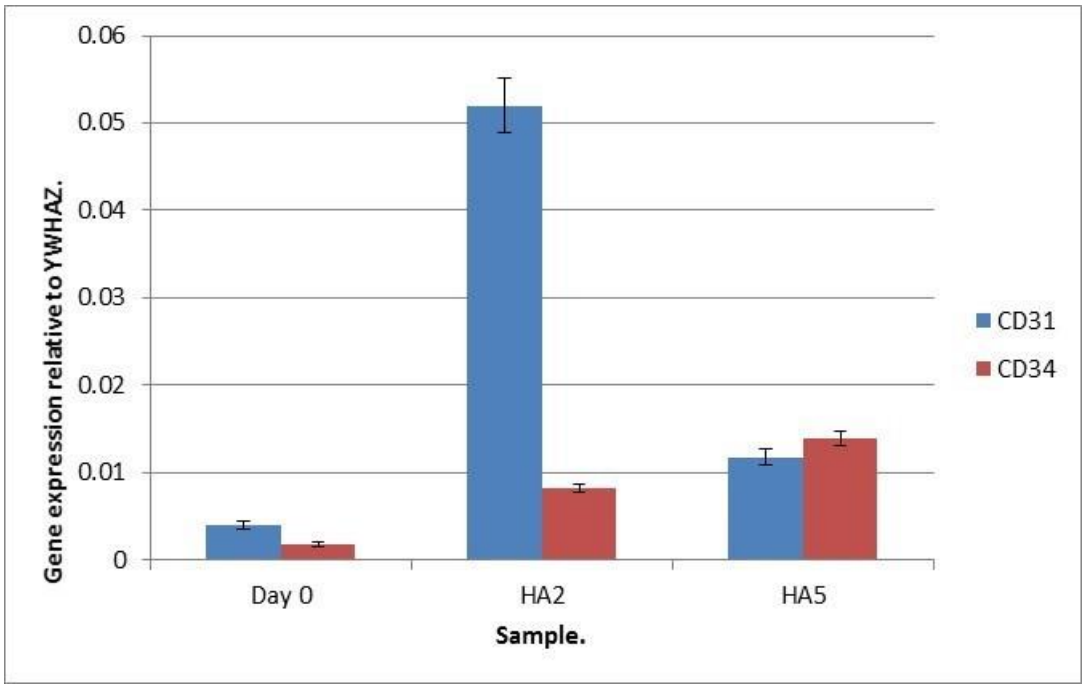

Figure 48. Bar chart showing changes in CD31 and CD34 expression from day 0 to days 2 and 5 in DPSCs cultured in 1% HyA with αMEM/10%FCS relative to *YWHAZ* housekeeping gene.

Comparing CD31 expression between day 0 and the HA2 and HA5 groups: from day 0 to day 2 in the HA2 group showed an extremely significant up regulation of CD31 expression, with $p < 0.001$. Between day 0 and day 5 the up regulation was much lower with $p = 1$. The difference between day 2 and 5 showed a significant down-regulation with $p < 0.001$.

Comparing CD34 expression between days 0, 2 and 5 for the HA group: the change in expression between days 0 and 2 wasn't statistically significant with a calculated value of $p = 0.432$. The change in expression between days 0 and 5 was statistically significant with a value of $p = 0.003$. The difference in expression between days 2 and 5 wasn't statistically significant with a value of $p = 0.702$.

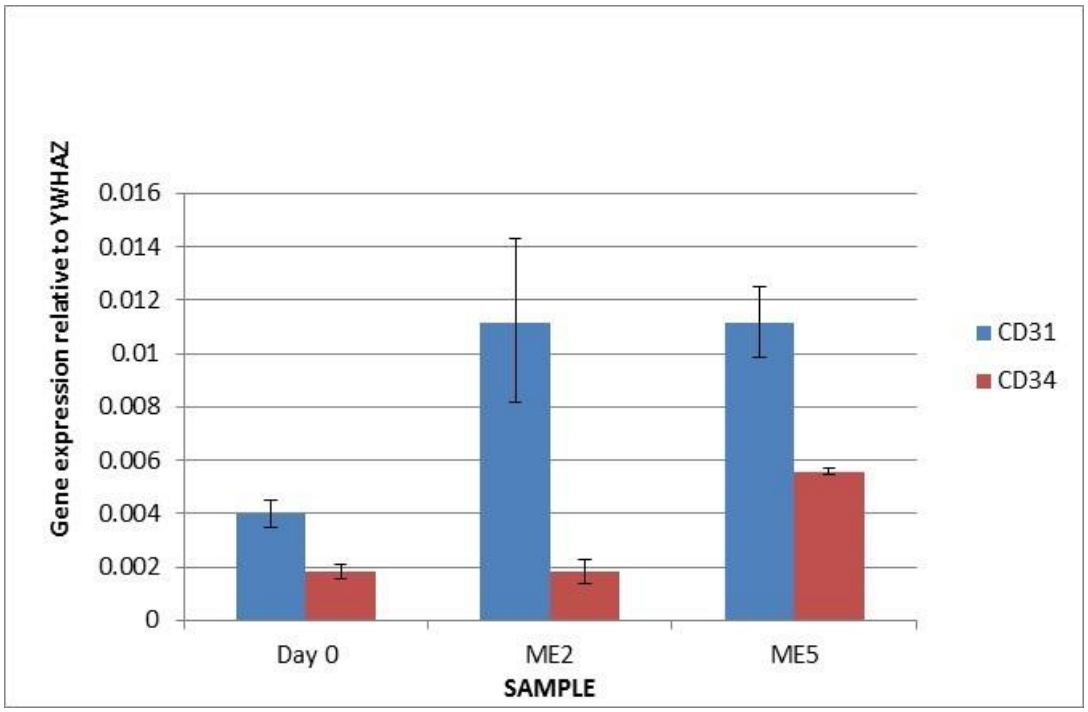

Figure 49. Bar chart showing changes in CD31 and CD34 expression in DPSCs at 2 and 5 days cultured on monolayer in EGM relative to *YWHAZ* housekeeping gene.

Comparing CD31 expression between days 0, 2 and 5 in the ME group; There is no statistically significant change in CD31 expression between days 0 and 2, or between days 0 and 5 in this group. There is also no statistically significant change in expression between days 2 and 5 with $p = 1$ in all cases.

Comparing the change in CD34 expression between days 0, 2 and 5 for the ME group: there was no statistically significant change in expression between day 0 and day 2, with $p = 1$. There was statistically significant change between days 0 and 5 with $p = 0.005$. There was no statistically significant change in expression between days 2 and 5 with $p = 1$.

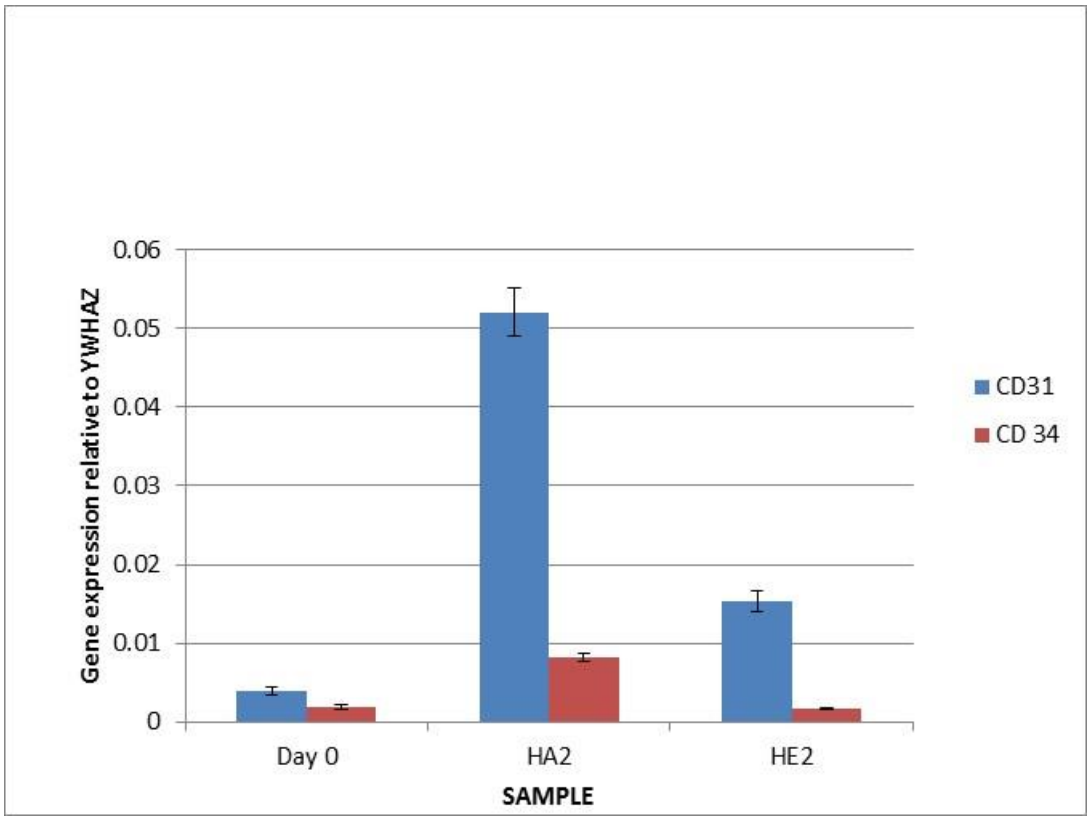

Figure 50. Bar chart showing changes in CD31 and CD34 expression in DPSCs at 2 days cultured on 1% HyA in αMEM/10%FCS or EGM relative to YWHAZ housekeeping gene.

Comparing CD31 expression between day 0 and the HA2 and HE2 groups: the change in CD31 expression between day 0 and the HA2 group is very statistically significant with $p < 0.001$. Between day 0 and the HE2 group it isn't statistically significant and the p value was calculated to be $p = 1$. Between the HA2 and the HE2 groups the difference is statistically very significant with a calculated value of $p < 0.001$.

Comparing CD34 expression between day 0 and day 2 in the HA and the HE2 samples: the difference in expression between day 0 and HA2 wasn't statistically significant with a value of $p = 0.432$. The difference in expression between day 0 and HE2 wasn't statistically significant with $p = 1$. The difference between HA2 and HE2 wasn't statistically significant with $p = 0.351$.

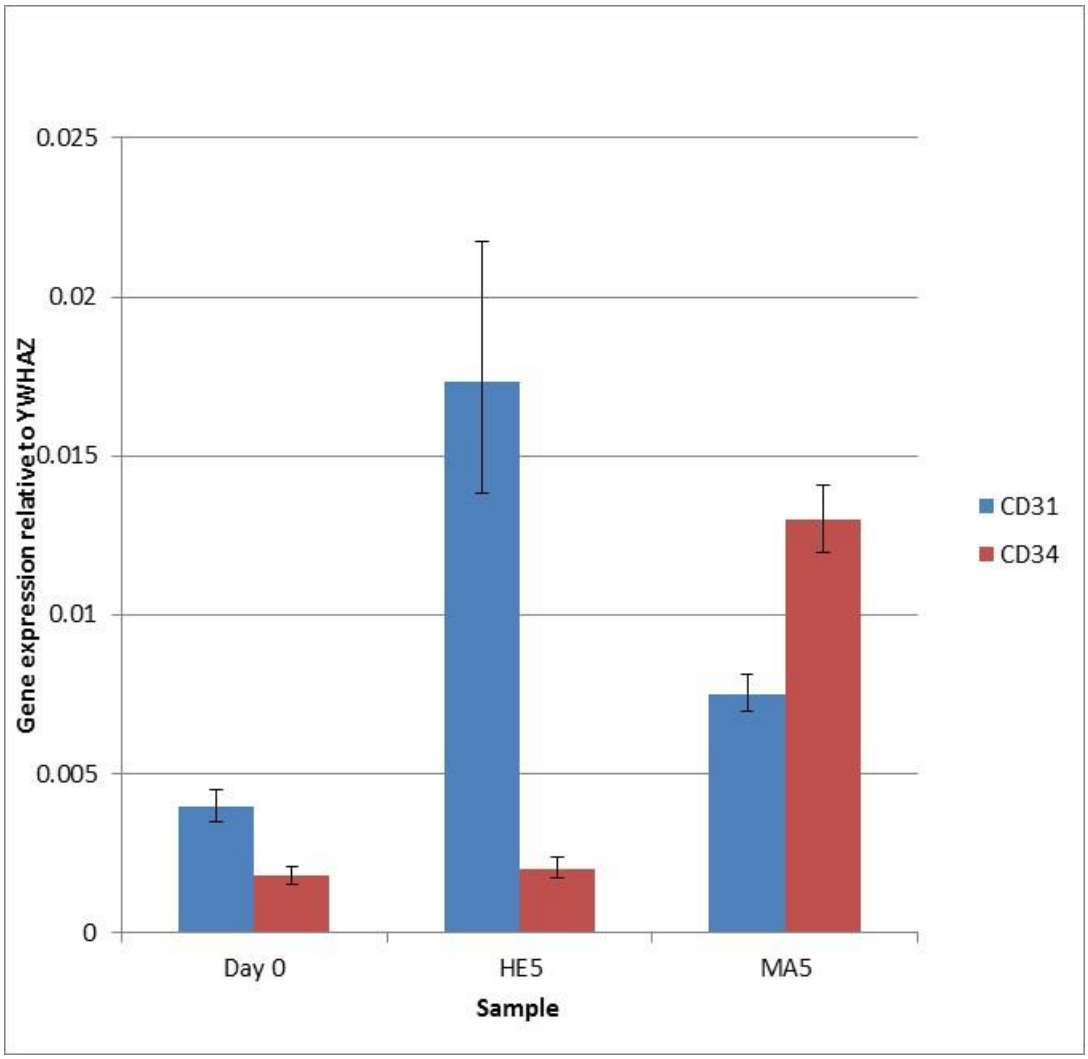

Figure 51. Bar chart showing changes in CD31 and CD34 expression in DPSCs at 5 days cultured on 1% HyA gel in EGM or on monolayer in αMEM/10%FCS relative to YWHAZ housekeeping gene.

Comparing CD31 expression between day 0 and days 5 in the HE5 and MA5 groups: although a slight increase is shown in the chart, there is no statistically significant difference in CD31 expression between day 0 and day 5 in the HE group, with a calculated value of $p = 0.419$. There is also no statistically significant difference in CD31 expression between day 0 and day 5 in the MA group with a calculated value of $p = 1$.

Comparing CD34 expression between day 0 and day 5 in the HE5 and MA5 groups: there was no statistically significant difference between day 0 and HA5 with $p = 1$. There was a statistically significant difference between day 0 and MA5 with $p = 0.005$. There was also a statistically significant difference between HE5 and MA5 with $p = 0.005$.

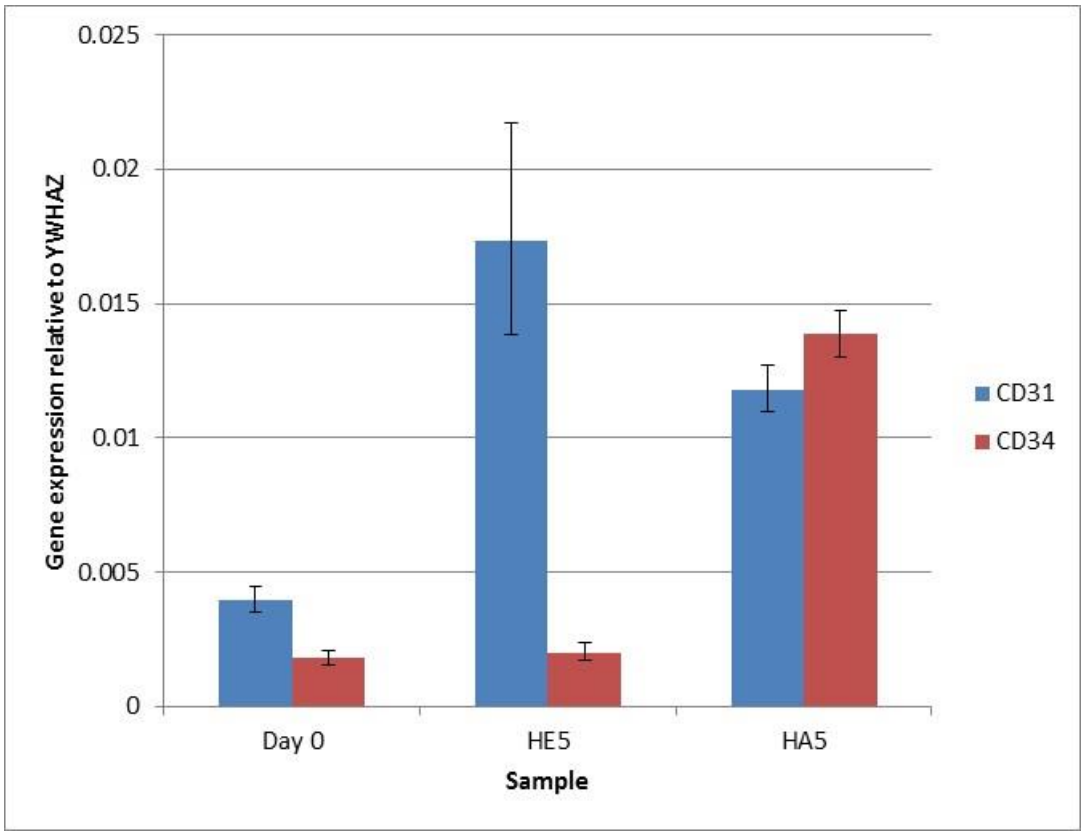

Figure 52. Bar chart showing changes in CD31 and CD34 expression in DPSCs at 5 days cultured on 1% HyA gel in EGM or on 1% HyA gel in αMEM/10%FCS relative to YWHAZ housekeeping gene.

Comparing the CD31 expression between day 0 and day 5 in the HE and HA group: there is no statistically significant difference in CD31 expression between day 0 and day 5 in the HE group with a calculated value of $p = 0.419$. there is no statistically significant difference between day 0 and day 5 of the HA group with a calculated value of $p = 1$ and the same for the HA5 group compared to the HE5 group.

Comparing CD34 expression between day 0 and the H5 and HA5 groups: there is no significant difference between day 0 and HE5 with $p = 1$. There is a significant difference between day 0 and HA5 with $p = 0.003$. There is also a significant difference between HE5 and HA5 with $p = 0.003$.

4.20 Retrieval of *in vivo* samples

After being euthanized at 28 days, the samples were dissected out from the animals and prepared for decalcification and sectioning (see section 3.17.2).

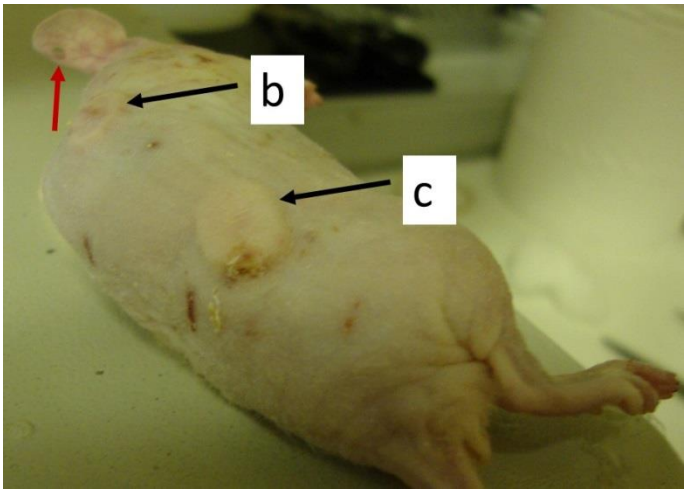

Figure 53. Euthanized mouse ready for dissection and retrieval of samples.

Image showing euthanized mouse with samples b, (right front, Type I and III collagen membrane with DPSCs) and c, (right rear, HyA with DPSCs) visible through the skin, indicated by the black arrows. The mouse seems to have been fighting with its siblings as can be seen from the scabs and scars on its back and right haunch. The red arrow indicates the single punched out hole in the ear, indicating that this is mouse number 1.

At dissection, all of the tooth slice constructs could be seen to have been encapsulated in fibrous tissue with a soft tissue pedicle attached.

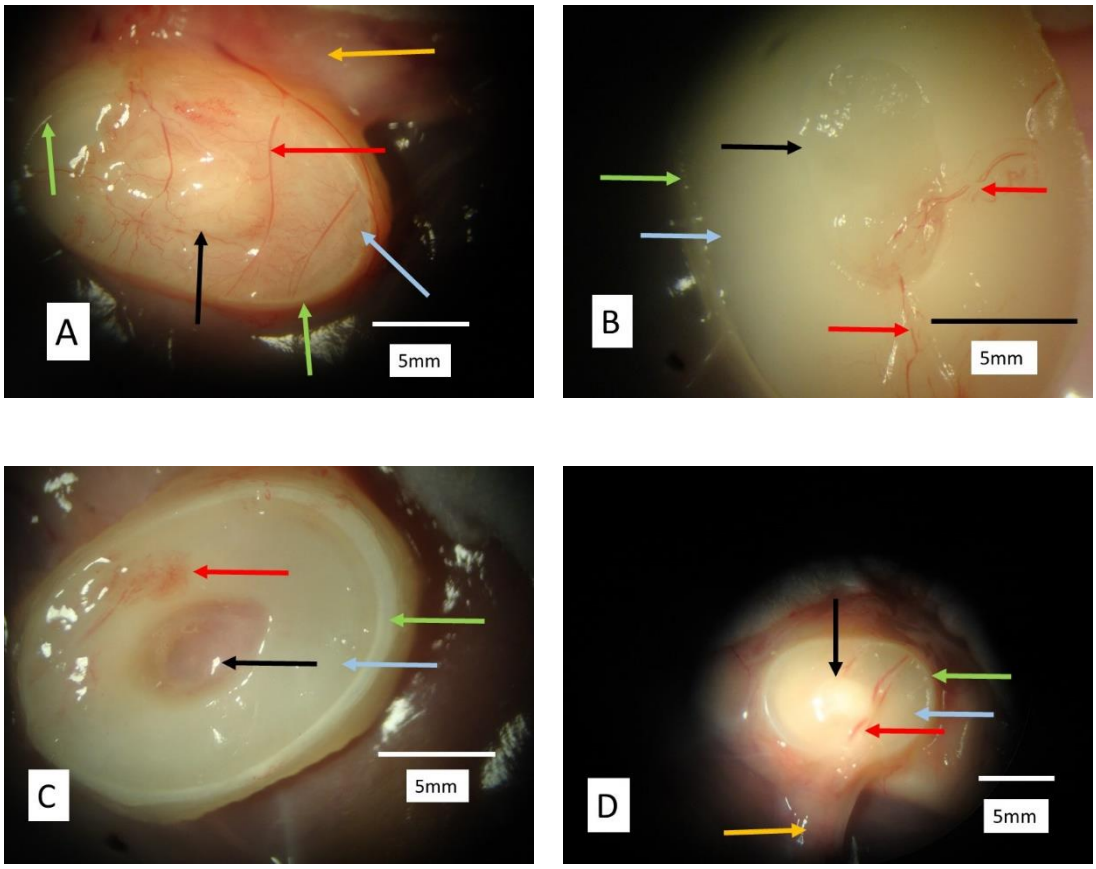

Figure 54. Dissected tooth slice samples from *in vivo* study.

A (sample a) shows the soft tissue pedicle attachment indicated by the gold arrow near the top of the image. The tooth enamel is indicated by the light green arrows, the dentine by the light blue arrow, the blood vessels of the capsule are indicated by the red arrow and the protuberance of the BioGide®/1% HyA central construct, with no seeding DPSCs is indicated by the black arrow. B (sample b) shows the same, the central construct being BioGide® with DPSCs. All coloured arrows indicating their respective structures, except there is no pedicle in the image. C (sample c), central construct being 1% HyA and DPSCs, again shows the same structures indicated by their respective coloured arrows, with the central construct appearing vascular in appearance. D (sample d) again shows enamel, dentine, blood vessels, central construct of BioGide®/1% HyA gel and DPSCs with an attachment pedicle, all indicated by their respective coloured arrows. Samples a,b,c and d correspond with the implantation sites in Figure 16, section 3.17.2.

4.21 Angiogenic change in tooth slice / DPSC-scaffold constructs following *in vivo* implantation

Previously (section 4.17), *in vitro* and *in situ* data suggested that a combination of DPSCs and BioGide® infiltrated with HyA supported cell growth and expression of angiogenic markers by DPSCs.

The four sets of tooth slices were prepared as described in section 3.16.1 and 3.16.2 containing 1) BioGide®/HyA only, with no DPSCs; 2) BioGide® and DPSCs; 3) 1% HyA plus DPSCs; 4) BioGide®/HyA plus DPSCs. Each tooth slice containing the constructs was implanted sub-cutaneously into Nu/Nu mice. After four weeks, the slices with constructs *in situ* were recovered, decalcified and tissue processed. The expression of angiogenic markers and evidence of early vasculature was assessed using immunohistochemistry.

4.21.1 BioGide®/HyA only

Figure 55 (A) (BioGide®/HyA only – no additional DPSCs seeded) shows evidence of cell ingrowth (white arrow) in to the BioGide®/HyA scaffold with BioGide® fragments (blue arrow). Dark brown staining tubule-like structures resembling predentine or dentine were seen, with a defined demarcation line between them and the dentinal tubules of the tooth slice. These tubules were contiguous with the dentine tubules of the endodontically prepared tooth slice which appeared to have picked up background staining. Cell bodies with dark blue staining cell nuclei (from the Harris Haematoxylin counter stain) were seen in intimate contact with the tubule-like material front, with cell processes visibly traversing through both the darker-staining tubule-like material and into the pre-existing dentinal tubules. This

suggested successful colonisation of the endodontically prepared space and continued cell growth enabling deposition of the tubule-like material. These samples were intended to provide negative controls and were not seeded with DPSCs, so the cells seen in the sections must have come from the host animal itself. This suggests the construct either having a passive role, allowing colonisation by the murine cells or an angio-dentinal inductive/conductive property for the tooth slice/combined scaffold material potentially affecting any cells allowed to colonise the prepared root canal within the tooth slice construct. Given that the only cells available for colonisation of these matrices must be murine, this would suggest that in a clinical application, other cells, not necessarily DPSCs, could potentially colonise from other tissues such as the periodontal ligament, which is anatomically adjacent to the tooth apex. As PDLCs are embryologically very close to DPSCs, this would be an interesting hypothesis to further explore.

Figure 55 (B) shows a higher power image of the same section as (A) revealing a close up of the cell ingrowth described previously. This showed that the cellular ingrowth did not only colonise the prepared root canal space but also began to grow cell processes along the existing dentinal tubules of the tooth slice. In (C) there was also evidence of cell ingrowth with the same tubule-like material contiguous with the dentine tubules of the tooth slice and cells in intimate contact with and arranged along the deposition front of the tubule-like material as described previously in the absence of pre-seeding with DPSCs. Finally, Figure 55 (D) demonstrates the arrangement of some cells within the construct in to a circular pattern, similar to vascular configuration (indicated by the white arrow). There was however, no evidence of any newly deposited tubule-like material in this particular section.

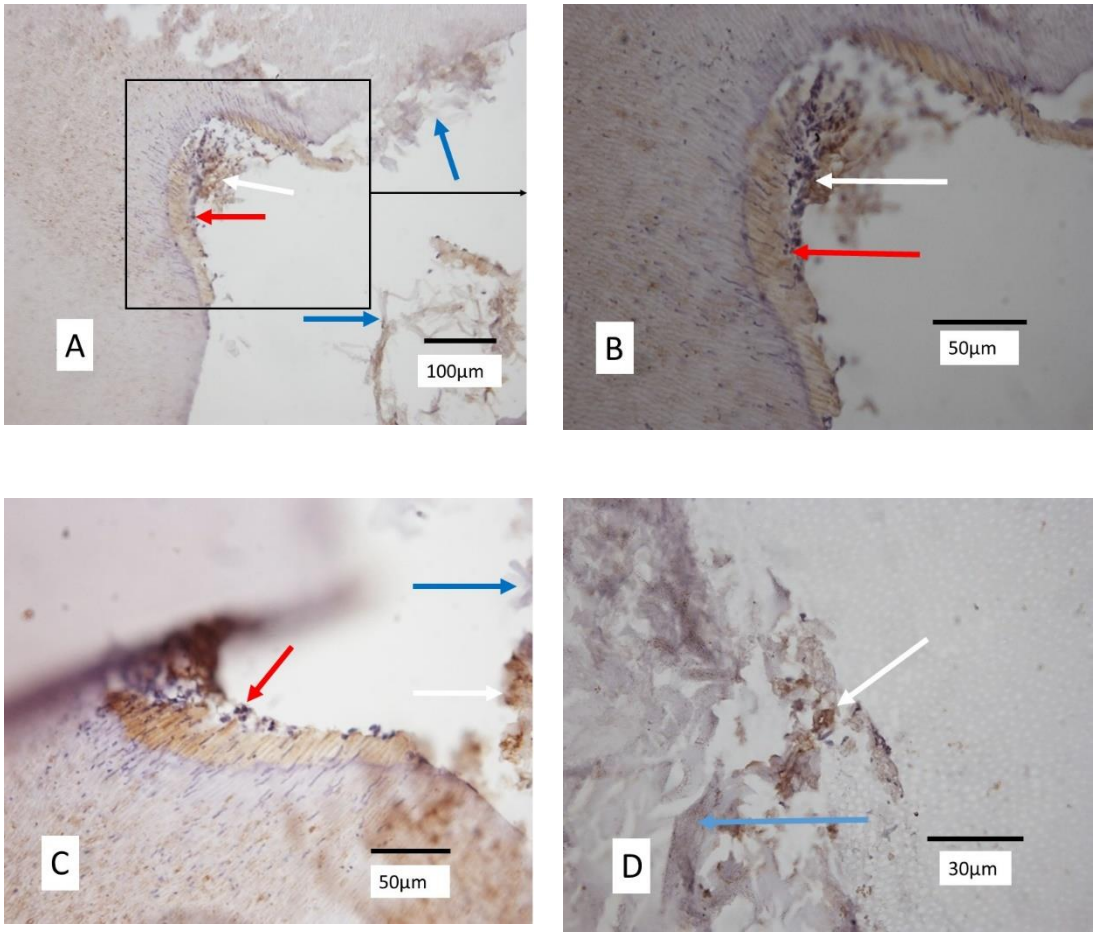

Figure 55. Immunohistochemical staining for CD31 and CD34 expression in sections of tooth slices containing constructs (without pre-seeding with DPSCs) *in vivo*.

A and B: Tooth slice containing BioGide®/1% HyA only (no DPSCs seeded on to the scaffold pre-implantation), with white arrows indicating cell accumulations, red arrows indicating new tubule-like material and blue arrows indicating BioGide® remnants. C and D: Tooth slice containing BioGide® membrane, with the white arrows indicating cell accumulations, red arrows indicating new tubule-like structure and blue arrows indicating BioGide® remnants. A, B and D were immunostained for CD31 antibody, C was stained for CD34 antibody. Positive staining appears brown, as does the new tubule-like material. A circular arrangement of cells, reminiscent of vascular structures is seen in image D, indicated by the white arrow.

4.21.2 BioGide® and DPSCs

When the combination of BioGide® and DPSCs (no HyA) were used, similar results were obtained as were found in the HyA/BioGide® (no DPSCs) samples as described previously.

Figure 56 (A) shows the same evidence of soft tissues ingrowth, new tubule-like material and cells in intimate contact with the same layer as that described and illustrated in Figure 55. Circular vascular structures were present showing brown positive staining to CD34. Figure 56 (B) shows a soft tissue ingrowth staining positively for CD31, detached from the dentine during processing, containing vascular structures with BioGide® fragments nearby and new tubule-like material contiguous with the tooth slice dentinal tubules. A magnified view of this is shown in Figure 56 (C), with the cells being arranged in an odontoblast-like fashion, with one cell in particular indicated by the purple arrow obviously running its process into an adjacent dentinal tubule.

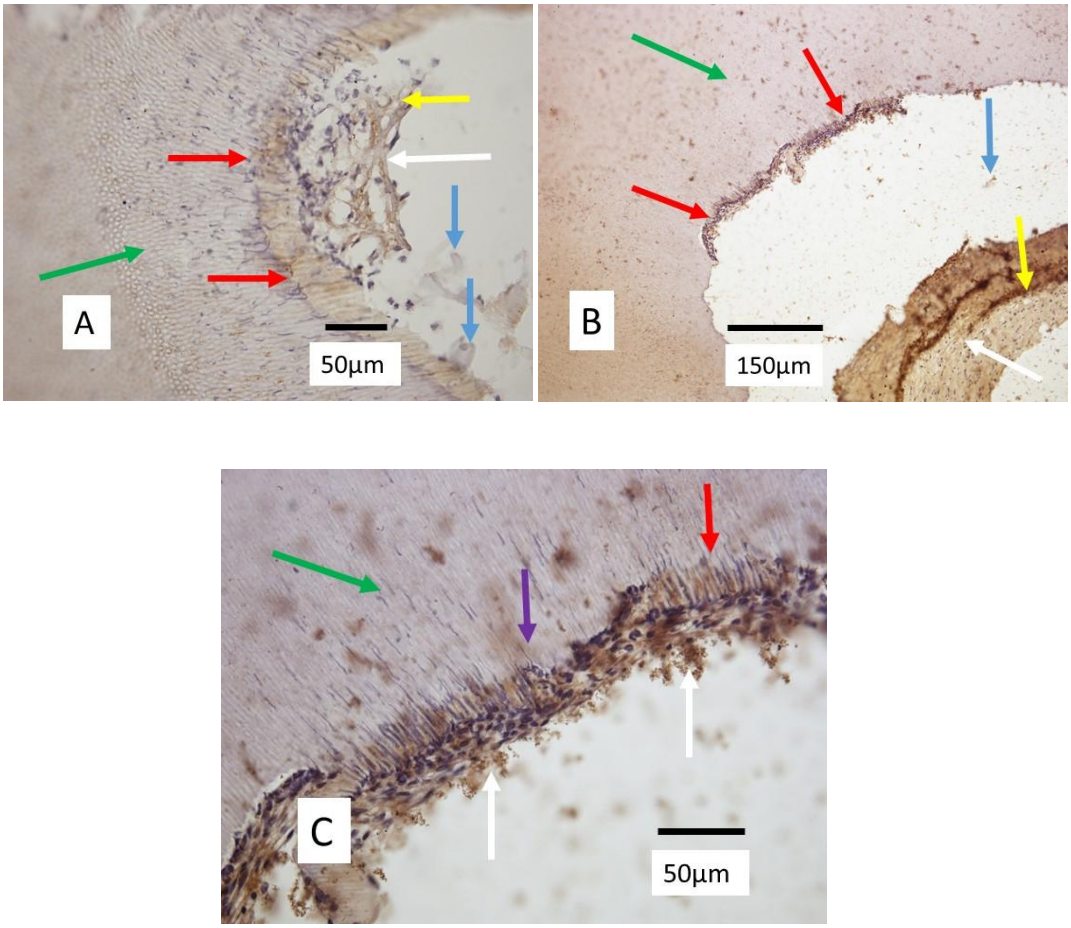

Figure 56. Immunohistochemical staining for CD34 and CD31 expression in tooth slices containing BioGide® and DPSCs only (no HyA).

A: staining for CD34. Green arrow shows dentine surface, red arrows show new material and cell processes at tooth slice margin, white arrows show soft tissue ingrowth, blue arrows indicate BioGide® fragments, yellow arrows indicate vascular structures. B: Staining for CD31. Green arrow shows dentine surface, red shows new tubular material, yellow shows vascular ingrowth, white shows soft tissue ingrowth, blue shows BioGide® fragments. C: Staining for CD31, magnified view. Same colour coding for arrows as before, but the purple arrow is to highlight a cell with its process running into the dentinal tubule.

4.21.3 1%HyA and DPSCs

When 1% HyA gel was used with DPSCs in the constructs to fill the prepared root canal within the tooth slices, results were similar to those described in the preceding sections, with evidence of soft tissue ingrowth staining positively for CD34 (see Figure 57). There was also a deposit of brown-staining tubule-like material with the tubules contiguous with the dentinal tubules of the tooth slice. Cell bodies appeared to be in intimate contact with the new material, with their processes transiting into the dentinal tubules of the tooth slice and a defined demarcation line between the new material and the dentine tubules of the tooth slice.

This soft tissue ingrowth was strongly positive for CD34 as evidenced by the brown colouration particularly towards its central region when stained using immuno-histochemistry. It also appeared to be attached to the dentine of the tooth slice by a pedicle-like structure (see Figure 57 (B and C)). There was also evidence (Figure 57 (B)) of a tubule-like material that stained a darker brown than the dentine of the tooth slice itself. These dark staining tubules were contiguous with the pre-existing dentinal tubules of the endodontically prepared tooth slice and exhibited dark blue staining nuclei of cells that appeared to be in intimate contact with the "deposition front" of the material. Evidence of vascular-like structures could also be seen, with some cells present within the lumen of the vascular structure exhibiting a biconcave disc morphology, strongly suggestive of a vascular structure containing erythrocytes.

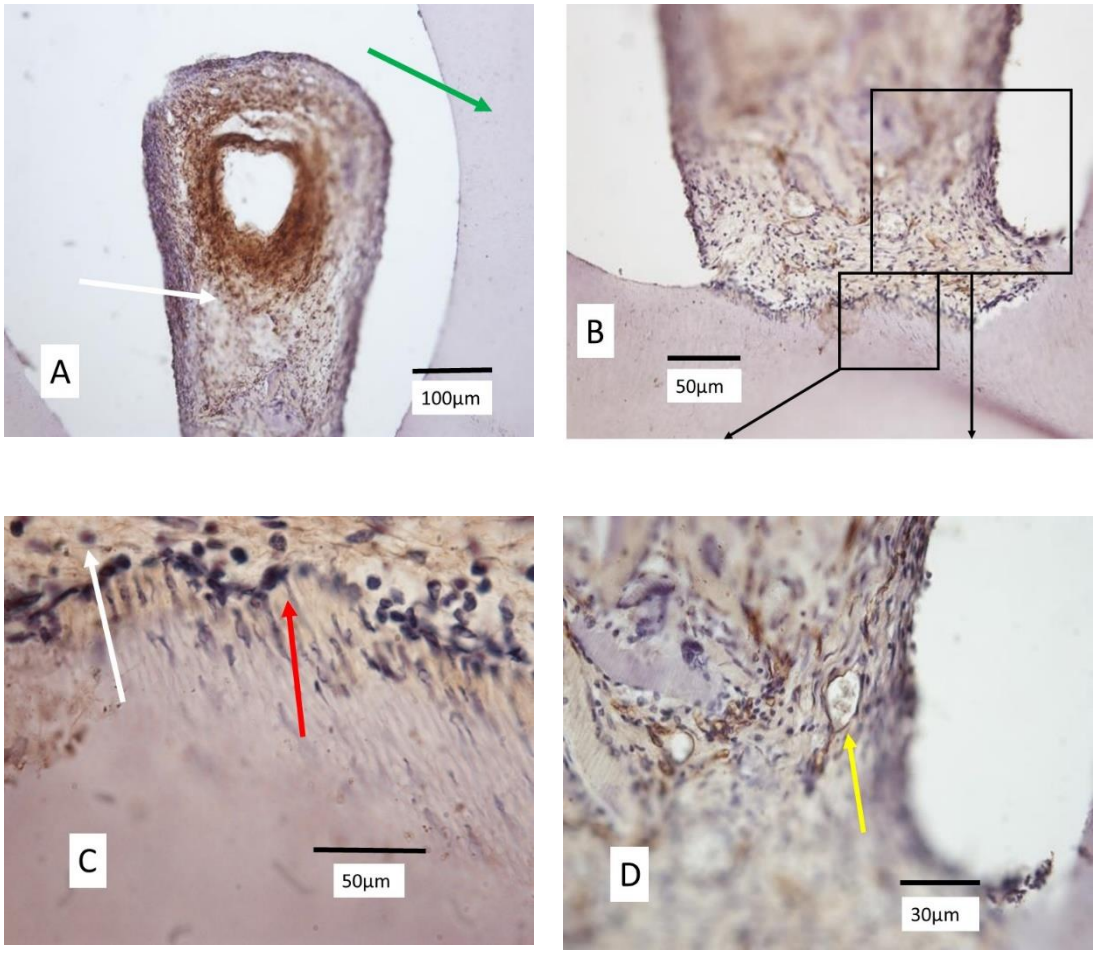

Figure 57. CD34 immunohistochemical staining of tooth slice containing 1% HyA gel and seeded with DPSCs following recovery from *in vivo* incubation for 28 days.

A: white arrow shows soft tissue ingrowth in to tooth slice lumen, staining strongly for CD34 marker, green arrow shows dentine slice. B: soft tissue attachment to tooth slice showing strong immunostaining for CD34 marker. Small box is enlarged in (C), large box is enlarged in (D). C: white arrow shows soft tissue staining strongly for CD34 marker, red arrow shows cell front and cell processes, transiting the darker staining tubule-like material, into the dentine tubules of the tooth slice. D: shows a vascular-like structure staining positively for CD34 marker with some pale-staining, non-nuclear cells present in the lumen. Positive immunostaining for CD34 (brown colour) was apparent in soft tissue ingrowth and new tubule-like structure formation.

When the tooth slices containing 1% HyA seeded with DPSCs were immune-stained using antibodies to the angiogenic marker CD31 after recovery from the animals following 28 days *in vivo* culture, cells staining with dark blue nuclei were seen to be in intimate contact with the instrumented canal lumen (Figure 58 (A)). Cell ingrowth was clearly apparent with strongly positive staining for the CD31 marker. The cells were apparently aligned along the deposition front of the new tubule-like material, contiguous with the dentinal tubules of the instrumented tooth slice (Figure 58 (B)). Cell processes were seen to be transiting the new tubule-like material and continuing through into the dentinal tubules of the tooth slice itself.

Figure 59 (A) is a negative control section of dental pulp (no first antibody). This showed no evidence of staining for the marker even in blood vessels while the corresponding positive control confirmed strong immunostaining for CD31 and CD34 (Figure 59 (B) and (C).

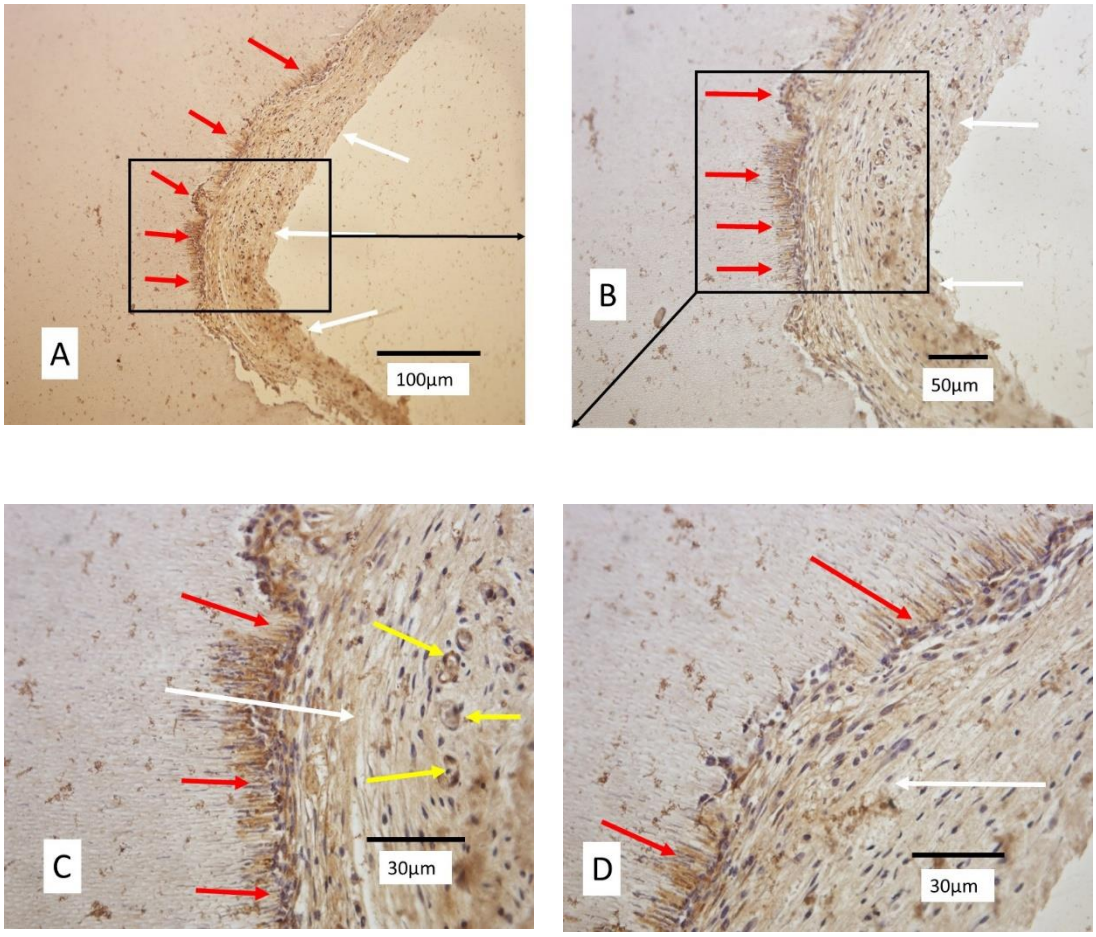

Figure 58. CD31 immunohistochemical staining of tooth slice containing 1% HyA gel and seeded with DPSCs.

A - D: soft tissue ingrowth indicated by the white arrows, positive staining for CD31 (brown colour) indicated by the yellow arrows and new tubule-like material deposited contiguous with the tooth slice dentine, indicated by the red arrows. The dark blue cell bodies can clearly been seen in intimate contact with the deposition front of the new material and there is a demarcation line between the same and the dentine of the tooth slice.

The following dental pulp sections were stained for each biomarker with a control section not being stained for either, thereby acting as a negative control.

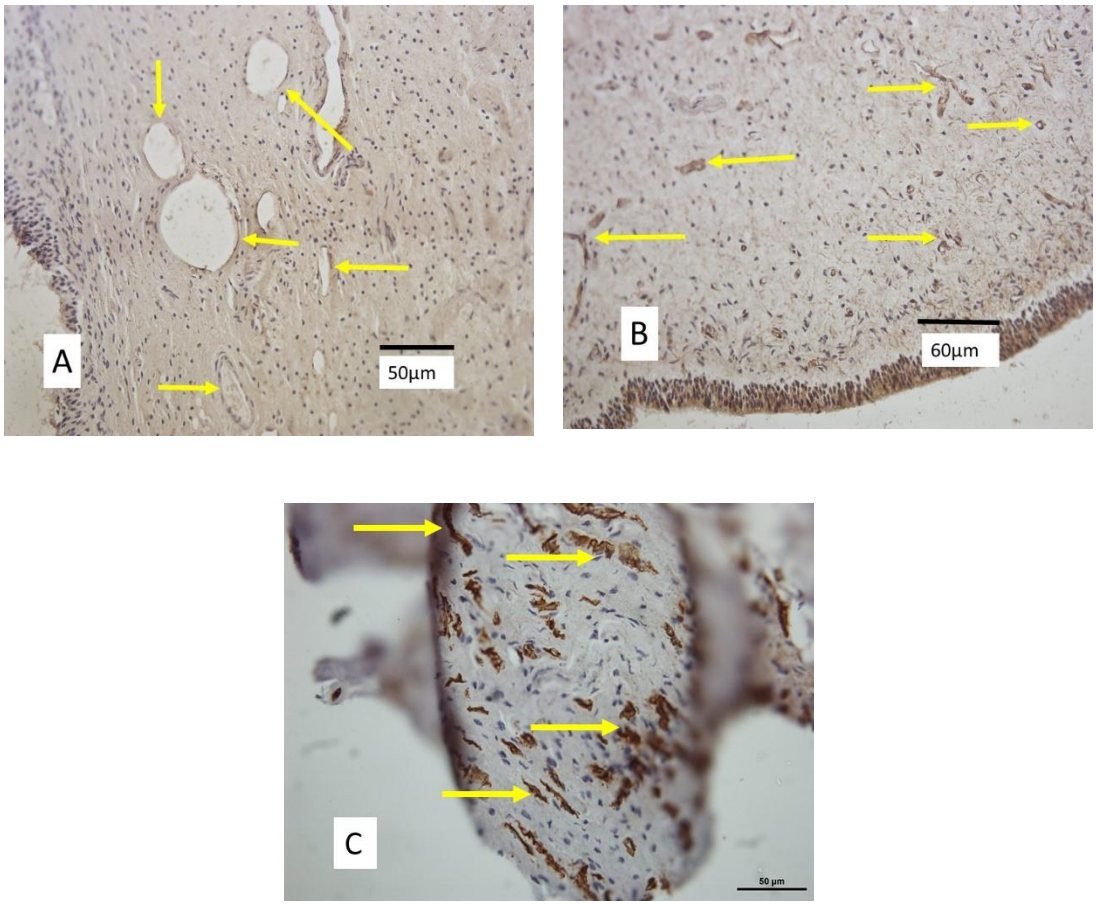

Figure 59. Dental pulp control sections immunostained for CD31 and CD34 marker.

A: no dark brown staining was seen for CD31/CD34 when the first antibody was omitted even around vascular structures (yellow arrows); (negative control dental pulp section). B: strong brown immunostaining for CD31 was seen in the positive control (dental pulp) including around the vessels (yellow arrows). C: strong brown immunostaining for CD34 is obvious in this positive control dental pulp section as indicated by the yellow arrows.

4.21.4 BioGide®/ 1% HyA with DPSCs

The final combination of constructs consisted of a combination of BioGide® collagen membrane plus 1% HyA gel seeded with DPSCs and was used as a within tooth slices followed by implantation *in vivo* and recovery after 28 days. Immuno-histochemistry to determine CD31 expression again revealed new tubule-like material with cells in intimate contact with the deposition front of the material and cell processes passing via the material into the dentinal tubules of the tooth slice (Figure 60 (A and B)). The BioGide® fragments appeared blue following staining and there was also extensive background staining over the dentine of the tooth slice. At higher magnification, cell ingrowth could be seen following the contour of the endodontically prepared tooth slice lumen with CD31 positively stained nuclei apparent (Figure 60 (B)). A region of tubule-like material (marked with a red arrow) with dark CD31 positive staining cell nuclei was seen in intimate contact with the deposition front of the tubule-like material which was in turn contiguous with the dentinal tubules of the tooth slice.

When immuno-histochemistry was repeated, this time using antibodies to CD34, similar results were seen (Figure 60 (C and D)).

The results indicate that a combination of BioGide® and 1% HyA gel plus DPSCs can lead to colonisation of the prepared root canal space, with new tubule-like material laid down contiguous with the dentinal tubules and with the cell layer responsible for elaborating this new material in intimate contact with the front of that newly laid down material. Positive staining with both CD31 and CD34 within this neo-tissue suggests early angiogenesis.

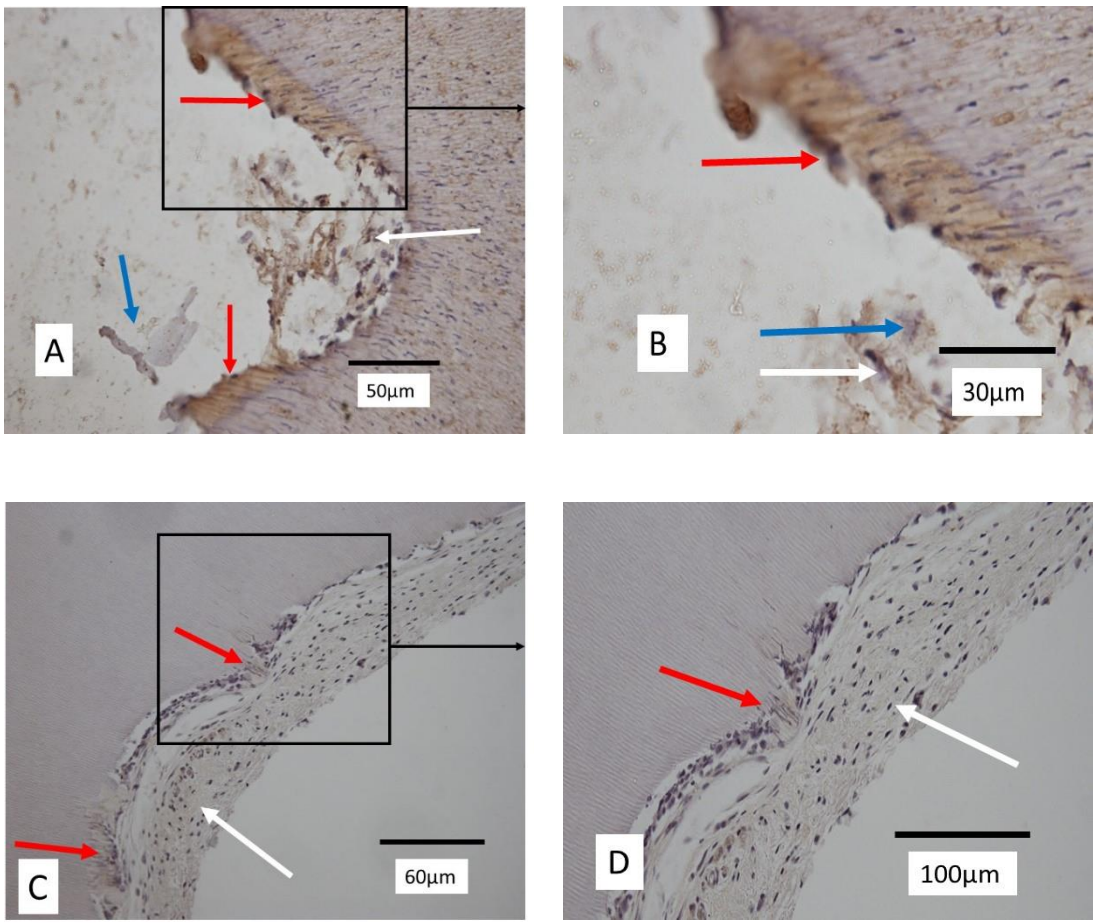

Figure 60. Immunohistochemical staining of *in vivo* samples of BioGide® membrane, 1% HyA and DPSCs stained for CD31 marker.

Images A, B, C and D: BioGide®/1%HyA/DPSCs. Images A and B: stained for CD31 antibody marker with soft tissue ingrowth indicated by the white arrows, BioGide® fragments indicated by the blue arrows and new, material with a visible demarcation line contiguous with the dentinal tubules indicated by the red arrows. Images C and D: stained for CD34 marker with soft tissue ingrowth indicated by white arrows, new material with a visible demarcation line contiguous with the dentinal tubules, by the red arrows.

5.Discussion

5.1 Introduction

5.1.1 Vasculogenesis and angiogenesis

During embryonic growth blood vessels develop through one of two processes;

Vasculogenesis where endothelial cells develop from progenitor cells and:

Angiogenesis where new vessels sprout from existing vessels (Risau, 1995, Risau and Flamme, 1995). Therefore in the adult all blood vessel production is a result of angiogenesis (Hanahan and Folkman, 1996). Outside of the nervous system endothelial cells are amongst the longest lived cells in the human body (as are odontoblasts) with a very low turnover of 1 in 10,000 of them being in cell division at any one time (Hobson and Denekamp, 1984), but given the appropriate stimulation a vasculature can become very active and start to grow new capillaries. Thus, the process of angiogenesis is very complex (Auerbach and Auerbach, 1994, Cockerill et al., 1995) which in turn implies there being multiple controls to oversee it.

5.1.2 Dental pulp regeneration

Dental pulp regeneration in endodontics has been the Holy Grail of Dentistry, and more recently the specialisation of Endodontics, for over half a century (Nygaard-Ostby, 1961, Nygaard-Ostby and Hjortdal, 1971). The American Association of Endodontists Glossary of Endodontic Terms (Endodontists, 2015) has defined

regenerative endodontics as ‘biologically based procedures designed to physiologically replace damaged tooth structures, including dentine and root structures, as well as cells of the pulp-dentine complex’. This started with histological investigations into tissue formation following dental pulp removal and apical ingrowth inside the root canal, initially following blood clot ingress and usually as sequelae of over-instrumentation during endodontic preparation (Nygaard-Ostby, 1961). Some tissue formation had also been seen inside root canals following pulp removal and filling of the root canal with a resorbable material (Engel, 1950, Erausquin and Muruzabal, 1968, Matsumiya and Kitamura, 1960, Stromberg, 1969). Studies in both animals and humans showed that such occurrences only happened if the root canal was allowed to fill with clotted blood from the adjacent instrumented periapical area (Erausquin and Muruzabal, 1968, Nygaard-Ostby, 1961). However, a separate study reported that following deliberate instrumentation beyond the apices of the teeth (admittedly by several millimetres), areas of periapical granulomas persisted and that granulomatous tissue was pervasive within the apical foramen (Seltzer et al., 1968) although this could well have been a consequence of the crude techniques employed, the resultant apical trauma sequelae and consequent compromised healing into an already fibrotic area.

More recently, these principles have been put to use in establishing a methodology to improve the treatment outcomes of immature teeth with open apices which have necrotic dental pulps. Historically, teeth like this have undergone apexification therapy where the treatment protocol entails root canal instrumentation along with periodic application and changes of $Ca(OH)_2$ to remove any necrotic or infected tissues until a calcific tissue barrier develops at the tooth apex (Banchs and Trope,

2004, Damle et al., 2012, Diogenes et al., 2013, Iwaya et al., 2001, Rule and Winter, 1966). Although successful in many cases, this protocol involves multiple surgery visits, thereby incurring higher clinical costs along with the potential for reinfection and consequent patient morbidity. An alternative to this is the application of an apical plug of mineral trioxide aggregate (MTA) which has the advantage of only one or two visits (Damle et al., 2012). However, like apexification, this procedure only promotes apical closure and doesn't allow for continuing root development or continued radicular dentine deposition within the lumen of the root canal to increase the strength of the tooth (Jadhav et al., 2012, Shivashankar et al., 2012). Hence, the current 'gold standard' treatment for immature open-apex teeth is a strategy of revascularisation which has been proven to induce both root extension (i.e. completion of root growth to the anatomically ideal correct length with a fully formed apex) and radicular strengthening by circumferential deposition of dentine inside the root canal lumen (Diogenes et al., 2013). When comparing the two methods, root extension does increase the survival rate of revascularised teeth when compared to apexified teeth by 100% v 77.2%, (Jeeruphan et al., 2012) and so can be regarded as an improvement.

Dental pulp survival following injury is an important aspect of dentistry and successful pulp capping with calcium hydroxide eventually results in pulp cells adhering to an osteodentine layer before differentiation into odontoblasts and production of dentine (Schroder, 1985). Long term studies have shown that success rates for this vary dramatically, with one long term study giving results of 80.1% after one year, tapering down to 58.7% after nine years (Willershausen et al., 2011). Although calcium hydroxide has been the accepted gold standard material of choice

for many years, a Cochrane review has revealed that there is limited evidence as to the most appropriate pulp capping material (Miyashita et al., 2007). With such a lack of common thought amongst the profession, brought about by both the limitations of the current techniques and materials in use, along with blinkered attitudes amongst practitioners, tissue engineering (provided it is properly thought through and applied) is ideally placed to provide a definitive answer to problems which have bedevilled the profession for decades such as bone loss around post/crown restored anterior teeth (Eliasson et al., 1995) and their premature loss (Aptekar and Ginnan, 2006, Murray et al., 2007).

The traditional tissue engineering triad of cells, scaffold and morphogens or growth differentiation signals (Alsberg et al., 2001) will invariably be different for dental pulp regeneration of immature teeth with open apices and those with complete apices, given their likely age groups of application. Both will have devitalised or necrotic tissues to contend with, where exposure to inflammatory cytokines such as tumour necrosis factor alpha (TNF-α) will cause loss of differentiation and mineralisation abilities in DPSCs (Boyle et al., 2014) which in turn interferes with the odontogenic differentiation of apical cells in developing teeth which is necessary for root formation (Sonoyama et al., 2008). Hence, root canal debridement is achieved by a combination of intracanal medicaments and chemomechanical means. Revascularisation protocols only employ mechanical instrumentation in about a third of cases (Kontakiotis et al., 2015), showing the importance and necessity of endodontic irrigation and medicaments. To preserve apical papilla cells, lower strength 1.5% sodium hypochlorite solution is used and 17% EDTA has been shown to promote release of growth factors resulting in hard tissue formation (Becerra et

al., 2014, Galler et al., 2015, Martin et al., 2014). Disinfection is achieved by $Ca(OH)_2$ or triple antibiotic paste (TAP) with the latter being most commonly used, although $Ca(OH)_2$ also gives successful results (Chen et al., 2012) as it appears to aid proliferation of periapical cells whereas TAP, in high concentrations shows detrimental effects (Ruparel et al., 2012). Failure to revascularise has been attributed to persistence of post canal debridement bacterial biofilms and smear layer, indicating inadequate infection control (Lin et al., 2014).

To date, no combination of Type I and III collagen membrane material with a 1% HyA gel has been used in any study or protocol to revascularise an immature open apex tooth, as reported in the literature. In this current study, a novel but everyday combination of 'High Street' materials, with their concomitant advantages of already being commercially licenced, ready availability, cost benefit and comparative ease of possible clinical use was investigated to determine their potential for use in tissue engineering a new dental pulp with potential applications in this particular sphere.

In a clinical setting, dental pulp revascularisation of a mature adult tooth with a fully formed apex in a patient has yet to be achieved (Albuquerque et al., 2014) although evidence of both the safety and efficacy of one treatment modality necessary for clinical use has been presented (Nakashima and Iohara, 2014) as a prerequisite to the initiation of a clinical trial. Almost every investigator and publication reports the use of a different combination of scaffold material, cells and/or morphogens to achieve their end results, both *in vivo* or *in vitro* as the following selection of citations shows: (Akkouch et al., 2014, Bottino et al., 2013 (a), Bottino et al., 2013 (b), Cavalcanti et al., 2013, Cordeiro et al., 2008, Coyac et al., 2013, Dobie et al., 2002,

Feng et al., 2010, Galler et al., 2008, Galler et al., 2011(a), Galler et al., 2011(b), Galler et al., 2012, Huang et al., 2010, Iohara et al., 2014, Iohara et al., 2013, Ishimatsu et al., 2009, Ishizaka et al., 2012, Murakami et al., 2013, Nakashima and Iohara, 2011, Nakashima and Iohara, 2014, Rosa et al., 2013, Wang et al., 2011, Yang et al., 2012, Yang et al., 2010, Zhang et al., 2012). This makes meaningful direct peer to peer comparisons impossible and is reminiscent of the debate surrounding what might be the best endodontic filling material at the beginnings of the twentieth century (Gethro, 1919) before the dental profession finally settled on a 3-D gutta-percha condensation in combination with a sealant paste (Schilder, 1967). There have been moves to at least rationalise the cell types used in these investigations with the suggestion that they be fully characterised to provide the knowledge of candidate cell gene expression to avoid spurious comparisons and ensure that everyone is 'singing from the same hymn sheet' (Ruparel et al., 2013) and also to inform good manufacturing processes for DPSC sourcing and proliferation (La Noce et al., 2014).

5.2 Study overview

The current study used a mixed tissue engineering scaffold material consisting of a combination of a commercially available BioGide® Type I and III collagen membrane combined with a commercially available hyaluronic acid product which has never before been reported as having been used experimentally in dental pulp tissue engineering, although each separate component has been used in differing

combinations in other applications and for different tissues. HyA has been used to investigate angiogenic change and cell attachment whilst cross-linked to Type I collagen derived from bovine Achilles tendon (Perng et al., 2009) in a study examining new blood vessel development. This study also showed that short chain HyA of low Molecular Weight (MW) 6.5 kDa, or oligosaccharide (o-HyA) was better at generating a higher density of new blood vessels than its longer chain high MW comparator (MW 220 kDa). HyA has also been investigated for its material properties of mechanical degradation whilst cross-linked to Type I collagen as a component of cartilage tissue engineering using human Mesenchymal Stem Cells (hMSCs) (Kim et al., 2012) and for compression, swelling and degradation properties whilst cross-linked to collagen as a scaffold for use in brain tissue engineering using neural stem cells (Wang and Spector, 2009). A cross-linked sponge collagen/HyA construct has been shown to have improved dissolution qualities and higher elastic collapse stress and compressive modulus than collagen-only controls when used to support the proliferation of 3T3-L1 pre-adipocytes in adipose tissue engineering for use in mammary tissues (Davidenko et al., 2010) and it has also been used in an *in vitro* study in conjunction with collagen combined with chondroitin sulphate as a potential cartilage tissue engineering scaffold (Zhang et al., 2010). If anything, the diversity of these studies highlights both the ubiquity and importance of the collagen/HyA combination in nature and as a potentially essential and desirable combination in any future tissue engineering clinical protocol.

5.3 Choice of cell procurement

Dental pulp cell harvesting

The dental pulp explant method is based on the outgrowth of DPSCs from sectioned pieces of dental pulp and their adherence to tissue culture plastic (Hilkens et al., 2013, La Noce et al., 2014, Spath et al., 2010). In this study, the dental pulp explant method (Park et al., 2004) proved to be both unpredictable and time-consuming in procuring adequate cell numbers for experimentation. The cell numbers required for experimental use also meant that there was a real potential that the results could be affected by cell senescence by the time sufficient DPSCs had been accumulated. Whilst quantitative data showing the comparative cell numbers obtained at set time points might have been useful to compare their doubling times, the obvious huge superiority of the collagenase digest method in obtaining DPSCs rendered this unnecessary. This was supported by data from other authors (Gronthos et al., 2000, Huang et al., 2006).

When comparing site-specific characteristics of dental pulp, the ALP activity (used as an early marker of osteogenic potential) was consistent in all of the three donor samples tested in that highest activity was seen in the coronal pulp explants with minimal activity in the radicular and apical pulp explant samples. This runs contrary to other authors (Liu et al., 2004, Sun et al., 2004) who found that the pulp explant method was better at harvesting DPSCs and that ALP activity was higher in root canal DPSCs compared with coronal DPSCs. However, the culture conditions were not identical as no mineralisation induction agents were used in this study, whereas theirs had included dexamethasone. This would thus reflect differences in inherent

ALP activity such as in this study and induced ALP activity as in the previous two studies just mentioned.

Several different types of cells have been used to investigate potential strategies in dental pulp tissue engineering. These include DPSCs (Yang et al., 2010), Stem cells from Human Exfoliated Deciduous teeth (SHED) (Cordeiro et al., 2008) both DPSCs and SHEDs together (Galler et al., 2008) DPSCs and SCAPs (Huang et al., 2010), canine dog pulp $CD105^{+}/CD31^{-}$ side population cells (Nakashima and Iohara, 2011), HPDLSCs (Galler et al., 2011(a)) and BMSCs (Galler et al., 2011(a)). In particular, $CD31^{+}$ BMSCs (i.e. non-endothelial cells) have recently been shown to possess better vasculogenic and angiogenic properties than their $CD31^{-}$ counterparts. In a recent review article (Albuquerque et al., 2014) of the studies examined, 18 out of the 27 used DPSCs and a total of 21 used some form of either DPSCs, SHEDs or SCAP cells either on their own or in combination. Hence, the logical choice of cells for this study were DPSCs, based upon their availability and comparability to other studies in the established literature. It is worthwhile noting that other authors have noted that DPSCs have a predilection towards angiogenic differentiation, which would also make them suitable for this study (d'Aquino et al., 2007, Ishizaka et al., 2013, Laino et al., 2005, Trubiani et al., 2003).

In addition, as they are derived from the tissue which is the object of the intended regeneration process, it should follow that any successful scaffold construct used would have a better chance of success *in dente*. At the initial stage of the study, DPSCs were cultured from dental pulp explants and the resultant DPSCs harvested and passaged on for experimental use. As previously noted in the results section

(4.1.1 and 4.1.2) this gave very variable results, concurring with the findings of Moule et al., 1995 and so was abandoned for a modification of the enzymatic digest method adopted by Gronthos et al., 2000, which gave consistently better cell proliferation. Whilst it would have been useful to have obtained quantitative data to support this, the obvious inter-donor variability plus the marked difference in cell numbers derived from each method showed the obvious superiority of the collagenase digest method. During this study the DPSCs generated using the collagenase digestion method showed the ability to proliferate on the BioGide® Type I and III collagen scaffold material and showed their ability to both colonise onto and undergo early angiogenic change on the 1% HyA scaffold.

5.4 Choice of scaffold materials and investigative model

As any scaffold material can have an effect on the eventual outcomes and findings of the study, it was important to choose that which, after an investigation of the literature, would be suitable but without unduly adversely affecting the outcome in any particular direction. This concurs with the findings of other investigators (Smith et al., 2015) who found that DPSCs cultured on elements of the ECM maintained their phenotype better, compared with those cultured on normal tissue culture plastic.

5.4.1 Tooth slice model

The tooth slice model (Goncalves et al., 2007, Magloire et al., 1996, Mullane et al., 2008, Sloan et al., 1998) is a well-established investigative protocol and the results obtained in this thesis broadly concur with those obtained immunohistochemically by other authors, where CD31 was identified in a tooth slice culture of SHED cells albeit following culture with $_{rh}VEGF_{165}$ (Sakai et al., 2010). In this thesis, the use of EGM as a culture medium was consistent with minimising the potentially random effects of FCS as well as its successful use in other studies culturing such diverse endothelial cell types such as 1° human iliac artery endothelial cells (Riessen et al., 2001), endothelial cells from the corpus cavernosum of the human penis (Pilatz et al., 2005(a), Pilatz et al., 2005(b)) and 1° human corneal endothelial cells (Schulz et al., 2013), although in this latter study, the EGM was modified by supplementing it with 10% FCS.

The *in vivo* experiment results obtained in this thesis were more definitive and stronger than the *in vitro* experiments, probably because the living organism is a better bioreactor than a tissue culture plastic 6 well plate and the animal has a much more subtly responsive physiology and microecology than the (relatively speaking) crude environment of the laboratory. Notwithstanding the last sentence, the experiment was carried out upon an animal with a minimally functioning immune system and so any positive results should be viewed with a degree of caution and not extrapolated directly to humans. The *in vitro* culture of DPSCs, seeded onto a combined Type I and III collagen membrane infiltrated with 1% HyA gel (described in the *in vitro* materials and methods and the results sections, 3.16 and 4.18 respectively) showed cells which stained positively for both CD31 and CD34, but

with less evidence of residual scaffold material than was expected due to Type I and III collagen scaffold loss during floating out and mounting of the cut immunohistochemical sections. This technical problem was an issue throughout and unfortunately reduced the number of useful sections available for full interpretation. All four variants of scaffold used in the *in vivo* results (Type I and III collagen membrane plus 1% HyA with no DPSCs; Type I and III collagen membrane plus DPSCs: 1% HyA gel plus DPSCs; Type I and III collagen membrane infiltrated with 1% HyA plus DPSCs) showed much better cell proliferation, along with deposition of material exhibiting a tubular structure contiguous with the pre-existing dentinal tubules than was seen *in vitro*. The newly deposited tubular-structured material was in intimate contact with an overlying cell layer and had cell processes transiting the new material into the dentinal tubules of the surrounding prepared tooth slice. Perhaps the most interesting result was that from the Type I and III collagen membrane/1% HyA only sample which showed the same result as the others but with no seeding cells having been added. This would imply that a cell-free procedure could be a possibility in the future with the scaffold itself exerting both an angioinductive and proliferative effect on any cells populating it. The possibility of a scaffold-inducing angiogenic effect was further supported by the qRT-PCR data shown here, which demonstrated *CD31/34* upregulation in basal medium in the absence of additional angiogenic cues provided by EGM. An angioinductive scaffold would negate the need for cell-seeding and the associated difficulties as is more fully expounded in the Future Work section. The findings in this study were consistent with the findings of other investigators (Cordeiro et al., 2008, Sakai et al., 2010), although both of these investigators only removed the pulp tissue from the

tooth slice leaving the predentine untouched and uninstrumented by files, a situation with potential to leave necrotic debris behind in the clinical setting, although each tooth slice was treated with EDTA. Any blood vessels in the soft tissues deposited within the tooth slice lumen stained positively to CD31 and CD34. There was also evidence of blood vessel-like structures, possibly containing red blood cells and closely resembling dental pulp both in architecture and immunohistological findings. These findings are consistent with those from previous studies (Cordeiro et al., 2008, Sakai et al., 2010) although the scaffolds involved in the current study differed from those in the cited studies which were poly-L-lactic acid (PLLA) and cast into the pulp space *in situ*. Also, there was obvious visual evidence of a definite demarcation line between the newly laid down tubule-like material and the pre-existing dentine of the tooth slice, consistent with the findings of other investigators (Huang et al., 2010).

5.4.2 CD31 and CD34 biomarkers

As already stated in sections 1.15.1.and 1.15.2 respectively, CD31 and CD34 are important biomarkers for angiogenesis and neovascularisation (Pinter et al., 1997). As a bioactive molecule, CD31 has been shown to be involved in numerous biological processes such as platelet aggregation and homeostasis, thrombosis, maintenance of the vascular endothelial barrier function, mechanosensing of endothelial cell response to fluid shear stress (Woodfin et al., 2007), leucocyte migration during the inflammatory response to sites of injury and bacterial ingress

and development of the vasculature (DeLisser et al., 1997, Ferrero et al., 1995, Thompson et al., 2001).

CD34 has been used for the isolation of haematopoietic stem and progenitor cells and as a marker to identify some tissue specific stem cells such as muscle satellite cells and epidermal cell precursors. In these capacities it has been widely used both as a haematopoietic stem cell marker and a vascular endothelial cell marker (Fina et al., 1990, Hristov and Weber, 2008, Sato et al., 1999). In this study CD31 and CD34 stained well both in experimental samples and for control sections of dental pulp tissues, with the only shortcomings being down to handling/storage errors and operator error. The qRT-PCR data presented in this thesis showed interesting significant differences in the timing of expression of *CD31* and *CD34*, with C*D31* expression apparently occurring earlier during the culture conditions compared with *CD34*. This would need further work to investigate whether such changes are relevant *in vivo*.

5.4.3 OsseoGuard® and BioGide® Type I and III collagen membranes scaffold material

In selecting an appropriate scaffold, the ultimate decision to proceed with BioGide® as a source of collagen scaffold was primarily based on ease of acquisition. OsseoGuard® is a highly purified bovine Type I collagen membrane derived from Achilles tendon whereas BioGide® is a veterinary-certified porcine sourced pure Type I and III collagen membrane (Almazrooa et al., 2014, Willershausen et al., 2014). BioGide® is obtained following inactivation of all potential microorganisms

and removal of any fatty and other tissue residues before being sterilised by gamma irradiation. BioGide® is FDA approved and CE marked (as is OsseoGuard®) and consists of Types I and III collagen without further cross-linking or chemical treatment (Ghanaati, 2012). Results for BioGide® obtained under SEM investigation of its structure, are consistent with those obtained by other investigators (Li, 2015, Schlegel et al., 1997). It (BioGide®) has been shown to be less susceptible to proliferation of three different strains of bacteria than OsseoGuard® (Slutzkey et al., 2015) although neither membrane has any definitive antibacterial properties nor are they marketed as possessing any. BioGide® also showed better results in an attachment assay at 24 hours and 5 days when compared to OsseoGuard® in a study examining attachment and proliferation of human osteoblast-like cells (Papaioannou et al., 2011). Both materials showed suitable pore size and interconnectivity for cell attachment, colonisation and proliferation (see section 4.7). This corresponds well with the findings of other authors (Loh and Choong, 2013, Yang et al., 2002). BioGide® also exhibits surface roughness due to not being cross-linked in any way, and the randomness of its structure also promotes better cell adhesion than an aligned structure (Zhong et al., 2006). Being of a 'fabric' construction, it keeps its size and shape and doesn't shrink, which can be a problem with collagen gels (Huang et al., 2006).

Both of these membranes are primarily comprised of Types I and III collagen. Type I collagen is a major structural protein of the ECM where it supports the growth of a wide variety of tissues and provides properties such as mechanical strength (Harley et al., 2007). In hydrogel form it has also been shown to align and stabilise collagen fibrils and DPSCs differentiating into Schwann cells in neural tissue engineering

(Georgiou et al., 2013, Martens et al., 2014). Type III collagen is co-expressed with Type I collagen and is deficient in the tissues of patients with Ehlers-Danlos syndrome type IV (Pope et al., 1975). It is widespread among the body's tissues, both elastic and skeletal, such as bone (Keene et al., 1991) in the epineurium along with collagens Type I and II (Platt et al., 2003) and also in the tympanic membrane where Type III collagen is the predominant type, giving the tympanic membrane its' elasticity and contributes to the healing response of that organ along with Type II collagen (Lim, 1995, Stenfeldt et al., 2013). Type III collagen has been shown to be present in early wound repair at a detectable level 48 hours after healing commenced, when only procollagen of Type I collagen was found, with Type I collagen only being detectable at 72 hours and increasingly thereafter until at day 9 when it was the predominant collagen being synthesised (Gay et al., 1978). Thus, the presence of Type III collagen in BioGide® could have an effect on the early establishment of nascent neo-pulpal tissues, paving the way for the later onset of a more fibroblastic morphology prior to the shift to predominantly collagen Type I expression. In the dental field, BioGide® collagen Type I and III membrane has shown itself capable of maintaining dental pulp vitality and supporting an increased number of blood vessels when used as a pulp-capping agent (Marsan et al., 2003). Other investigators have used collagen impregnated with antibiotics (Biofil-AB™) as a pulpotomy capping agent in deciduous teeth where it was found to be a potential alternative to the current 'gold standard' material formocresol, showing itself to be biologically compatible with deciduous dental pulp tissue, increased pulp healing capacity and promoting better vascularisation where it showed better

biocompatibility than the other material being studied - Pulpotec cement (Kakarla, 2013).

In this study, BioGide® collagen Type I and III membrane was also seen to be compatible with DPSC attachment over a 15 day period as seen when measuring DNA content using the PicoGreen® assay (section 4.10) and for longer periods of up to 28 days, as shown by the confocal microscopy images (section 4.9.2) and also by the SEMs taken on BioGide® and Osseoguard® membranes at 28 days of culture (sections 4.8.1 and 4.8.2). This is consistent with findings of other investigators who cultured DPSCs and oral fibroblasts for 14 days in Type I collagen gels (Lee et al., 2004).

5.4.4 Hyaluronic Acid as a scaffold material

As an important part of the ECM, HyA plays a pivotal role both in signal transduction and cell instruction (DeAngelis, 2008, Toole, 2001). It has been mooted that there are two distinct but continuous forms of ECM, the widespread general intercellular ECM and another more closely cell-associated ECM called the glycocalyx, first imaged using electron microscopy (Luft, 1966) and since then subjected to widespread investigation for its influence on endothelial and pathophysiological processes (Arkill et al., 2011, Erickson and Stern, 2012, Reitsma et al., 2007, Rola, 2013). The endothelial glycocalyx is predominantly localised on the luminal (i.e. inward-facing) surface of the endothelium where it interacts directly with passing blood flow. It has important roles in mediation of leucocyte adhesion (Lipowsky, 2011, Tarbell, 2010), vascular permeability (Curry and Adamson, 2012,

Tarbell, 2010) and endothelial mechanotransduction (Fu and Tarbell, 2013, Pries et al., 2000, Tarbell and Ebong, 2008). This extension of the HyA into the vascular lumen also enables it to control the diffusion of low MW solutes and permeability (Gao and Lipowsky, 2010, Henry and Duling, 1999, Henry and Duling, 2000). It is an extremely versatile molecule and can be chemically modified (Schalte et al., 2011), enabling it at a high molecular weight of 1.6×10^6 Da to support Schwann cells for neural tissue regeneration (Suri and Schmidt, 2010), made into microspheres for sustained gene delivery with site-specific targeting (Yun, 2004), electrospun into nanofibrous scaffolds (Ji et al., 2006), and used as a delivery vehicle for growth factor complexes (Xie et al., 2011). It also has the advantage of complete degradation by the body's cells following use as a scaffold material (Solchaga et al., 1999) and may reduce postsurgical inflammation when added to a surgical site thereby improving treatment outcomes (Jentsch et al., 2003, Peattie et al., 2004, Prato et al., 2003). HyA has also been shown to have some limited bacteriostatic activity (Pirnazar et al., 1999). HyA usually occurs as a high molecular-mass glycosaminoglycan, widely found in mammalian tissues and of sizes between 6×10^5 to 1×10^6 Daltons (Da) and is a component in the haematopoietic stem cell (HSC) niche in the bone marrow where it not only provides a support or physical scaffold within the marrow to facilitate retention and localisation of HSCs to the stem cell niche but is also able to affect the cellular functions of HSCs through ligation with its counter receptors (Haylock and Nilsson, 2006). Whereas high molecular weight HyA is found in many biological contexts, much lower molecular weight HyA is easily detectable in many cancers where it is thought to aid in tumour angiogenesis and also assist cell motility and invasion

(Lokeshwar and Selzer, 2000). HyA degradation products have been shown to have different biological properties and functions depending on their chain length (Stern et al., 2006). o-HyAs are short chains or oligomers of HyA most often with a weight of $\leq 10^4$ Da, which corresponds to between 2 to 40-mers (Cui et al., 2009). These o-HyAs have been shown to initiate gene activation and expression affecting cell function, proliferation, and migration (Entwistle et al., 1996, Noble, 2002, Sherman et al., 1994) with differing functions from those found in the normal, more usual high molecular mass HyA polymer. Short chain HyA is also involved in angiogenesis with o-HyAs of between 4-25 disaccharides (approximately 1×10^4 to 1.6×10^6 Da) exhibiting angiogenic effects on endothelial cells (West and Kumar, 1989) and so should probably be worthy of further investigation re dental pulp revascularisation as more specific angiogenic agents. Their proliferative effects on endothelial cells are thought to be mediated by action on two of the ERM (Ezrin, Radixin and Moesin) group proteins ezrin and merlin, where HUVECs treated with o-HyA showed an increase in the expression and activation of ezrin but treatment with native high MW HyA (n-HyA) gave no significant change in ezrin expression or activation. Conversely, treatment with n-HyA gave no increase in ezrin expression and activation but did give increase that of merlin (Mo et al., 2011). Whereas longer chain HyA has a tendency to inhibit angiogenesis, it can also enhance the production of Type I and Type VIII collagens by endothelial cells (Rooney et al., 1993). More defined investigation of narrower ranges of o-HyAs have shown short chains of 3-10 disaccharide units (but not greater than 10 units) to have the ability to stimulate endothelial cells' proliferation, migration and sprout formation resulting in angiogenesis when used in the chicken chorioallantoic

membrane (CAM) model (Toole et al., 2008) and also in infarction of the myocardium (Slevin et al., 2002). Following depolymerisation into o-HyAs, common or garden 'native' HyA may show different novel functions or bioactive behaviour (Cui et al., 2009). It has been shown that o-HyAs compete with higher molecular weight HyA at cell surface receptors such as CD44 (Misra et al., 2005) and the receptor for HyA-mediated motility (RHAMM) (Slevin et al., 2007). Native high molecular weight HyA has an important role in inhibiting endothelial cell proliferation and migration, as shown in a three-dimensional collagen gel model (Lokeshwar and Selzer, 2000, West et al., 1985) and it is thought that o-HyAs acting in an antagonistic fashion may inhibit many of these interactions via differing pathways (Gao et al., 2008, Slevin et al., 2004). The specificity of o-HyA chain size has been shown by Cui et al., 2009, who synthesised o-HyAs of 4, 6, 8 and 10 disaccharide fragment lengths. The 4 o-HyA chain length had no statistically significant effects on either HUVECs proliferation (which were being used as controls during this experiment) or chicken CAM angiogenesis, whereas the 6, 8 and 10 o-HyA significantly stimulated both HUVEC proliferation and chicken CAM angiogenesis. This was in agreement with previous studies which had shown that oligosaccharides of between 6 – 20 disaccharides could both bind to the CD44 receptor site on endothelial cells and also promote angiogenesis there once *in situ* (Stern et al., 2006) and in a study which showed that o-HyA complexes promote wound healing in the murine wound healing model at twice the rate of nHyA complexes (Gao et al., 2010), this study also found that compared to nHyA, o-HyA promoted the up-regulation of endothelial nitric oxide synthase expression; also E-selectin, integrin β3, procollagen-1 and procollagen-3. Matrix metalloproteinase-9

(MMP-9) and MMP-13 were downregulated. One further advantage of HyA over $_{rh}VEGF_{165}$ is that its physiological effects can continue for an extended period of several days, whereas the half-life of $_{rh}VEGF_{165}$ is between 3 to 6 minutes *in vivo* (George et al., 2000) and about one hour *in vitro* (Shi et al., 2001).

In vivo experimentation using HyA has shown that it can potentially have a role to play in pulp capping and reparative dentinogenesis either alone, using MW 1500-2000 kDa or in combination with other biomaterials (Bogovic et al., 2011, Inuyama et al., 2010, Kuo et al., 2008, Sasaki and Kawamata-Kido, 1995). An *in vitro* study has recently shown a construct of HyA seeded with DPSCs to be able to develop a dental pulp-like tissue and also aid in the repair of calvarial defects in rats when used *in vivo* (Ferroni et al., 2015).

As already shown in the results section (Section 4) GenGiGel®-derived HyA can support cell growth of DPSCs (section 4.4; section 4.15), G292 cells (sections 4.4; 4.16.1), HUVECs (section 4.15.2) and HPDLCs (section 4.16.2) so it can support more than one type of cell, which is important but unsurprising given its ubiquity throughout the ECM and the fact that almost every cell type expresses its most common receptor, CD44. The HyA powder supplied by OralDent® for this study is available commercially as GenGiGel® in several concentrations. On the company's website, it is listed as being of patented high molecular weight and is commonly used in periodontal therapies and for mouth ulceration. It therefore has a track record of use in the oral cavity but the reported high MW would appear to be less than ideal given the enhanced angiogenic properties associated with o-HyAs and described above. This high versus low molecular weight could account for the limited

angiogenic change seen experimentally and in the qRT-PCR results in this thesis when using the GenGiGel® powder. However, the high MW of the HyA used here could also be an explanation for the dentine-like deposition seen in all of the immunohistochemistry samples described in section 4.21 and as this phenomenon has previously been documented in the literature in the direct pulp-capping model (Sasaki and Kawamata-Kido, 1995) in association with high MW HyA. It would provide an explanation as well, for the nodule-like formation seen in the cultures of G292 cells with HyA described in section 4.3.1. Previous tooth slice models have dwelt on angiogenesis as their main result and don't seem to have reported any dentine-like deposition as a finding for whatever reason (Goncalves et al., 2007, Mullane et al., 2008), although maintenance of the pulpal soft tissues was confirmed and evidence of continued ECM production and tooth slice dental pulp homeostasis has been seen (Sloan et al., 1998).

The 1% HyA gel used in the study has shown itself to be able to initiate early angiogenic change in DPSCs as indicated by positive immunohistochemical staining for CD31 and CD34 markers both in the presence and absence of $_{rh}VEGF_{165}$ (section 4.16) and also weakly to CD31 marker in HPDLCs under identical culture conditions (section 4.16). This is perhaps surprising given its high MW, although the high MW chains could have been degraded to smaller fragments during the autoclaving process used for sterilisation. In addition, the qRT-PCR data showed an upregulation in gene expression for CD31 and CD34 which may also explain the level of angiogenic change sufficient to increase angiogenic marker activity as seen in the immunohistochemical results (section 4.18) but show no evidence of budding or sprouting in the *in vitro* DPSC cultures as seen in the low MW studies (Cui et al.,

2009). This would suggest that a more precise mixture of high and low MW HyA could be a more clinically applicable, appropriate and ultimately successful scaffold material for dental pulp tissue engineering, potentially able to give suitable cues for both angiogenesis and hard tissue formation in a single material. As well as HyA, there are other examples of tissue culture scaffolds which can show angiogenic change in DPSCs, without the necessity of adding $_{rh}VEGF_{165}$ (El-Gendy et al., 2015).

5.4.5 Collagen/HyA in combination as scaffold material

HyA has been used in combination with collagens in other investigative areas and other tissues such as the brain (Wang and Spector, 2009) and in cartilage tissue engineering (Liao et al., 2007, Pfeiffer et al., 2008). The combination has not, however, been used in dental pulp engineering to date and particularly as a membrane and gel combination. The natural presence of the two materials in the majority of tissues in the body combined with the biocompatibility of the two materials and their biodegradability makes them particularly favourable as potential scaffolds both for the delivery of cells, and as building blocks for new tissues and consequently for tissue reconstruction in three-dimensions (Vickers et al., 2006, Wang et al., 2006).

As shown in the *in vitro* results, section (Section 4.12), Type I and III collagen membranes on their own were unable to initiate early angiogenic change in DPSCs seeded and grown on them for a period of several days. However, the *in vitro* results (section 4.19) shows that early angiogenic change for DPSCs was induced by

culture in a relatively non-molecular weight-specific gel matrix of 1% HyA in the presence of an endothelial culture medium without $_{rh}VEGF_{165}$. The *in vivo* tooth slice results (section 4.21) showed that DPSCs seeded onto Type I and III collagen/1% HyA and also Type I and III collagen/1% HyA on its own can result in a soft tissue ingrowth staining positively for CD31 and CD34, markers of angiogenic change and also give rise to a newly deposited, organised, tubule-like tissue contiguous with the original dentinal tubules of the endodontically prepared tooth slice along with formation of a layer of cells in intimate contact with the new organised tubule-like material boundary, similar to the layer of odontoblasts anatomically and histologically found at the pulpo-dentine interface of the normal healthy tooth (Goncalves et al., 2007, Mullane et al., 2008, Sakai et al., 2011). They also showed that similar results could be obtained in the absence of seeded DPSCs. This must mean that as a sub-cutaneous model had been used where the tooth slice/scaffold material/seeding cell construct is inserted into a pocket beneath the cutaneous layer (Goncalves et al., 2007, Mullane et al., 2008) and without resorting to implantation in intra-peritoneally placed diffusion chambers, any cells found in the BioGide®/HyA cohort of results had to be derived from the animal host, there being no other source for them. This in turn means that there is potential for a successful therapeutic protocol based on a 'no implanted or seeded cells' basis, leading back to the possibility of recruiting adjacent HPDLCs or other cells migrating along the blood stream via an opened up or expanded apical orifice with all of the potential advantages expounded in Section 7: Future Work, the least of which would be not needing to negotiate many of the regulatory difficulties involved

in current cell-based therapies. It would also lessen the inherent difficulties of donor cell collection, isolation, proliferation and placement.

Previous studies have used species-specific antibodies to differentiate between cells and tissues derived from the seeding cells and those from the host animal. Preliminary work was begun on this but wasn't continued due to constraints on antibody optimisation and time available.

6. Conclusion

To summarise, this study has shown that:

1. It is possible to induce changes commensurate with early angiogenesis in an unselected population of DPSCs by the application of a broad, non-specific but predominantly high MW commercially available HyA gel.
2. Type I and III commercially available collagen membrane materials can support DPSCs, allowing them to attach and colonise and then proliferate over an extended period of time, but not induce angiogenic change.
3. A combination of these two commercially available materials, ± DPSCs can promote the growth of CD31/CD34 positive vascular-like structures within an experimental tooth slice model without recourse to expensive or customised scaffold materials and without a specifically selected i.e. an intentionally broad DPSC population. They have also shown similar results when used unseeded, which means that the cells therein observed had to be host-derived, implying an inductive/conductive property to the scaffold materials.
4. The results obtained here using this novel scaffold combination correlate with those obtained by previous investigators of dental pulp revascularisation using alternative strategies but in addition, show that the deposition of a tubular material which was contiguous with the dentinal tubules of the tooth slice *in situ*, with a layer of cells in intimate contact with that tubular material whose cell processes transit the new

material and run into the dentinal tubules of the tooth slice. As such, this newly deposited material was strongly reminiscent of dentine or predentine in histological appearance.

5. The results obtained in this study provide a basis for future work focussing upon the definitive goal of tissue engineering a dental pulp *in situ*.

7 Future work

The results of the present study have highlighted several main areas of investigation deserving of further study:

1. As the PCR results were fragmentary and n only equalled 1, more detailed PCR investigation would give better insight as to the exact nature of the angiogenic change achieved by the 1% HyA scaffold material.
2. Further immunohistochemical investigation of the tubule-like material laid down in the tooth slice samples during the *in vivo* experiment by specific markers such as those for DSPP could elicit a more definitive answer as to its' exact composition, as would investigation of the adjacent cell layer for evidence of enamelysin, a marker for odontoblasts.
3. Given the proximity of an easily available source of stromal cells in the periodontal ligament, the predictable success of apexification procedures and the probable hierarchy of other therapeutic loci in which cell sources such as DPSCs are much more likely to be utilised for major organ repair, regeneration or replacement, not to mention the costs and possible risks involved in harvesting, expanding and storing DPSCs, it would be logical to evaluate *in situ* HPDLCs as a potential source of new cells to repopulate an engineered dental pulp. This would require further investigation into the best method of accessing them using some modified form of Patency Filing via the tooth apex to ensure optimal preservation of their survivability and proliferation *in situ* but would make sense as the periodontal ligament is a

self-renewing source of cells with a rapid natural turnover, it has a healthy vascular supply provided there are no perio/endo or other dental complications and would require no further harvesting of cells from other donor sources. In turn, this would minimise the amount of time taken to acquire cells, reduce the potential risks of laboratory contamination and problems from senescence during proliferation, lessen patient morbidity consequent to harvesting donor cells from other sites and at the same time maximise use of the 'patient as the bioreactor'. As apexification or revitalisation often leads to a fibro-osseous deposition inside the root canal lumen, further investigation would be needed to elucidate the optimal scaffold material instead of the current blood clot which takes the entire process along a ***repair*** pathway, not a ***regenerative*** one. In a mature tooth, this would probably involve opening up i.e. widening the tooth apex, but as has been seen in the case of apexification and other occurrences, not only soft tissues but also hard tissues can be deposited given the appropriate stimulation and conditions (see Figure below).

4. Optimisation of HyA chain length needs to be carried out to improve and optimise the vascular and proliferation response from any cell source used for dental pulp regeneration. The size of o-HyA required for dermal and other wound healing has already been expounded and although they might be predicted to behave in the same way, any cells used in dental pulp regeneration will need a more specifically optimised scaffold to proliferate rapidly to repopulate an instrumented root canal before the onset of bacterial

ingress. This would also fit in with more accurately establishing the temporality of CD31 and CD34 expression during culture.

5. There is a probable role for collagen Type I and III possibly in endodontic point form or gel-supported fibrils as opposed to membrane form. This could originate from decellularised dental pulp from bovine or porcine origin which would furnish both the necessary fibrillar tissue clues as well as provide a template *in situ* from the various collagen types necessary for any cell ingrowth to tissue engineer a new dental pulp.

   It could also have potential (a) as a carrier for attached or sequestered morphogens or morphogen precursors, or (b) as an easily-degraded source of scaffold material for the regenerating dental pulp. Overall, this would mean it is based primarily on an organic (i.e. in the classical organic chemistry definition such as predominantly oxygen/carbon/nitrogen based materials and biologically resorbable scaffold materials) as opposed to an inorganic (i.e. in the classical chemistry definition such as predominantly calcium/silicon/sodium/phosphorous materials) basis.

6. Finally as the following Figure shows, it is possible to stimulate growth of hard tissues (in the presence of orthodontic forces and tooth movement) down a root canal with an open apex which has been appropriately prepared by adequate filing and disinfection followed by insertion of a suitable nucleating scaffold material such as $Ca(OH)_2$ as in the clinical example shown below.

   A soft tissue should not lie beyond the abilities of dental science and future application as a clinical endodontic dental pulp regenerative therapy.

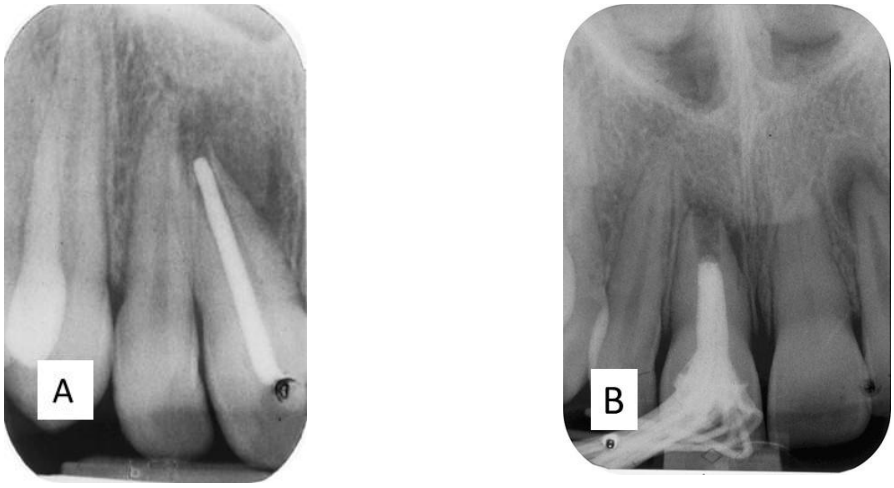

Figure 61. Image of bone deposition inside the root canal of an open apex, orthodontically repositioned upper right central incisor.

The above incisor was partially endodontically treated when this patient was 8-9 years old. A: in her early twenties it was repositioned orthodontically following removal of the single gutta percha point (which doesn't even touch the sides) then endodontic instrumentation, disinfection with sodium hypochlorite, drying, then application of $Ca(OH)_2$ paste and the access cavity sealed. B: several millimetres of bone have been deposited inside the root canal lumen during orthodontic movement as can be seen by the trabecular structure of the bone in the apical portion of the root canal, limiting the extent of the new gutta percha root canal filling. Note the absence of any periodontal structures inside the root canal, such as lamina dura, periodontal ligament, or periodontal ligament space, where the bone deposition has occurred. This would imply ankylosis, although there is still radiographic evidence of periodontal structure on the external root surface.

(Images courtesy of L.D.I.).

List of References

AARS, H., BRODIN, P. & ANDERSEN, E. 1993. A study of cholinergic and beta-adrenergic components in the regulation of blood flow in the tooth pulp and gingiva in man. *Acta Physiol Scand,* 148**,** 441-7.

AINLEY, J. E. 1970. Fluorometric assay of the apical seal of root canal fillings. *Oral Surg Oral Med Oral Pathol,* 29**,** 753-62.

AKKOUCH, A., ZHANG, Z. & ROUABHIA, M. 2014. Engineering bone tissue using human dental pulp stem cells and an osteogenic collagen-hydroxyapatite-poly (L-lactide-co-epsilon-caprolactone) scaffold. *J Biomater Appl,* 28**,** 922-36.

ALBUQUERQUE, M. T. P., VALERA, M. C., NAKASHIMA, M., NOR, J. E. & BOTTINO, M. C. 2014. Tissue-engineering-based Strategies for Regenerative Endodontics. *Journal of Dental Research.,* 93**,** 1222-1231.

ALMAZROOA, S. A., NOONAN, V. & WOO, S. B. 2014. Resorbable collagen membranes: histopathologic features. *Oral Surg Oral Med Oral Pathol Oral Radiol,* 118**,** 236-40.

ALSBERG, E., HILL, E. E. & MOONEY, D. J. 2001. Craniofacial tissue engineering. *Crit Rev Oral Biol Med,* 12**,** 64-75.

ANDREASEN, J. O. A. A., F.M. 1994. Textbook and Color Atlas of Traumatic Injuries to the Teeth. 3rd Edition. *Textbook and Color Atlas of Traumatic Injuries to the Teeth. 3rd Edition.* Copenhagen and St. Louis.: Munksgaard and Mosby.

ANDREW, D. & MATTHEWS, B. 2000. Displacement of the contents of dentinal tubules and sensory transduction in intradental nerves of the cat. *J Physiol,* 529 Pt 3**,** 791-802.

ANNEROTH, G. & BANG, G. 1972. The effect of allogeneic demineralized dentin as a pulp capping agent in Java monkeys. *Odontol Revy,* 23**,** 315-28.

APTEKAR, A. & GINNAN, K. 2006. Comparative Analysis of Microleakage and Seal for 2 Obturatin Materials: Resilon/Epiphany and Gutta-apercha. *J Can Dent Assoc,* 72**,** 245-245d.

ARKILL, K. P., KNUPP, C., MICHEL, C. C., NEAL, C. R., QVORTRUP, K., ROSTGAARD, J. & SQUIRE, J. M. 2011. Similar endothelial glycocalyx structures in microvessels from a range of mammalian tissues: evidence for a common filtering mechanism? *Biophys J,* 101**,** 1046-56.

ARTESE, L., RUBINI, C., FERRERO, G., FIORONI, M., SANTINELLI, A. & PIATTELLI, A. 2002. Vascular endothelial growth factor (VEGF) expression in healthy and inflamed human dental pulps. *J Endod,* 28**,** 20-3.

ARTHUR, A., RYCHKOV, G., SHI, S., KOBLAR, S. A. & GRONTHOS, S. 2008. Adult human dental pulp stem cells differentiate toward functionally active neurons under appropriate environmental cues. *Stem Cells,* 26**,** 1787-95.

AUERBACH, W. & AUERBACH, R. 1994. Angiogenesis inhibition: a review. *Pharmacol Ther,* 63**,** 265-311.

AVERY, J. K., COX, C. F. & CHIEGO, D. J., JR. 1980. Presence and location of adrenergic nerve endings in the dental pulps of mouse molars. *Anat Rec,* 198**,** 59-71.

BADYLAK, S. F. 2002. The extracellular matrix as a scaffold for tissue construction. *Cell and developmental Biology.,* 13**.,** 377-383.

BADYLAK, S. F. 2007. The extracellular matrix as a biologic scaffold material. *Biomaterials.,* 28**,** 3587-3593.

BANCHS, F. & TROPE, M. 2004. Revascularization of immature permanent teeth with apical periodontitis: new treatment protocol? *J Endod,* 30**,** 196-200.

BARRAS, C. 2012. Oldest dental filling is found in a Stone Age tooth. *New Scientist.*

BARRON, M. J., MCDONNELL, S. T., MACKIE, I. & DIXON, M. J. 2008. Hereditary dentine disorders: dentinogenesis imperfecta and dentine dysplasia. *Orphanet J Rare Dis,* 3**,** 31.

BAUMGARDNER, K. R., WALTON, R. E., OSBORNE, J. W. & BORN, J. L. 1996. Induced hypoxia in rat pulp and periapex demonstrated by 3H-misonidazole retention. *J Dent Res,* 75**,** 1753-60.

BAUMHETER, S., SINGER, M. S., HENZEL, W., HEMMERICH, S., RENZ, M., ROSEN, S. D. & LASKY, L. A. 1993. Binding of L-selectin to the vascular sialomucin CD34. *Science,* 262**,** 436-8.

BECERRA, P., RICUCCI, D., LOGHIN, S., GIBBS, J. L. & LIN, L. M. 2014. Histologic study of a human immature permanent premolar with chronic apical abscess after revascularization/revitalization. *J Endod,* 40**,** 133-9.

BERNICK, S. & NEDELMAN, C. 1975. Effect of aging on the human pulp. *J Endod,* 1**,** 88-94.

BHUSSARY, B. R. Modification of the Dental Pulp Organ during development and aging. *In:* FINN, S. B., ed. Biology of the Dental Pulp Organ: a Symposium., 1968 Birmingham, Alabama, USA.: University of Alabama Press.

BIANCO, P. & COSSU, G. 1999. Uno, nessuno e centomila: searching for the identity of mesodermal progenitors. *Exp Cell Res,* 251**,** 257-63.

BIESTERFELD, R. C., TAINTOR, J. F. & MARSH, C. L. 1979. The significance of alterations of pulpal respiration. A review of literature. *J Oral Pathol,* 8**,** 129-39.

BISHOP, M. A. & YOSHIDA, S. 1992. A permeability barrier to lanthanum and the presence of collagen between odontoblasts in pig molars. *J. Anat.,* 181**.,** 29-38.

BLANEY, J. R. 1928. The Medicinal Treatment and the Filling of Root Canals. . *Journal of the American Dental Association,* 15.

BOGOVIC, A., NIZETIC, J., GALIC, N., ZELJEZIC, D., MICEK, V. & MLADINIC, M. 2011. The effects of hyaluronic acid, calcium hydroxide, and dentin adhesive on rat odontoblasts and fibroblasts. *Arh Hig Rada Toksikol,* 62**,** 155-61.

BOHL, K. S., SHON, J., RUTHERFORD, B. & MOONEY, D. J. 1998. Role of synthetic extracellular matrix in development of engineered dental pulp. *J Biomater Sci Polym Ed,* 9**,** 749-64.

BONADIO, J., SMILEY, E., PATIL, P. & GOLDSTEIN, S. 1999. Localized, direct plasmid gene delivery in vivo: prolonged therapy results in reproducible tissue regeneration. *Nat Med,* 5**,** 753-9.

BOTTINO, M. C., KAMOCKI, K., YASSEN, G. H., PLATT, J. A., VAIL, M. M., EHRLICH, Y., SPOLNIK, K. J. & GREGORY, R. L. 2013 (a). Bioactive nanofibrous scaffolds for regenerative endodontics. *J Dent Res,* 92**,** 963-9.

BOTTINO, M. C., YASSEN, G. H., PLATT, J. A., LABBAN, N., WINDSOR, L. J., SPOLNIK, K. J. & BRESSIANI, A. H. 2013 (b). A novel three-dimensional scaffold for regenerative endodontics: materials and biological characterizations. *J Tissue Eng Regen Med*.

BOUVIER, M., JOFFRE, A. & MAGLOIRE, H. 1990. In vitro mineralisation of a three-dimensional collagen matrix by human dental pulp cells in the presence of chondroitin sulphate. *Arch Oral Biol,* 35**,** 301-309.

BOY, S. C. & STEENKAMP, G. 2004. Neural innervation of the tusk pulp of the African elephant (Loxodonta africana). *Vet Rec,* 154**,** 372-4.

BOYAN, B. D., LOHMANN, C. H., ROMERO, J. & SCHWARTZ, Z. 1999. Bone and cartilage tissue engineering. *Clin Plast Surg,* 26**,** 629-45, ix.

BOYLE, M., CHUN, C., STROJNY, C., NARAYANAN, R., BARTHOLOMEW, A., SUNDIVAKKAM, P. & ALAPATI, S. 2014. Chronic inflammation and angiogenic signaling axis impairs differentiation of dental-pulp stem cells. *PLoS One,* 9**,** e113419.

BRADAMANTE, Z., PECINA-HRNCEVIC, A. & CIGLAR, I. 1980. Oxytalan fibres in dental pulp. *Cellular and Molecular Life Sciences.,* 36**,** 1210-1211.

BRADY, J. M. & DEL RIO, C. E. 1975. Corrosion of endodontic silver cones in humans: a scanning electron microscope and X-ray microprobe study. *J Endod,* 1**,** 205-10.

BRANNSTROM, M. 1966(a). Sensitivity of dentine. *Oral Surg Oral Med Oral Pathol,* 21**,** 517-26.

BRANNSTROM, M. 1966(b). The hydrodynamics of the dental tubule and pulp fluid: its significance in relation to dentinal sensitivity. *Annu Meet Am Inst Oral Biol,* 23**,** 219.

BROWN, J., GREAVES, M. F. & MOLGAARD, H. V. 1991. The gene encoding the stem cell antigen, CD34, is conserved in mouse and expressed in haemopoietic progenitor cell lines, brain, and embryonic fibroblasts. *Int Immunol,* 3**,** 175-84.

BUCHANAN, L. S. 1989. Management of the curved root canal. *J Calif Dent Assoc,* 17**,** 18-25, 27.

BUTLER, W. T., BHOWN, M., BRUNN, J. C., D'SOUZA, R. N., FARACH-CARSON, M. C., HAPPONEN, R.-P., SCHROHENLOHER, R. E., SEYER, J. M., SOMERMAN, M. J., FOSTER, R. A., TOMANA, M. & VAN DIJK, S. 1992. Isolation, characterisation and Immunolocalization of a 53-kDal dentin Sialoprotein (DSP). *Matrix.,* 12.**,** 343-351.

BYERS, M. R. & KISH, S. J. 1976. Delineation of Somatic Nerve Endings in Rat Teeth by Radioautography of Axon-Transported Protein. *Journal of Dental Research.,* 55**,** 419-425.

BYERS, M. R. & NARHI, M. V. 1999. Dental injury models: experimental tools for understanding neuroinflammatory interactions and polymodal nociceptor functions. *Crit Rev Oral Biol Med,* 10**,** 4-39.

BYERS, M. R. & SUGAYA, A. 1995. Odontoblast processes in dentin revealed by fluorescent Di-I. *J Histochem Cytochem,* 43**,** 159-68.

BYERS, M. R., SUZUKI, H. & MAEDA, T. 2003. Dental neuroplasticity, neuro-pulpal interactions, and nerve regeneration. *Microsc Res Tech,* 60**,** 503-15.

BYERS, M. R. & TAYLOR, P. E. 1993. Effect of sensory denervation on the response of rat molar pulp to exposure injury. *J Dent Res,* 72**,** 613-8.

CAMPBELL, J. H., EFENDY, J. L. & CAMPBELL, G. R. 1999. Novel vascular graft grown within recipient's own peritoneal cavity. *Circ Res,* 85**,** 1173-8.

CAO, G., O'BRIEN, C. D., ZHOU, Z., SANDERS, S. M., GREENBAUM, J. N., MAKRIGIANNAKIS, A. & DELISSER, H. M. 2002. Involvement of human PECAM-1 in angiogenesis and in vitro endothelial cell migration. *Am J Physiol Cell Physiol,* 282**,** C1181-90.

CAVALCANTI, B. N., ZEITLIN, B. D. & NOR, J. E. 2013. A hydrogel scaffold that maintains viability and supports differentiation of dental pulp stem cells. *Dent Mater,* 29**,** 97-102.

CHAN, B. P. & LEONG, K. W. 2008. Scaffolding in tissue engineering: general approaches and tissue specific considerations. *European Spine Journal.,* 17**,** 467-479.

CHARADRAM, N., FARAHANI, R. M., HARTY, D., RATHSAM, C., SWAIN, M. V. & HUNTER, N. 2012. Regulation of reactionary dentin formation by odontoblasts in response to polymicrobial invasion of dentin matrix. *Bone,* 50**,** 265-75.

CHEN, M. Y., CHEN, K. L., CHEN, C. A., TAYEBATY, F., ROSENBERG, P. A. & LIN, L. M. 2012. Responses of immature permanent teeth with infected

necrotic pulp tissue and apical periodontitis/abscess to revascularization procedures. *Int Endod J,* 45**,** 294-305.

CHEN, N. N. 1987. *A transmission electron microscope study of early changes in hypoxic pulps* PhD., Loma Linda.

CHIEN, S. 1987. Hemodynamics of the dental pulp. *Journal of Dental Research.,* 64**,** 602-606.

CHUDLER, E. H., DONG, W. K. & KAWAKAMI, Y. 1985. Tooth pulp-evoked potentials in the monkey: cortical surface and intracortical distribution. *Pain,* 22**,** 221-33.

CIVIN, C. I., STRAUSS, L. C., BROVALL, C., FACKLER, M. J., SCHWARTZ, J. F. & SHAPER, J. H. 1984. Antigenic analysis of hematopoiesis. III. A hematopoietic progenitor cell surface antigen defined by a monoclonal antibody raised against KG-1a cells. *J Immunol,* 133**,** 157-65.

COCKERILL, G. W., GAMBLE, J. R. & VADAS, M. A. 1995. Angiogenesis: models and modulators. *Int Rev Cytol,* 159**,** 113-60.

COHEN, P. 2001. Open Wide. *New Scientist.*

COLE, W. G. 2002. Advances in osteogenesis imperfecta. *Clin Orthop Relat Res***,** 6-16.

CORDEIRO, M. M., DONG, Z., KANEKO, T., ZHANG, Z., MIYAZAWA, M., SHI, S., SMITH, A. J. & NOR, J. E. 2008. Dental pulp tissue engineering with stem cells from exfoliated deciduous teeth. *J Endod,* 34**,** 962-9.

COUBLE, M. L., FARGES, J. C., BLEICHER, F., PERRAT-MABILLON, B., BOUDEULLE, M. & MAGLOIRE, H. 2000. Odontoblast differentiation of human dental pulp cells in explant cultures. *Calcif Tissue Int,* 66**,** 129-38.

COUVE, E. 1986. Ultrastructural changes during the life cycle of human odontoblasts. *Archives of Oral Biology.,* 31**,** 643-651.

COYAC, B. R., CHICATUN, F., HOAC, B., NELEA, V., CHAUSSAIN, C., NAZHAT, S. N. & MCKEE, M. D. 2013. Mineralization of dense collagen hydrogel scaffolds by human pulp cells. *J Dent Res,* 92**,** 648-54.

CUI, X., XU, H., ZHOU, S., ZHAO, T., LIU, A., GUO, X., TANG, W. & WANG, F. 2009. Evaluation of angiogenic activities of hyaluronan oligosaccharides of defined minimum size. *Life Sci,* 85**,** 573-7.

CURRY, F. E. & ADAMSON, R. H. 2012. Endothelial glycocalyx: permeability barrier and mechanosensor. *Ann Biomed Eng,* 40**,** 828-39.

CVEK, M. 1978. A clinical report on partial pulpotomy and capping with calcium hydroxide in permanent incisors with complicated crown fracture. *J. Endod.,* 4**,** 232-237.

D'AQUINO, R., GRAZIANO, A., SAMPAOLESI, M., LAINO, G., PIROZZI, G., DE ROSA, A. & PAPACCIO, G. 2007. Human postnatal dental pulp cells co-differentiate into osteoblasts and endotheliocytes: a pivotal synergy leading to adult bone tissue formation. *Cell Death Differ,* 14**,** 1162-71.

D'SOUZA, R. 2002. Selzer and bender's dental pulp. *In:* HARGREAVES, K. M. & GOODI, H. E. (eds.). Carol Stream, IL.: Quintessence Publishing Co.

D'SOUZA, R. N., BACHMAN, T., BAUMGARDNER, K. R., BUTLER, W. T. & LITZ, M. 1995. Characterization of cellular responses involved in reparative dentinogenesis in rat molars. *J Dent Res,* 74**,** 702-9.

DAMLE, S. G., BHATTAL, H. & LOOMBA, A. 2012. Apexification of anterior teeth: a comparative evaluation of mineral trioxide aggregate and calcium hydroxide paste. *J Clin Pediatr Dent,* 36**,** 263-8.

DAMMASCHKE, T. 2008. The history of direct pulp capping. *J Hist Dent,* 56**,** 9-23.

DAVIDENKO, N., CAMPBELL, J. J., THIAN, E. S., WATSON, C. J. & CAMERON, R. E. 2010. Collagen-hyaluronic acid scaffolds for adipose tissue engineering. *Acta Biomater,* 6**,** 3957-68.

DE WEVER, O., DEMETTER, P., MAREEL, M. & BRACKE, M. 2008. Stromal myofibroblasts are drivers of invasive cancer growth. *Int J Cancer,* 123**,** 2229-38.

DEAN, M. C. & COLE, T. J. 2013. Human life history evolution explains dissociation between the timing of tooth eruption and peak rates of root growth. *PLoS One,* 8**,** e54534.

DEANGELIS, P. L. 2008. Hot topic: hyaluronan, a very useful sugar polymer. *Curr Pharm Biotechnol,* 9**,** 235.

DELISSER, H. M., CHRISTOFIDOU-SOLOMIDOU, M., STRIETER, R. M., BURDICK, M. D., ROBINSON, C. S., WEXLER, R. S., KERR, J. S., GARLANDA, C., MERWIN, J. R., MADRI, J. A. & ALBELDA, S. M. 1997. Involvement of endothelial PECAM-1/CD31 in angiogenesis. *Am J Pathol,* 151**,** 671-7.

DEMARCO, F. F., CONDE, M. C., CAVALCANTI, B. N., CASAGRANDE, L., SAKAI, V. T. & NOR, J. E. 2011. Dental pulp tissue engineering. *Braz Dent J,* 22**,** 3-13.

DIMITROVA-NAKOV, S., BAUDRY, A., HARICHANE, Y., KELLERMANN, O., GOLDBERG, M. & DR ES SCIENCES, N. 2014. Pulp stem cells: implication in reparative dentin formation. *J Endod,* 40**,** S13-8.

DIOGENES, A., HENRY, M. A., TEIXEIRA, F. B. & HARGREAVES, K. M. 2013. An update on clinical regenerative endodontics. *Endodontic Topics.***,** 2-23.

DOBIE, K., SMITH, G., SLOAN, A. J. & SMITH, A. J. 2002. Effects of alginate hydrogels and TGF-beta 1 on human dental pulp repair in vitro. *Connect Tissue Res,* 43**,** 387-90.

DONG, W. K., CHUDLER, E. H. & MARTIN, R. F. 1985. Physiological properties of intradental mechanoreceptors. *Brain Res,* 334**,** 389-95.

EL-GENDY, R., KIRKHAM, J., NEWBY, P. J., MOHANRAM, Y., BOCCACCINI, A. R. & YANG, X. B. 2015. Investigating the Vascularization of Tissue-Engineered Bone Constructs Using Dental Pulp Cells and 45S5 Bioglass(R) Scaffolds. *Tissue Eng Part A,* 21**,** 2034-43.

ELIASSON, S., BERGSTROM, J. & SANDA, A. 1995. Periodontal bone loss of teeth with metal posts. A radiographic study. *J Clin Periodontol,* 22**,** 850-3.

ENDODONTISTS, A. A. O. 2015. AAE Glossary of Endodontic Terms. *American Association of Endodontists.* 2015. ed. 211 E. Chicago Ave., Suite 1100, Chicago, Il. 60611-2691.: American Association of Endodontists.

ENDODONTISTS., A. A. O. 1994. Contemporary terminology of Endodontics. *American Association of Endodontists.* Suite 211 E. Chicago Ave., Suite 1100, Chicago, Il., 60611-2691.: American Association of Endodontists.

ENGEL, H. 1950. [Comparative roentgenologic and histologic studies of results obtained with Walkhoff's method in the treatment of root canal infections and granuloma]. *SSO Schweiz Monatsschr Zahnheilkd,* 60**,** 1077-109.

ENTWISTLE, J., HALL, C. L. & TURLEY, E. A. 1996. HA receptors: regulators of signalling to the cytoskeleton. *J Cell Biochem,* 61**,** 569-77.

ERAUSQUIN, J. & MURUZABAL, M. 1968. Evaluation of blood clot after root canal treatment. *Journal of Dental Research.,* 47**,** 34-40.

ERICKSON, M. & STERN, R. 2012. Chain gangs: new aspects of hyaluronan metabolism. *Biochem Res Int,* 2012**,** 893947.

FAGAN, D. A., BENIRSCHKE, K., SIMON, J. H. & ROOCROFT, A. 1999. Elephant dental pulp tissue: where are the nerves? *J Vet Dent,* 16**,** 169-72.

FELSCHOW, D. M., MCVEIGH, M. L., HOEHN, G. T., CIVIN, C. I. & FACKLER, M. J. 2001. The adapter protein CrkL associates with CD34. *Blood,* 97**,** 3768-75.

FENG, J. Q., YE, L., CHEN, D., HUANG, H., ZHANG, J., LU, Y. & AL., E. 2002. DPM1 deficient mice develop dwarfism, chondroplasia, and exhibit disorganised bone mineralisation during post-natal development (abstract). *Journal of Bone Mineralisation Research.,* 17**.,** S 127.

FENG, K., SUN, H., BRADLEY, M. A., DUPLER, E. J., GIANNOBILE, W. V. & MA, P. X. 2010. Novel antibacterial nanofibrous PLLA scaffolds. *J Control Release,* 146**,** 363-9.

FERRERO, E., FERRERO, M. E., PARDI, R. & ZOCCHI, M. R. 1995. The platelet endothelial cell adhesion molecule-1 (PECAM1) contributes to endothelial barrier function. *FEBS Lett,* 374**,** 323-6.

FERRONI, L., GARDIN, C., SIVOLELLA, S., BRUNELLO, G., BERENGO, M., PIATTELLI, A., BRESSAN, E. & ZAVAN, B. 2015. A hyaluronan-based scaffold for the in vitro construction of dental pulp-like tissue. *Int J Mol Sci,* 16**,** 4666-81.

FINA, L., MOLGAARD, H. V., ROBERTSON, D., BRADLEY, N. J., MONAGHAN, P., DELIA, D., SUTHERLAND, D. R., BAKER, M. A. & GREAVES, M. F. 1990. Expression of the CD34 gene in vascular endothelial cells. *Blood,* 75**,** 2417-26.

FISHER, A. K. 1967. Respiratory Variations Within the Normal dental Pulp. *J Dent Res,* 46**,** 424-428.

FISHER, A. K., SCHUMACHER, E. R., ROBINSON, N. P. & SHARBONDY, G. P. 1957. Effects of dental drugs and materials on the rate of oxygen consumption in bovine dental pulp. *J Dent Res,* 36**,** 447-50.

FISHER, A. K. & WALTERS, V. E. 1968. Anaerobic Glycolisis in Bovine dental Pulp. *J Dent Res,* 47**,** 717-719.

FISHER, L. W., TORCHIA, D. A., FOHR, B., YOUNG, M. F. & FEDARKO, N. S. 2001. Flexible structures of SIBLING proteins, bone sialoprotein, and osteopontin. *Biochem Biophys Res Commun,* 280**,** 460-5.

FITZGERALD, M. 1979. Cellular mechanics of dentinal bridge repair using 3H-thymidine. *J Dent Res,* 58**,** 2198-206.

FITZGERALD, M., CHIEGO, D. J. & HEYS, D. R. 1990. Autoradiographic analysis of odontoblast replacement following pulp exposure in primate teeth. *Arch Oral Biol,* 35**,** 707-715.

FRANTZ, C., STEWART, K. M. & WEAVER, V. M. 2010. The extracellular matrix at a glance. *J Cell Sci,* 123**,** 4195-200.

FREIRE, A. & ARCHEGAS, L. R. 2010. Porcelain laminate veneer on a highly discoloured tooth: a case report. *J Can Dent Assoc,* 76**,** a126.

FRIED, K., RISLING, M., EDWALL, L. & OLGART, L. 1992. Immuno-electron-microscopic localization of laminin and collagen type IV in normal and denervated tooth pulp of the cat. *Cell Tissue Res,* 270**,** 157-64.

FRISTAD, I. 1997. Dental innervation: functions and plasticity after peripheral injury. *Acta Odontol Scand,* 55**,** 236-54.

FU, B. M. & TARBELL, J. M. 2013. Mechano-sensing and transduction by endothelial surface glycocalyx: composition, structure, and function. *Wiley Interdiscip Rev Syst Biol Med,* 5**,** 381-90.

GALLER, K. M., BUCHALLA, W., HILLER, K. A., FEDERLIN, M., EIDT, A., SCHIEFERSTEINER, M. & SCHMALZ, G. 2015. Influence of root canal disinfectants on growth factor release from dentin. *J Endod,* 41**,** 363-8.

GALLER, K. M., CAVENDER, A., YUWONO, V., DONG, H., SHI, S., SCHMALZ, G., HARTGERINK, J. D. & D'SOUZA, R. N. 2008. Self-assembling peptide amphiphile nanofibers as a scaffold for dental stem cells. *Tissue Eng Part A,* 14**,** 2051-8.

GALLER, K. M., CAVENDER, A. C., KOEKLUE, U., SUGGS, L. J., SCHMALZ, G. & D'SOUZA, R. N. 2011(a). Bioengineering of dental stem cells in a PEGylated fibrin gel. *Regen Med,* 6**,** 191-200.

GALLER, K. M., D'SOUZA, R. N., FEDERLIN, M., CAVENDER, A. C., HARTGERINK, J. D., HECKER, S. & SCHMALZ, G. 2011(b). Dentin conditioning codetermines cell fate in regenerative endodontics. *J Endod,* 37**,** 1536-41.

GALLER, K. M., HARTGERINK, J. D., CAVENDER, A. C., SCHMALZ, G. & D'SOUZA, R. N. 2012. A customized self-assembling peptide hydrogel for dental pulp tissue engineering. *Tissue Eng Part A,* 18**,** 176-84.

GAO, F., LIU, Y., HE, Y., YANG, C., WANG, Y., SHI, X. & WEI, G. 2010. Hyaluronan oligosaccharides promote excisional wound healing through enhanced angiogenesis. *Matrix Biol,* 29**,** 107-16.

GAO, F., YANG, C. X., MO, W., LIU, Y. W. & HE, Y. Q. 2008. Hyaluronan oligosaccharides are potential stimulators to angiogenesis via RHAMM mediated signal pathway in wound healing. *Clin Invest Med,* 31**,** E106-16.

GAO, L. & LIPOWSKY, H. H. 2010. Composition of the endothelial glycocalyx and its relation to its thickness and diffusion of small solutes. *Microvasc Res,* 80**,** 394-401.

GARBEROGLIO, R. & BRANNSTROM, M. 1976. Scanning electron microscopic investigation of human dentinal tubules. *Arch Oral Biol,* 21**,** 355-62.

GAY, S., VIJANTO, J., RAEKALLIO, J. & PENTTINEN, R. 1978. Collagen types in early phases of wound healing in children. *Acta Chir Scand,* 144**,** 205-11.

GEORGE, M. L., ECCLES, S. A., TUTTON, M. G., ABULAFI, A. M. & SWIFT, R. I. 2000. Correlation of plasma and serum vascular endothelial growth factor levels with platelet count in colorectal cancer: clinical evidence of platelet scavenging? *Clin Cancer Res,* 6**,** 3147-52.

GEORGIOU, M., BUNTING, S. C., DAVIES, H. A., LOUGHLIN, A. J., GOLDING, J. P. & PHILLIPS, J. B. 2013. Engineered neural tissue for peripheral nerve repair. *Biomaterials,* 34**,** 7335-43.

GETHRO, F. M. 1919. The treatment and filing of root-canals. *Journal of the American Dental Association,* 9**,** 812.

GHANAATI, S. 2012. Non-cross-linked porcine-based collagen I-III membranes do not require high vascularization rates for their integration within the implantation bed: a paradigm shift. *Acta Biomater,* 8**,** 3061-72.

GLICK, M., TROPE, M. & PLISKIN, M. E. 1989. Detection of HIV in dental pulp of a patient with AIDS. *Journal of the American Dental Association,* 119**,** 649-650.

GOLDBERG, M., SEPTIER, D., LECOLLE, S., CHARDIN, H., QUINTANA, M. A., ACEVEDO, A. C., GAFNI, G., DILLOUYA, D., VERMELIN, L., THONEMANN, B. & ET AL. 1995. Dental mineralization. *Int J Dev Biol,* 39**,** 93-110.

GOLDBERG, M. & SMITH, A. J. 2004. Cells and Extracellular Matrices of Dentin and Pulp: A Biological Basis for Repair and Tissue Engineering. *Crit Rev Oral Biol Med,* 15**,** 13-27.

GOLDONI, S. & IOZZO, R. V. 2008. Tumor microenvironment: Modulation by decorin and related molecules harboring leucine-rich tandem motifs. *Int J Cancer,* 123**,** 2473-9.

GONCALVES, S. B., DONG, Z., BRAMANTE, C. M., HOLLAND, G. R., SMITH, A. J. & NOR, J. E. 2007. Tooth slice-based models for the study of human dental pulp angiogenesis. *J Endod,* 33**,** 811-4.

GOODMAN, A., SCHILDER, H. & ALDRICH, W. 1974. The thermomechanical properties of gutta-percha. II. The history and molecular chemistry of gutta-percha. *Oral Surg Oral Med Oral Pathol,* 37**,** 954-61.

GORDON, M. K. & HAHN, R. A. 2010. Collagens. *Cell Tissue Res,* 339**,** 247-57.

GOTJAMANOS, T. 1969. The odontoblastic and subodontoblastic cell layers of the rat incisor pulp. *Australian Dent. J.,* 14**,** 302-311.

GOTO, Y., CEYHAN, J. & CHU, S. J. 2009. Restorations of endodontically treated teeth: new concepts, materials, and aesthetics. *Pract Proced Aesthet Dent,* 21**,** 81-9.

GREEN, D. 1956. A stereomicroscopic study of the root apices of 400 maxillary and mandibular anterior teeth. *Oral Surg Oral Med Oral Pathol,* 9**,** 1224-32.

GRONTHOS, S., BRAHIM, J., LI, W., FISHER, L. W., CHERMAN, N., BOYDE, A., DENBESTEN, P., ROBEY, P. G. & SHI, S. 2002. Stem cell properties of human dental pulp stem cells. *J Dent Res,* 81**,** 531-5.

GRONTHOS, S., MANKANI, M., BRAHIM, J., ROBEY, P. G. & SHI, S. 2000. Postnatal human dental pulp stem cells (DPSCs) in vitro and in vivo. *Proc Natl Acad Sci U S A,* 97**,** 13625-30.

GROSSMAN, E. S. & AUSTIN, J. C. 1983. Scanning electron microscope observations on the tubule content of freeze-fractured peripheral vervet monkey dentine (Cercopithecus pygerythrus). *Arch Oral Biol,* 28**,** 279-281.

GROSSMAN, L. I. 1976. Endodontics 1776-1976: a bicentennial history against the background of general dentistry. *J Am Dent Assoc,* 93**,** 78-87.

GYSI, A. 1900. An attempt to explain the sensitiveness of dentine. *Br J Dent Sci.,* 43**,** 865-868.

HAHN, C.-L., FALKLER, W. A. & SIEGEL, M. A. 1989. A study of T and B cells in pulpal pathosis. *J Endod,* 15**,** 20-26.

HAMERSKY, P. A., WEIMER, A. D. & TAINTOR, J. F. 1980. The effect of orthodontic force application on the pulpal tissue respiration rate in the human premolar. *Am J Orthod,* 77**,** 368-78.

HAN, S. S. 1968. *The fine structure of cells and intercellular substances of the dental pulp.,* Birmingham., University of Alabama Press.

HANAHAN, D. & FOLKMAN, J. 1996. Patterns and emerging mechanisms of the angiogenic switch during tumorigenesis. *Cell,* 86**,** 353-64.

HARLEY, B. A., LEUNG, J. H., SILVA, E. C. & GIBSON, L. J. 2007. Mechanical characterization of collagen-glycosaminoglycan scaffolds. *Acta Biomater,* 3**,** 463-74.

HARRIS, R. & GRIFFIN, C. J. 1968. Fine structure of nerve endings in the human dental pulp. *Arch Oral Biol,* 13**,** 773-8.

HATTYASY, D. 1961. Continuous regeneration of the dentinal nerve endings. *Nature,* 189**,** 72-4.

HAYLOCK, D. N. & NILSSON, S. K. 2006. The role of hyaluronic acid in hemopoietic stem cell biology. *Regen Med,* 1**,** 437-45.

HENRY, C. B. & DULING, B. R. 1999. Permeation of the luminal capillary glycocalyx is determined by hyaluronan. *Am J Physiol,* 277**,** H508-14.

HENRY, C. B. & DULING, B. R. 2000. TNF-alpha increases entry of macromolecules into luminal endothelial cell glycocalyx. *Am J Physiol Heart Circ Physiol,* 279**,** H2815-23.

HERMANN, B. W. 1952. [On the reaction of the dental pulp to vital amputation and calxyl capping]. *Dtsch Zahnarztl Z,* 7**,** 1446-7.

HEYERAAS, K. J. & BERGGREEN, E. 1999. Interstitial fluid pressure in normal and inflamed pulp. *Crit Rev Oral Biol Med,* 10**,** 328-36.

HEYERAAS, K. J., KVINNSLAND, I., BYERS, M. R. & JACOBSEN, E. B. 1993. Nerve fibers immunoreactive to protein gene product 9.5, calcitonin gene-related peptide, substance P, and neuropeptide Y in the dental pulp, periodontal ligament, and gingiva in cats. *Acta Odontol Scand,* 51**,** 207-21.

HEYERASS, K. J. & KVINNSLAND, I. 1992. Tissue pressure and blood flow in pulpal inflammation. *Proc Finn Dent Soc,* 88**,** 383-401.

HIKIJI, A., YAMAMOTO, H., SUNAKAWA, M. & SUDA, H. 2000. Increased blood flow and nerve firing in the cat canine tooth in response to stimulation of the second premolar pulp. *Arch Oral Biol,* 45**,** 53-61.

HILKENS, P., GERVOIS, P., FANTON, Y., VANORMELINGEN, J., MARTENS, W., STRUYS, T., POLITIS, C., LAMBRICHTS, I. & BRONCKAERS, A. 2013. Effect of isolation methodology on stem cell properties and multilineage differentiation potential of human dental pulp stem cells. *Cell Tissue Res,* 353**,** 65-78.

HILLMAN, G. & GUERTSEN, W. 1997. Light-microscopal investigation of the distribution of extracellular matrix molecules and calcifications in human dental pulps of various ages. *Cell Tissue Res,* 289.**,** 145-154.

HOBSON, B. & DENEKAMP, J. 1984. Endothelial proliferation in tumours and normal tissues: continuous labelling studies. *Br J Cancer,* 49**,** 405-13.

HOLLAND, G. H. & TORABINEJAD, M. 2009. *Endodontics: Principles and Practice.*

HOLLAND, G. R. 1976. The extent of the odontoblast process in the cat. *J. Anat.,* 121**,** 133-149.

HOLLAND, G. R. 1985. The odontoblast process: form and function. *J Dent Res,* 64 Spec No**,** 499-514.

HOLLAND, G. R. 1994. Morphological features of dentine and pulp related sensitivity. *Arch Oral Biol,* 39**,** S3-S11.

HOLLAND, R., DE SOUZA, V., MURATA, S. S., NERY, M. J., BERNABE, P. F., OTOBONI FILHO, J. A. & DEZAN JUNIOR, E. 2001. Healing process of dog dental pulp after pulpotomy and pulp covering with mineral trioxide aggregate or Portland cement. *Braz Dent J,* 12**,** 109-13.

HOVLAND, E. J. & DUMSHA, T. C. 1985. Leakage evaluation in vitro of the root canal sealer cement Sealapex. *Int Endod J,* 18**,** 179-82.

HRISTOV, M. & WEBER, C. 2008. Endothelial progenitor cells in vascular repair and remodeling. *Pharmacol Res,* 58**,** 148-51.

HUA, C. T., GAMBLE, J. R., VADAS, M. A. & JACKSON, D. E. 1998. Recruitment and activation of SHP-1 protein-tyrosine phosphatase by human platelet endothelial cell adhesion molecule-1 (PECAM-1). Identification of immunoreceptor tyrosine-based inhibitory motif-like binding motifs and substrates. *J Biol Chem,* 273**,** 28332-40.

HUANG, G. T., SONOYAMA, W., CHEN, J. & PARK, S. H. 2006. In vitro characterization of human dental pulp cells: various isolation methods and culturing environments. *Cell Tissue Res,* 324**,** 225-36.

HUANG, G. T., YAMAZA, T., SHEA, L. D., DJOUAD, F., KUHN, N. Z., TUAN, R. S. & SHI, S. 2010. Stem/progenitor cell-mediated de novo regeneration of dental pulp with newly deposited continuous layer of dentin in an in vivo model. *Tissue Eng Part A,* 16**,** 605-15.

IBUKI, T., KIDO, M. A., KIYOSHIMA, T., TERADA, Y. & TANAKA, T. 1996. An ultrastructural study of the relationship between sensory trigeminal nerves and odontoblasts in rat dentin/pulp as demonstrated by the anterograde transport of wheat germ agglutinin-horseradish peroxidase (WGA-HRP). *J Dent Res,* 75**,** 1963-70.

INOUE, K., CREVELING, C. R., KARASAWA, N., ISOMURA, G. & NAGATSU, I. 1994. Measurement of dopa and immunolocalization of L-dopa-positive nerve fibers in rat dental pulp. *Brain Res,* 657**,** 307-9.

INUYAMA, Y., KITAMURA, C., NISHIHARA, T., MOROTOMI, T., NAGAYOSHI, M., TABATA, Y., MATSUO, K., CHEN, K. K. & TERASHITA, M. 2010. Effects of hyaluronic acid sponge as a scaffold on odontoblastic cell line and amputated dental pulp. *J Biomed Mater Res B Appl Biomater,* 92**,** 120-8.

IOHARA, K., MURAKAMI, M., NAKATA, K. & NAKASHIMA, M. 2014. Age-dependent decline in dental pulp regeneration after pulpectomy in dogs. *Exp Gerontol,* 52**,** 39-45.

IOHARA, K., MURAKAMI, M., TAKEUCHI, N., OSAKO, Y., ITO, M., ISHIZAKA, R., UTUNOMIYA, S., NAKAMURA, H., MATSUSHITA, K.

& NAKASHIMA, M. 2013. A novel combinatorial therapy with pulp stem cells and granulocyte colony-stimulating factor for total pulp regeneration. *Stem Cells Transl Med,* 2**,** 521-33.

IOHARA, K., NAKASHIMA, M., ITO, M., ISHIKAWA, M., NAKASIMA, A. & AKAMINE, A. 2004. Dentin regeneration by dental pulp stem cell therapy with recombinant human bone morphogenetic protein 2. *J Dent Res,* 83**,** 590-5.

IOZZO, R. V. & MURDOCH, A. D. 1996. Proteoglycans of the extracellular environment: clues from the gene and protein side offer novel perspectives in molecular diversity and function. *FASEB J,* 10**,** 598-614.

IOZZO, R. V., ZOELLER, J. J. & NYSTROM, A. 2009. Basement membrane proteoglycans: modulators Par Excellence of cancer growth and angiogenesis. *Mol Cells,* 27**,** 503-13.

ISHIMATSU, H., KITAMURA, C., MOROTOMI, T., TABATA, Y., NISHIHARA, T., CHEN, K. K. & TERASHITA, M. 2009. Formation of dentinal bridge on surface of regenerated dental pulp in dentin defects by controlled release of fibroblast growth factor-2 from gelatin hydrogels. *J Endod,* 35**,** 858-65.

ISHIZAKA, R., HAYASHI, Y., IOHARA, K., SUGIYAMA, M., MURAKAMI, M., YAMAMOTO, T., FUKUTA, O. & NAKASHIMA, M. 2013. Stimulation of angiogenesis, neurogenesis and regeneration by side population cells from dental pulp. *Biomaterials,* 34**,** 1888-97.

ISHIZAKA, R., IOHARA, K., MURAKAMI, M., FUKUTA, O. & NAKASHIMA, M. 2012. Regeneration of dental pulp following pulpectomy by fractionated stem/progenitor cells from bone marrow and adipose tissue. *Biomaterials,* 33**,** 2109-18.

IWAYA, S. I., IKAWA, M. & KUBOTA, M. 2001. Revascularization of an immature permanent tooth with apical periodontitis and sinus tract. *Dent Traumatol,* 17**,** 185-7.

IZUMI, T., KOBAYASHI, I., OKAMURA, K. & SAKAI, H. 1995. Immunohistochemical study on the immunocompetent cells of the pulp in human non-carious and carious teeth. *Arch Oral Biol,* 40**,** 609-14.

JACKSON, D. E., WARD, C. M., WANG, R. & NEWMAN, P. J. 1997. The protein-tyrosine phosphatase SHP-2 binds platelet/endothelial cell adhesion molecule-1 (PECAM-1) and forms a distinct signaling complex during platelet aggregation. Evidence for a mechanistic link between PECAM-1- and integrin-mediated cellular signaling. *J Biol Chem,* 272**,** 6986-93.

JADHAV, G., SHAH, N. & LOGANI, A. 2012. Revascularization with and without platelet-rich plasma in nonvital, immature, anterior teeth: a pilot clinical study. *J Endod,* 38**,** 1581-7.

JARVELAINEN, H., SAINIO, A., KOULU, M., WIGHT, T. N. & PENTTINEN, R. 2009. Extracellular matrix molecules: potential targets in pharmacotherapy. *Pharmacol Rev,* 61**,** 198-223.

JEERUPHAN, T., JANTARAT, J., YANPISET, K., SUWANNAPAN, L., KHEWSAWAI, P. & HARGREAVES, K. M. 2012. Mahidol study 1: comparison of radiographic and survival outcomes of immature teeth treated with either regenerative endodontic or apexification methods: a retrospective study. *J Endod,* 38**,** 1330-6.

JENTSCH, H., POMOWSKI, R., KUNDT, G. & GOCKE, R. 2003. Treatment of gingivitis with hyaluronan. *J Clin Periodontol,* 30**,** 159-64.

JERNVALL, J., KETTUNEN, P., KARAVANOVA, I., MARTIN, L. B. & THESLEFF, I. 1994. Evidence for the role of the enamel knot as a control center in mammalian tooth cusp formation: non-dividing cells express growth stimulating Fgf-4 gene. *Int J Dev Biol,* 38**,** 463-9.

JI, Y., GHOSH, K., SHU, X. Z., LI, B., SOKOLOV, J. C., PRESTWICH, G. D., CLARK, R. A. & RAFAILOVICH, M. H. 2006. Electrospun three-dimensional hyaluronic acid nanofibrous scaffolds. *Biomaterials,* 27**,** 3782-92.

JONES, P. A., TAINTOR, J. F. & ADAMS, A. B. 1979. Comparative dental material cytotoxicity measured by depression of rat incisor pulp respiration. *J Endod,* 5**,** 48-55.

JONTELL, M., BERGENHOLTZ, G., SCHEYNIUS, A. & AMBROSE, W. 1988. Dendritic cells and macrophages expressing class II antigens in the normal rat incisor pulp. *J Dent Res,* 67**,** 1263-6.

JONTELL, M., GUNRAJ, M. N. & BERGENHOLTZ, G. 1987. Immunocompetent Cells in the Normal Dental Pulp. *J Dent Res,* 66**,** 1149-1153.

JULLIG, M., ZHANG, W. V. & STOTT, N. S. 2004. Gene therapy in orthopaedic surgery: the current status. *ANZ J Surg,* 74**,** 46-54.

KAKARLA, P., AVULA, J.S.S., MELLELA, G.M., BANDI, S. AND ANCHE S. 2013. Dental response to collagen and pulpotec cement as pulpotomy agents in primary dentition: A histological study. *Journal of Conservative Dentistry.,* 16**,** 434-438.

KAKEHASHI, S., STANLEY, H. R. & FITZGERALD, R. J. 1965. The Effects of Surgical Exposures of Dental Pulps in Germ-Free and Conventional Laboratory Rats. *Oral Surg Oral Med Oral Pathol,* 20**,** 340-9.

KARJALAINEN, S., SODERLING, E., PELLINIEMI, L. & FOIDART, J. M. 1986. Immunohistochemical localization of types I and III collagen and fibronectin in the dentine of carious human teeth. *Arch Oral Biol,* 31**,** 801-6.

KAWASHIMA, N. 2012. Characterisation of dental pulp stem cells: a new horizon for tissue regeneration? *Arch Oral Biol,* 57**,** 1439-58.

KEANE, H. C. 1944. *A century of service to dentistry, 1844-1944*, Philidelphia, White, S.S.

KEENE, D. R., SAKAI, L. Y. & BURGESON, R. E. 1991. Human bone contains type III collagen, type VI collagen, and fibrillin: type III collagen is present

on specific fibers that may mediate attachment of tendons, ligaments, and periosteum to calcified bone cortex. *J Histochem Cytochem,* 39**,** 59-69.

KELLEY, K. W., BERGENHOLTZ, G. & COX, C. F. 1981. The extent of the oodontoblast process in rhesus monkeys (mucaca mulatta) as observed by scanning electron microscopy. *Arch Oral Biol,* 26**,** 893-879.

KENMOTSU, M., MATSUZAKA, K., KOKUBU, E., AZUMA, T. & INOUE, T. 2010. Analysis of side population cells derived from dental pulp tissue. *Int Endod J,* 43**,** 1132-42.

KIM, J. W. & SIMMER, J. P. 2007. Hereditary dentin defects. *J Dent Res,* 86**,** 392-9.

KIM, M., GARRITY, S., ERICKSON, I. E., HUANG, A. H., BURDICK, J. A. & MAUCK, R. L. 2012. Optimization of macromer density in human MSC-laden hyaluronic acid (HA) hydrogels. *Bioengineering conference (NEBEC) 2012 38th Annual Northeast.*: IEEE.

KIM, S. 1985. Microcirculation of the dental pulp in health and disease. *J Endod,* 11**,** 465-71.

KIM, S., DORSCHER-KIM, J. E. & LIU, M. 1989. Microcirculation of the dental pulp and its autonomic control. *Proc Finn Dent Soc,* 85**,** 279-87.

KIM, S., EDWALL, L., TROWBRIDGE, H. & CHIEN, S. 1984. Effects of local anesthetics on pulpal blood flow in dogs. *J Dent Res,* 63**,** 650-2.

KIM, S., SCHUESSLER, G. & CHIEN, S. 1983. Measurement of blood flow in the dental pulp of dogs with the 133xenon washout method. *Arch Oral Biol,* 28**,** 501-5.

KISHI, Y., TAKAHASHI, K. & TROWBRIDGE, H. O. 1995. Changes in the vascular network of the oral epithelium and reduced enamel epithelium during tooth eruption. *Acta Anat (Basel),* 153**,** 168-80.

KITASAKO, Y., SHIBATA, S., COX, C. F. & TAGAMI, J. 2002. Location, arrangement and possible function of interodontoblastic collagen fibres in association with calcium hydroxide-induced hard tissue bridges. *Int Endod J,* 35**,** 996-1004.

KLING, M., CVEK, M. & MEJARE, I. 1986. Rate and predictability of pulp revascularization in therapeutically reimplanted permanent incisors. *Endod Dent Traumatol,* 2**,** 83-9.

KONTAKIOTIS, E. G., FILIPPATOS, C. G., TZANETAKIS, G. N. & AGRAFIOTI, A. 2015. Regenerative endodontic therapy: a data analysis of clinical protocols. *J Endod,* 41**,** 146-54.

KRAMER, I. R. H. 1968. *The distribution of blood vessels in the human dental pulp.*, Birmingham, Alabama, USA., University of Alabama Press.

KRELL, K. V., MCMURTREY, L. G. & WALTON, R. E. 1994. Vasculature of the dental pulp of atherosclerotic monkeys: light and electron microscopic findings. *J Endod,* 20**,** 469-73.

KUO, T. F., HUANG, A. T., CHANG, H. H., LIN, F. H., CHEN, S. T., CHEN, R. S., CHOU, C. H., LIN, H. C., CHIANG, H. & CHEN, M. H. 2008. Regeneration of dentin-pulp complex with cementum and periodontal ligament formation using dental bud cells in gelatin-chondroitin-hyaluronan tri-copolymer scaffold in swine. *J Biomed Mater Res A,* 86**,** 1062-8.

L'HEUREUX, N. L., PAQUET, S., LABBE, R., GERMAIN, L. & AUGER, F. 1997. A completely biological tissue-engineered human blood vessel. *The FASEB journal.,* 12**.,** 47-56.

LA NOCE, M., PAINO, F., SPINA, A., NADDEO, P., MONTELLA, R., DESIDERIO, V., DE ROSA, A., PAPACCIO, G., TIRINO, V. & LAINO, L. 2014. Dental pulp stem cells: state of the art and suggestions for a true translation of research into therapy. *J Dent,* 42**,** 761-8.

LAINO, G., D'AQUINO, R., GRAZIANO, A., LANZA, V., CARINCI, F., NARO, F., PIROZZI, G. & PAPACCIO, G. 2005. A new population of human adult dental pulp stem cells: a useful source of living autologous fibrous bone tissue (LAB). *J Bone Miner Res,* 20**,** 1394-402.

LANGELAND, K. & LANGELAND, L. K. 1965. Histologic study of 155 impacted teeth. *Odontol Tidskr,* 73**,** 527-49.

LANGER, R. & VACANTI, J. P. 1993. Tissue engineering. *Science,* 260**,** 920-6.

LECHNER, J. H. & KALNITSKY, G. 1981. The presence of large amounts of type III collagen in bovine dental pulp and its significance with regard to the mechanism of dentinogenesis. *Arch Oral Biol,* 26**,** 265-73.

LEE, G.-H., HUH, S.-Y. & PARK, S.-H. 2004. Tissue engineering of dental pulp on type I collagen. . *Journal of Korean Academy of Conservative dentistry.,* 29**,** 370-377.

LI, S.-T. Y., D; MARTIN, D.; LEE, N.S. 2015. A comparative study of a New Porcine Collagen Membrane to Bio-Gide. *Science, Technology, Innovation,* February, 2015**,** 1-5.

LI, Y., LU, X., SUN, X., BAI, S., LI, S. & SHI, J. 2011. Odontoblast-like cell differentiation and dentin formation induced with TGF-beta1. *Arch Oral Biol,* 56**,** 1221-9.

LIAO, E., YASZEMSKI, M., KREBSBACH, P. & HOLLISTER, S. 2007. Tissue-engineered cartilage constructs using composite hyaluronic acid/collagen I hydrogels and designed poly(propylene fumarate) scaffolds. *Tissue Eng,* 13**,** 537-50.

LIM, D. J. 1995. Structure and function of the tympanic membrane: a review. *Acta Otorhinolaryngol Belg,* 49**,** 101-15.

LIN, L. M., RICUCCI, D. & HUANG, G. T. 2014. Regeneration of the dentine-pulp complex with revitalization/revascularization therapy: challenges and hopes. *Int Endod J,* 47**,** 713-24.

LINDE, A. 1973. Glycosaminoglycans of the Odontoblast-Predentine Layer in dentinogenically Active Porcine Teeth. *Calcified Tissue Research,* 12**,** 281-294.

LINDE, A. 1985. The extracellular matrix of the dental pulp and dentin. *J Dent Res,* 64 Spec No**,** 523-9.

LINDEN, L.-A., KALLSKOG, O. & WOLGAST, M. 1995. Human dentine as a hydrogel. *Arch Oral Biol,* 40**,** 991-1004.

LIPOWSKY, H. H. 2011. Protease Activity and the Role of the Endothelial Glycocalyx in Inflammation. *Drug Discov Today Dis Models,* 8**,** 57-62.

LIU, L. & SHI, G. P. 2012. CD31: beyond a marker for endothelial cells. *Cardiovasc Res,* 94**,** 3-5.

LIU, S. H., WEI, F. C., SUN, S. Z., ZHANG, C. Y. & LIU, Y. S. 2004. Investigation of primary cell culture for dental pulp: comparing of coronal pulp and root pulp. *Shanghai Kou Qiang Yi Xue,* 13**,** 103-5.

LOCKE, M. 2008. Structure of ivory. *J Morphol,* 269**,** 423-50.

LOH, Q. L. & CHOONG, C. 2013. Three-dimensional scaffolds for tissue engineering applications: role of porosity and pore size. *Tissue Eng Part B Rev,* 19**,** 485-502.

LOKESHWAR, V. B. & SELZER, M. G. 2000. Differences in hyaluronic acid-mediated functions and signaling in arterial, microvessel, and vein-derived human endothelial cells. *J Biol Chem,* 275**,** 27641-9.

LORENZ, U. 2009. SHP-1 and SHP-2 in T cells: two phosphatases functioning at many levels. *Immunol Rev,* 228**,** 342-59.

LU, W., JI, K., KIRKHAM, J., YAN, Y., BOCCACCINI, A. R., KELLETT, M., JIN, Y. & YANG, X. B. 2014. Bone tissue engineering by using a combination of polymer/Bioglass composites with human adipose-derived stem cells. *Cell Tissue Res,* 356**,** 97-107.

LUCERO, H. A. & KAGAN, H. M. 2006. Lysyl oxidase: an oxidative enzyme and effector of cell function. *Cell Mol Life Sci,* 63**,** 2304-16.

LUFT, J. H. 1966. Fine structures of capillary and endocapillary layer as revealed by ruthinium red. *Fed. Proc.,* 25**,** 1773-1783.

LUKINMAA, P. L. & WALTIMO, J. 1992. Immunohistochemical localization of types I, V, and VI collagen in human permanent teeth and periodontal ligament. *J Dent Res,* 71**,** 391-7.

LUMSDEN, A. G. 1988. Spatial organization of the epithelium and the role of neural crest cells in the initiation of the mammalian tooth germ. *Development,* 103 Suppl**,** 155-69.

LUUKKO, K., KETTUNEN, P., FRISTAD, I. & BERGGREEN, E. 2011. *Structure and Functions of the Dentin-Pulp Complex.,* St. Louis, Missouri., MOSBY Elsevier.

MABIE, P. C., MEHLER, M. F. & KESSLER, J. A. 1999. Multiple roles of bone morphogenetic protein signaling in the regulation of cortical cell number and phenotype. *J Neurosci,* 19**,** 7077-88.

MACARTHUR, B. D. O., R.O.C. 2005. Bridging the Gap. *Nature,* 433**,** 19.

MACDOUGALL, M., SIMMONS, D., LUAN, X., NYDEGGER, J., FENG, J. & GU, T. T. 1997. Dentin phosphoprotein and dentin sialoprotein are cleavage products expressed from a single transcript coded by a gene on human chromosome 4. Dentin phosphoprotein DNA sequence determination. *J Biol Chem,* 272**,** 835-42.

MACKIE, A. R. & LOSORDO, D. W. 2011. CD34-positive stem cells: in the treatment of heart and vascular disease in human beings. *Tex Heart Inst J,* 38**,** 474-85.

MAEDA, T. & BYERS, M. R. 1996. Different localizations of growth-associated protein (GAP-43) in mechanoreceptors and free nerve endings of adult rat periodontal ligament, dental pulp and skin. *Arch Histol Cytol,* 59**,** 291-304.

MAGLOIRE, H., JOFFRE, A. & BLEICHER, F. 1996. An in vitro model of human dental pulp repair. *J Dent Res,* 75**,** 1971-8.

MAGLOIRE, H., JOFFRE, A., GRIMAUD, J. A., HERBAGE, D., COUBLE, M. L. & CHAVRIER, C. 1982. Distribution of type III collagen in the pulp parenchyma of the human developing tooth. Light and electron microscope immunotyping. *Histochemistry,* 74**,** 319-28.

MALKONDU, O., KARAPINAR KAZANDAG, M. & KAZAZOGLU, E. 2014. A review on biodentine, a contemporary dentine replacement and repair material. *Biomed Res Int,* 2014**,** 160951.

MARION, D., JEAN, A., HAMEL, H., KEREBEL, L.-M. & KEREBEL, B. 1991. Scanning electron microscopic study of odontoblasts and circumpulpal dentin in a human tooth. *Oral Surgery, Oral medicine, Oral Pathology.,* 72**,** 473-478.

MARSAN, T., PRPIC-MEHICIC, G., KARLOVIC, I., SOSTARIC, B., ANIC, I. & KARLOVIC, Z. 2003. Pulpal Response to Direct Pulp capping with Collagen Bioresorbable Membrane. *Acta Stomatologica Croatia.,* 37**.,** 59-62.

MARTENS, W., SANEN, K., GEORGIOU, M., STRUYS, T., BRONCKAERS, A., AMELOOT, M., PHILLIPS, J. & LAMBRICHTS, I. 2014. Human dental pulp stem cells can differentiate into Schwann cells and promote and guide neurite outgrowth in an aligned tissue-engineered collagen construct in vitro. *FASEB J,* 28**,** 1634-43.

MARTIN, D. E., DE ALMEIDA, J. F., HENRY, M. A., KHAING, Z. Z., SCHMIDT, C. E., TEIXEIRA, F. B. & DIOGENES, A. 2014. Concentration-dependent effect of sodium hypochlorite on stem cells of apical papilla survival and differentiation. *J Endod,* 40**,** 51-5.

MATSUMIYA, S. & KITAMURA, M. 1960. Histo-pathological and histo-bacterial studies of the relation between the conditions of sterilization of the interior of

the root canal and the healing process of the periapical tissues in experimentally infected root canal treatment. *Bulletin of Tokyo Dental College.,* 1**,** 1-19.

MATSUSHITA, K., MOTANI, R., SAKUTA, T., YAMAGUCHI, N., KOGA, T., MATSUO, K., NAGAOKA, S., ABEYAMA, K., MARUYAMA, I. & TORII, M. 2000. The role of vascular endothelial growth factor in human dental pulp cells: induction of chemotaxis, proliferation, and differentiation and activation of the AP-1-dependent signaling pathway. *J Dent Res,* 79**,** 1596-603.

MATTHEWS, B., ANDREW, D., AMESS, T. R., IKEDA, H. & VONGSAVAN, N. 1996. *Dentin/Pulp Complex.,* Tokyo., Quintessence Publishing Company.

MATTHEWS, B. & HOLLAND, G. R. 1975. Coupling between nerves in teeth. *Brain Res,* 98**,** 354-8.

MATTHEWS, B. & VONGSAVAN, N. 1994. Interactions between neural and hydrodynamic machanisms in dentine and pulp. *Arch Oral Biol,* 39**,** S87-S89.

MEYER, M. W. 1993. Pulpal blood flow: use of radio-labelled microspheres. *Int Endod J,* 26**,** 6-7.

MEYER, M. W. & PATH, M. G. 1979. Blood flow in the dental pulp of dogs determined by hydrogen polarography and radioactive microsphere methods. *Arch Oral Biol,* 24**,** 601-5.

MINA, M. & KOLLAR, E. J. 1987. The induction of odontogenesis in non-dental mesenchyme combined with early murine mandibular arch epithelium. *Archives of Oral Biology.,* 32**,** 123-127.

MINOZZI, S., FORNACIARI, G., MUSCO, S. & CATALANO, P. 2007. A gold dental prosthesis of Roman imperial age. *Am J Med,* 120**,** e1-2.

MISRA, S., GHATAK, S. & TOOLE, B. P. 2005. Regulation of MDR1 expression and drug resistance by a positive feedback loop involving hyaluronan, phosphoinositide 3-kinase, and ErbB2. *J Biol Chem,* 280**,** 20310-5.

MIYASHITA, H., WORTHINGTON, H. V., QUALTROUGH, A. & PLASSCHAERT, A. 2007. Pulp management for caries in adults: maintaining pulp vitality. *Cochrane Database Syst Rev***,** CD004484.

MJOR, I. A. & NORDAHL, I. 1996. The density and branching of dentinal tubules in human teeth. *Arch Oral Biol.,* 41**,** 401-412.

MO, W., YANG, C., LIU, Y., HE, Y., WANG, Y. & GAO, F. 2011. The influence of hyaluronic acid on vascular endothelial cell proliferation and the relationship with ezrin/merlin expression. *Acta Biochim Biophys Sin (Shanghai),* 43**,** 930-9.

MONTANO, I., SCHIESTL, C., SCHNEIDER, J., PONTIGGIA, L., LUGINBUHL, J., BIEDERMANN, T., BOTTCHER-HABERZETH, S., BRAZIULIS, E., MEULI, M. & REICHMANN, E. 2010. Formation of human capillaries in

vitro: the engineering of prevascularized matrices. *Tissue Eng Part A,* 16**,** 269-82.

MORAND, M. A., SCHILDER, H., BLONDIN, J., STONE, P. J. & FRANZBLAU, C. 1981. Collagenolytic and elastinolytic activities from diseased human dental pulps. *J Endod,* 7**,** 156-60.

MORENO-HIDALGO, M. C., CALEZA-JIMENEZ, C., MENDOZA-MENDOZA, A. & IGLESIAS-LINARES, A. 2014. Revascularization of immature permanent teeth with apical periodontitis. *Int Endod J,* 47**,** 321-31.

MOULE, A. J., LI, H. & BARTOLD, P. M. 1995. Donor variability in the proliferation of human dental pulp fibroblasts. *Aust Dent J,* 40**,** 110-4.

MULLANE, E. M., DONG, Z., SEDGLEY, C. M., HU, J. C., BOTERO, T. M., HOLLAND, G. R. & NOR, J. E. 2008. Effects of VEGF and FGF2 on the revascularization of severed human dental pulps. *J Dent Res,* 87**,** 1144-8.

MURAKAMI, M., HORIBE, H., IOHARA, K., HAYASHI, Y., OSAKO, Y., TAKEI, Y., NAKATA, K., MOTOYAMA, N., KURITA, K. & NAKASHIMA, M. 2013. The use of granulocyte-colony stimulating factor induced mobilization for isolation of dental pulp stem cells with high regenerative potential. *Biomaterials,* 34**,** 9036-47.

MURPHY, C. M., HAUGH, M. G. & O'BRIEN, F. J. 2010. The effect of mean pore size on cell attachment, proliferation and migration in collagen-glycosaminoglycan scaffolds for bone tissue engineering. *Biomaterials,* 31**,** 461-6.

MURPHY, C. M. & O'BRIEN, F. J. 2010. Understanding the effect of mean pore size on cell activity in collagen-glycosaminoglycan scaffolds. *Cell Adh Migr,* 4**,** 377-81.

MURPHY, C. M., O'BRIEN, F. J., LITTLE, D. G. & SCHINDELER, A. 2013. Cell-scaffold interactions in the bone tissue engineering triad. *Eur Cell Mater,* 26**,** 120-32.

MURRAY, P. E., ABOUT, I., LUMLEY, P. J., FRANQUIN, J.-C., REMUSAT, M. & SMITH, A. J. 2000. Human odontoblastic cell numbers after dental injury. *Journal Of Dentistry.,* 28**,** 277-285.

MURRAY, P. E., GARCIA-GODOY, F. & HARGREAVES, K. M. 2007. Regenerative endodontics: a review of current status and a call for action. *J Endod,* 33**,** 377-90.

MYLLYHARJU, J. & KIVIRIKKO, K. I. 2004. Collagens, modifying enzymes and their mutations in humans, flies and worms. *Trends Genet,* 20**,** 33-43.

NAGAOKA, S., MIYAZAKI, Y., LIU, H. J., IWAMOTO, Y., KITANO, M. & KAWAGOE, M. 1995. Bacterial invasion into dentinal tubules of human vital and nonvital teeth. *J Endod,* 21**,** 70-3.

NAKASHIMA, M. 1990. The induction of reparative dentine in the amputated dental pulp of the dog by bone morphogenetic protein. *Arch Oral Biol,* 35**,** 493-7.

NAKASHIMA, M. 1994. Induction of dentin formation on canine amputated pulp by recombinant human bone morphogenetic proteins (BMP)-2 and -4. *J Dent Res,* 73**,** 1515-22.

NAKASHIMA, M. & IOHARA, K. 2011. Regeneration of dental pulp by stem cells. *Adv Dent Res,* 23**,** 313-9.

NAKASHIMA, M. & IOHARA, K. 2014. Mobilized dental pulp stem cells for pulp regeneration: initiation of clinical trial. *J Endod,* 40**,** S26-32.

NAKASHIMA, M. & REDDI, A. H. 2003. The application of bone morphogenetic proteins to dental tissue engineering. *Nat Biotechnol,* 21**,** 1025-32.

NALDINI, L., BLOMER, U., GALLAY, P., ORY, D., MULLIGAN, R., GAGE, F. H., VERMA, I. M. & TRONO, D. 1996. In vivo gene delivery and stable transduction of nondividing cells by a lentiviral vector. *Science,* 272**,** 263-7.

NANCI, A. 2012. *Ten Cate's Oral Histology,* St. Louis, Missouri., Elsevier.

NARHI, M. V. 1985. Dentin sensitivity: a review. *J Biol Buccale,* 13**,** 75-96.

NEWMAN, P. J. 1997. The biology of PECAM-1. *J Clin Invest,* 100**,** S25-9.

NG, Y. L., MANN, V. & GULABIVALA, K. 2011. A prospective study of the factors affecting outcomes of nonsurgical root canal treatment: part 1: periapical health. *Int Endod J,* 44**,** 583-609.

NIELSEN, J. S. & MCNAGNY, K. M. 2008. Novel functions of the CD34 family. *J Cell Sci,* 121**,** 3683-92.

NIKLASON, L. E. 1999. Techview: medical technology. Replacement arteries made to order. *Science,* 286**,** 1493-4.

NOBLE, P. W. 2002. Hyaluronan and its catabolic products in tissue injury and repair. *Matrix Biol,* 21**,** 25-9.

NOR, J. E., PETERS, M. C., CHRISTENSEN, J. B., SUTORIK, M. M., LINN, S., KHAN, M. K., ADDISON, C. L., MOONEY, D. J. & POLVERINI, P. J. 2001. Engineering and characterization of functional human microvessels in immunodeficient mice. *Lab Invest,* 81**,** 453-63.

NOSRAT, I. V., SMITH, C. A., MULLALLY, P., OLSON, L. & NOSRAT, C. A. 2004. Dental pulp cells provide neurotrophic support for dopaminergic neurons and differentiate into neurons in vitro; implications for tissue engineering and repair in the nervous system. *Eur J Neurosci,* 19**,** 2388-98.

NYGAARD-OSTBY, B. 1961. The role of the blood clot in Endodontic Therapy an Experimental Histologic Study. *Acta Odontol Scand,* 19**,** 323-353.

NYGAARD-OSTBY, B. & HJORTDAL, O. 1971. Tissue formation in the root canal following pulp removal. *Scandinavian Journal of Dental Research.,* 79**.,** 333-348.

O'BRIEN, F. J. 2011. Biomaterials and Scaffolds for Tissue Engineering. *Materials Today.,* 14**,** 88-95.

OKAMURA, K., KOBAYASHI, I., MATSUO, K., TANIGUCHI, K., ISHIBASHI, Y., IZUMI, T., KITAMURA, K. & SAKAI, H. 1995. An immunohistochemical and ultrastructural study of vasomotor nerves in the microvasculature of human dental pulp. *Arch Oral Biol,* 40**,** 47-53.

OKIJI, T., JONTELL, M., BELICHENKO, P., BERGENHOLTZ, G. & DAHLSTROM, A. 1997. Perivascular dendritic cells of the human dental pulp. *Acta Physiologica Scandinavica,* 159**,** 163-169.

OKIJI, T., KAWASHIMA, N., KOSAKA, T., MATSUMOTO, A., KOBAYASHI, C. & SUDA, H. 1992. An immunohistochemical study of the distribution of immunocompetent cells, especially macrophages and Ia antigen-expressing cells of heterogeneous populations, in normal rat molar pulp. *J Dent Res,* 71**,** 1196-202.

OLGART, L. 1996. Neural control of pulpal blood flow. *Crit Rev Oral Biol Med,* 7**,** 159-71.

ORBAN, B. 1928. Growth and movement of the Tooth Germs and Teeth. *Journal of the American Dental Association.,* 15**.,** 1004-1016.

ORBAN, B. 1930. Why root canals should be filled to the dentinocemental junction. *Journal of the American Dental Association,* 17**,** 1086-1087.

ORLOWSKI, W. A. 1977. The turnover of collagen in the dental pulp of rat incisors. *J Dent Res,* 56**,** 437-40.

PANKOV, R. & YAMADA, K. M. 2002. Fibronectin at a glance. *J Cell Sci,* 115**,** 3861-3.

PANNESE, E. 1962. Observations on the ultrastructure of the enamel organ: III. Internal and external enamel epithelia. *Journal of Ultrastructure Research,* 6**,** 186-204.

PAPACCIO, G., GRAZIANO, A., D'AQUINO, R., GRAZIANO, M. F., PIROZZI, G., MENDITTI, D., DE ROSA, A., CARINCI, F. & LAINO, G. 2006. Long-term cryopreservation of dental pulp stem cells (SBP-DPSCs) and their differentiated osteoblasts: a cell source for tissue repair. *J Cell Physiol,* 208**,** 319-25.

PAPAIOANNOU, K. A., MARKOPOULOU, C. E., GIONI, V., MAMALIS, A. A., VAYOURAKI, H. N., KLETSAS, D. & VROTSOS, I. A. 2011. Attachment and proliferation of human osteoblast-like cells on guided bone regeneration (GBR) membranes in the absence or presence of nicotine: an in vitro study. *Int J Oral Maxillofac Implants,* 26**,** 509-19.

PARIKH, S. N. 2004. Gene therapy: principles and clinical applications in orthopedics. *Orthopedics,* 27**,** 294-303; quiz 304-5.

PARK, S. H., HSIAO, G. Y. & HUANG, G. T. 2004. Role of substance P and calcitonin gene-related peptide in the regulation of interleukin-8 and monocyte chemotactic protein-1 expression in human dental pulp. *Int Endod J,* 37**,** 185-92.

PASHLEY, D. H. 1996. Dynamics of the pulpo-dentin complex. *Crit Rev Oral Biol Med,* 7**,** 104-33.

PASHLEY, D. H., GALLOWAY, S. E. & STEWART, F. 1984. Effects of fibrinogen in vivo on dentine permeability in the dog. *Arch Oral Biol,* 29**.,** 725-728.

PASHLEY, D. H. & LIEWEHR, F. 2006. *Pathways of the Pulp, 9th Edition.,* St. Louis, MO, USA., Mosby Elsevier.

PATERSON, R. C. 1976. Bacterial contamination and the exposed pulp. *Br Dent J,* 140**,** 231-6.

PATH, M. G. & MEYER, M. W. 1977. Quantification of pulpal blood flow in developing teeth of dogs. *J Dent Res,* 56**,** 1245-54.

PEATTIE, R. A., NAYATE, A. P., FIRPO, M. A., SHELBY, J., FISHER, R. J. & PRESTWICH, G. D. 2004. Stimulation of in vivo angiogenesis by cytokine-loaded hyaluronic acid hydrogel implants. *Biomaterials,* 25**,** 2789-98.

PERNG, C.-K., WANG, Y.-J., TSI, C.-H. & MA, H. 2009. *In vivo* Angiogenesis Effect of Porous collagen Scaffold with Hyaluronic Oligisaccharides. *Journal of Surgical Research.,* 168**.,** 9-15.

PFEIFFER, E., VICKERS, S. M., FRANK, E., GRODZINSKY, A. J. & SPECTOR, M. 2008. The effects of glycosaminoglycan content on the compressive modulus of cartilage engineered in type II collagen scaffolds. *Osteoarthritis Cartilage,* 16**,** 1237-44.

PICTON, D. C. 1989. The periodontal enigma: eruption versus tooth support. *Eur J Orthod,* 11**,** 430-9.

PILATZ, A., SCHULTHEISS, D., GABOUEV, A. I., SCHLOTE, N., MERTSCHING, H., JONAS, U. & STIEF, C. G. 2005(a). In vitro viability of human cavernosal endothelial and fibroblastic cells after exposure to papaverine/phentolamine and prostaglandin E1. *BJU Int,* 95**,** 1351-7.

PILATZ, A., SCHULTHEISS, D., GABOUEV, A. I., SCHLOTE, N., MERTSCHING, H., JONAS, U. & STIEF, C. G. 2005(b). Isolation of primary endothelial and stromal cell cultures of the corpus cavernosum penis for basic research and tissue engineering. *Eur Urol,* 47**,** 710-8; discussion 718-9.

PINTER, E., BARREUTHER, M., LU, T., IMHOF, B. A. & MADRI, J. A. 1997. Platelet-endothelial cell adhesion molecule-1 (PECAM-1/CD31) tyrosine phosphorylation state changes during vasculogenesis in the murine conceptus. *Am J Pathol,* 150**,** 1523-30.

PIRNAZAR, P., WOLINSKY, L., NACHNANI, S., HAAKE, S., PILLONI, A. & BERNARD, G. W. 1999. Bacteriostatic effects of hyaluronic acid. *J Periodontol,* 70**,** 370-4.

PLATT, C. I., KREKOSKI, C. A., WARD, R. V., EDWARDS, D. R. & GAVRILOVIC, J. 2003. Extracellular matrix and matrix metalloproteinases in sciatic nerve. *J Neurosci Res,* 74**,** 417-29.

POHTO, P. & ANTILA, R. 1972. Innervation of blood vessels in the dental pulp. *Int Dent J,* 22**,** 228-39.

POMERAT, C. M. & CONTINO, R. M. 1965. The Cultivation of Dental Tissues. *Oral Surg Oral Med Oral Pathol,* 19**,** 628-32.

POPE, F. M., MARTIN, G. R., LICHTENSTEIN, J. R., PENTTINEN, R., GERSON, B., ROWE, D. W. & MCKUSICK, V. A. 1975. Patients with Ehlers-Danlos syndrome type IV lack type III collagen. *Proc Natl Acad Sci U S A,* 72**,** 1314-6.

PRASAD, M., ZHU, Q., SUN, Y., WANG, X., KULKARNI, A., BOSKEY, A., FENG, J. Q. & QIN, C. 2011. Expression of dentin sialophosphoprotein in non-mineralized tissues. *J Histochem Cytochem,* 59**,** 1009-21.

PRATO, G. P., ROTUNDO, R., MAGNANI, C., SORANZO, C., MUZZI, L. & CAIRO, F. 2003. An autologous cell hyaluronic acid graft technique for gingival augmentation: a case series. *J Periodontol,* 74**,** 262-7.

PRIES, A. R., SECOMB, T. W. & GAEHTGENS, P. 2000. The endothelial surface layer. *Pflugers Arch,* 440**,** 653-66.

PUSZTASZERI, M. P., SEELENTAG, W. & BOSMAN, F. T. 2006. Immunohistochemical expression of endothelial markers CD31, CD34, von Willebrand factor, and Fli-1 in normal human tissues. *J Histochem Cytochem,* 54**,** 385-95.

QIN, C., BABA, O. & BUTLER, W. T. 2004. Post-translational modifications of sibling proteins and their roles in osteogenesis and dentinogenesis. *Crit Rev Oral Biol Med,* 15**,** 126-36.

QIN, C., BRUNN, J. C., JONES, J., GEORGE, A., RAMACHANDRAN, A., GORSKI, J. P. & BUTLER, W. T. 2001. A comparative study of sialic acid-rich proteins in rat bone and dentin. *Eur J Oral Sci,* 109**,** 133-41.

RAMAMOORTHI, M., BAKKAR, M., JORDAN, J. & TRAN, S. D. 2015. Osteogenic Potential of Dental Mesenchymal Stem Cells in Preclinical Studies: A Systematic Review Using Modified ARRIVE and CONSORT Guidelines. *Stem Cells Int,* 2015**,** 378368.

RAY, H. A. & TROPE, M. 1995. Periapical status of endodontically treated teeth in relation to the technical quality of the root filling and the coronal restoration. *Int Endod J,* 28**,** 12-8.

REITSMA, S., SLAAF, D. W., VINK, H., VAN ZANDVOORT, M. A. & OUDE EGBRINK, M. G. 2007. The endothelial glycocalyx: composition, functions, and visualization. *Pflugers Arch,* 454**,** 345-59.

RIESSEN, R., FENCHEL, M., CHEN, H., AXEL, D. I., KARSCH, K. R. & LAWLER, J. 2001. Cartilage oligomeric matrix protein (thrombospondin-5) is expressed by human vascular smooth muscle cells. *Arterioscler Thromb Vasc Biol,* 21**,** 47-54.

RISAU, W. 1995. Differentiation of endothelium. *FASEB J,* 9**,** 926-33.

RISAU, W. & FLAMME, I. 1995. Vasculogenesis. *Annu Rev Cell Dev Biol,* 11**,** 73-91.

ROBERTS-CLARK, D. J. & SMITH, A. J. 2000. Angiogenic growth factors in human dentine matrix. *Arch Oral Biol,* 45**,** 1013-6.

ROBINS, S. P. 2007. Biochemistry and functional significance of collagen cross-linking. *Biochem Soc Trans,* 35**,** 849-52.

ROLA, P. 2013. The Glycocalyx: An Overview for the Clinician. *PulmCCM*.

ROONEY, P., WANG, M., KUMAR, P. & KUMAR, S. 1993. Angiogenic oligosaccharides of hyaluronan enhance the production of collagens by endothelial cells. *J Cell Sci,* 105 (Pt 1)**,** 213-8.

ROSA, V., ZHANG, Z., GRANDE, R. H. & NOR, J. E. 2013. Dental pulp tissue engineering in full-length human root canals. *J Dent Res,* 92**,** 970-5.

ROZARIO, T. & DESIMONE, D. W. 2010. The extracellular matrix in development and morphogenesis: a dynamic view. *Dev Biol,* 341**,** 126-40.

RUCH, J. V. 1985. Odontoblast differentiation and the formation of the odontoblast layer. *J Dent Res,* 64 Spec No**,** 489-98.

RULE, D. C. & WINTER, G. B. 1966. Root growth and apical repair subsequent to pulpal necrosis in children. *Br Dent J,* 120**,** 586-90.

RUPAREL, N. B., DE ALMEIDA, J. F., HENRY, M. A. & DIOGENES, A. 2013. Characterization of a stem cell of apical papilla cell line: effect of passage on cellular phenotype. *J Endod,* 39**,** 357-63.

RUPAREL, N. B., TEIXEIRA, F. B., FERRAZ, C. C. & DIOGENES, A. 2012. Direct effect of intracanal medicaments on survival of stem cells of the apical papilla. *J Endod,* 38**,** 1372-5.

RUTHERFORD, R. B. & GU, K. 2000. Treatment of inflamed ferret dental pulps with recombinant bone morphogenetic protein-7. *Eur J Oral Sci,* 108**,** 202-6.

SACHLOS, E. & CZERNUSZKA, J. T. 2003. Making Tissue Engineering Scaffolds Work. Review: The application of solid freeform fabrication technology to the production of tissue engineering scaffolds. *European cells and materials.,* 5**,** 29-40.

SAITO, T., OGAWA, M., HATA, Y. & BESSHO, K. 2004. Acceleration effect of human recombinant bone morphogenetic protein-2 on differentiation of human pulp cells into odontoblasts. *J Endod,* 30**,** 205-8.

SAKAI, V. T., CORDEIRO, M. M., DONG, Z., ZHANG, Z., ZEITLIN, B. D. & NOR, J. E. 2011. Tooth slice/scaffold model of dental pulp tissue engineering. *Adv Dent Res,* 23**,** 325-32.

SAKAI, V. T., ZHANG, Z., DONG, Z., NEIVA, K. G., MACHADO, M. A., SHI, S., SANTOS, C. F. & NOR, J. E. 2010. SHED differentiate into functional odontoblasts and endothelium. *J Dent Res,* 89**,** 791-6.

SAKAMOTO, N., NAKAJIMA, T., IKUNAGA, K., SHIDAHARA, H., OKAMOTO, H. & OKUDA, K. 1981. Identification of hyaluronidase activity in rabbit dental pulp. *J Dent Res,* 60**,** 850-4.

SAKURAI, K., OKIJI, T. & SUDA, H. 1999. Co-increase of nerve Fibers and HLA-DR-and/or Factor-XIIIa-expressing Dendritic cells in Dentinal Caries-affected Regions of the Human dental Pulp: An immunohistochemical study. . *J Dent Res,* 78**,** 1596-1608.

SALEHRABI, R. & ROTSTEIN, I. 2004. Endodontic treatment outcomes in a large patient population in the USA: an epidemiological study. *J Endod,* 30**,** 846-50.

SARKAR, S., DADHANIA, M., ROURKE, P., DESAI, T. A. & WONG, J. Y. 2005. Vascular tissue engineering: microtextured scaffold templates to control organization of vascular smooth muscle cells and extracellular matrix. *Acta Biomater,* 1**,** 93-100.

SASAKI, S. 1959. Studies on the respiration of the dog tooth germ. *Journal of Biochemistry (Tokyo).* 46**,** 269-279.

SASAKI, T. & GARANT, P. R. 1996. Structure and organization of odontoblasts. *Anat Rec,* 245**,** 235-49.

SASAKI, T. & KAWAMATA-KIDO, H. 1995. Providing an environment for reparative dentine induction in amputated rat molar pulp by high molecular-weight hyaluronic acid. *Arch Oral Biol,* 40**,** 209-19.

SASANO, T., KURIWADA, S., SHOJI, N., SANJO, D., IZUMI, H. & KARITA, K. 1994. Axon reflex vasodilatation in cat dental pulp elicited by noxious stimulation of the gingiva. *J Dent Res,* 73**,** 1797-802.

SASANO, T., SHOJI, N., KURIWADA, S., SANJO, D., IZUMI, H. & KARITA, K. 1995. Absence of parasympathetic vasodilatation in cat dental pulp. *J Dent Res,* 74**,** 1665-70.

SATO, T., LAVER, J. H. & OGAWA, M. 1999. Reversible expression of CD34 by murine hematopoietic stem cells. *Blood,* 94**,** 2548-54.

SAWA, Y., YOSHIDA, S., ASHIKAGA, Y., KIM, T., YAMAOKA, Y. & SUZUKI, M. 1998. Immunohistochemical demonstration of lymphatic vessels in human dental pulp. *Tissue Cell,* 30**,** 510-6.

SCHAEFER, L. & SCHAEFER, R. M. 2010. Proteoglycans: from structural compounds to signaling molecules. *Cell Tissue Res,* 339**,** 237-46.

SCHALTE, C. E., ZUBER, G., HERLIN, C. & VANDAMME, T. F. 2011. Chemical modifications of hyaluronic acid for the synthesis of derivatives for a broad range of biomedical applications. *Carbohydrate Polymers.,* 85**,** 469-489.

SCHILDER, H. 1967. Filling root canals in three dimensions. *Dent Clin North Am***,** 723-44.

SCHLEGEL, A. K., MOHLER, H., BUSCH, F. & MEHL, A. 1997. Preclinical and clinical studies of a collagen membrane (Bio-Gide). *Biomaterials,* 18**,** 535-8.

SCHLINGEMANN, R. O., RIETVELD, F. J., DE WAAL, R. M., BRADLEY, N. J., SKENE, A. I., DAVIES, A. J., GREAVES, M. F., DENEKAMP, J. & RUITER, D. J. 1990. Leukocyte antigen CD34 is expressed by a subset of cultured endothelial cells and on endothelial abluminal microprocesses in the tumor stroma. *Lab Invest,* 62**,** 690-6.

SCHNEIDER, S. W. 1971. A comparison of canal preparations in straight and curved root canals. *Oral Surg Oral Med Oral Pathol,* 32**,** 271-5.

SCHRODER, U. 1985. Effects of calcium hydroxide-containing pulp-capping agents on pulp cell migration, proliferation, and differentiation. *J Dent Res,* 64 Spec No**,** 541-8.

SCHULZ, S., STEINBERG, T., BECK, D., TOMAKIDI, P., ACCARDI, R., TOMMASINO, M., REINHARD, T. & EBERWEIN, P. 2013. Generation and evaluation of a human corneal model cell system for ophthalmologic issues using the HPV16 E6/E7 oncogenes as uniform immortalization platform. *Differentiation,* 85**,** 161-72.

SEDGLEY, C. M. & MESSER, H. H. 1992. Are endodontically treated teeth more brittle? *J Endod,* 18**,** 332-5.

SELTZER, S., SOLTANOFF, W., SINAI, I., GOLDENBERG, A. & BENDER, I. B. 1968. Biologic aspects of endodontics. 3. Periapical tissue reactions to root canal instrumentation. *Oral Surg Oral Med Oral Pathol,* 26**,** 694-705.

SENZAKI, H. 1980. A histological study of reparative dentinogenesis in the rat incisor after colchicine administration. *Arch Oral Biol,* 25**,** 737-43.

SHALAK, R. F., C.F. 1988. *Preface,* New York, Alan R. Liss.

SHERMAN, L., SLEEMAN, J., HERRLICH, P. & PONTA, H. 1994. Hyaluronate receptors: key players in growth, differentiation, migration and tumor progression. *Curr Opin Cell Biol,* 6**,** 726-33.

SHI, Q., LE, X., WANG, B., ABBRUZZESE, J. L., XIONG, Q., HE, Y. & XIE, K. 2001. Regulation of vascular endothelial growth factor expression by acidosis in human cancer cells. *Oncogene,* 20**,** 3751-6.

SHI, S. & GRONTHOS, S. 2003. Perivascular niche of postnatal mesenchymal stem cells in human bone marrow and dental pulp. *J Bone Miner Res,* 18**,** 696-704.

SHIVASHANKAR, V. Y., JOHNS, D. A., VIDYANATH, S. & KUMAR, M. R. 2012. Platelet Rich Fibrin in the revitalization of tooth with necrotic pulp and open apex. *J Conserv Dent,* 15**,** 395-8.

SHUTTLEWORTH, C. A., BERRY, L. & WILSON, N. 1980. Collagen synthesis in rabbit dental pulp fibroblast cultures. *Arch Oral Biol,* 25**,** 201-5.

SHUTTLEWORTH, C. A., WARD, J. L. & HIRSCHMANN, P. 1978. The presence of type III collagen in the developing tooth. *Biochimica et Biophysica Acta (BBA).* 535**,** 348-355.

SIDNEY, L. E., BRANCH, M. J., DUNPHY, S. E., DUA, H. S. & HOPKINSON, A. 2014. Concise review: evidence for CD34 as a common marker for diverse progenitors. *Stem Cells,* 32**,** 1380-9.

SIEMERINK, M. J., KLAASSEN, I., VOGELS, I. M., GRIFFIOEN, A. W., VAN NOORDEN, C. J. & SCHLINGEMANN, R. O. 2012. CD34 marks angiogenic tip cells in human vascular endothelial cell cultures. *Angiogenesis,* 15**,** 151-63.

SIGAL, M. J., AUBIN, J. E., TEN CATE, A. R. & PITARU, S. 1984(a). The odontoblast process extends to the dentinoenamel junction: an immunocytochemical study of rat dentine. *J Histochem Cytochem,* 32**,** 872-7.

SIGAL, M. J., PITARU, S., AUBIN, J. E. & TEN CATE, A. R. 1984(b). A combined scanning electron microscopy and immunofluorescence study demonstrating that the odontoblast process extends to the dentinoenamel junction in human teeth. *Anat Rec,* 210**,** 453-62.

SLEVIN, M., KRUPINSKI, J., GAFFNEY, J., MATOU, S., WEST, D., DELISSER, H., SAVANI, R. C. & KUMAR, S. 2007. Hyaluronan-mediated angiogenesis in vascular disease: uncovering RHAMM and CD44 receptor signaling pathways. *Matrix Biol,* 26**,** 58-68.

SLEVIN, M., KUMAR, S. & GAFFNEY, J. 2002. Angiogenic oligosaccharides of hyaluronan induce multiple signaling pathways affecting vascular endothelial cell mitogenic and wound healing responses. *J Biol Chem,* 277**,** 41046-59.

SLEVIN, M., WEST, D., KUMAR, P., ROONEY, P. & KUMAR, S. 2004. Hyaluronan, angiogenesis and malignant disease. *Int J Cancer,* 109**,** 793-4; author reply 795-6.

SLOAN, A. J., SHELTON, R. M., HANN, A. C., MOXHAM, B. J. & SMITH, A. J. 1998. An in vitro approach for the study of dentinogenesis by organ culture of the dentine-pulp complex from rat incisor teeth. *Arch Oral Biol,* 43**,** 421-30.

SLUTZKEY, S., KOZLOVSKY, A., ARTZI, Z. & MATALON, S. 2015. Collagen barrier membranes may accelerate bacterial growth in vitro: a potential clinical risk to regenerative procedures. *Quintessence Int,* 46**,** 43-50.

SMITH, A. J. & LESOT, H. 2001. Induction and regulation of crown dentinogenesis: embryonic events as a template for dental tissue repair? *Crit Rev Oral Biol Med,* 12**,** 425-37.

SMITH, J. G., SMITH, A. J., SHELTON, R. M. & COOPER, P. R. 2015. Dental Pulp Cell Behavior in Biomimetic Environments. *J Dent Res,* 94**,** 1552-9.

SMITH, M. L., GOURDON, D., LITTLE, W. C., KUBOW, K. E., EGUILUZ, R. A., LUNA-MORRIS, S. & VOGEL, V. 2007. Force-induced unfolding of fibronectin in the extracellular matrix of living cells. *PLoS Biol,* 5**,** e268.

SOLCHAGA, L. A., DENNIS, J. E., GOLDBERG, V. M. & CAPLAN, A. I. 1999. Hyaluronic acid-based polymers as cell carriers for tissue-engineered repair of bone and cartilage. *J Orthop Res,* 17**,** 205-13.

SONOYAMA, W., LIU, Y., YAMAZA, T., TUAN, R. S., WANG, S., SHI, S. & HUANG, G. T. 2008. Characterization of the apical papilla and its residing stem cells from human immature permanent teeth: a pilot study. *J Endod,* 34**,** 166-71.

SPATH, L., ROTILIO, V., ALESSANDRINI, M., GAMBARA, G., DE ANGELIS, L., MANCINI, M., MITSIADIS, T. A., VIVARELLI, E., NARO, F., FILIPPINI, A. & PAPACCIO, G. 2010. Explant-derived human dental pulp stem cells enhance differentiation and proliferation potentials. *J Cell Mol Med,* 14**,** 1635-44.

SREENATH, T., THYAGARAJAN, T., HALL, B., LONGENECKER, G., D'SOUZA, R., HONG, S., WRIGHT, J. T., MACDOUGALL, M., SAUK, J. & KULKARNI, A. B. 2003. Dentin sialophosphoprotein knockout mouse teeth display widened predentin zone and develop defective dentin mineralization similar to human dentinogenesis imperfecta type III. *J Biol Chem,* 278**,** 24874-80.

STANLEY, H. R. 1962. The cells of the dental pulp. *Oral Surg Oral Med Oral Pathol,* 15**,** 849-58.

STENFELDT, K., JOHANSSON, C., ERIKSSON, P. O. & HELLSTROM, S. 2013. Collagen Type II is produced in healing pars tensa of perforated tympanic membranes: an experimental study in the rat. *Otol Neurotol,* 34**,** e88-92.

STERN, R., ASARI, A. A. & SUGAHARA, K. N. 2006. Hyaluronan fragments: an information-rich system. *Eur J Cell Biol,* 85**,** 699-715.

STROMBERG, T. 1969. Wound healing after total pulpectomy in dogs. A comparative study between rootfillings with calciumhydroxide, dibasic calciumphosphate, and gutta percha. *Odontol Revy,* 20**,** 147-63.

SUN, S. Z., LIU, S. H., WEI, F. C., ZHANG, C. Y. & LIU, Y. S. 2004. The ALP activity of cultured dental coronal and root pulp cells in vitro. *Shanghai Kou Qiang Yi Xue,* 13**,** 531-3.

SURI, S. & SCHMIDT, C. E. 2010. Cell-laden hydrogel constructs of hyaluronic acid, collagen, and laminin for neural tissue engineering. *Tissue Eng Part A,* 16**,** 1703-16.

TAKAGI, M., HISHIKAWA, H., HOSOKAWA, Y., KAGAMI, A. & RAHEMTULLA, F. 1990. Immunohistochemical localization of glycosaminoglycans and proteoglycans in predentin and dentin of rat incisors. *J Histochem Cytochem,* 38**,** 319-24.

TARBELL, J. M. 2010. Shear stress and the endothelial transport barrier. *Cardiovasc Res,* 87**,** 320-30.

TARBELL, J. M. & EBONG, E. E. 2008. The endothelial glycocalyx: a mechano-sensor and -transducer. *Sci Signal,* 1**,** pt8.

THOMAS, H. F. 1979. The extent of the odontoblast process in human dentin. *J Dent Res,* 58**,** 2207-18.

THOMAS, H. F. & PAYNE, R. C. 1983. The ultrastructure of Dentinal Tubules from unerupted Human Premolar Teeth. *J Dent Res,* 62**,** 532-536.

THOMPSON, R. D., NOBLE, K. E., LARBI, K. Y., DEWAR, A., DUNCAN, G. S., MAK, T. W. & NOURSHARGH, S. 2001. Platelet-endothelial cell adhesion molecule-1 (PECAM-1)-deficient mice demonstrate a transient and cytokine-specific role for PECAM-1 in leukocyte migration through the perivascular basement membrane. *Blood,* 97**,** 1854-60.

THORPE., K. A. 1909. A History of Dentistry vols. 2 and 3.

TONDER, K. J. H. 1976. Effect of Vasodilating Drugs on External Carotid and Pulpal Blood Flow in Dogs: "Stealing " of Dental Perfusion Pressure. . *Acta Physiologica Scandinavica,* 97**,** 75-87.

TONDREAU, T., MEULEMAN, N., DELFORGE, A., DEJENEFFE, M., LEROY, R., MASSY, M., MORTIER, C., BRON, D. & LAGNEAUX, L. 2005. Mesenchymal stem cells derived from CD133-positive cells in mobilized peripheral blood and cord blood: proliferation, Oct4 expression, and plasticity. *Stem Cells,* 23**,** 1105-12.

TOOLE, B. P. 2001. Hyaluronan in morphogenesis. *Semin Cell Dev Biol,* 12**,** 79-87.

TOOLE, B. P., GHATAK, S. & MISRA, S. 2008. Hyaluronan oligosaccharides as a potential anticancer therapeutic. *Curr Pharm Biotechnol,* 9**,** 249-52.

TORABINEJAD, M. & CHIVIAN, N. 1999. Clinical applications of mineral trioxide aggregate. *J Endod,* 25**,** 197-205.

TORABINEJAD, M. & LEMON, R. R. 2009. *Endodontics: Principles and Practice.,* St. Louis, Missouri, USA., Saunders Elsevier.

TORABINEJAD, M., PETERS, D. L., PECKHAM, N., RENTCHLER, L. R. & RICHARDSON, J. 1993. Electron microscopic changes in human pulps after intraligamental injection. *Oral Surg Oral Med Oral Pathol,* 76**,** 219-24.

TROWBRIDGE, H. O. & KIM, S. 1998. *Pathways of the Pulp,* St. Louis., Mosby.

TRUBIANI, O., TRIPODI, D., DELLE FRATTE, T., CAPUTI, S. & DI PRIMIO, R. 2003. Human dental pulp vasculogenesis evaluated by CD34 antigen expression and morphological arrangement. *J Dent Res,* 82**,** 742-7.

TSAI-FANG, T. 1984. Endodontic treatment in China. *International Endodontic Journal.,* 17.**,** 163.

TSUZAKI, M., YAMAUCHI, M. & MECHANIC, G. L. 1990. Bovine dental pulp collagens: characterization of types III and V collagen. *Arch Oral Biol,* 35**,** 195-200.

TZIAFAS, D. 2004. The future role of a molecular approach to pulp-dentinal regeneration. *Caries Res,* 38**,** 314-20.

TZIAFAS, D., ALVANOU, A., PAPADIMITRIOU, S., GASIC, J. & KOMNENOU, A. 1998. Effects of recombinant basic fibroblast growth factor, insulin-like growth factor-II and transforming growth factor-beta 1 on dog dental pulp cells in vivo. *Arch Oral Biol,* 43**,** 431-44.

TZIAFAS, D. & KOLOKURIS, I. 1990. Inductive influences of demineralized dentin and bone matrix on pulp cells: an approach of secondary dentinogenesis. *J Dent Res,* 69**,** 75-81.

UITTO, V.-J. & ANTILA, R. 1971. Characterisation of Collagen Biosynthesis in Rabbit Dental Pulp In Vitro. *Acta Odontol Scand,* 29**,** 609-617.

UITTO, V.-J. & LARJAVA, H. 1991. Extracellular Matrix Molecules and their Receptors: An overview with Special Emphasis on Periodontal Tissues. *Critical Reviews in Oral Biology and Medicine.,* 2**,** 323-354.

URIST, M. R. 1965. Bone: formation by autoinduction. *Science,* 150**,** 893-9.

VACANTI, C. A. 2006. History of tissue engineering and a glimpse into its future. *Tissue Eng,* 12**,** 1137-42.

VACANTI, C. A. & VACANTI, J. P. 2000. The science of tissue engineering. *Orthop Clin North Am,* 31**,** 351-6.

VAN AMERONGEN, J. P., LEMMENS, I. G. & TONINO, G. J. 1983. The concentration, extractability and characterization of collagen in human dental pulp. *Arch Oral Biol,* 28**,** 339-45.

VICKERS, S. M., SQUITIERI, L. S. & SPECTOR, M. 2006. Effects of cross-linking type II collagen-GAG scaffolds on chondrogenesis in vitro: dynamic pore reduction promotes cartilage formation. *Tissue Eng,* 12**,** 1345-55.

VONGSAVAN, N. & MATTHEWS, B. 1992. Fluid flow through cat dentine in vivo. *Arch Oral Biol,* 37**.,** 175-185.

WANG, J., MA, H., JIN, X., HU, J., LIU, X., NI, L. & MA, P. X. 2011. The effect of scaffold architecture on odontogenic differentiation of human dental pulp stem cells. *Biomaterials,* 32**,** 7822-30.

WANG, T. W. & SPECTOR, M. 2009. Development of hyaluronic acid-based scaffolds for brain tissue engineering. *Acta Biomater,* 5**,** 2371-84.

WANG, T. W., WU, H. C., HUANG, Y. C., SUN, J. S. & LIN, F. H. 2006. Biomimetic bilayered gelatin-chondroitin 6 sulfate-hyaluronic acid biopolymer as a scaffold for skin equivalent tissue engineering. *Artif Organs,* 30**,** 141-9.

WEBER, D. F. & ZAKI, A. E. 1986. Scanning and transmission electron microscopy of tubular structures presumed to be human odontoblast processes. *J Dent Res,* 65**,** 982-6.

WEINBERG, C. B. & BELL, E. 1986. A blood vessel constructed from collagen and cultured vascular cells. *Science,* 231**.,** 397-400.

WEST, D. C., HAMPSON, I. N., ARNOLD, F. & KUMAR, S. 1985. Angiogenesis induced by degradation products of hyaluronic acid. *Science,* 228**,** 1324-6.

WEST, D. C. & KUMAR, S. 1989. The effect of hyaluronate and its oligosaccharides on endothelial cell proliferation and monolayer integrity. *Exp Cell Res,* 183**,** 179-96.

WEST, J. 2006. Endodontic update 2006. *J Esthet Restor Dent,* 18**,** 280-300.

WEST, N. X., LUSSI, A., SEONG, J. & HELLWIG, E. 2013. Dentin hypersensitivity: pain mechanisms and aetiology of exposed cervical dentin. *Clin Oral Investig,* 17 Suppl 1**,** S9-19.

WILLERSHAUSEN, B., WILLERSHAUSEN, I., ROSS, A., VELIKONJA, S., KASAJ, A. & BLETTNER, M. 2011. Retrospective study on direct pulp capping with calcium hydroxide. *Quintessence Int,* 42**,** 165-71.

WILLERSHAUSEN, I., BARBECK, M., BOEHM, N., SADER, R., WILLERSHAUSEN, B., KIRKPATRICK, C. J. & GHANAATI, S. 2014. Non-cross-linked collagen type I/III materials enhance cell proliferation: in vitro and in vivo evidence. *J Appl Oral Sci,* 22**,** 29-37.

WISE, S. G. & WEISS, A. S. 2009. Tropoelastin. *Int J Biochem Cell Biol,* 41**,** 494-7.

WOODFIN, A., VOISIN, M. B. & NOURSHARGH, S. 2007. PECAM-1: a multi-functional molecule in inflammation and vascular biology. *Arterioscler Thromb Vasc Biol,* 27**,** 2514-23.

XIAO, S., YU, C., CHOU, X., YUAN, W., WANG, Y., BU, L., FU, G., QIAN, M., YANG, J., SHI, Y., HU, L., HAN, B., WANG, Z., HUANG, W., LIU, J., CHEN, Z., ZHAO, G. & KONG, X. 2001. Dentinogenesis imperfecta 1 with or without progressive hearing loss is associated with distinct mutations in DSPP. *Nat Genet,* 27**,** 201-4.

XIE, Y., UPTON, Z., RICHARDS, S., RIZZI, S. C. & LEAVESLEY, D. I. 2011. Hyaluronic acid: evaluation as a potential delivery vehicle for vitronectin:growth factor complexes in wound healing applications. *J Control Release,* 153**,** 225-32.

XU, T., BIANCO, P., FISHER, L. W., LONGENECKER, G., SMITH, E., GOLDSTEIN, S., BONADIO, J., BOSKEY, A., HEEGAARD, A. M., SOMMER, B., SATOMURA, K., DOMINGUEZ, P., ZHAO, C., KULKARNI, A. B., ROBEY, P. G. & YOUNG, M. F. 1998. Targeted disruption of the biglycan gene leads to an osteoporosis-like phenotype in mice. *Nat Genet,* 20**,** 78-82.

YAMADA, T., NAKAMURA, K., IWAKU, M. & FUSAYAMA, T. 1983. The extent of the odontoblast process in normal and carious human dentin. *J Dent Res,* 62**,** 798-802.

YAMAKOSHI, Y., HU, J. C., FUKAE, M., ZHANG, H. & SIMMER, J. P. 2005. Dentin glycoprotein: the protein in the middle of the dentin sialophosphoprotein chimera. *J Biol Chem,* 280**,** 17472-9.

YAMAMURA, T. 1985. Differentiation of pulpal cells and inductive influences of various matrices with reference to pulpal wound healing. *J Dent Res,* 64 Spec No**,** 530-40.

YANG, J., SHI, G., BEI, J., WANG, S., CAO, Y., SHANG, Q., YANG, G. & WANG, W. 2002. Fabrication and surface modification of macroporous poly(L-lactic acid) and poly(L-lactic-co-glycolic acid) (70/30) cell scaffolds for human skin fibroblast cell culture. *J Biomed Mater Res,* 62**,** 438-46.

YANG, X., HAN, G., PANG, X. & FAN, M. 2012. Chitosan/collagen scaffold containing bone morphogenetic protein-7 DNA supports dental pulp stem cell differentiation in vitro and in vivo. *J Biomed Mater Res A.*

YANG, X., YANG, F., WALBOOMERS, X. F., BIAN, Z., FAN, M. & JANSEN, J. A. 2010. The performance of dental pulp stem cells on nanofibrous PCL/gelatin/nHA scaffolds. *J Biomed Mater Res A,* 93**,** 247-57.

YANG, X. B., WEBB, D., BLAKER, J., BOCCACCINI, A. R., MAQUET, V., COOPER, C. & OREFFO, R. O. 2006. Evaluation of human bone marrow stromal cell growth on biodegradable polymer/bioglass composites. *Biochem Biophys Res Commun,* 342**,** 1098-107.

YU, C. & ABBOTT, P. V. 2007. An overview of the dental pulp: its functions and responses to injury. *Aust Dent J,* 52**,** S4-16.

YU, C. Y., BOYD, N. M., CRINGLE, S. J., ALDER, V. A. & YU, D. Y. 2002. Oxygen distribution and consumption in rat lower incisor pulp. *Arch Oral Biol,* 47**,** 529-36.

YUN, Y. H. G., D.G.; YELLEN, P.; CHEN, W. 2004. Hyaluronan microspheres for sustained gene delivery and site-specific targeting. *Biomaterials,* 25**,** 147-157.

ZACH, L., TOPAL, R. & COHEN, G. 1969. Pulpal repair following operative procedures. Radioautographic demonstration with tritiated thymidine. *Oral Surg Oral Med Oral Pathol,* 28**,** 587-97.

ZAVAN, B., BRESSAN, E., SIVOLELLA, S., BRUNELLO, G., GARDIN, C., FERRARESE, N., FERRONI, L. & STELLINI, E. 2011. *Dental pulp stem cells and tissue engineering strategies for clinical application on odontoiatric field.,* Rijeka, Croatia., Intech.

ZHANG, H., LIU, S., ZHOU, Y., TAN, J., CHE, H., NING, F., ZHANG, X., XUN, W., HUO, N., TANG, L., DENG, Z. & JIN, Y. 2012. Natural mineralized scaffolds promote the dentinogenic potential of dental pulp stem cells via the

mitogen-activated protein kinase signaling pathway. *Tissue Eng Part A,* 18**,** 677-91.

ZHANG, J. Q., NAGATA, K. & IIJIMA, T. 1998. Scanning electron microscopy and immunohistochemical observations of the vascular nerve plexuses in the dental pulp of rat incisor. *Anat Rec,* 251**,** 214-20.

ZHANG, L., LI, K., XIAO, W., ZHENG, L., XIAO, Y., FAN, H. & AL., E. 2010. Preparation of collagen-chondroitin sulphate-hyaluronic acid hybrid hydrogel scaffolds and cell compatability *in vitro*. *Carbohydrate Polymers.,* 84**.,** 118-125.

ZHANG, S., WANG, D., ESTROV, Z., RAJ, S., WILLERSON, J. T. & YEH, E. T. 2004. Both cell fusion and transdifferentiation account for the transformation of human peripheral blood CD34-positive cells into cardiomyocytes in vivo. *Circulation,* 110**,** 3803-7.

ZHANG, X., ZHAO, J., LI, C., GAO, S., QIU, C., LIU, P., WU, G., QIANG, B., LO, W. H. & SHEN, Y. 2001. DSPP mutation in dentinogenesis imperfecta Shields type II. *Nat Genet,* 27**,** 151-2.

ZHONG, S., TEO, W. E., ZHU, X., BEUERMAN, R. W., RAMAKRISHNA, S. & YUNG, L. Y. 2006. An aligned nanofibrous collagen scaffold by electrospinning and its effects on in vitro fibroblast culture. *J Biomed Mater Res A,* 79**,** 456-63.

ZIAS, J. & NUMEROFF, K. 1987. Operative dentistry in the second century BC. *J Am Dent Assoc,* 114**,** 665-6.

List of Abbreviations

5-CMFDA	5-chloromethylfluorodiacetate
ABI	Applied Biosystems
ALP	Alkaline phosphatase
APES	3-aminopropyltriethoxysilane
BDNF	Brain derived neurotrophic factor
BMPs	Bone morphogenic proteins
BMSCs	Bone marrow stem cells
BSP	Bone sialoprotein
CAM	Chorioallantoic membrane
CD	Cluster of differentiation
CGRP	Calcitonin gene-related peptide
DMEM	Dulbecco’s modified Eagle’s medium
DMP1	Dentine matrix protein-1
DMSO	Dimethyl sulphoxide

DNA	Deoxyribonucleic acid
DPSCs	Dental pulp stromal cells
DPX	Dibutylphthalate
DSPP	Dentine sialophosphoprotein
ECACC	European collection of cell cultures
ECM	Extra Cellular Matrix
EDTA	Ethylenediaminetetracetic acid
EGFIR	Epidermal growth factor
EGM	Essential growth medium
FCS	Foetal calf serum
FEGSEM	Field emission gun scanning electron microscope
FN	Fibronectin
GAG	Glycosaminoglycan
GDNF	Glial derived neurotrophic factor
H&E	Haematoxylin and Eosin
HIV	Human Immunodeficiency Virus

hMSCs	Human Mesenchymal Stem Cells
HPDLC	Human Periodontal Ligament Cells
HRP	Horseradish Peroxidase
HSC	Haematopoietic Stem Cell
HUVECs	Human umbilical vein endothelial cells
HyA	Hyaluronic Acid
IGFIR	Insulin-like growth factor 1
ITIMs	Immunoreceptor tyrosine inhibitory motifs
kDa	kilo Dalton
LDI	Leeds Dental Institute
LOX	Lysil oxidase
LOXL	Lysil oxidase-like
MEPE	Matrix extracellular phosphoglycoprotein
MHCs	Major histocompatibility complexes
mRNA	Messenger Ribonucleic Acid
MTA	Mineral trioxide aggregate

MW	Molecular weight
NBF	Neutral buffered formaldehyde
NCPs	Non collagenous proteins
NGF	Nerve growth protein
NGS	Normal goat serum
n-HyA	Native High Molecular weight Hyaluronic Acid.
o-HyA	Oligo- Hyaluronic Acid
OP	Osteopontin
PBS	Phosphate buffered saline
PDLLA	Poly (DL-lactic acid)
PG	Proteoglycan
PLLA	Poly-L-lactic acid
PTPs	Protein-tyrosine phosphates
RER	Rough endoplasmic reticulum
RHAMM	Receptor for Hyaluronan Mediated Motility
$_{rh}VEGF_{165}$	Recombinant human VEGF 165

SCAP	Stem Cells from the Apical Papilla
SCID	Severe Combined Immunodeficient
SEM	Scanning electron microscope
SHED	Stem cells from Human Exfoliated deciduous Teeth
SHPs	Src homology region 2 domain-containing phosphates
SIBLINGS	Small integrin binding ligand N-linked glycoproteins
SLRPS	Small leucine rich proteins
STRO-1	Stromal Cell Surface Marker 1
TE	Trizema hydrochloride ethylenediaminetetracetic acid
TGFβ	Transforming growth factor Beta
TOPRO	TOPRO-3 iodide
TRIS	Tris(hydroxymethyl)aminomethane
UV	Ultra Violet

vWF	Von Willebrand Factor
YWHAZ	Tyrosine 3-monooxygenase/tryptophan 5-monooxygenase activation protein, zeta polypeptide
αMEM	Alpha modified essential media

Appendix A Histology protocols

1.1 Alkaline Phosphatase staining.

Positive alkaline phosphatase stain produces a strong dark red-purple colouration indicative of a tissues' or cells' ability to form mineralised tissue under the appropriate culture conditions.

1) The cell explants were first stopped in 98% ethanol overnight in their 6 well plate.
2) Next day the ethanol is drained off and replaced with PBS for 10 minutes.
3) Add 0.4mL of Naphthol A5-MX solution to 9.6 mL of distilled water.
4) To this mixture add 2.4mg of Fast Violet B salt and mix thoroughly.
5) Remove the PBS from the samples and add sufficient reagent mixture to cover the samples.
6) Leave with lid on for at least 30 minutes or longer if necessary until no further colour change is apparent.
7) Take images.

1.2 Alcian Blue/Sirius Red Staining.

Alcian blue positive cells produce the proteoglycan aggrecan, a component of cartilage.

1. Stain the sections on the slides with Weigart haematoxylin. Using a plastic Pasteur pipette, gently wash the Weigart haematoxylin over each section and leave for 10 minutes.
2. Take each slide and rinse gently through a water bath then replace the slides in the staining tray.
3. Place the tray into the water bath and rinse for 10 minutes.
4. Dip the slides 3x in acid/alcohol(20mL HCl + 2litres 50% methanol).
5. Rinse slides in water bath for 1 minute.
6. Stain slides in molybdophosphoric acid for 20 minutes.
7. Rinse in water bath for 1 minute.
8. Stain with Sirius red for 60 minutes.
9. Rinse in water 1 minute.
10. Dip tray in 100% ethanol 1 for 30 minutes then 100% ethanol 2 for 30 minutes.
11. Mount in DPX.

1.3 CD31/34 staining for formalin fixed paraffin embedded dental pulp sections and in vitro and in vivo samples.

For CD31: AbCam ab28364. CD34: AbCam ab 81289. STRO-1: AbCam ab102969.

1. Place slides in staining tray and place in Xylene 1 for 20 minutes.
2. Place in Xylene 2 for 20 minutes.
3. Place in alcohol 1 for 5 minutes.
4. Place in alcohol 2 for 5 minutes.
5. Tap water wash for 5 minutes minimum.
6. Place in 2% hydrogen peroxide/methanol solution for 20 minutes
7. Wash in PBS in washbox with magnetic stirrer for 5 minutes minimum.
8. For antigen retrieval, place slides in a plastic coplin jar containing 10mM sodium citrate buffer (pH6) and place coplin jar(s) in a water bath preheated to 65°C. Cover the water bath and leave for 1 hour.
9. Replace slides in staining racks and wash in PBS in washbox with stirrer for minimum of 5 minutes.
10. Quickly load slides into Shandon 67650002 Sequenza developer and top up well at top of each coverplate slide holder with PBS. N.B. if PBS drains through rapidly, slide is not seated properly.
11. Add 1/5 normal goat serum (NGS) for 5 minutes.
12. Add primary antibody at desired concentration (usually 1:100) and leave overnight at room temperature, with box cover on and some PBS in bottom of container to prevent drying out.

13. Top up coverplate well with PBS and leave for 5 minutes minimum.
14. Add 2 drops of EnVision solution A from Dako kit K5007 per slide and leave for 30 minutes.
15. Quickly unload the slides and place into a humidity chamber and add 120µL of EnVision solution (1mL of solution B plus 20µL of solution C) to each slide. After 5 minutes check staining under microscope. Repeat if necessary.
16. Was in PBS/washbox for 5 minutes minimum.
17. Counterstain in Harris haematoxylin for 1 minute.
18. Wash in tap water for 5 minutes minimum until water runs clear.
19. Immerse in Scott's tap water for 1 minute.
20. Wash in tap water for 5 minutes.
21. Dehydrate in alcohol 3 & 4 for 5 minutes each.
22. Clear in xylene 1 & 2 for 5 minutes each.
23. Mount slides under appropriate sized coverslip in DPX (**D**ibutyl**P**hthalate in solution with **X**ylene).

1.4 Haematoxylin and Eosin (H&E) staining.

1. Place sections in a slide rack and immerse in xylene for 5 minutes.

2. Immerse sections in absolute ethyl alcohol 1 for 5 minutes.

3. Immerse sections in absolute alcohol 2 for 5 minutes.

4. Wash under running tap water for 5 minutes.

5. Stain with Harris' haematoxylin solution for 3 minutes.

6. Wash under running tap water for 5 minutes.

7. Differentially stain the nuclei by dipping the sections in 1% acid alcohol for (literally) 3 quick dips. Check under the light microscope for contrast and repeat if necessary.

8. Wash under running tap water for 5 minutes.

9. 'Blue' the sections by immersion in Scott's tap water for 2 minutes.

10. Wash under running tap water for 5 minutes.

11. counterstain by immersing the sections in 1% aqueous Eosin for 30 seconds.

12. Wash under running tap water for 5 minutes.

13. Dehydrate in absolute alcohol 3 for 5 minutes.

14. Dehydrate in absolute alcohol 4 for 5 minutes.

15 Clear the alcohol by immersion in xylene for 5 minutes

16. Mount the sections in DPX, under a coverslip.

1.5 DPSCs, HUVECs and G292 cells cultured on collagen I gel, 1% HyA gel in 12 well plates or on coverslips. CD31 AbCam ab28364. CD34 AbCam ab 81289.

Use a new disposable plastic Pasteur pipette for each stage and do not mix them up between stages to avoid reagent contamination.

1 Remove culture medium and wash in PBS for 5 minutes.

2.Remove PBS and fix cells in 10% NBF for 30 minutes.

3. Remove NBF and wash gel with 3 x 5 minutes tap water.

4. Remove tap water and immerse in 2% hydrogen peroxide/methanol for 20 minutes.

5. Remove H_2O_2/methanol and wash with PBS 3 x 5 minutes.

6. Apply 20% NGS in PBS for 5 minutes.

7. Remove excess NGS but do not wash (for negative control leave covered with NGS overnight.

8. Add primary antibody at desired concentration (usually 1:100) and seal the plate around with parafilm, placing PBS in any unused wells to prevent desiccation.

9. Add 2 drops EnVision solution A for 30 minutes at room temperature.

10. Wash with PBS for 3 x 5 minutes.

11. Add EnVision solution (1mL of B with 20µL of C) 150µL per well for 2 x 5 minutes.

12. Wash thoroughly with tap water for at least 2 x 10 minutes. Tap water should be clear at last wash.

13. Counterstain with Harris haematoxylin for 1 minute.

14. Wash thoroughly with tap water and repeat until clear.

15. Immerse with Scott's tap water for 1 minute.

16. Wash with tap water 3 x 5 minutes.

17. If cells cultured on a cover slip, mount face down onto a slide with aqueous mounting medium then seal edges with nail varnish. If cultured in a 12 well plate, seal lid with PARAFILM® "M" laboratory film and record images as soon as possible.

1.6 RNA Isolation and Reverse Transcription

Each 6 well plate was stopped at the appropriate time point by draining the media and washed twice with 3 mL of PBS for 20mins each. It was then drained and 1 mL of trypsin/EDTA reagent (Invitrogen, UK) was added then the plates were placed in a tissue culture incubator until the cells had detached or in the case of those cultured on HyA, until they had visibly shrunken under microscope examination. Then each well was scoured with a disposable cell scraper (Fisherbrand® Scientific) to ensure maximal cell harvest. The contents of each group of wells (monolayer or HyA) were then moved into a 50 mL test tube, topped up with PBS to 30 mL, vortexed for 1 minute and then spun down for 10 minutes at 2000 rpm. The supernatant was then removed and the resealed tubes were stored at minus 80°C until RNA extraction.

The RNA was obtained from the cells in accordance with the instructions found in the Qiagen RNeasy® Mini Kit (50) (Cat. No. 74104) as follows:

The cell pellet was defrosted in 1 × PBS at room temperature then agitated to mix the contents. It was then centrifuged at 2000 rpm for ten minutes, the supernatant was aspirated and cells were disrupted by adding 1.5 mL of RLT buffer, to which had previously been added β-mercaptoethanol at a concentration of 10µL per mL. As the cells had been pelleted the cell pellet was pipetted up and down to loosen it up and aid cell lysis during mixing. The mixture was transferred to a 2 mL tube and vortexed for 1 minute at 1400. 350 µL of 70% ethanol was added to the tube and the mixture pipetted to mix. 700µL of each sample (including any precipitate) was transferred to a labelled RNeasy spin column, placed in a 2mL spin column which is

then spun at 10000 rpm for 15 seconds. The flow-through is discarded, then to remove any potential genomic DNA, an on-column DNase digestion is performed: 350µL of Buffer RW1 is added to each spin column and centrifuged at 10000 rpm for 15 seconds and the flow-through is discarded. 10µL of DNase stock solution (DNase 1 kit, Invitrogen, UK) is added to 70µL of RDD buffer for each sample (i.e.80µL per sample), added to each spin column centrifuged very briefly and left for 20 minutes at room temperature. 350 µL of Buffer RW1 is then added to each spin column and centrifuged at 10000 rpm for 15 seconds. Discard the flow-through. 500µL of Buffer RPE is added to each column and spun for 2 minutes at 10000 rpm. Using a new collection tube, 50µL of RNase free water is added to each column and spun for 1 minute at 10000rpm to elute the RNA. Discard the follow-through and repeat.

The RNA quality was checked using a Thermo Scientific NanoDrop 2000 machine which measured the quantity and purity of the RNA obtained. A 2 µL sample of the extracted mRNA is quantified by measuring the 260/280 ratios, which were all found to be between 1.8 and 2, indicating acceptable purity.

The RNA obtained is then processed into cDNA using a High Capacity RNA-to-cDNA Kit (applied Biosystems, Carlsbad, USA) to obtain 200ng of cDNA in 20 µL reaction volumes in accordance with the manufacturer's instructions. These were then run on a MJ Research PTC-100 Thermo Cycler for 1 hour at 37°C and then at 95°C for five minutes.

Appendix B List of Conferences Attended

7th April 2007 BSDR Annual General Meeting, Durham (Poster).

27th June 2007 White Rose Health Innovation Partnership – Dentistry Workshop (Oral Presentation).

16th October 2008 2nd Leeds-Michigan Tissue Engineering Symposium.

19th November 2008 Leeds Dental Institute postgraduate student annual meeting.

18th November 2009 Leeds Dental Institute postgraduate student annual meeting.

17th November 2010 Leeds Dental Institute postgraduate student annual meeting (Poster).

27th July 2011 Leeds Dental Institute postgraduate annual meeting.

11th July 2012 Leeds Dental Institute postgraduate annual meeting (oral presentation).

10th July 2013 Leeds Dental Institute postgraduate annual meeting.

9th July 2014 Leeds Dental Institute postgraduate annual meeting.

10th July 2015 Leeds Dental Institute postgraduate annual meeting.

Appendix C List of Courses Attended

26th January 2011	Human Tissue Ethics Training Workshop.
10th February 2011	Protecting your ideas – Understanding the process.
16th March 2013	University Research Ethics Workshop.
1st May 2013	How to write a great research paper and get it accepted by a good journal.
28th January 2015	Preparing for your viva.

Appendix D Bibliography

Cohen's Pathways of the Pulp, 10th edition: Eds: Hargreaves, K.M. and Berman, L.H. Mosby, 2016. ISBN13: 9780323185868.

Ten Cate's Oral Histology, 8th edition. Ed: Antonio Nanci. Mosby, 2013. ISBN13: 9780323078467.

Ingle's Endodontics, 6th edition: Eds: Ingle, J.I., Bakland, L.K., Baumgartner, J.C. B. C. Decker, Inc. ISBN13: 9781550093339.

Appendix E Publications

Automated electrophysiological and pharmacological evaluation of human pluripotent stem cell-derived cardiomyocytes. Denning, C. et al. Submitted to Stem Cells and development, subject to corrections and revision.